

Role of Chemistry for Sustainable Future



Dr. V. D. Tripathi

Kripa Drishti Publications, Pune.

**ROLE OF
CHEMISTRY
FOR SUSTAINABLE FUTURE**

Editor

Dr. V. D. Tripathi

Assistant Professor,
Department of Chemistry,
C.M. Science College,
Darbhanga.

Kripa-Drishti Publications, Pune.

Book Title: **Role of Chemistry for Sustainable Future**

Editor By: **Dr. V. D. Tripathi**

Price: ₹475

1st Edition

ISBN: 978-81-19149-17-9



Published: **July 2023**

Publisher:



Kripa-Drishti Publications

A/ 503, Poorva Height, SNO 148/1A/1/1A,
Sus Road, Pashan- 411021, Pune, Maharashtra, India.

Mob: +91-8007068686

Email: editor@kdpublications.in

Web: <https://www.kdpublications.in>

© **Copyright Dr. V. D. Tripathi**

All Rights Reserved. No part of this publication can be stored in any retrieval system or reproduced in any form or by any means without the prior written permission of the publisher. Any person who does any unauthorized act in relation to this publication may be liable to criminal prosecution and civil claims for damages. [The responsibility for the facts stated, conclusions reached, etc., is entirely that of the author. The publisher is not responsible for them, whatsoever.]

PREFACE

The edited book "**Role of Chemistry for Sustainable Future**" assists chemistry instructors in strengthening connections in the college chemistry curriculum to the local, regional, and global challenges that we face on our planet. These multifaceted and multidisciplinary challenges include providing clean energy, protecting and stewarding the environment and its resources, employing wise agricultural practises to supply food, and ensuring clean water and clean air for all communities. The carbon cycle, as a chemical concept, is linked to problems like these. It is presented as a possibility for strengthening curriculum connections to sustainability.

Chemical Sciences have made remarkable advances in Sustainable Technology and Development. Chemical sciences play a critical role in moving society closer to being able to control and manage a stable, improved ecosphere. The application of this knowledge allows for the development of sustainable technology. The ideas, concepts, achievements, and challenges of chemical sciences, as well as their applications in sustainable technological developments, must be established. The special issue's goal is to introduce cutting-edge research activities in Chemical Sciences, demonstrating vigorously innovative technologies, methods, and novel integrated devices for next-generation technological developments in a variety of fields such as pharmaceuticals, biomedical, polymer, petrochemicals, agriculture, food safety, and environmental monitoring.

CONTENT

1. Bio-fertilizer: A key Player in Sustainable Agriculture - Sidhu Murmu, Arup Sarkar, Kanu Murmu, Priya Das	1
1.1 Introduction:	1
1.2 Key Concepts of Sustainable Agriculture:.....	2
1.3 Classification of Bio-fertilizers:	3
1.3.1 Nitrogen Fixing Bio-fertilizers:	4
1.3.2 Phosphorus Solubilizing Bio-Fertilizers:	8
1.3.3 Phosphorus Mobilizing Bio-Fertilizers: Mycorrhiza	8
1.3.4 Potassium (K)-Solubilizing Bio-Fertilizers:.....	9
1.3.5 Plant-Growth-Promoting Rhizobacteria (PGPR):.....	10
1.3.6 Organic Matter Decomposer:.....	11
1.4 Bio-fertilizer: Application for Sustainable Economic Development:	12
1.5 Conclusions:	13
1.6 References:	13
2. Multicomponent Reactions: Minimizing the Impact of Chemical Synthesis - Pragati Sharma, Pragma Sinha	16
2.1 Introduction:	16
2.2 Anticancer Compounds Obtained from MCRs Approaches:.....	18
2.3 Conclusions:.....	24
2.4 References:	24
3. Drug Delivery Formulations - Dr. Mir Kaisar Ahmad.....	27
3.1 Introduction:	27
3.2 Route of Administration	28
3.2.1. Peroral Route:	28
3.2.2. Parenteral Route:.....	28
3.2.3. Pulmonary Route:.....	29
3.2.4. Nasal Route:.....	29
3.2.5. Transdermal Route:	29
3.2.6 Implants:	29
3.3. Target Sites:	30
3.3.1. Brain Targeting:	30
3.3.2. Colon Targeting:	30
3.3.3 Cancer Tissues Targeting:	30
3.4. Drug Delivery Formulations:	31
3.5. Conclusions:	31

**4. Chemistry of Metal Ferrite Nanoparticles: Synthesis and Characterization -
Chinmay, Vishaka Chauhan, Anjaneyulu Bendi32**

4.1 Introduction:.....	32
4.2 Chemistry of Metal Ferrite Nanoparticles and their Nanocomposites:	33
4.2.1 Synthesis and Characterization of ZnFe ₂ O ₄ Nanoparticles:.....	33
4.2.2 Synthesis and Characterization of NiFe ₂ O ₄ Nanoparticles:	34
4.2.3 Synthesis and Characterization of CuFe ₂ O ₄ Nanoparticles:.....	34
4.2.4 Synthesis and Characterization of CoFe ₂ O ₄ /Cu (OH) ₂ Nanocomposite:	35
4.2.5 Synthesis and Characterization of ZnFe ₂ O ₄ /Cu Nanocomposite:.....	36
4.2.6 Synthesis and Characterization of NiFe ₂ O ₄ / Geopolymer Nanocomposite:	37
4.3 Conclusion:	37
4.5 Acknowledgments:	37
4.6 References:.....	38

**5. Deep Eutectic Solvents (DESs): A Benign and Sustainable Approach in
Amphiphilic Self-Assembly - Yagnik Vora, Ketan Kuperkar.....40**

5.1 Introduction to Deep Eutectic Solvents (DESs):.....	40
5.1.1 General assumption:.....	40
5.1.2 Historical Perspective:.....	40
5.2 Preparation and Classification of DESs:.....	41
5.3 Physicochemical Properties of DESs	43
5.3.1 Freezing Point:	43
5.3.2 Density (ρ):	44
5.3.3 Viscosity (η):	44
5.3.4 Rheology:.....	44
5.3.5 Conductivity (κ):	45
5.3.6 Surface Tension (γ):	45
5.3.7 Refractive Index (n_D):.....	45
5.4 Applications of DESs:	47
5.4.1 Electrochemistry:	47
5.4.2 Catalysis:	47
5.4.3 Drug Solubilization Biomedical and Pharmaceuticals:	48
5.4.4 Metal Oxide Solubility:	48
5.4.5 Biomass Dissolution:	48
5.4.6 Organic Synthesis:	49
5.4.7 CO ₂ Capturing:	49
5.4.8 Nanoparticle Synthesis:.....	49
5.5 Self-Assembly of Amphiphiles In DES:.....	49
5.6 Conclusions and Future Prospective:	52
5.7 References:.....	53

6. Basic Principles of Green Chemistry - Dr. Shubhendu Dhara..... 55

6.1 Introduction:.....	55
6.2 Background of Green Chemistry:.....	56
6.3 Objective of Green Chemistry Approaches:	57
6.4 Few Terminologies Used in Green Chemistry ³	58
6.4.1 Atom Economy (AE):	58
6.4.2 Environmental factor (E-factor):.....	59
6.4.3 Life cycle assessment (LCA):.....	60
6.5 Limitations in Pursuing Strategies of Green Chemistry:	60
6.6 Principles of Green Chemistry:	61
6.7 Conclusion:	69
6.8 Reference:	70

7. Green Chemistry: A Sustainable Approach to Chemistry - Jhinuk De..... 71

7.1 Introduction:.....	71
7.2 Definition of the Green Chemistry by These 12 Principles:.....	72
7.2.1 Pollution Prevention:.....	72
7.2.2 Atom Economy:	72
7.2.3 Less Hazardous Chemical Synthesis:.....	72
7.2.4 Designing Safer Chemicals:	72
7.2.5 Used Safer Solvents and Auxiliaries:.....	72
7.2.6 Design A Chemical Process for Energy Efficiency:.....	72
7.2.7 Use of Renewable Feed Stocks:.....	72
7.2.8 Reduce Derivatives:	73
7.2.9 Catalysis of a Chemical Reaction:	73
7.2.10 Design for Degradation - While Designing a New Chemical:	73
7.2.11 Real-Time Analysis for Pollution Avoidance:.....	73
7.2.12 Essentially Safer Chemistry for Accident Prevention:.....	73
7.3 Sustainable Synthesis and Manufacturing:	74
7.4 Solvent Selection and Design:.....	74
7.5 What Is Solvent Free Reaction?	74
7.6 Waste Minimization and Valorisation:	74
7.7 Life Cycle Assessment and Sustainability Metrics:	75
7.8 Green Chemistry in Industry and Academia:.....	75
7.9 Challenges and Future Directions:	75
7.10 Conclusion:	75
7.11 References:.....	76

8. Ceric Ammonium Nitrate: An Alternative Over Metaal Catalysts for Multicomponent Synthesis - Vishwa Deepak Tripathi, Sanjeev Kumar Jha 77

8.1 Introduction:.....	77
8.2 General Information:	78
8.3 Characterization Data for Synthesized Compounds:.....	79

8.4 Results and Discussion:	85
8.4.2 Scheme 2:	87
8.4.3 Scheme 3:	88
8.5 Conclusion:	91
8.6 References:.....	91

9. Natural Product in Research and Drug Discovery - Vishwa Deepak Tripathi, Anand Mohan Jha93

9.1 Natural Product in Research and Drug Discovery:	93
9.2 History:	94
9.3 Today:.....	96
9.4 Natural Product Inspired Synthesis:	98
9.5 Marketed Drugs Based on Natural Molecules:	98
9.6 Lovastatin:.....	99
9.7 Paclitaxel:.....	100
9.8 Sirolimus, Rapamycin:	101
9.9 Artemisinin:	102
9.10 Vincristine:.....	102
9.11 Penicillin:	103
9.12 Vancomycin:	104
9.13 Erythromycin:	105
9.14 Doxorubicin:	106
9.15 Calanolide A:	107
9.16 Morphine:.....	107
9.17 Streptomycin:	108
9.18 Quinine:	109
9.19 Reference:	110

10. A Summarized Study of Recent Advances in Biologically Active Quinazolines - Vishwa Deepak Tripathi112

10.1 Introduction:.....	112
10.2 Summary of Quinazolines with Biological Potential Against Different Targets:	114
10.2.1 Analgesic Activity:	114
10.2.2 Anti-Inflammatory Activity:.....	118
10.2.3 Anticonvulsant Activity:	121
10.2.4 Antiviral Activity:.....	124
10.2.5 Anticancer Activity:	126
10.2.6 Anti-tubercular Activity:	131
10.2.7 Anti-Histaminic Activity:.....	132
10.3 References:.....	134

11. Photocatalytic Investigations of Organic Dyes Using Phosphate and Tungstate Based Nanomaterials - Indumukhi B. C, Vinayaka S, Ishwarya S, Harini H. V, Nagaswarupa H. P 139

11.1 Introduction: 139
11.2 Mechanism of Photocatalysis Using Phosphate and Tungstate Nanomaterials: 140
11.3 Dye and Their Structure: 141
11.4 Methods of Synthesis: 142
11.5 Characterization: 147
 11.5.1 XRD: 147
 11.5.2 FTIR: 148
 11.5.3 SEM: 148
 11.5.4 TEM: 149
 11.5.5 EDAX: 149
 11.5.6 UV-Visible: 149
 11.5.7 BET: 150
 11.5.8 Raman Spectroscopy 150
11.6 Photocatalytic Application: 150
 11.6.1 Photocatalysis of RhB: 151
 11.6.2 Photocatalysis of MO: 151
 11.6.3 Photocatalysis of EBT: 152
 11.6.4 Photocatalysis of 2,4-DNP: 152
11.7 Future Prospects: 152
11.8 Reference: 152

12. Functional Materials for Energy Storage Applications - V. V. Deshmukh, H. P. Nagaswarupa 158

12.1 Introduction: 158
12.2 Classification of Energy Storages: 159
 12.2.1 Thermal Energy Storage: 159
 12.2.2 Mechanical Energy Storage: 159
 12.2.3 Chemical Energy Storage: 160
 12.2.4 Electrochemical Energy Storage: 160
 12.2.5 Electromagnetic Energy Storage: 160
12.3 Types of Materials Used for Energy Storages: 161
 12.3.1 Common Materials: 161
 12.3.2 Advanced Materials for Energy Storage: 166
 12.3.3 Advances and Challenges of Green Materials: 169
12.4 Applications of Energy Storage: 169
 12.4.1 Fuel Cells: 169
 12.4.2 Batteries: 170
 12.4.3 Supercapacitors: 170
 12.4.4 Emerging Storage Technologies: 170
12.5 Sustainable Developments: Constraints and Reality: 172

12.5.1 Materials Recycling	172
12.5.2 Energy Management:	173
12.6 Challenges and Prospects:.....	173
12.7 Conclusion:	173
12.8 References:.....	174

1. Bio-fertilizer: A key Player in Sustainable Agriculture

Sidhu Murmu

Department of Agricultural Chemistry and Soil Science,
Bidhan Chandra Krishi Viswavidyalaya.

Arup Sarkar, Kanu Murmu, Priya Das

Department of Agronomy,
Faculty of Agriculture,
Bidhan Chandra Krishi Viswavidyalaya.

1.1 Introduction:

Agriculture and agriculture resources are the sole factors for sustenance for human civilization. The majority of people in the world depend on agriculture to support a healthy lifestyle and provide food, feed, and other essentials like fiber, wood, gums, and secondary products with medicinal properties. According to the trend of population growth, researchers, agricultural scientists, and agro-industries must create appropriate strategies for sustainable agriculture if they are to feed the growing population's hunger needs. The primary goal of any civilized society is to control agricultural operations to a degree that may effectively eliminate the need for hunger. Traditional agricultural practices solely provide food and feed for domestic consumption. Only the farmer's families and their local village communities are permitted to use traditional practices (Jehangir et al. 2017; Pandey 2018). The concept of sustainable agriculture is not only to maximize the limit of crop growth but also to maintain the ecology is the decisive factor behind the success of sustainable agriculture (Barragan-Ocana and Rivera 2016). To increase crop output, agricultural operations use a variety of hormones, artificial fertilizers, and other synthetic minerals. The health of the soil and the plant system are both impacted by these synthetic chemicals and minerals (Campos et al. 2018). Chemical fertilizers, which are byproducts of fossil fuels (coal + petroleum), are the principal synthetic inputs that modern agriculture is increasingly dependent upon for a stable supply. Due to the excessive and unbalanced usage of these synthetic inputs, negative impacts are being seen. By this point, the soils are biologically dead. This circumstance has helped researchers uncover risk-free inputs like bio-fertilizers and biopesticides. Sustainability in agriculture system can be possible without sacrificing the ability of future generations to meet their own needs and the environment's resources (Calabi-Floody et al. 2018). + A new era of industry might begin if bio-fertilizers are used in place of chemicals in the agricultural system. Bio-fertilizers may be useful for giving crop plants the nutrients they need without harming the environment (Mishra and Dash 2014). The market and society are under pressure from environmentalists all around the world to transition to organic farming and bio-fertilizers. Organic farming focuses on protecting biodiversity and the preservation of natural resources in order to produce food in a way that is more ecologically friendly and sustainable. High standards for animal welfare are also emphasized, as is avoiding synthetic chemical inputs like pesticides, fertilizers, and genetically engineered organisms (GMOs).

1.2 Key Concepts of Sustainable Agriculture:

The USDA first used the phrase "sustainable agriculture" in 1977 to refer to an integrated system of plant and animal production techniques that are site-specific and will, in the long run:

- A. Meet the demands of human food and fiber
- B. Improve environmental quality and the natural resource base that supports the agriculture economy
- C. Utilize nonrenewable resources and on-farm resources as effectively as possible and include, as necessary, natural biological cycles and controls
- D. Maintain the agriculture operations' ability to make a profit
- E. Improve the standard of living for farmers and society at large.

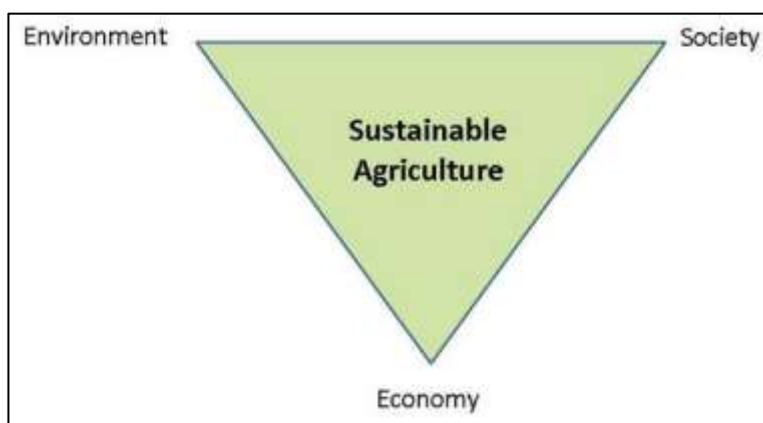


Figure 1.1: Sustainable agriculture gives equal weight to environmental, social, and economic concerns in agriculture.

The foundation of agricultural sustainability is the idea that we must satisfy our needs today without jeopardizing the ability of future generations to satisfy their own needs. Therefore, short-term economic gain is just as important as long-term stewardship of both natural and human resources. Stewardship of human resources includes taking into account social duties such as laborers' living and working conditions, the needs of rural communities, and the current and long-term health and safety of consumers. Land and natural resource stewardship entails preserving or improving the quality of these resources and utilizing them in ways that enable future regeneration. When making stewardship decisions in farm enterprises that use cattle, considerations for animal welfare must be made. The current trajectory of agricultural production development is unsustainable due to its detrimental effects on the environment and natural resources. Up to 75% of crop genetic variety has been lost, one-third of farmland has been destroyed, and 22% of animal breeds are under danger. Over the previous ten years, almost 13 million hectares of forests per year were converted into other land uses, and more than half of fish sources are fully utilized. The primary issues at hand are the increasing scarcity and rapid deterioration of natural resources at a time when there is a rising demand for food, feed, fiber, and other products and services from agriculture (including crops, livestock, forests, fisheries, and aquaculture).

In regions with a high rate of food insecurity and a reliance on agriculture, some of the biggest population growth is anticipated. Sustainability needs to be viewed as a process rather than a clearly defined goal that must be attained in order to deal with the accelerated rate of change and growing unpredictability. In turn, this necessitates the creation of technological, policy, governance, and financial frameworks that aid resource managers and agricultural producers who are actively engaged in a dynamic innovation process.

A. What is Bio-Fertilizers?

Bio-fertilizers are the products containing one or more viable microorganisms which have ability to increase the soil fertility by increasing availability of plant nutrients through several biological processes such as nitrogen fixation, phosphorus solubilization, excretion of plant growth promoting substances or cellulose and lignin degradation etc. Use of bio-fertilizers is one of the important constituents of integrated nutrient management as they are the cost effective and adequate renewable sources of plant nutrients in supplement of chemical fertilizers for sustainable development in agriculture.



Figure 1.2: Bio-Fertilizers

1.3 Classification of Bio-fertilizers:

A. Types of Bio-fertilizers on the basis of Beneficial Microorganisms and their Functions:

Bio-fertilizers are substances that contain microorganisms that can trigger a biological process that promotes plant growth and development. These bacteria perform more than just a simple fertilizing task. They change the unavailable forms of soil components into ones that plants can access. Contrarily, microorganisms steadily and consistently increase the stability and phytosanitation of the soil. Additionally, microorganisms assist plants in producing hormones, vitamins, and amino acids that are crucial for developing disease resistance. Six categories can be used to classify the numerous bio-fertilizers that support plant growth at different stages of development:

- A. Nitrogen fixing bio-fertilizers
- B. Phosphorus solubilizing bio-fertilizers
- C. Phosphorus mobilizing bio-fertilizers: Mycorrhiza
- D. Potassium (K)-solubilizing bio-fertilizers
- E. Plant-growth-promoting rhizobacteria (PGPR)
- F. Organic matter decomposers

1.3.1 Nitrogen Fixing Bio-fertilizers:

Nitrogen is the most limiting nutrient to plant growth although the atmosphere contains about 80% nitrogen because plants cannot take the nitrogen from air. Some microorganisms are capable of fixing atmospheric nitrogen for plant uptake. Nitrogen fixing bio-fertilizers are bacteria and blue green algae. Bacteria are both symbiotic and non-symbiotic. Bacteria become associated with different plant parts and fix the nitrogen and make the nitrogen able to plant uptake.

A. Symbiotic Nitrogen Fixing Bacteria:

The best known and effective symbiotic nitrogen fixing bacteria are belonged to the family Rhizobiaceae (Rhizobia) and the following families are included into this family: Rhizobium, Bradyrhizobium, Sinorhizobium, Azorhizobium, Mesorhizobium, and Allorhizobium (Vance, 1998; Graham and Vance, 2000). The N₂-fixing capability of rhizobia varies greatly up to 450 Kg N/ha⁻¹ depending on host plant species and bacterial strains (Stamford et al., 1997; Unkovich and Pate, 2000). Inoculation is very important because local and resident soil rhizobia population are absent or very low in some particular soil conditions like acidic soils generally contain no or low population densities of the alfalfa rhizobial symbiont *Sinorhizobium meliloti*, whereas basic soils contain a low inoculum potential of *Bradyrhizobium* sp., a rhizobial symbiont of *Lupinus* spp. (Catroux et al., 2001). Rhizobia inoculant is very effective and cost-effective in terms of proper use, as if the rhizobia are present in high quantities in the soil then the application of inoculation becomes unnecessary and loss of investment. Catroux et al. (2001) suggested that when rhizobial population density is lower than 100 rhizobia per gram of soil, inoculation is likely to be beneficial for crop productivity.

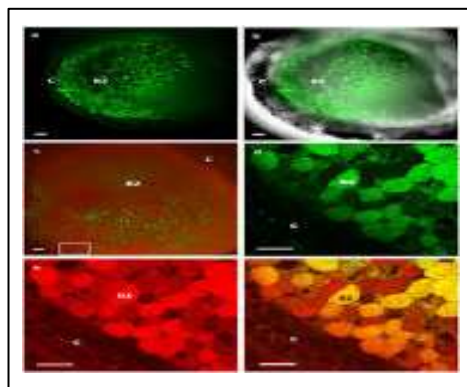


Figure 1.3: Symbiotic Nitrogen Fixing Bacteria

Table 1.1: A list of Common legumes and the Rhizobium strains by which they are inoculated

Rhizobium spp.	Legumes inoculated
1. Rhizobium meliloti	a) Melilotus (Sweet clover) b) Medicago (Alfalfa) c) Trigonella (Fenugreek)
2. R. trifoli	Trifolium (Clover)
3. R. leguminosarum	a) Pisum (Pea) b) Vicia (Vetch) c) Lathyrus (Sweet peas) d) Lens (Lentil)
4. R. phaseoli	Phaseolus (Beans)
5. R. lupini	a) Lupinus (Lupine)
6.R. japonicum	a) Glycine (Soybean) b) Vigna (Cowpea) c) Arachis (Groundnut) d) Crotalaria

B. Free living Nitrogen Fixing Bacteria:

Many free-living bacteria also fix atmospheric nitrogen such as free-living bacteria such as Azotobacter, Beijerinckia, and Clostridium. The estimation of the N₂ fixation by free-living bacteria is quite difficult. In an alfalfa (*Medicago sativa*) stand, the contribution of free-living N₂-fixing bacteria was estimated to range from 3 to 10 kg N/ha⁻¹ (Roper et al., 1995).

In a greenhouse experiment using different types of bacterial inoculation methods (leaf spray, seed soaking, side dressing), Beijerinckia mobilis and Clostridium spp. stimulated growth in cucumber and barley plants (Polyanskaya et al., 2002). But the inoculation of these free-living bacteria helps in the plant growth especially in non-legumes fixing atmospheric nitrogen without forming nodules. Azotobacter act in temperate zone with the pH range 6.5-8.0 whereas in tropical zone Beijerinckia act with wide pH range 5.0-9.0. Clostridium are tolerant in anaerobic conditions with pH range 5.0-9.0.

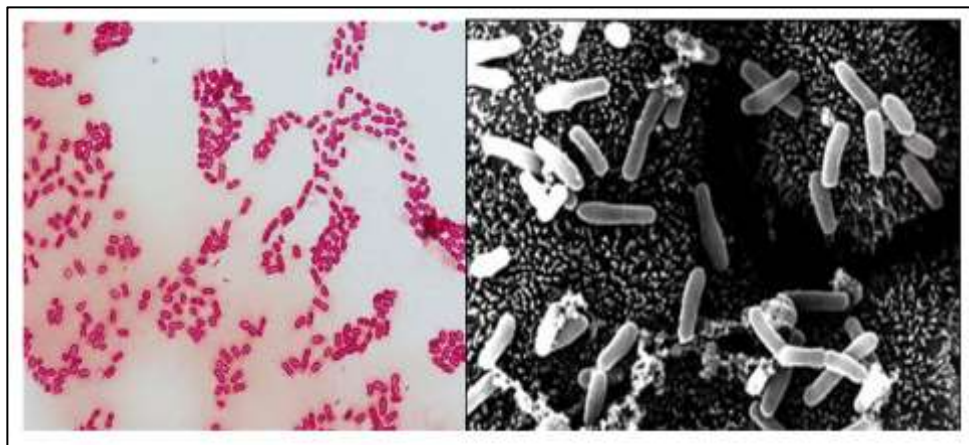


Figure 1.4: Free Living Nitrogen Fixing Bacteria

C. Nitrogen fixing associated Bacteria:

Besides symbiotic and free-living nitrogen fixation, some bacteria are capable of nitrogen fixing with association living within the roots of several crop plants like sorghum, pearl millet, rice, maize, wheat and sugarcane. Examples of such bacteria include *Acetobacter diazotrophicus* and *Herbaspirillum spp.* associated with sugarcane, sorghum, and maize (James et al., 1997; Boddey et al., 2000), *Azoarcus spp.* associated with kallar grass (*Leptochloa fusca*) (Malik et al., 1997), and *Alcaligenes*, *Azospirillum*, *Bacillus*, *Enterobacter*, *Herbaspirillum*, *Klebsiella*, *Pseudomonas*, and *Rhizobium* associated with rice and maize (James, 2000). They possess not only as a great root colonizer but also can increase the growth of plants. These include sunflower, carrot, oak, sugarbeet, tomato, eggplant, pepper, and cotton in addition to wheat and rice (Bashan and Holguin, 1997). The yield increases can be substantial, up to 30 percent, but generally range from 5 to 30 percent.

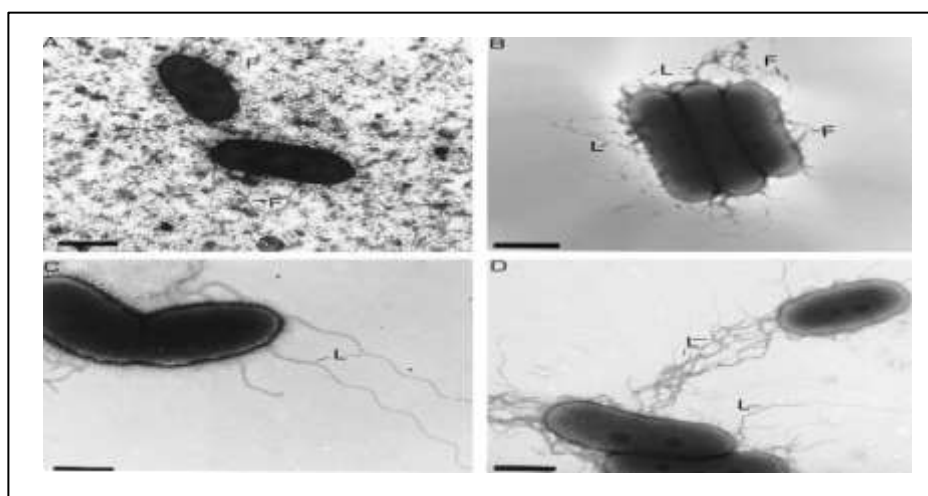


Figure 1.5: Nitrogen Fixing Associated Bacteria

D. Blue Green Algae or Cyanobacteria:

Soil algae are microscopic, chlorophyll containing organisms which can fix atmospheric nitrogen by obtaining energy from sunlight. Blue green algae are also known as Cyanobacteria. The first agronomic potential of blue green algae in rice was recognized by P. K. Dey (1939). The rice field ecosystem provides a favorable environment for development of blue green algae with respect to their requirements like light, water, temperature, air, nutrient requirements etc. They contribute about 20-30 kg N/ha and they can also add organic matter, excrete several growth promoting substances and also amend the physical and chemical properties of the soil. Nostoc, Anabaena, Calothrix, Tolypothrix, Aulosira etc. are considered as dominant nitrogen fixers and can be used as soil based mixed algal cultures for growth of rice plants.

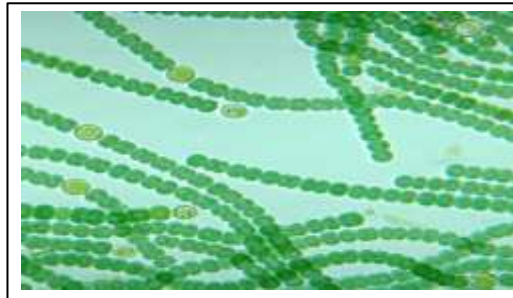


Figure 1.6: Blue Green Algae or Cyanobacteria

E. Azolla:

Azolla are the free-floating water which fix the atmospheric nitrogen in symbiotic association with blue green algae in rice fields. They fix nitrogen by using energy through sunlight through photosynthesis contributing about 40-60 kg N/ha/year. There are several species of Azolla present in the environment, among them Azolla pinnata is most widely distributed in India. Azolla can be used both as green manure before transplanting and as a dual crop after transplanting of rice.



Figure 1.7: Azolla

1.3.2 Phosphorus Solubilizing Bio-Fertilizers:

The total phosphorus determines the amount of phosphorus availability to the plants. The solubility of phosphate compounds is of great concern. Most of the soils are deficient to soluble forms of phosphorus thus causing deficiency syndromes. It is the second most limiting nutrient after N₂ that consists of 0.2% of the total plant dry weight (Schachtman et al., 1998). Bone meal, fish meal and other plant residue consists of organic phosphate compounds.

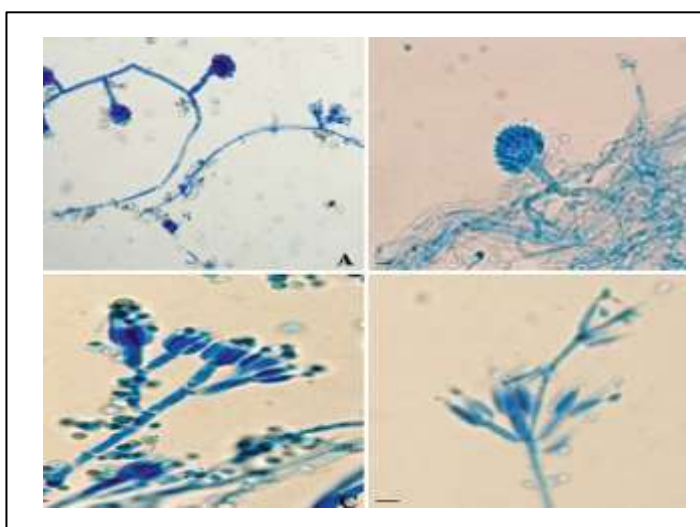


Figure 1.8: Phosphorus solubilizing bio-fertilizers

Microorganisms such as bacteria and fungi play a vital role converting them into plant available form. They are able to solubilize and mineralize the inorganic and organic forms respectively. *Pseudomonas*, *Bacillus*, *Penicillium*, *Aspergillus* etc. are some of the important fungi and bacterial species that act as PSM which consists of 0.5 - 1% of the total soil microbial population mainly from the bacterial species.

1.3.3 Phosphorus Mobilizing Bio-Fertilizers: Mycorrhiza

The symbiosis between the plant and the root colonizing mycorrhizal fungi may be a facultative or an obligatory relationship. Fungus is mostly dependent on the host for the carbon, photosynthates and energy. In return they provide several benefits to the host plant. The extended surface area of the hyphal structure of the mycorrhiza is capable of extracting nutrients from a larger volume of soil matrix. Thus, this type of symbiosis increases the crop yield demonstrated by many scientists.

They are also heavy metal accumulators and moisture absorbers and help them avoid toxicity and drought. Mycorrhizal growth on plant roots also increases the soil aggregation and provides better soil health. The mycorrhizal growth formed due to fungal association may be classified into two major categories, as follows

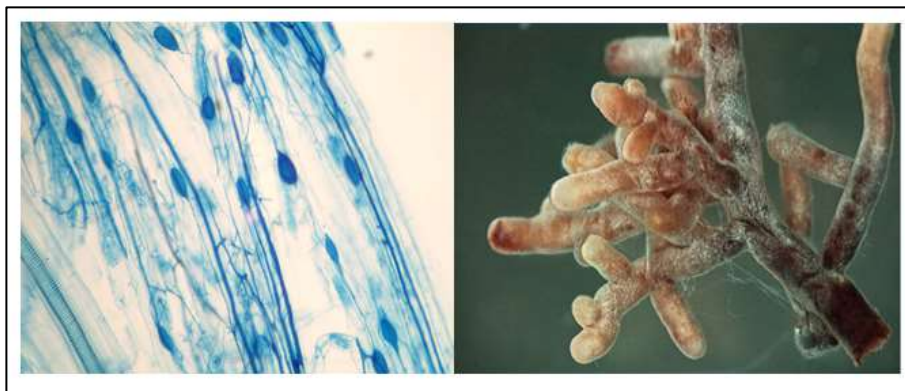


Figure 1.9: Phosphorus mobilizing bio-fertilizers: Mycorrhiza

A. Vesicular Arbuscular Mycorrhizal Fungi:

This type of inoculation can be made through the application of spores, fragments or roots along with some carrier substances like pumice or clay, sand, vermiculite. The hyphal system creates vascular (vesicles and arbuscules) structure inside the host body, this is also known as “endomycorrhiza”.

This obligate symbiont plays a key role in efficient use of Phosphate fertilizers and enhancing nitrogen fixation. They also enhance the uptake of K, S, Cu and Zn. The arbuscules help in nutrient transfer and vesicles store phospholipids. Application of excess P-fertilizers ceases their further growth and mostly proliferates in agroforestry. Sorghum, barley, wheat, upland rice, tobacco, citrus, cotton, guava, apple showed beneficial effects of VAM inoculation.

B. Ectomycorrhizal Fungi:

Ectomycorrhizal symbiosis of the fungi are the externally infected fungi species that connect with the hosts through infectious peg. The fungi suck root sap through the infectious peg and also provides nutritional elements to the host plant. Frank (1885) hypothesized the presence of ectomycorrhizal fungi and their benefits. *Pisolithus tinctorius* is one of the widespread ectomycorrhizal species in the plantation orchards. Inoculum for the ectomycorrhizal fungi can be developed through vegetative mycelium in a peat of vermiculite carrier. Alternative techniques as application of liquid and spore based mycelial inoculum were lately introduced. But their proliferation time may vary due to delayed establishment and fragmentation.

1.3.4 Potassium (K)-Solubilizing Bio-Fertilizers:

The third critical ingredient for plant growth is potassium (K). Some rhizobacteria have the capacity to dissolve potassium salts that are intractable. *Paenibacillus glucanolyticus* has been discovered to enhance the dry weight of black pepper, and *Bacillus edaphicus* has been reported to boost potassium uptake in wheat.

Higher biomass yields were produced by Sudan grass that had been inoculated with the potassium-solubilizing bacterium *Bacillus mucilaginosus*. Additionally, co-inoculation of the phosphate-solubilizing *Bacillus megaterium* and *Bacillus mucilaginosus* improved the development of eggplant, pepper, and cucumber.

1.3.5 Plant-Growth-Promoting Rhizobacteria (PGPR):

The term "plant-growth-promoting rhizobacteria" (PGPR) refers to a category of rhizosphere bacteria (rhizobacteria) that promotes the growth of plants. Bacteria that, in some frequently unidentified way, can promote plant development are denoted by the abbreviation PGPR. They come from a number of different genera, including *Agrobacterium*, *Achromobacter*, *Alcaligenes*, *Arthrobacter*, *Actinoplanes*, *Azotobacter*, *Bacillus*, *Pseudomonas* sp., *Rhizobium*, *Bradyrhizobium*, *Erwinia*, *Enterobacter*, *Amorphosporangium*, *Cellulomonas*, *Flavobacterium*, *Streptomyces*, and *Xanthomona*. These bacteria range in how they stimulate plant development, but they often do so by increasing nutrient intake, producing plant growth hormones, or solubilizing phosphate.

They can also produce a variety of antimicrobial chemicals that have diverse modes of action. Bertrand et al. (2000) demonstrated that an *Achromobacter* rhizobacterium could increase the quantity and length of roots hairs in oilseed rape (*Brassica napus*). By being specifically recognised by membrane proteins, the released iron-chelating chemicals recognise ferric ions (Fe^{3+}) and bind them before being taken up by microbial cells (Srivastava and Shalini, 2008). Two distinct siderophores, pseudobactin and pyoverdine, are produced by *Pseudomonas* species. Because the siderophores produced by some fungal diseases have a lower affinity for iron than those produced by biocontrol bacteria, the former microbes can scavenge the majority of the iron that is available and stop the growth of fungal pathogens. Many environmental and genetic factors affect the antifungal activity of PGPRs.

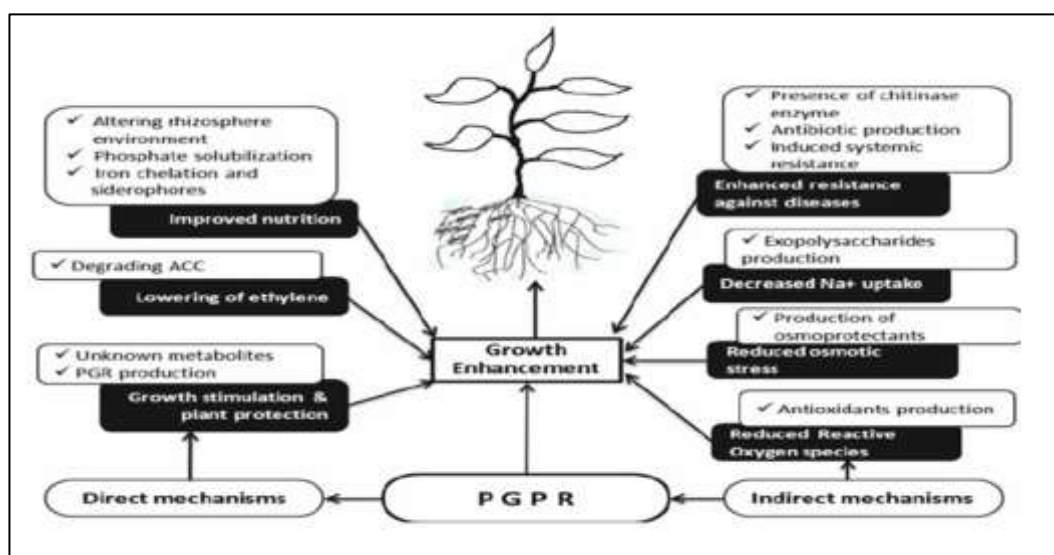


Figure 1.10: Plant-growth-promoting rhizobacteria (PGPR)

1.3.6 Organic Matter Decomposer:

Composting is a fruitful technology to use a wide variety of organic wastes including rural and urban wastes. This process takes a long time about 4-6 months for maturity but it is very rich in plant nutrients. In order to increase the decomposition of the organic wastes, there are some microorganisms present in the composting mass.

They are mainly two types: cellulolytic and ligninolytic microorganisms. These microorganisms decompose the organic matter at a much faster rate and make the compost ready within 2-3 months for application. The efficient microorganisms for rapid decomposition used as bio-fertilizers are *Trichoderma viride*, *Trichurus spiralis*, *Aspergillus niger*, *Phaenerocheate cryosporium*, *Paecilomyces fusisporus* etc.

Table 1.2: Bio-fertilizers and their mode of action, host crops, methods of application and rate of inoculants used

Name of the organisms	Mode of action	Host crops which used	Method of application	Rate of application	Remarks
Rhizobium strain	Symbiotic nitrogen fixation	Legumes (pulses, soybean, groundnut)	Seed treatment	200 g/ 10 kg seed	Leaves residual nitrogen in soil for next crop
Azotobacter	Non-symbiotic nitrogen fixation	Cereals, millets, cotton, vegetables	Seed treatment	200 g/10 kg seed	Also control certain diseases
Azospirillum	Associated nitrogen fixation	Non-legumes (maize, barley, oats, sorghum, millets, sugarcane etc.)	Seed treatment	200 g/ 10 kg seed	Produces growth promoting substances
Phosphate solubilizes	Phosphate solubilization	Soil application for all crops	Seed treatment	200 g/ 10 kg seed	Can be mixed with rock phosphate
Blue green algae (BGA)	Non-symbiotic nitrogen fixation	Rice	Soil application	10 kg/ha	Reduces soil alkalinity; has growth promoting effects

Name of the organisms	Mode of action	Host crops which used	Method of application	Rate of application	Remarks
Azolla	Symbiotic nitrogen fixation	Rice	Soil application	1 t/ha (dried material)	Increases organic carbon, soil physico-chemical properties
Mycorrhiza (VAM/AM)	Symbiotic association	Many trees and crops, wheat, sorghum	Soil application	Varied	Usually, seedlings are inoculated

1.4 Bio-fertilizer: Application for Sustainable Economic Development:

Bio-fertilizer technology must satisfy the fundamental conditions for its primary dimensions in order to be an unchangeable component of sustainable agriculture. Technology for bio-fertilizers must be:

- **Economically feasible and viable:** ability can be applied by all farmers, regardless of their financial situation and position, in terms of the return on investment;
- **Environmentally friendly:** improving the environment or, at the very least, not deteriorating the agro-ecological conditions already in place;
- **Stable:** In the long run, the benefits of the technology must continue to hold true;
- **Efficient:** a method of using inputs to produce useful and environmentally friendly outputs;
- **Adaptable:** able to adjust to current regional conditions;
- **Social acceptance and sustainability:** meeting individual demands while being acceptable to various societal sectors;
- **Renewable:** use and re-use without major additional inputs
- **Productive:** Productiveness is a characteristic of sustainable agriculture and refers to the rate and volume of output per unit of land or input, as well as yield per unit of area (or labor input, or investment).

However, the adoption of programs for increasing awareness among bio-fertilizer producers and consumers is essential for the successful marketing of bio-fertilizer technology in sustainable agriculture. It appears that bio-fertilizers are a low-cost, sustainable source of agricultural input that is both farmer- and ecologically friendly.

A. Advantages of Bio-Fertilizers:

- They are eco- friendly as well as cost effective
- Their use leads to soil enrichment and the quality of the soil improves with time.
- These fertilizers harness atmospheric nitrogen and make it directly available to the plants.

- Bio-fertilizers improve root proliferation due to the release of growth promoting hormones.
- Microorganism converts complex nutrients into simple nutrients for the availability of the plants.
- Bio-fertilizers contain microorganisms which promote the adequate supply of nutrients to the host plants and ensure their proper development of growth and regulation in their physiology.
- They help in increasing the crop yield by 10-25%.
- Bio-fertilizers can also protect plants from soil borne diseases to a certain degree.

B. Disadvantages of Bio-Fertilizers:

- Biofertilizers require special care for long-term storage because they are alive. They must be used before their expiration date.
- If other microorganisms contaminate the carrier medium or if growers use the wrong strain, they are not as effective.
- The soil must contain adequate nutrients for bio-fertilizer organisms to thrive and work.
- Biofertilizers lose their effectiveness if the soil is too hot or dry.
- Excessively acidic or alkaline soils also hamper successful growth of the beneficial microorganisms; moreover, they are less effective if the soil contains an excess of their natural microbiological enemies.
- Shortages of particular strains of microorganisms or of the best growing medium reduce the availability of some biofertilizers.

1.5 Conclusions:

Productivity is dropping at a never-before-seen rate, and environmental stresses are turning into a significant issue. Because of our reliance on chemical fertilizers and pesticides, companies that produce dangerous chemicals that are not only harmful for human consumption but also have the potential to upset the ecological balance are flourishing. The issue of feeding a growing world population can be resolved with the aid of biofertilizers at a time when agriculture is dealing with a number of environmental pressures. Biofertilizers make plant nutrients more accessible and can support long-term soil fertility management.

As was previously mentioned, several microbes play advantageous roles in the biological fixation of nitrogen to provide nitrogen to crops. In the upcoming years, biofertilizers will play a greater role due to the shifting landscape of agricultural methods and the environmental risks connected with chemical fertilizers. Therefore, biofertilizers are affordable, renewable, and environmentally beneficial, but they cannot completely replace chemical fertilizers.

1.6 References:

1. Barragán-Ocaña, A. and del Carmen del-Valle-Rivera, M., 2016. Rural development and environmental protection through the use of biofertilizers in agriculture: An alternative for underdeveloped countries? *Technology in Society*, 46, pp.90-99.

2. Bashan, Y. and Holguin, G. (1997). Azospirillum-plant relationships: Environmental and physiological advances (1990-1996). *Canadian Journal of Microbiology* 43: 103-121.
3. Bertrand, H., Plassard, C., Pinochet, X., Touraine, B., Normand, P. and J.C. Cleyet-Marel, (2000). Stimulation of the ionic transport system in *Brassica napus* by a plant growth promoting rhizobacterium (*Achromobacter* sp.). *Can J Microbiol.* 46: 229–236
4. Boddey, R.M., Da Silva, L.G., Reis, V., Alves, B.J.R., and Urquiaga, S. (2000). Assessment of bacterial nitrogen fixation in grass species. In E.W. Triplett (ed.), *Prokaryotic nitrogen fixation: A model system for analysis of a biological process* (pp. 705-726). Wymondham, UK: Horizon Scientific Press.
5. Calabi-Floody, M., Medina, J., Rumpel, C., Condron, L.M., Hernandez, M., Dumont, M. and de La Luz Mora, M., 2018. Smart fertilizers as a strategy for sustainable agriculture. *Advances in agronomy*, 147, pp.119-157.
6. Campos, E.V., Proença, P.L., Oliveira, J.L., Bakshi, M., Abhilash, P.C. and Fraceto, L.F., 2019. Use of botanical insecticides for sustainable agriculture: Future perspectives. *Ecological Indicators*, 105, pp.483-495.
7. Catroux, G., Hartmann, A., and Revellin, C. (2001). Trends in rhizobial inoculant production and use. *Plant and Soil* 230: 21-30.
8. Frank, A.B. (1885). Über die auf Wurzelsymbiose beruhende Ernährung gewisser Bäume durch unterirdische Pilze. *Berichte der Deutschen Botanischen Gesellschaft* 3: 128-145.
9. James, E.K. (2000). Nitrogen fixation in endophytic and associative symbiosis. *Field Crops Research* 65: 197-209.
10. James, E.K., Olivares, F.L., Baldani, J.I., and Döbereiner, J. (1997). *Herbaspirillum*, an endophytic diazotroph colonizing vascular tissue in leaves of *Sorghum bicolor* L. Moench. *Journal of Experimental Botany* 48: 785-797.
11. Jehangir IA, Mir MA, Bhat MA, Ahangar MA (2017) Biofertilizers an approach to sustainability in agriculture: a review. *Int J Pure Appl Biosci* 5:327–334
12. Malik, K.A., Bilal, R., Mehnaz, S., Rasul, G., Mirza, M.S., and Ali, S. (1997). Association of nitrogen-fixing, plant growth-promoting rhizobacteria (PGPR) with kallar grass and rice. *Plant and Soil* 194: 37-44.
13. Mishra, P. and Dash, D., 2014. Rejuvenation of biofertilizer for sustainable agriculture and economic development. *Consilience*, (11), pp.41-61.
14. Pandey, G., 2018. Challenges and future prospects of agri-nanotechnology for sustainable agriculture in India. *Environmental Technology & Innovation*, 11, pp.299-307.
15. Polyanskaya, L.M., Vedina, O.T., Lysak, L.V., and Zvyagintsev, D.G. (2002). The growth-promoting effects of *Beijerinckia mobilis* and *Clostridium* sp. cultures on some agricultural crops. *Microbiology* 71: 109-115.
16. Roper, M.M., Gault, R.R., and Smith, N.A. (1995). Contribution to the N status of soil by free-living N₂-fixing bacteria in a Lucerne stand. *Soil Biology and Biochemistry* 27: 467-471.
17. Shalini, S.R. and Srivastav, R., 2008. Antifungal activity screening and HPLC analysis of crude extract from *Tectona grandis*, *Shilajit*, *Valeriana wallachi*. *The International Journal of Alternative Medicine*, 5(2), pp.1540-2584.
18. Stamford, N.P., Ortega, A.D., Temprano, F., and Santos, D.R. (1997). Effects of phosphorus fertilization and inoculation of *Bradyrhizobium* and mycorrhizal fungi on

- growth of *Mimosa caesalpiniaefolia* in an acid soil. *Soil Biology and Biochemistry* 29: 959-964.
19. Unkovich, M.J. and Pate, J.S. (2000). An appraisal of recent field measurements of symbiotic N₂ fixation by annual legumes. *Field Crops Research* 65: 211-228.
 20. Vance, C.P. (1998). Legume symbiotic nitrogen fixation: agronomic aspects, In H.P. Spaink, A. Kondorosi, and P.J.J. Hooykaas (eds.), *The Rhizobiaceae* (pp. 509- 530). Dordrecht, the Netherlands: Kluwer Academic Publishers.

2. Multicomponent Reactions: Minimizing the Impact of Chemical Synthesis

Pragati Sharma, Pragya Sinha

Department of Chemistry,
The IIS University,
Jaipur, India.

Abstract:

The creation of effective chemical syntheses of complex, high added value chemicals has been made possible by the strong foundation that sustainable or green chemistry has developed. On the other hand, multicomponent reactions are a relatively new addition to the synthetic chemist's toolkit.

Nevertheless, there is still a lack of understanding regarding the usefulness of these kinds of reactions in meeting many of the standards established by the green chemistry philosophy to direct organic chemists and process chemists in the design, synthesis, and further advancement of truly sustainable manufacturing processes of pharmaceuticals, food additives, catalysts, or advanced materials.

We emphasise the value of multicomponent reactions as green synthesis techniques in this perspective.

Keywords:

Sustainability, Multicomponent reactions, Antineoplastic drugs.

2.1 Introduction:

Efficiency is typically thought of by synthetic chemists in terms of yield, selectivity, and number of steps.

The development of effective chemical syntheses of complex, high-valued compounds has been made possible by the establishment of sustainable or green chemistry, which has solid footing and offers crucial design requirements.

However, the green chemistry viewpoint is much broader and considers requirements for waste generation, reagent and solvent consumption, use of potentially harmful compounds, energy intensity, and general safety.

All of these standards are included in the 12 principles that Anastas and Warner developed in 1998 (**Figure 2.1**)¹.

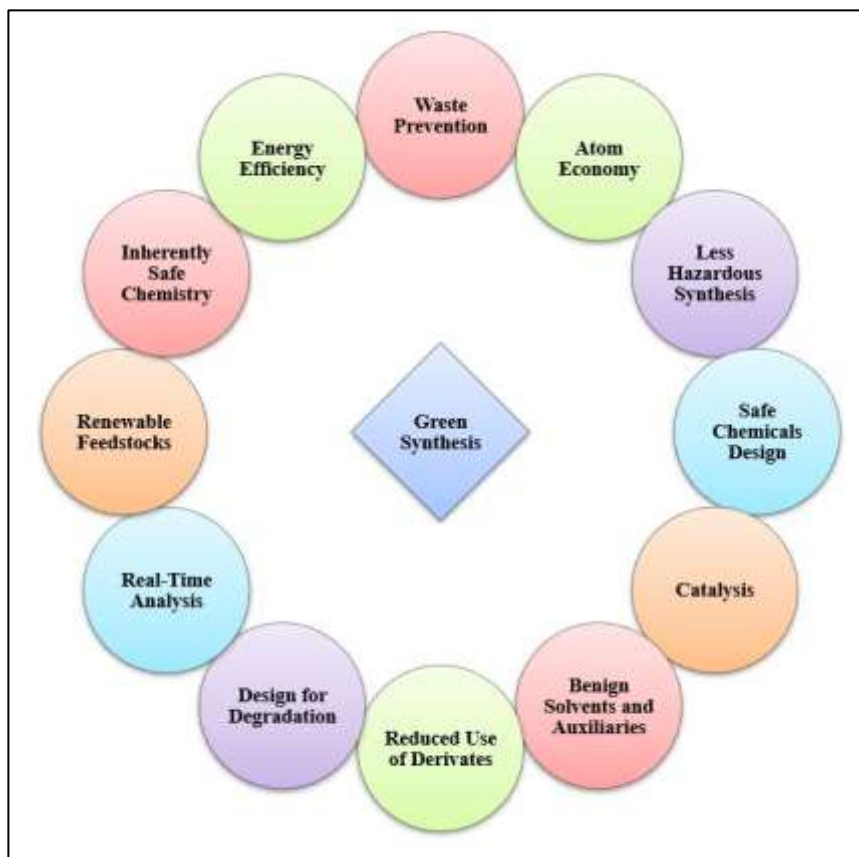


Figure 2.1: Principles of Green Chemistry

The goal of green chemistry is to change how chemists think about synthesis; as a result, its actions don't always center on the creation of novel techniques but rather on sustainable alternatives to already-developed ones and, most importantly, on various synthetic strategies that incorporate environmental considerations as early as possible in the process design stage.

Multicomponent Reactions (MCRs) are useful in this situation. Multicomponent reactions combine at least three reactants in one vessel to produce a final product that contains the majority (ideally all) of the atoms of the initial components. Their general compatibility with green solvents, efficiency, moderate circumstances, high convergence, and concurrent step economy merits a prominent position in the toolkit of sustainable synthesis methodologies^{2,3}.

Only recently has the importance of multicomponent reactions been acknowledged as a significant expansion of the synthetic chemist's toolkit for fulfilling many of the criteria established by the green chemistry philosophy to direct organic chemists and process chemists in the design, synthesis, and further development of truly sustainable manufacturing processes of pharmaceuticals, food additives, catalysts, or advanced materials⁴. As will be emphasised in the following section, a characteristic of many MCRs

is that they do not produce large molecular weight by-products. Additionally, isolation is frequently straightforward and doesn't utilise excessive volumes or amounts of chromatographic materials or solvents, which would also have a positive impact on the sustainability of the process from the perspective of waste prevention: both the quantity and harmful nature of waste generated by MCRs⁵.

Reaction telescoping, or the one-pot blending of various distinct chemical transformations, has high practical value because the fine chemicals industry has long sought to reduce the number of stages of a process, envisaging time, solvent (including solvent for cleaning the reactors), and energy savings⁶.

Although the chemical advantages of MCRs (convergence/divergence, diversity-oriented synthesis, library generation) are widely known and discussed, the sustainability element of this chemistry is only sporadically acknowledged and discussed in the literature⁷. With this viewpoint, we hope to highlight the advantages of using MCRs giving environmentally friendly synthesis and process design for significant pharmaceuticals in recent years.

Uncontrolled cell proliferation is a process that leads to the growth of a tumour that grows abnormally (sometimes for years) and causes the development of cancer. Cancer starts as a local illness that has the potential to spread to other organs or crucial systems, compromising their functionality.

Cancer is viewed as a multifactorial disease because a multitude of influencing factors, including genetic alterations, pollution, food toxins, viruses, chemicals, and ionising radiation, interact with one another⁸.

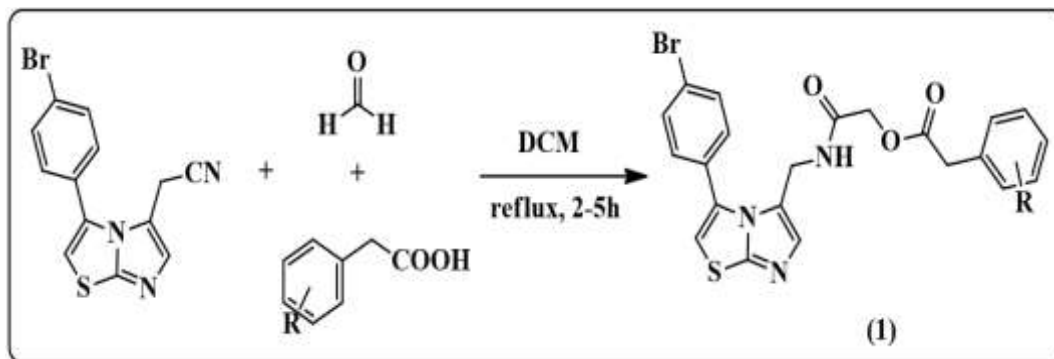
Every year, eight to ten million individuals worldwide pass away from cancer^{9,10} making it one of the leading causes of mortality. By the year 2025, predictions show that there would be an additional 20 million cancer diagnoses worldwide¹¹.

2.2 Anticancer Compounds Obtained from MCRs Approaches:

In this chapter, representative and recent (from 2018) examples of the exploitation of MCRs for the discovery and optimization of antineoplastic drugs are selected. The selected case studies are classified according to the MCR employed in the publication.

In 2021, Griglio et al.¹² used the Passerini multicomponent reaction (**Scheme 2.1**) and the Ugi multicomponent reaction (illustrated in the following paragraph) to create a series of imidazothiazole derivatives based on the previously synthesised compound (1) (IC₅₀ = 77 nM) and investigated their inhibitory activities against human Indoleamine 2,3-dioxygenase 1 (rhIDO1).

An in vitro cell-based assay was used to test the compounds' ability to inhibit the rhIDO1 enzyme activity in order to assess both their inhibitory effect and their ability to penetrate cell membranes. The human melanoma A375 cell line was chosen for the cellular experiment because, under typical growth conditions, it does not express either the rhIDO1 gene or protein.

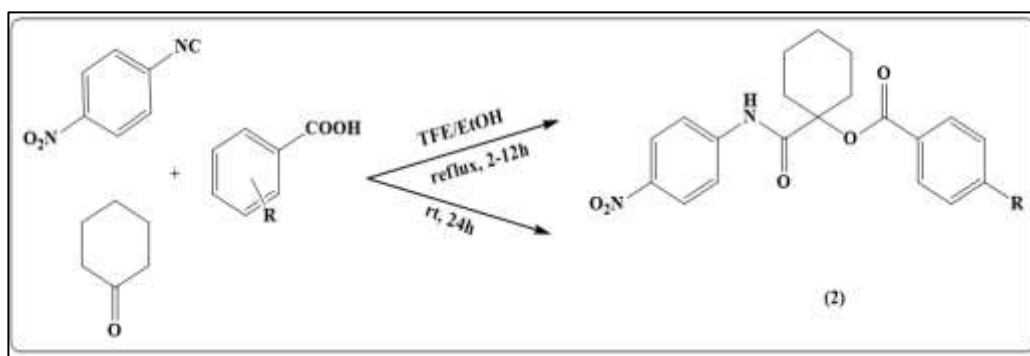


Scheme 2.1: Three-Component Passerini Synthesis of α -acyloxyamides

In comparison to the comparable α -acylaminoamides, acyloxyamides often shown a stronger inhibitory effect (illustrated in the following paragraph). Any position of the electron-withdrawing groups (R1), such as nitro and chlorine, resulted in a reduction of activity. When placed at position 3, the cyano group or hydroxyl groups had no impact on IDO1 inhibition, but when placed at position 4, they significantly increased activity.

The enzymatic IC₅₀ values for compounds (1), which were tested against the rhIDO1 enzyme, were 0.58 M, 0.24 M, and 0.20 M, respectively. Some of these compounds had IC₅₀ values below 1.0 M. This paper provides a fresh avenue for their research by describing the multicomponent technique as an easy tool to quickly access IDO1 inhibitors.

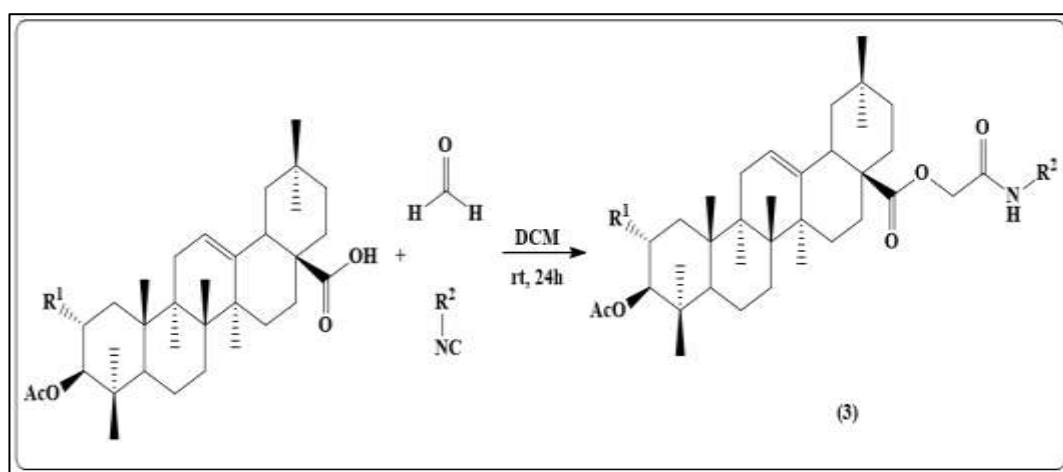
A new set of Passerini products that were synthesised and assessed as strong caspase-dependent apoptotic inducers were described by Ayoup et al. in 2019¹³. p-Nitrophenyl isocyanide, cyclohexanone, and other carboxylic acids were used to make a number of α -acyloxy carboxamides (2), and the main amide-based scaffold was effectively decorated with a variety of substituents (**Scheme 2.2**). Using the 3-(4,5-dimethylthiazol-2-yl)-2,5-diphenyl-2H-tetrazolium bromide (MTT) assay, all of the synthesised compounds were tested for cytotoxicity against normal human fibroblasts and for their potential anticancer activities against three human cancer cell lines: MCF-7 (breast), NFS-60 (myeloid leukaemia), and HepG-2 (liver).



Scheme 2.2: Three-Component Passerini Synthesis of α -acyloxyamides

Many of the tested compounds exhibit superior IC₅₀ values for various cell lines than the reference chemical. Some of them also have strong selectivity index (SI) values, and as a result, good safety values. Synthesized compounds (2) were more effective than doxorubicin against the cancer cell lines NFS-60, MCF-7, and HepG-2 (IC₅₀ = 0.0087 M, 0.0050 M, and 0.0077 M, respectively). Additionally, these compounds were the safest, exhibiting the highest selectivity profiles in comparison to the other investigated compounds and doxorubicin against the cancer cell lines MCF-7, NFS-60, and all three substances dramatically increased caspase activity to cause apoptosis in all.

New medications are frequently developed as inspiration from natural compounds¹⁴⁻¹⁷ by focusing on the combination of natural compounds and their derivatization via isocyanide-based multicomponent reactions (IMCRs). Wiemann et al.¹⁸ took a step in this direction. As a result, a set of 3-4 CR Ugi and 3CR Passerini products (**Scheme 2.3**) were successfully made from natural triterpenoids, namely oleanolic acid (OA) and maslinic acid (MA), and their cytotoxicity was then assessed biologically by using colorimetric SRB assays on the novel -acylamino carboxamides and -acyloxy carboxamides.



Scheme 2.3: Passerini products from natural triterpenoids: oleanolic acid (OA) and maslinic acid (MA)

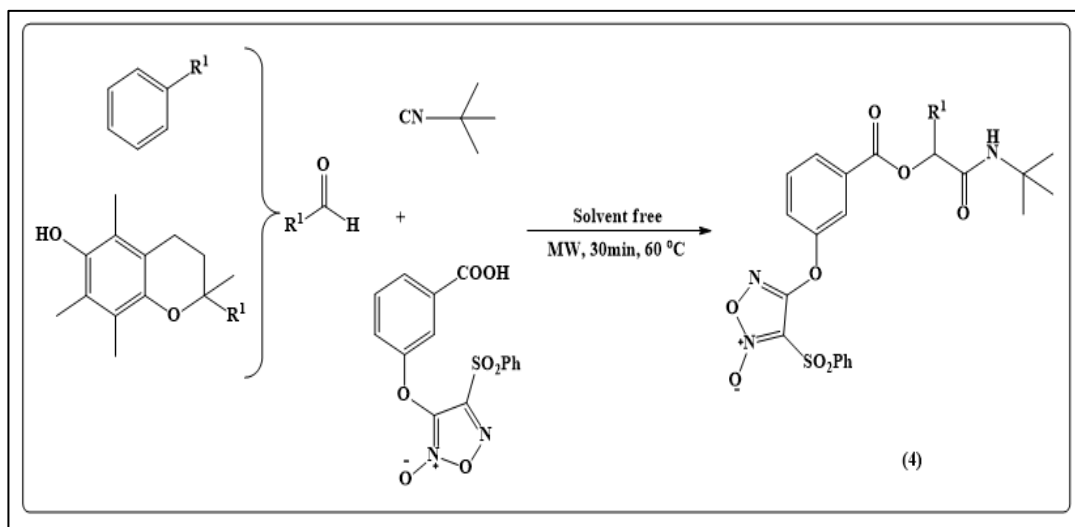
A faster reaction rate was seen in comparison to U-4CR, which was most likely brought on by the acid component of dichloromethane's (DCM) higher solubility. The biological activity of these compounds was examined in colorimetric sulforhodamine B (SRB) assays, and the EC₅₀ values were determined for six human tumour cell lines: 518A2 (melanoma), A2780 (ovarian carcinoma), HT29 (colorectal carcinoma), MCF7 (breast carcinoma), A549 (lung adenocarcinoma), 8505C (thyroid carcinoma) and non-malignant mouse fibroblasts (NIH 3T3).

The measured EC₅₀ values for the Ac-OA and Ac-MA Ugi under investigation were comparable. The EC₅₀ values for compound (3) were 8.8–20.0 M, 6.4–11.3 M, and 1.0–7.3 M, respectively. The selectivity index, however, showed a sharp drop, which reduced the medicinal value of the α-acyloxy carboxamides.

The Ugi Reaction (shown in the next paragraph) and the Passerini reaction were utilised in 2019 by Ingold et al.¹⁹ to concentrate on a library of NO-donor chemicals with optimised yields under green chemistry settings (**Scheme 2.4**).

In order to assess whether the position of the NO-donor moiety plays a fundamental role in the biological activity compared to the previous series and, thus, to explore the chemical space in search of new chemotypes with improved antitumor activity, nitroxyl or furoxanyl groups were incorporated into the carboxylic acid component.

It was found that the reaction may be carried out under solvent-free circumstances using MW irradiation, ultrasound, or green solvents such water or ethanol, either at room temperature or under microwave irradiation (MW).



Scheme 2.4: Three-Component Passerini Synthesis of NO-Donor Compounds

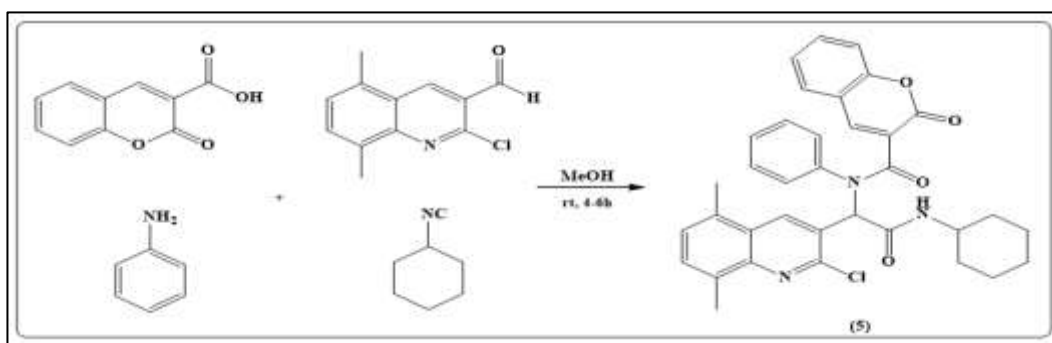
To expand the functional variety of the library for structure-activity relationship (SAR) studies, compounds have occasionally additionally been Boc-protected.

The furoxan systems found in Passerini derivatives (4), each of which serves as a NO-donor, are effective anticancer agents with GI₅₀ values that range from 0.021 to 5.8 M against all cells.

In comparison to cisplatin and etoposide, compound (4) was nearly seven times more effective against breast cancer cells HBL-100 and nearly 30 times more powerful and nearly 140 times more potent against cancer cells SW1573.

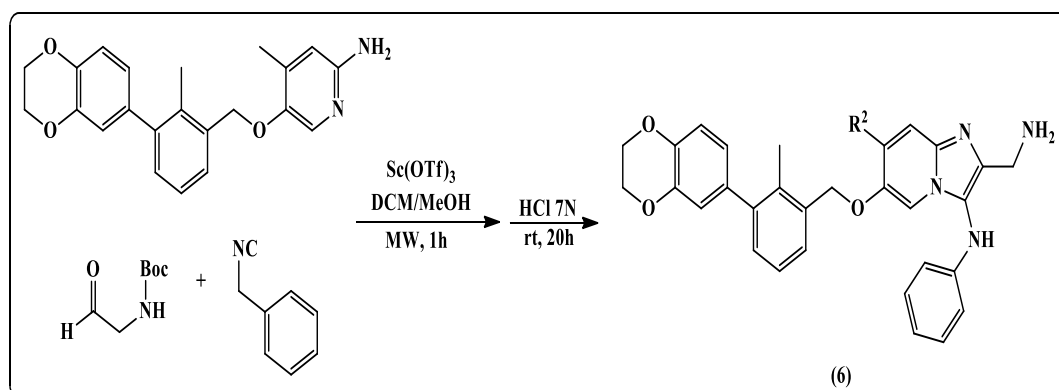
Additionally, this substance demonstrated decreased potency against human keratinocytes (HaCaT), demonstrating a preference against malignant cells. Additionally, compound (4) was able to cause HeLa cells to emit NO, and as a result, the antiproliferative effects decreased.

Taheri et al.²⁰ developed an effective four-component Ugi synthesis of quinoline-coumarin hybrids. The utilisation of coumarin-3-carboxylic acid, various 2-chloroquinoline-3-carbaldehydes, aniline derivatives, and aliphatic isocyanides in methanol at room temperature were involved by this easy access to quinoline-coumarin derivatives (Scheme 2.5).



Scheme 2.5: Formation of diamide Ugi reaction compounds

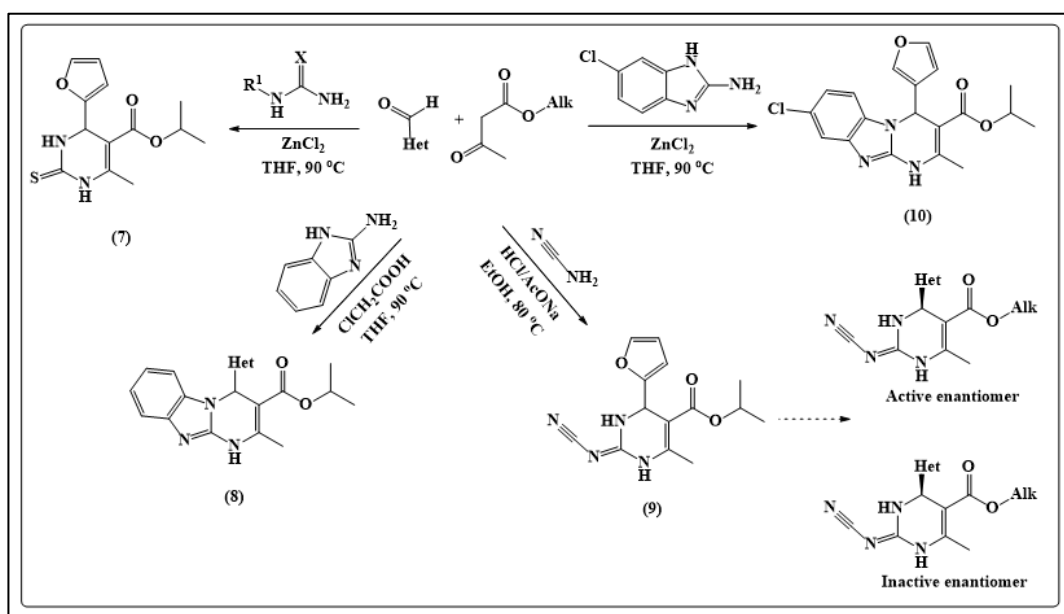
Fourteen items' cytotoxic potential was examined in A2780 human ovarian cancer cells. Cell viability, the induction of apoptosis, a mitochondrial membrane potential (MMP) assay, the measurement of intracellular ROS, a caspase 9 and 3 activity assay were among the other techniques used. With an IC₅₀ value of 25 g/mL (0.042 M), compound (5) interestingly demonstrated remarkable anticancer activity. Hybrids were applied to A2780 cells at doses ranging from 0 to 100 g/mL for 24 hours, and the vitality of the cells was assessed using a 3-(4,5-dimethylthiazol-2-yl)-2,5-diphenyl-2H-tetrazolium bromide assay. By using MCR synthesis in 2021, Butera et al.²¹ concentrated on developing innovative therapeutic modalities like peptides or small compounds. In order to determine the structure-activity connection of imidazo[1,2-a] pyridine-based inhibitors, a small library of compounds was synthesised utilising the GBB-3CR (**Scheme 2.6**). Using a variety of biophysical assays, these inhibitors were examined for their biological action, yielding powerful candidates with low-micromolar PD-L1 affinities.



Scheme 2.6: GBB-3CR products of imidazo[1,2-a] pyridine-based inhibitors

The authors discovered that the presence of scandium triflate (10 mol%) as a catalyst, 2:1 DCM/MeOH as the solvent system, a concentration of 0.3 M regarding the amidine, and 1.7 equivalent of the isocyanide and aldehyde components produced the best reaction conditions for the utilised substrates. Good to excellent yields (48–86%) of the relevant GBB products were produced after 1 hour of microwave-assisted heating. Through a variety of biological experiments, the products were evaluated for their ability to inhibit cell proliferation. Compound (6)'s IC₅₀ value was 16.8–1.8 M at a concentration of 50 M. These findings pave the way for a novel class of PD-L1 antagonists and an intriguing bioactive scaffold.

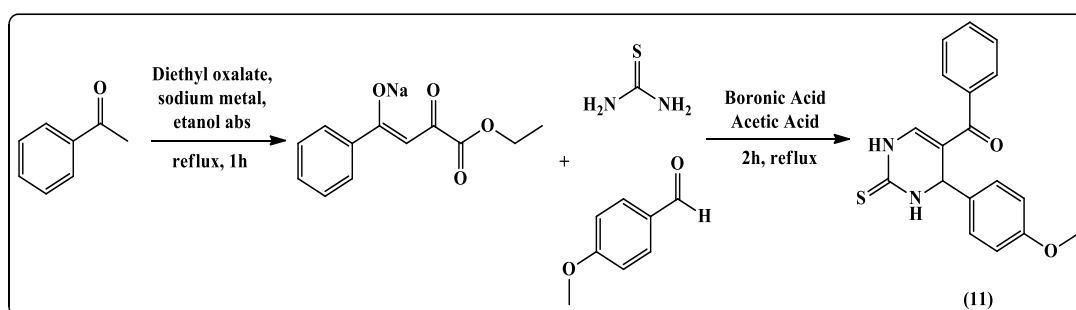
Sotelo et al.²²⁻²⁶ discovered several families of (monocyclic, bicyclic, or tricyclic) pyrimidine derivatives (**Scheme 7**) that were quickly and effectively assembled through a three-component Biginelli reaction with the goal of creating novel cancer immunotherapeutic agents via the modulation of the A2B adenosine receptor.



Scheme 2.7: Three-component Biginelli synthesis of A2B antagonists

The antagonistic activity of the synthesised compounds towards the adenosine receptors was assessed. Many substances have produced excellent selectivity profiles for receptor subtypes and good K_i values in A2B (K_i 25 nM). The monocyclic compounds (7) and (9), with K_i values of 10.2 nM and 24.3 nM respectively, as well as the tricyclic compounds (8), with K_i values of 3.49 nM and 11.40 nM, are the most promising for A2B. A2A/A2B duals that work synergistically on the immune system and tumour cells are of special interest in cancer immunotherapy during the course of the investigation. With K_i = 176.2 and 6.1 nM for A2A and A2B, respectively, (10) is the most promising candidate. The affinities of the two enantiomers were first assessed on (9) and validated in subsequent investigations, demonstrating that the affinities. In order to create novel dihydropyrimidines in 2021, an environmentally friendly Biginelli reaction method was modified²⁷. 59 human cancer cell

lines representing various cancer types, including leukaemia and melanoma, as well as lung, colon, ovarian, renal, prostate, and breast cancer, were used to test all of the synthesised compounds for their anticancer potential. A single dose of 105 M was used to demonstrate the anticancer activity as a percentage growth inhibition of various human cell lines. With a percentage of growth inhibition of 29.04-71.68% after a single dosage injection (105 M), Compound (11) (**Scheme 2.8**) demonstrated strong broad spectrum anticancer action towards the majority of the tested cancer cell lines. Particularly, the majority of leukaemia and colon cancer cell lines were extremely susceptible to the antitumor effect of compound (11), with a growth inhibiting effect exceeding 50%, as well as the colon cancer HT29 cell line (53.16%) and the leukemia cell lines, K-562 (64.97%) and SR (71.68%).



Scheme 2.8: Synthesis of compound (11) of new dihydropyrimidines

2.3 Conclusions:

The investigation of small molecule anticancer drugs built using MCRs has been highlighted in the present study, underscoring the enormous potential and broad chemical space to examine the scope of medicinal chemistry and drug discovery.

2.4 References:

1. Anastas P. T. and Warner J. C. (1998). *Green Chemistry: Theory and Practice*. Oxford University Press, New York.
2. Brauch, S., van Berkel S.S. and B. Westermann, (2013). Higher-order multicomponent reactions: beyond four reactants. *Chem. Soc. Rev.*, 42, 4948–4962.
3. Zhu J. and Bienaymé H. (2005). *Multicomponent Reactions*, Wiley-VCH, Weinheim.
4. Dunn, P. J. (2012). *Chem. Soc. Rev.* The importance of Green Chemistry in Process Research and Development, 41, 1452-1461. <https://doi.org/10.1039/C1CS15041C>
5. Jiang, B., Rajale, T., Wever, W., Tu, S. J., and Li, G. (2010). Multicomponent reactions for the synthesis of heterocycles. *Chemistry—An Asian Journal*, 5(11), 2318-2335.
6. Vaxelaire, C., Winter, P. and Christmann, P. (2011). One-Pot Reactions Accelerate the Synthesis of Active Pharmaceutical Ingredients. *Angew. Chem., Int. Ed.*, 50, 3605–3607.
7. (a) Andraos, J. (2013). On the Probability That Ring-Forming Multicomponent Reactions Are Intrinsically Green: Setting Thresholds for Intrinsic Greenness Based on Design Strategy and Experimental Reaction Performance. *ACS Sustainable Chem. Eng.*, 1, 496– 512.

8. (b) Huang, Y., Yazbak, A. and Dömling, A. (2012). *Green Techniques for Organic Synthesis and Medicinal Chemistry*. John Wiley & Sons, Ltd, Chichester, UK, 497–522; (c) Zhu, J., Wang, Q. and Wang, M.X. (2010). *Handbook of Green Chemistry*, Wiley-VCH Verlag GmbH & Co. KGaA (d) da Silva, E. N. (2007). *Res. J. Chem. Environ.*, 11, 90–91; (e) Andraos, J. (2005). *Org. Process Res. Dev.*, 9, 404–431
9. Hanahan, D.; Weinberg, R.A. (2011). *Hallmarks of Cancer: The next Generation*. *Cell*, 144, 646–674.
10. Bray, F.; Laversanne, M.; Weiderpass, E.; Soerjomataram, I. (2021). *The Ever-Increasing Importance of Cancer as a Leading Cause of Premature Death Worldwide*. *Cancer*, 127, 3029–3030
11. Sung, H., Ferlay, J., Siegel, R.L., Laversanne, M., Soerjomataram, I., Jemal, A., Bray, F. (2021). *Global Cancer Statistics 2020: GLOBOCAN Estimates of Incidence and Mortality Worldwide for 36 Cancers in 185 Countries*. *CA Cancer J. Clin.*, 71, 209–249.
12. Sikora, K.; Timbs, O. *Cancer 2025: Introduction*. *Expert Rev. Anticancer Ther.* 2004, 4, S11–S12.
13. Griglio, A.; Torre, E.; Serafini, M.; Bianchi, A.; Schmid, R.; Coda Zabetta, G.; Massarotti, A.; Sorba, G.; Pirali, T.; Fallarini, S. 2018. *A Multicomponent Approach in the Discovery of Indoleamine 2,3-Dioxygenase 1 Inhibitors: Synthesis, Biological Investigation and Docking Studies*. *Bioorg. Med. Chem. Lett.*, 28, 651–657
14. Salah Ayoup, M.; Wahby, Y.; Abdel-Hamid, H.; Ramadan, E.S.; Teleb, M.; Abu-Serie, M.M.; Noby, A. (2019). *Design, Synthesis and Biological Evaluation of Novel α -Acyloxy Carboxamides via Passerini Reaction as Caspase 3/7 Activators*. *Eur. J. Org. Chem.*, 168, 340–356
15. Najmi, A.; Javed, S.A.; Al Bratty, M.; Alhazmi, H.A. (2022). *Modern Approaches in the Discovery and Development of Plant-Based Natural Products and Their Analogues as Potential Therapeutic Agents*. *Molecules*, 27, 349. [
16. Huang, B.; Zhang, Y. *Teaching an Old Dog New Tricks: Drug Discovery by Repositioning Natural Products and Their Derivatives*. *Drug Discov. Today* 2022, 27, 1936–1944.
17. Wainwright, C.L.; Teixeira, M.M.; Adelson, D.L.; Braga, F.C.; Buenz, E.J.; Campana, P.R.V.; David, B.; Glaser, K.B.; Harata-Lee, Y.; Howes, M.-J.R.; et al. 2022. *Future Directions for the Discovery of Natural Product-Derived Immunomodulating Drugs: An IUPHAR Positional Review*. *Pharmacol. Res.*, 177, 106076.
18. Atanasov, A.G.; Zotchev, S.B.; Dirsch, V.M.; Supuran, C.T. (2021). *Natural Products in Drug Discovery: Advances and Opportunities*. *Nat. Rev. Drug. Discov.*, 20, 200–216
19. Wiemann, J.; Heller, L.; Csuk, R. (2018). *An Access to a Library of Novel Triterpene Derivatives with a Promising Pharmacological Potential by Ugi and Passerini Multicomponent Reactions*. *Eur. J. Org. Chem.*, 150, 176–194.
20. Ingold, M.; Colella, L.; Hernández, P.; Batthyány, C.; Tejedor, D.; Puerta, A.; García-Tellado, F.; Padrón, J.M.; Porcal, W.; López, G.V. 2019. *A Focused Library of NO-Donor Compounds with Potent Antiproliferative Activity Based on Green Multicomponent Reactions*. *Chem. Med. Chem.*, 14, 1669–1683.
21. Taheri, S.; Nazifi, M.; Mansourian, M.; Hosseinzadeh, L.; Shokohinia, Y. *Ugi Efficient Synthesis, Biological Evaluation and Molecular Docking of Coumarin-Quinoline Hybrids as Apoptotic Agents through Mitochondria-Related Pathways*. 2019. *Bioorg. Chem.*, 91, 103147

22. Butera, R.; Ważyńska, M.; Magiera-Mularz, K.; Plewka, J.; Musielak, B.; Surmiak, E.; Sala, D.; Kitel, R.; de Bruyn, M.; Nijman, H.W.; et al. (2021), Design, Synthesis, and Biological Evaluation of Imidazopyridines as PD-1/PD-L1 Antagonists. *ACS Med. Chem. Lett.*, 12, 768–773
23. El Maatougui, A.; Azuaje, J.; González-Gómez, M.; Miguez, G.; Crespo, A.; Carbajales, C.; Escalante, L.; García-Mera, X.; Gutiérrez-De-Terán, H.; Sotelo, E. (2016). Discovery of Potent and Highly Selective A2B Adenosine Receptor Antagonist Chemotypes. *J. Med. Chem.*, 59, 1967–1983.
24. Crespo, A.; El Maatougui, A.; Biagini, P.; Azuaje, J.; Coelho, A.; Brea, J.; Loza, M.I.; Cadavid, M.I.; García-Mera, X.; Gutiérrez-de-Terán, H.; et al. (2013). Discovery of 3,4-Dihydropyrimidin-2(1H)-Ones as a Novel Class of Potent and Selective A2B Adenosine Receptor Antagonists. *ACS Med. Chem. Lett.*, 4, 1031–1036.
25. Carbajales, C.; Azuaje, J.; Oliveira, A.; Loza, M.I.; Brea, J.; Cadavid, M.I.; Masaguer, C.F.; García-Mera, X.; Gutiérrez-de-Terán, H.; Sotelo, E. (2017). Enantiospecific Recognition at the A2B Adenosine Receptor by Alkyl 2-Cyanoimino-4-Substituted-6-Methyl-1,2,3,4-Tetrahydropyrimidine-5-Carboxylates. *J. Med. Chem.*, 60, 3372–3382.
26. Tay, A.H.M.; Prieto-Díaz, R.; Neo, S.; Tong, L.; Chen, X.; Carannante, V.; Önfelt, B.; Hartman, J.; Haglund, F.; Majellaro, M.; et al. (2022). A2B Adenosine Receptor Antagonists Rescue Lymphocyte Activity in Adenosine-Producing Patient-Derived Cancer Models. *J. Immunother. Cancer*, 10, e004592.
27. Prieto-Díaz, R.; González-Gómez, M.; Fojo-Carballo, H.; Azuaje, J.; El Maatougui, A.; Majellaro, M.; Loza, M.I.; Brea, J.; Fernández-Dueñas, V.; Paleo, M.R.; et al. (2023). Exploring the Effect of Halogenation in a Series of Potent and Selective A2B Adenosine Receptor Antagonists. *J. Med. Chem.*, 66, 890–912
28. El-Malah, A.; Mahmoud, Z.; Hamed Salem, H.; Abdou, A.M.; Soliman, M.M.H.; Hassan, R.A. (2021). Design, Ecofriendly Synthesis, Anticancer and Antimicrobial Screening of Innovative Biginelli Dihydropyrimidines Using β -Aroylpyruvates as Synthons. *Green Chem. Lett. Rev.*, 14, 221–233.

3. Drug Delivery Formulations

Dr. Mir Kaisar Ahmad

Assistant Professor,
Department of Biochemistry,
Government Medical College,
Doda, Jammu and Kashmir, India.

3.1 Introduction:

Drug delivery, a technology that is utilized to present the drug to the desired body site for drug release and absorption, or the subsequent transport of the active ingredients across the biological membranes to the site of action. A drug delivery system is a formulation or a device that enables the introduction of a therapeutic substance in the body and improves its efficacy and safety by controlling the rate, time and place of release of drugs in the body.

The increasing interest in sustained release originated the concept of the drug delivery looking for biologically precise and accurate controlled delivery systems with more biological and fewer materials-oriented characteristics. Efficient drug delivery plays a crucial role in disease treatment and remains an important challenge in medicine.

The aim of drug formulation design is to develop systems suitable for the administration of therapeutics that can be maintained at a desired concentration and duration to achieve the optimal therapeutic effect. These systems are referred to as drug delivery systems (DDSs). Recent advances in pharmaceutical formulation design have been used to develop tailored systems for the deliver therapeutics to specific cells, tissues, or organs.

For efficient DDS, polymers are believed to be the backbone of technology as they are used as drug carriers, reservoirs, matrices, coatings, or membranes.

The main role of polymers in drug delivery is to protect the incorporated therapeutics from the physiological environment, improve drug stability, and control the release rate of the drug. However, selecting the right material for drug delivery is challenging because of the diversity of the currently available polymers that can be used directly or tailored to suit the desired clinical purpose. It is important to thoroughly understand the required chemical, interfacial, mechanical, and biological properties of the formulation before selecting a suitable biomaterial for drug delivery purposes.

The developments in polymer science have introduced “smart” polymeric hydrogel systems that can regulate the delivery of therapeutics in response to a specific stimulus. Thus, before developing a pharmaceutical formulation, it is crucial to first understand what is required of the DDS, the route of administration, the target site, type of incorporated therapeutics, and the desired rate of drug delivery.

3.2 Route of Administration

A variety of drug administration/ application routes and appropriate dosage forms have been postulated time to time (Figure 3.1).

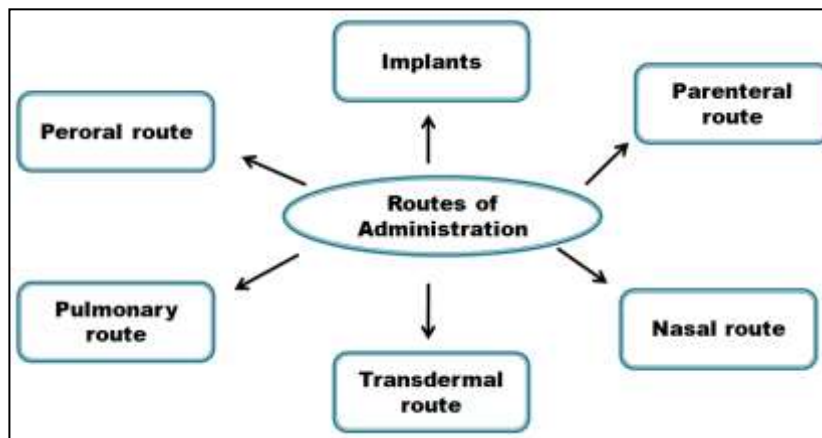


Figure 3.1: Various Routes of Administration

3.2.1. Peroral Route:

The most common route of administration of therapeutics is the peroral route, where drugs are delivered via ingestion of either liquid (solution, suspension, emulsion) or solid dosage forms (tablets or capsules) through the mouth. DDSs that are designed for oral delivery pass through the gastrointestinal system where the drugs can be degraded, which makes this route unsuitable for sensitive therapeutics like peptides and proteins and encapsulating the medication with resistant microspheres can help to protect them degradation. Coating with various pH-resistant materials such as cellulose or vinyl acetate polymers can also help protect the incorporated drugs.

For example, gelatine polymeric microspheres can be coated with various concentrations of sodium alginate and cross-linked with calcium chloride to increase their resistance to the gastrointestinal medium.

3.2.2. Parenteral Route:

The most common parenteral routes include intravenous (IV), intramuscular (IM), or subcutaneous (SC); the drug-carrying vehicle is injected into those sites to reach the systemic circulation. The IV route leads to immediate drug availability in the circulation, which is an advantage if the rapid action of the drug is required; however, this route of delivery has a short drug circulation time. Polymers used for IV delivery should be water-soluble. On the other hand, IM and SC injections usually form a drug “depot” that controls the release of the medication into the systemic circulation for a long period of time. Flupentixol is an antipsychotic medication that is formulated in oil to be administered as IM injections every 1 or 3 months. Some of the most commonly used, FDA-approved

biodegradable polymers that have been used to prolong the release of parenteral drugs are polylactic acid, poly glycolic acid, a copolymer of lactic and glycolic acid named poly lactic-co-glycolic acid. Poly lactic-co-glycolic acid is widely used due to its excellent biocompatibility, biodegradability, and mechanical strength. Various molecules have been incorporated in those biodegradable polymers including vaccines, peptides, proteins, and drug micro molecules.

3.2.3. Pulmonary Route:

Pulmonary DDSs are formulated for direct delivery of therapeutics to the lungs via inhalation and enable the direct application of drugs to the lungs, and therefore require the use of low drug doses thereby minimizing any associated side effects. Polymer and lipid-based nanoparticles have been widely used in pulmonary DDSs.

3.2.4. Nasal Route:

Nasal delivery is where the formulation is inserted through the nasal opening in the form of nasal drops or sprays for either a local or systemic action. The nasal delivery route is especially useful for delivering immunization vaccines as the nasal mucosa can filter the pathogens before entering the body. Nanocarrier DDSs can be good vehicles for delivery of vaccines as they offer protection and efficient transport of the enclosed antigens. Nanocarriers can also be designed to offer improved and effective antigen recognition by immune cell. Nasal and pulmonary routes are currently used to deliver systemic drugs to the blood as an alternative to parenteral drug delivery, especially in the case of peptide and protein therapeutics. Formulations including liposomes, microspheres, and gels have been exploited for drug delivery via nasal and pulmonary routes. Factors that must be considered when formulating a DDS for these routes include biocompatibility, the ability to be transferred into an aerosol, stability against the generated forces during aerosolization, and degradation within an acceptable period of time.

3.2.5. Transdermal Route:

Transdermal DDSs adhere to the skin surface to allow the passage of the active ingredients across the skin layers for either a local or systemic effect via transdermal sprays, creams, patches, or implantable devices. Transdermal patches usually have the drug entrapped in a reservoir with a porous membrane covering it or enclosed within an adhesive matrix that melts with body temperature and releases the embedded medication. Transdermal delivery is limited to small molecules that can penetrate the skin. The most famous transdermal patch is the nicotine patch that releases small amount of nicotine in the blood to help with smoking cessation.

3.2.6 Implants:

Implants are useful in cancer therapy as they control the delivery of drugs into the targeted tissue over a long period of time and implants can be tailored to deliver therapeutics into such specific locations. This method of delivery is advantageous as it offers greater convenience to patients compared to conventional chemotherapy approaches.

3.3. Target Cites:

3.3.1. Brain Targeting:

It can be challenging to deliver pharmaceuticals to some sites in the body, including the brain, colon, and cancer cells. Drug targeting to the brain is challenging due to the presence of the endothelial cells lining the cerebral microvasculature which forms a blood brain barrier. This barrier protects the brain from the fluctuations in plasma composition, and from the circulating neurotransmitters and xenobiotics capable of disturbing neural function. The lipid blood brain barrier is closely packed with very tight junctions that prevent the passage of molecules and ions, and this makes it hard to deliver various Alzheimer and anti-epilepsy medications to the brain. Several drugs have properties such as high lipid solubility, low molecular size, and positive charge which do not allow them to pass the blood brain barrier. A common noninvasive approach for delivering water-soluble drugs through the blood brain barrier is by formulating a lipid-soluble prodrug DDS or loading the drug into a polymeric or lipid-based nanocarriers that can pass the blood brain barrier due to their small size.

3.3.2. Colon Targeting:

The colon is an organ that requires special DDS formulation design that ensures the safe arrival of therapeutics to the colon following their passage through the GIT. The long transit time and varying pH levels that the DDS faces following its ingestion until it reaches the colon led to the degradation of the drugs before reaching their target site. Drugs targeted to reach the colon can be designed to either act locally in the colon or to get delivered to the systemic circulation. Locally acting colon therapeutics are designed for treatment of conditions such as ulcerative colitis, chronic inflammatory bowel disease (Crohn's disease), and colorectal cancer. Colonic systemic absorption is also a way of delivering peptide and protein drug molecules and other drugs that are poorly absorbed from the upper GIT to the blood.

Recent developments in pharmaceutical technology formulations designed for colon targeting include coating drugs with pH-sensitive polymers, embedding in bacterial degradable matrices and pro-drug formation. Another common way for colon targeting is enteric-coated drugs with polysaccharide polymers that dissolve in the colon and not in the upper GIT. Polysaccharide coatings such as guar gum are pH-resistant and thus prevent the degradation of the DDS in the GIT. Enteric coated films degrade by colon-specific bacteria to release the drugs at their target site. Some DDSs have recently been developed for colon drug targeting and include pressure-controlled colon delivery capsules, colon targeted drug delivery system, and osmotic-controlled drug delivery.

3.3.3 Cancer Tissues Targeting:

Most anticancer drugs have poor aqueous solubility and the potential to adversely effect on healthy tissue, thereby limiting their clinical efficacy and therapeutic safety. Solubilizers can be used to enhance the drug solubility, but this might increase the side effects of the medication. Moreover, to achieve therapeutic efficacy for cancer therapeutics, it is often

necessary to administer high doses of drugs due to their short circulation time in the blood plasma, low specificity, and poor pharmacokinetics. Several approaches are used to achieve drug targeting of polymeric carriers in order to overcome these limitations. Active drug targeting to cancerous cells can be achieved via carrier functionalized coatings or ligands. Nanoparticles can be coated with or attached to a hydrophilic polymer such as PEG which protects the drug from macrophages ingestion and prevents particle adsorption by blood serum proteins, and thus prolongs their circulation time. The incorporation of ligands over the nanoparticle surface is another common approach for active drug targeting

3.4. Drug Delivery Formulations:

An ideal formulation that is beneficial for all subsets of the population should provide sufficient bioavailability of the active pharmaceutical ingredient, be palatable or at least acceptable, contain non-toxic, safe excipients, enable a safe and easy administration, own socio-cultural acceptance and provide precise advice in the product information. The following is the list of basic criteria for drug formulations (Table 3.1). The table is extremely helpful to elaborate a rough idea on the opportunities and challenges of drug administration.

Table 3.1: Criteria for Drug Formulations

Sr. No.	Criteria/ Parameters for formulations
1.	Sufficient bioavailability
2.	Safe excipients
3.	Palatable and/or acceptable properties
4.	Acceptable dose uniformity
5.	Easy and safe administration
6.	Socio-cultural acceptability
7.	Precise and clear product information
8.	Parent/caregiver friendly

3.5. Conclusions:

Drug delivery is still a major challenge and the key issues are age-appropriate formulations, safety of excipients, suitability of drug delivery devices and therapy compliance. Some improvements have been made recently and the most promising in oral drug delivery are or dispersible mini-tablets and thin film strips. In parenteral drug delivery age-adapted devices and profound knowledge on the preparation of extemporaneous or enabling formulations are of major importance. In pulmonary drug delivery new in vitro deposition models, adapted to physiological properties of an individual, may lead to better formulations and delivery devices. The new formulations will as such stimulate the research and development in the medicines.

4. Chemistry of Metal Ferrite Nanoparticles: Synthesis and Characterization

Chinmay, Vishaka Chauhan, Anjaneyulu Bendi

Department of Chemistry,
Faculty of Science,
SGT University,
Gurugram, Haryana, India.

Abstract:

In the past three decades, metal ferrites have been extensively studied for catalysis, energy storage, microwave screening, and biomedical applications. Nanoparticles of metal ferrite catalyse decomposition (particularly photocatalytic), dehydrogenation, oxidation, alkylation, and C-C coupling reactions. Due to their chemical stability, high saturation magnetization, high permeability, insolubility in most reaction solvents, low toxicity, ease of accessibility, low cost, simple recovery, and reusability, as well as their Lewis acidic and basic properties, transition metal ferrites (MFe₂O₄) have garnered a great deal of interest among the various magnetic nanoparticles used as catalysts in the synthesis of a variety of heterocycles. Using spinel ferrite nanoparticles and their composites as a catalyst for producing heterocycles gives drug discovery a new dimension. This chapter describes the synthesis and characterization of various metal ferrites and their nanocomposites employed as heterogeneous catalysts in various organic transformations.

4.1 Introduction:

Nanotechnology is a branch of science and technology concerned with manipulating and controlling matter at the atomic and molecular levels. It is one of the fascinating modern technologies helpful in turning the theoretical applications of nanoscience into real-world applications. According to Norio Taniguchi, the main applications of nanotechnology involve manipulating materials using only one atom or molecule to process, separate, consolidate, and distort them. [1-3] The characteristics and behaviours of nanoscale and macroscale materials are distinct due to the increased surface area, quantum effects, and other phenomena that become prominent at the nanoscale. Nanotechnology can potentially revolutionize many scientific, technological, and industrial fields. In recent decades, the use of heterogeneous and environmentally-friendly catalysts in organic reactions has garnered a great deal of chemists' and chemical industries' attention. [4-6]

In chemical reactions, interest in using magnetic nanoparticles (MNPs) as heterogeneous catalysts has increased due to their super magnetic behaviour, easy separation from reaction media, large surface area, low toxicity, exceptional stability, and potential for fictionalization. Transition metal oxides have been recognized as highly efficient, non-corrosive, highly durable, and recyclable catalysts in heterogeneous chemical reactions among the available magnetic nanomaterials. [7-9]

Ferrites are incredibly strong and delicate ceramic materials and have a dark grey or black color. The word "ferrite" is used to designate a magnetic material class displaying ferrimagnetic activity. It comes from the Latin word "ferrum," which means iron. Ferric ions make up the majority of ferrites, which are oxides. Several methods, such as high-temperature solid-state reaction, sol-gel, co-precipitation, pulsed laser deposition, high-energy ball milling, and hydrothermal process, can produce ferrites in powder or thin film forms. [10-11]

Based on their crystal structures, ferrites may be divided into spinel ferrites, garnet, orthoferrites, and hexagonal ferrites. Spinel metal ferrites' intriguing magnetic quality has attracted the scientific community's interest. Spinel metal ferrites and their nanocomposites have been used in a variety of applications, including gas sensors, semiconductor photocatalysts, anode materials for lithium-ion batteries, and catalysis. Spinel ferrites are represented by the chemical formula MFe_2O_4 , where M stands for divalent metal ions (Zn^{2+} , Co^{2+} , Mn^{2+} , Ni^{2+} , etc.). Among the various metal-based nanoparticles, a few have attracted the greatest attention due to their extraordinary magnetic and optical properties, making them desirable competitors for several applications.[12] Spinel metal nanoparticles can be created using a variety of techniques, including co-precipitation, hydrothermal, microwave irradiation, solution combustion, hydrothermal, conventional heating, sono chemical, polymeric precursor, etc. Based on the above observations, we have decided to compile the data related to some spinel metal ferrite nanoparticle and their nanocomposites in this book chapter. The synthesis of metal ferrite nanoparticles with adequate physical and chemical properties has become an important area of research and development. Numerous synthesis techniques, including sol-gel, hydrothermal, combustion, co-precipitation, thermal decomposition, and micro-emulsion, are used to produce metal ferrite nanoparticles.

4.2 Chemistry of Metal Ferrite Nanoparticles and their Nanocomposites:

4.2.1 Synthesis and Characterization of $ZnFe_2O_4$ Nanoparticles:

$ZnFe_2O_4$ Nanoparticles have been used as heterogeneous catalysts in the synthesis of isatinyldenethiazol-4-ones, quinazolines, tetrahydro pyranoquinolines, benzopyrans, imidazoles, quinoxalines, pyrazoles, tetrazoles, triazoles, isoquinolines, acridines, and pyridines.[13]

Andhare D. et al. synthesized $ZnFe_2O_4$ Nanoparticles by co-precipitation method. The co-precipitation method is simple, cost-effective, and requires no organic fuel. The co-precipitation technique has many excellent advantages, including low temperature, tiny particle size, high porosity, quick preparation time, high purity, strong chemical homogeneity, crystallinity, and simplicity of the procedure.[14] Initially, a mixture of $ZnCl_2$ and $FeCl_3$ solution was prepared in distilled water with a 1:2 molar ratio. To keep the pH of the solution stable while stirring continuously, NaOH was added drop by drop. The solution was cooled after the aging process had taken place for 60 minutes. In order to get rid of the sodium hydroxide and any remaining water, the precipitate was washed with hot DI water or acetone. The precipitate is then employed in the centrifugal separator, where it is settled many times before being washed and filtered. The freshly obtained precipitate was crushed and subjected to calcination at $900^\circ C$ in a muffle furnace to get the zinc ferrite nanoparticles.

To investigate the structural and chemical characteristics of prepared samples, XRD and FTIR measurements were made. By using XRD, it was possible to determine that Zn-ferrite formed as a single phase with the Fd-3m space group, and the impact of several synthesis methods on structural characteristics was also investigated. ZnFe₂O₄ was discovered to have crystallites that were 26.11 nm in size.

The creation of the ferrite phase was confirmed by the FTIR spectra, which revealed two anticipated bands in the ranges of 550-560 cm⁻¹ and 400-410 cm⁻¹.

4.2.2 Synthesis and Characterization of NiFe₂O₄ Nanoparticles:

NiFe₂O₄ Nanoparticles have been used as heterogenous catalysts in the synthesis of acetyl ferrocene chalcones, 4H-chromene derivatives, phthalazine-triones, benzoimidazo pyrimidine derivatives, 2, 4, 5 trisubstituted imidazoles and benzoxazoles.[15]

Hariani P. et al. have recently developed a method to synthesize NiFe₂O₄ nanoparticles by Solution Combustion Method using urea as fuel.[16] Given its straightforward process, speed, and low-temperature requirement, the solution combustion approach is particularly well suited for the synthesis of these ferrite nanoparticles. High uniformity and purity offer an easy way to characterize the finished product. Moreover, this method has a high success rate. The study's fuel of choice was urea since it is affordable, secure, and non-toxic. [17-18] A solution of urea and distilled water was initially prepared and added Ni (NO₃)₂.6H₂O and Fe (NO₃)₃.9H₂O subsequently. The mixture was subjected to heating at the rate of 5°C/min, and the formed solid was washed with water and calcined for three hours.



X-ray diffraction (XRD) analysis was used to characterize the synthesized NiFe₂O₄ nanoparticles. The Scherrer equation was used to determine the average crystal size and observed 8.6 nm. The spinel structure was verified by identifying two peaks from the FTIR spectrum with wavenumbers of 580-620 and 420-435 cm⁻¹. The stretching vibration of the nickel and oxygen (Ni-O) bonds was suggested by a significant peak at 580.57 cm⁻¹, whereas the stretching vibration of the iron and oxygen (Fe-O) links was indicated by the wave number at 433.98 cm⁻¹. The stretching vibration of the OH group is shown by the broad spectrum seen between wave numbers 3200 and 3500 cm⁻¹. The measured magnetization saturation value was 47.32 emu/g. small particle size has a relationship with the usual magnetization saturation. The size of crystallites affects magnetic characteristics. Poor crystallinity is indicated by the decreased crystallite size. The saturation magnetization is growing due to the growth in crystallite size. The NiFe₂O₄ nanoparticles have a 14.70% Ni, 38.20% Fe, and 47.10% O element composition according to the EDS results. This composition demonstrates that the NiFe₂O₄ nanoparticles were successfully synthesized.

4.2.3 Synthesis and Characterization of CuFe₂O₄ Nanoparticles:

CuFe₂O₄ Nanoparticles have been used as heterogeneous catalysts in the synthesis of pyrazoles, benzodiazepines, indoles, Imidazoles, polysubstituted pyrroles, benzothiazoles, 4H-chromene-3-carbonitriles, and benzimidazoles.[19]

Amulya M. et al. developed a new method to synthesize CuFe_2O_4 nanoparticles using the sonochemical method. [20] In a sonication flask, Copper (II) Nitrate (0.1 M) and Iron (III) Nitrate (0.2 M) were mixed in a stoichiometric ratio of 1:2 and subjected to a 2-hour sonication process at 40°C .

The pH was kept between 10 and 12 by using 2M NaOH. After the precipitation reaction was finished, the solution was centrifuged, and the precipitate was filtered and collected. To get rid of extra NaOH, it was repeatedly rinsed with distilled water and ethanol. After being dried in a hot air oven at 80°C for 10 minutes, the precursor to CuFe_2O_4 was then calcined for 3 hours at 800°C , and NPs were subsequently sonicated with a less powerful ultrasound.

The synthesized CuFe_2O_4 NPs have an average crystal size of 35–40 nm, according to powder X-ray diffraction (PXRD) examination. The band-gap energy was measured using diffuse-reflectance spectroscopy (DRS), which revealed the semiconductor behavior. CuFe_2O_4 NPs have modest ferromagnetic behavior, as demonstrated by vibrating sample magnetometry (VSM) tests carried out at 300K. For the purpose of examining the electrochemical characteristics of the NPs, electrochemical impedance spectroscopy (EIS) and cyclic voltammetry (CV) have been used. In comparison to a basic media (0.1 M NaOH), an acidic medium (0.1 M HCl) elicited a stronger response from a CuFe_2O_4 NP electrode. The electrode also demonstrated high sensitivity for paracetamol, strong cycling stability, and high-rate capabilities. The CuFe_2O_4 NPs displayed pseudocapacitive properties based on EIS measurements.

4.2.4 Synthesis and Characterization of $\text{CoFe}_2\text{O}_4/\text{Cu}(\text{OH})_2$ Nanocomposite:

CoFe_2O_4 Nanoparticles have been used as heterogeneous catalysts in the synthesis of Xanthene-ones, benzimidazoles, benzoxazoles, phthalazine-triones, and benzoimidazo pyrimidines.[18] $\text{CoFe}_2\text{O}_4/\text{Cu}(\text{OH})_2$ Nanocomposite has been widely used in the synthesis of dihydropyrimidinone derivatives and triazoles.[21]

Bendi A. et al. synthesized $\text{CoFe}_2\text{O}_4/\text{Cu}(\text{OH})_2$ nanocomposite by co-precipitation method and used it as an expeditious and magnetically recoverable heterogeneous catalyst for the construction of biologically active 3,4-dihydropyrimidin-2(1H)-one C5 esters (DHPMs).[22]

Initially, 0.5M $\text{Co}(\text{NO}_3)_2 \cdot 4\text{H}_2\text{O}$ and 1.0M $\text{Fe}(\text{NO}_3)_3 \cdot 9\text{H}_2\text{O}$ were dissolved in distilled water separately and thoroughly mixed at a temperature of 70°C using a magnetic stirrer. With the use of a burette, 6.0 M NaOH solution was then added dropwise until the pH of the solution reached 12. The NaOH addition was then discontinued, and the stirring kept going. A precipitate was seen to form, which was agitated at 70°C before being filtered, washed with ethanol, then washed again with deionized water until pH 7 was attained.

The precipitate was subsequently dried at 60°C . The resultant powder was calcined at 300°C to produce CoFe_2O_4 nanoparticles. In order to create the $\text{CoFe}_2\text{O}_4/\text{Cu}(\text{OH})_2$ nanocomposite, freshly made CoFe_2O_4 nanoparticles were first mixed vigorously with $\text{CuCl}_2 \cdot 2\text{H}_2\text{O}$ in an aqueous solution before being added dropwise to the sodium hydroxide solution.

It was noted that a precipitate with a black-blue color formed and accumulated by magnetic separation. It was dried after being cleaned with deionized water. TEM, powder X-ray diffraction (XRD), VSM, and IR Spectroscopy were used to characterize the synthesized $\text{CoFe}_2\text{O}_4/\text{Cu}(\text{OH})_2$ magnetic nanocomposite. Powder X-ray Diffraction (PXRD) measurement was used to validate the purity of synthesized nanoparticles. The Debye-Scherrer Analysis was used to determine the nanocomposite's crystallite size, which was discovered to be 15.17 nm. Without any agglomeration, TEM revealed a consistent distribution of nanowires and nanospheres in the sample. According to VSM, the magnetic saturation of the $\text{CoFe}_2\text{O}_4/\text{Cu}(\text{OH})_2$ nanocomposite is lower (40 emu g^{-1}). Strong absorption bands at 563 and 676 cm^{-1} in the FT-IR spectra of the $\text{CoFe}_2\text{O}_4/\text{Cu}(\text{OH})_2$ nanocomposite indicate the stretching vibrations of the metal-oxygen (M-O) bonds, confirming the spinel ferrite structure.

4.2.5 Synthesis and Characterization of $\text{ZnFe}_2\text{O}_4/\text{Cu}$ Nanocomposite:

$\text{ZnFe}_2\text{O}_4/\text{Cu}$ Nanocomposite has been widely used in the synthesis of N-aryl nitrogen-containing heterocycles.[13]

Zhang R. et al. synthesized $\text{Cu}/\text{ZnFe}_2\text{O}_4$ for Catalytic Reduction of Nitroarenes And C-N Bond Formation Reactions.[23] By co-precipitating with ultrasonic assistance, Cu species were loaded onto zinc ferrite particles to create the $\text{Cu}/\text{ZnFe}_2\text{O}_4$ catalyst.

To synthesize the composite, $\text{Cu}(\text{NO}_2)_2$ was dissolved in 100 mL of diethanolamine, which was then rapidly agitated while being slowly heated to 150°C . As the reaction continued, the mixture's color changed to crimson red. Centrifugation was used to produce copper precipitates after cooling. Then, 100 mL of deionized water containing a solution of FeCl_3 and ZnCl_2 was sonicated for 3 hours. After that, 30 mL of NaOH (3 M) was added to the mixture. The ultrasonic water bath was then heated to 60°C for one hour, and ZnFe_2O_4 was subsequently removed using magnetic suction. A combination of the previously obtained copper precipitate and 50 mL of ethanol was added after the acquired ZnFe_2O_4 had been dissolved in 100 mL of deionized water. The resultant mixture was then heated to 80°C while being stirred. After using a magnetic bar to separate the solid precipitate, it was washed with distilled water and anhydrous ethanol. The $\text{Cu}/\text{ZnFe}_2\text{O}_4$ composite was then produced after drying at 160°C .

By using FT-IR, XRD, TGA, EDS, TEM, and SEM, the structure of the synthesized zinc ferrite and $\text{Cu}/\text{ZnFe}_2\text{O}_4$ materials was identified. The Fe-O vibration from the magnetic basement is responsible for the absorption peak at 556 cm^{-1} . The presence of copper nanoparticles was revealed by the absorption peak at 618 cm^{-1} . The $\text{Cu}/\text{ZnFe}_2\text{O}_4$ TGA curves demonstrate at 700°C , the $\text{Cu}/\text{ZnFe}_2\text{O}_4$ catalyst's mass did not considerably drop, indicating the catalyst has strong thermal stability. $\text{Cu}/\text{ZnFe}_2\text{O}_4$ XRD data show that the ZnFe_2O_4 crystal structure was preserved throughout the Cu loading procedures. EDS analysis was used to establish the elemental composition, and the findings showed the presence of O, Cu, Zn, and Fe elements as well as further supporting the structure of $\text{Cu}/\text{ZnFe}_2\text{O}_4$. The SEM and TEM demonstrate how the surface of ZnFe_2O_4 is altered by the addition of Cu nanoparticles and how needle-like Cu single crystals are loaded on the initially smooth surface.

4.2.6 Synthesis and Characterization of NiFe₂O₄/ Geopolymer Nanocomposite:

NiFe₂O₄/ Geopolymer Nanocomposite has been widely used in the synthesis of imidazole derivatives, benzoxazoles. [15]

Hajizadeh Z. et al. developed a novel and green NiFe₂O₄/geopolymer nanocatalyst based on bentonite by ultrasonic irradiations.[24] One of the most innovative and environmentally friendly methods for scientific and industrial research is sonochemistry, which is based on ultrasonic irradiations. A bentonite-based nanocomposite of NiFe₂O₄ and geopolymer was created using an ultrasonic method. NaOH powder was initially mixed with Na₂SiO₃ powder to create the geopolymer. The powder combination was then given a final addition of distilled water. The solution was allowed to stir for 10 minutes after the granules had dissolved. The mixture was then mixed while being supplemented with calcined bentonite powder (500 °C for 6 hours). The inclusion of bentonite resulted in the creation of a slurry-like fluid. NiFe₂O₄ spinel was formed, then added to the slurry solution, where it was disseminated using an ultrasonic bath. By placing the solution in the oven, the final nanocomposite was created. The crystalline phase of bentonite clay, synthetic geopolymer, and NiFe₂O₄/geopolymer nanocomposite are all identified using the X-ray diffraction pattern. The average diameter of the geopolymer's pores, which range from 130 to 140 nm, was thoroughly characterized. The TEM images of the NiFe₂O₄/geopolymer nanocomposite were used to determine the presence and dispersion of NiFe₂O₄ nanoparticles. VSM analysis used to assess the magnetic saturation value of functionalized and unfunctionalized magnetic nanostructures. In comparison to bare NiFe₂O₄ nanoparticles, the saturation magnetization value of the NiFe₂O₄/geopolymer nanocomposite was lower. Hence, the nanocomposite made of NiFe₂O₄ and geopolymer demonstrated good magnetic properties. The elemental composition of many types of materials may be determined using the effective and practical EDX analysis method. According to the results of the constructed NiFe₂O₄/geopolymer nanocomposite's EDX spectrum, the presence of iron, nickel, and oxygen peaks was connected to the structure of the artificial magnetic NiFe₂O₄ nanoparticles. Along with the oxygen peak, the inorganic geopolymer substrate was also responsible for the aluminium and silicon peaks.

4.3 Conclusion:

Metal ferrite nanoparticles and their nanocomposites have attracted the scientific community's attention due to their extensive use in catalysis, energy storage, microwave screening, and biomedical applications. This book chapter outlined the synthesis and characterization of some essential metal ferrite nanoparticles and their nanocomposites, extensively used as heterogeneous catalysts in synthesizing medicinally important heterocycles.

Conflict of Interest: The author declares no conflict of interest.

4.5 Acknowledgments:

The authors express their gratitude to the management of SGT University, Gurgaon, Haryana, India for the constant support to complete the work.

4.6 References:

1. Murugan, C., et al., Two-dimensional cancer theranostic nanomaterials: Synthesis, surface functionalization and applications in photothermal therapy. *Journal of Controlled Release*, 2019. 299: p. 1-20.
2. Patade, S.R., et al., Preparation and characterizations of magnetic nanofluid of zinc ferrite for hyperthermia. *Nanomaterials and Energy*, 2020: p. 1-6.
3. Somvanshi, S.B., et al., Hyperthermic evaluation of oleic acid coated nano-spinel magnesium ferrite: enhancement via hydrophobic-to-hydrophilic surface transformation. *Journal of Alloys and Compounds*, 2020: p. 155422.
4. Corma, A., García, H. and Llabrés i Xamena, F.X., 2010. Engineering metal organic frameworks for heterogeneous catalysis. *Chemical Reviews*, 110(8), pp.4606–4655.
5. Pourshojaei, Y., Jadidi, M.H., Eskandari, K., Foroumadi, A. and Asadipour, A., 2018. An eco-friendly synthesis of 4-aryl-substituted pyrano-fused coumarins as potential pharmacological active heterocycles using molybdenum oxide nanoparticles as an effective and recyclable catalyst. *Research on Chemical Intermediates*, 44(7), pp.4195–4212.
6. Karami, B., Eskandari, K. and Azizi, M., 2013. Tungstate sulfuric acid (TSA): A green and highly efficient catalyst for novel and known polysubstituted imidazoles synthesis. *Letters in Organic Chemistry*, 10(10), pp.722–732.
7. Royer, S. and Duprez, D., 2011. Catalytic oxidation of carbon monoxide over transition metal oxides. *ChemCatChem*, 3(1), pp.24–65.
8. Poorali, L., Karami, B., Eskandari, K. and Azizi, M., 2013. New and rapid access to synthesis of novel polysubstituted imidazoles using antimony trichloride and stannous chloride dihydrate as effective and reusable catalysts. *Journal of Chemical Sciences*, 125(3), pp.591–599.
9. Karami, B., Eskandari, K., Zare, Z. and Gholipour, S., 2014. A new access to 1,8-dioxooctahydroxanthenes using yttrium (III) nitrate hexahydrate and tin (II) chloride dihydrate as effective and reusable catalysts. *Chemistry of Heterocyclic Compounds*, 49(12), pp.1715–1722.
10. Sharma G.; Kumar A.; Sharma S.; Naushad M.; Prakash R.; Alothman Z.; Tessema G. *Journal of King Saud University- Science Novel Development of Nanoparticles to Bimetallic Nanoparticles and their Composites: A Review. J. King Saud Univ. Sci.* 2019, 31, 257–269, <https://doi.org/10.1016/j.jksus.2017.06.012>.
11. Sertkol M.; Koseoglu Y.; Baykal A.; Kavasa H.; Basaran C. *Journal of Magnetism and Magnetic Materials Synthesis and Magnetic Characterization of Zn_{0.6}Ni_{0.4}Fe₂O₄ Nanoparticles via a Polyethylene Glycol-Assisted Hydrothermal Route. J. Magn. Magn. Mater.* 2009, 321, 157–162, doi: 10.1016/j.jmmm.2008.08.083.
12. Sertkol M.; Koseoglu Y.; Baykal A.; Kavas H.; Bozkurt A.; Toprak M. *Journal of Alloys and Compounds Microwave Synthesis and Characterization of Zn-doped Nickel Ferrite Nanoparticles. J. Alloys Compds* 2009, 486, 325–329, doi: 10.1016/j.jallcom.2009.06.128.
13. Poonam; Singh R. *Current Organic Chemistry Use of Bimetallic Nanoparticles in the Synthesis of Heterocyclic Molecules. Curr. Org. Chem.* 2021, Volume 25, Number 3, 2021, pp. 351-360(10), <https://doi.org/10.2174/1385272824999200409115018>.

14. Andhare D.; Jadhav S.; Khedkar M.; More S.; Jadhav K. Journal of Physics Structural and Chemical Properties of ZnFe₂O₄ Nanoparticles Synthesised by Chemical Co-Precipitation Technique. *J. Phys.* 2020, 1644, 012014, doi:10.1088/1742-6596/1644/1/012014.
15. Adak L.; Ghosh T. Current Organic Chemistry Recent Progress in Iron-Catalyzed Reactions Towards the Synthesis of Bioactive Five- and Six-Membered Heterocycles. *Curr. Org. Chem.* 2020, Volume 24, Number 22, pp. 2634-2664(31), <https://doi.org/10.2174/1385272824999200714102103>.
16. Hariani P.; Said M.; Rachmat A.; Riyanti F.; Pratiwi H.; Rizki W. Bulletin of Chemical Reaction Engineering & Catalysis Preparation of NiFe₂O₄ Nanoparticles by Solution Combustion Method as Photocatalyst of Congo Red. *Bull. Chem. React. Eng.* 2021, 16 (3), 481-490, <https://doi.org/10.9767/bcrec.16.3.10848.481-490>.
17. Egizbek K.; Kozlovskiy A.; Ludzik K.; Zdorovets M.; Korolkov L.; Marciniak B.; Jazdzewska M.; Chudoba D.; Nazarova A.; Kontek R. Ceramics International Stability and Cytotoxicity Study of NiFe₂O₄ Nanocomposites Synthesized by Co-precipitation and Subsequent Thermal Annealing. *Ceram. Int.* 2020, 46, 16548–16555, doi: 10.1016/j.ceramint.2020.03.222.
18. Karakas Z.; Boncukcuoglu R.; Karakas I. Journal of Physics: Conference Series the Effects of Fuel in Synthesis of NiFe₂O₄ Nanoparticles by Microwave Assisted Combustion Method. *J. Phys. Conf. Ser.* 2016, 707, 1–11, doi:10.1088/1742-6596/707/1/012046.
19. Ghobadi M. Journal of Synthetic Chemistry Based on Copper Ferrite Nanoparticles (CuFe₂O₄ NPs): Catalysis in Synthesis of Heterocycles. *J. Synth. Chem.* 2022, 1, 84-96, 10.22034/jsc.2022.155234.
20. Amulya M.; Nagaswarupa H; Kumar M.; Ravikumar C.; Kusuma K.; Prashantha S. Journal of Physics and Chemistry of Solids Evaluation of Bifunctional Applications of CuFe₂O₄ Nanoparticles Synthesized by a Sonochemical Method. *J. Phys. Chem. Solids* 2020, 148 109756, <https://doi.org/10.1016/j.jpics.2020.109756>.
21. Kazemi M.; Ghobadi M.; Mirzaie A. Nanotechnology Reviews Cobalt ferrite nanoparticles (CoFe₂O₄ MNPs) as catalyst and support: magnetically recoverable nanocatalysts in organic synthesis. *Nanotechnol Rev* 2018; 7(1): 43–68, <https://doi.org/10.1515/ntrev-2017-0138>.
22. Bendi A.; Dharma G.; Sharma N.; Singh M. Results in Chemistry CoFe₂O₄/Cu (OH)₂ Nanocomposite: Expeditious and Magnetically Recoverable Heterogeneous Catalyst for the Four Component Biginelli/Transesterification Reaction and Their DFT Studies. *Results Chem.* 2021, 3, 100202, <https://doi.org/10.1016/j.rechem.2021.100202>.
23. Zhang R.; Chen T.; Wang G.; Guan Y.; Yan G.; Chen Z.; Hu J. Catalysis Letters Magnetic Recyclable Cu/ZnFe₂O₄ for Catalytic Reduction of Nitroarenes And C-N Bond Formation Reactions. *Catal Lett* 2022, 152, 3506–3516, <https://doi.org/10.1007/s10562-021-03906-z>.
24. Hajizadeh Z.; Radinekiyan F.; Keihan R.; Maleki A. Scientific Reports Development of Novel and Green NiFe₂O₄/Geopolymer Nanocatalyst Based on Bentonite for Synthesis of Imidazole Heterocycles by Ultrasonic Irradiations. *Sci. Rep.* 2020, 10, 11671, <https://doi.org/10.1038/s41598-020-68426-z>.

5. Deep Eutectic Solvents (DESs): A Benign and Sustainable Approach in Amphiphilic Self-Assembly

Yagnik Vora, Ketan Kuperkar

Department of Chemistry,
Sardar Vallabhbhai National Institute of Technology (SVNIT),
Udhana- Magdalla Road, Surat, Gujarat, India.

5.1 Introduction to Deep Eutectic Solvents (DESs):

5.1.1 General assumption:

Science and technology (S&T) are teeming with novel discoveries and inventions for the good of the human race. However, the advancement of S&T has its own set of advantages and disadvantages.

Though most of these advancements have been overwhelmingly beneficial to humanity, however, it has imposed long-term environmental impacts such as countless health risks to the human species, loss of flora and fauna, drastic climate changes, and many other imbalanced implications.

As a consequence, it is imperative that S&T technologies pay heed to their negative advances and ensure that any progress in them takes into account the current and potential needs and well-being of the human race, climate, and ecosystem. In today's situation, the need for sustainable growth is undeniable.

The World Summit on Sustainable Development convened in Johannesburg in 2002, a global consensus had started on how to design developments and technologies that are more environmentally sustainable. These advancements have also inspired researchers involved in the field of chemistry to focus their innovations more on 'greener/sustainable technologies' that must be devoid of all 'environmentally hazardous' instruments, procedures, or methods.

5.1.2 Historical Perspective:

At the turn of the century, Deep Eutectic solvents (DESs) have earned a great deal of interpretation around the globe, like ionic liquids (ILs). Although DESs can be derived from both ionic and non-ionic elements, they are not ILs. DESs have many benefits over typical ILs. They are relatively inexpensive non-toxic and environmentally friendly, easy to prepare simply combining cheap starting ingredients at a mild atmospheric pressure), chemically more inert, bio-degradable, and convenient to store¹.

These environmentally sustainable compounds combine HBD (Hydrogen Bond Donor) and other remaining component/s as HBA (Hydrogen Bond Acceptor) *via* hydrogen bonding interactions to shape a eutectic mixture with a melting/freezing point far lower than either of the components used to produce the DESs.

The most commonly studied DES is the complex formation of quaternary ammonium salts such as choline chloride (ChCl, 2-hydroxyethyltrimethylammonium chloride) with carboxylic acids, amides, or other hydroxyl HBDs.

As opposed to other inorganic salts, the cholinium cation is non-toxic, biodegradable, and comparatively inexpensive. It is classified as a provitamin in European countries and is mostly used as an animal nutrient. ChCl can be obtained from biomass or produced in a one-step gas phase reaction involving HCl, ethylene oxide, and trimethylamine that generates no by-products. As a result, DESs constitute a wide class of molten mixtures containing massive, asymmetric ions with low lattice energy and, as a result, melting points as low as 285.15 K.

The drastic change in the melting point in case of these novel solvents is due to the distribution of charge due to the extensive hydrogen bonding network between the halide atom of HBA and H atom of the HBD².

In contrast to ILs, where electrostatic interactions were witnessed between cations and anions, while DES have a massive hydrogen bonding network between HBA and HBD. However, there is no significant difference in the physical properties of DESs and ILs while the chemical properties are fairly different. Nevertheless, these DESs are fundamentally an extensive version of the ILs model *i.e.*, ILs analogues. Abbott and co-workers group at the University of Leicester were responsible for pioneering the development of this novel green and environmentally friendly DES¹.

The expression DESs was coined to distinguish these solvents from ILs and to denote the decrease in freezing point. Millions of combinations of DESs have been shaped by varying HBD and HBA as precursors that display unique physicochemical properties *viz.*, biodegradability, low cost, low volatility, easy preservation, less exposure to moisture, and low toxicity that has enable them to display a wide range of applications.

So far, the majority of DESs recorded are hydrophilic in nature. However, there are few studies on the new class of hydrophobic DES with HBD and quaternary ammonium salt having long alkyl chains which induce the hydrophobicity in DES.

5.2 Preparation and Classification of DESs:

The ease with which DESs can be prepared is extremely straightforward. The preparation of a homogeneous and transparent liquid is accomplished by combining the two or more components in precise molar ratios while constantly heating and stirring.

The essence of the relationship between the various HBDs and HBAs used throughout the formulation of DESs decides the necessary temperature (**Figure 5.1**).

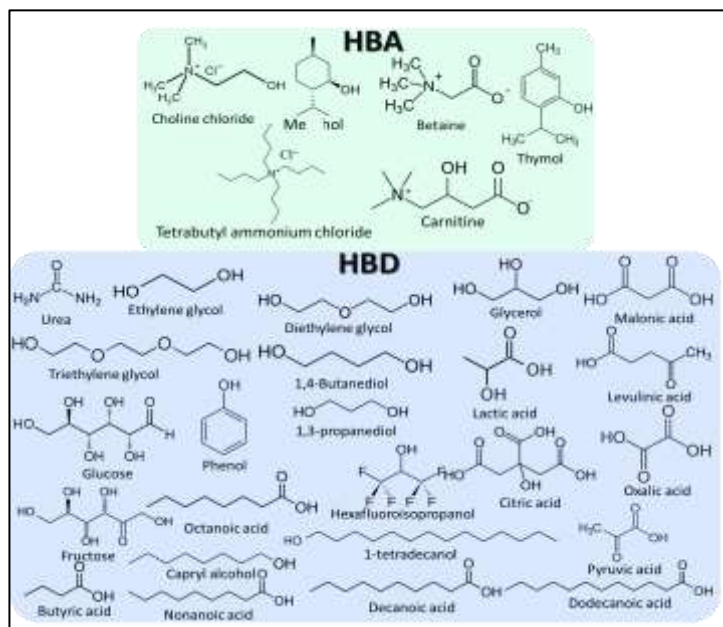


Figure 5.1: Structures of HBDs and HBAs used in the preparation of DESs

Although Abbott. group reported the first preparation of the DES as well as the systematic investigation by using several structurally different precursors like metal halides (MX_n , M = metal, $X = I, Br, Cl$ hydrated metal salt), and other HBDs. As a result, Abbott et al. suggested a general formula ($[R_1R_2R_3R_4N^+X^-] \cdot Y$) for distinguish various types of DESs. Where, $R_1, R_2, R_3,$ and R_4 are the substituents attached to the N atom of quaternary ammonium species. X^- is the halide anion of the HBA salt and Y is the HBD component. Studies have reported the classification of DESs into five groups (I - V) based on the essence of the complexation activity between HBDs and HBAs^{3,4} (Figure 5.2).

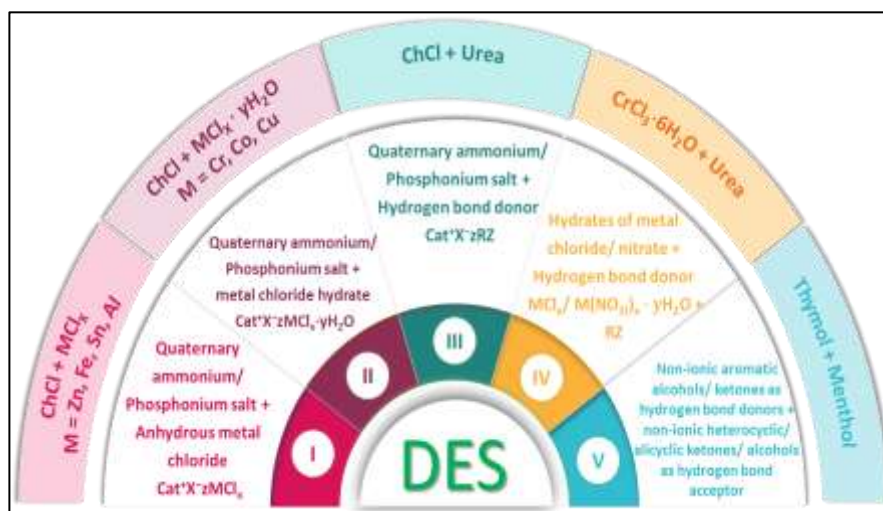


Figure 5.2: Different Type of DES Based on The Nature of The Complexing Agents

5.3 Physicochemical Properties of DESs

DESs and ILs have almost identical physical properties; furthermore, the chemical properties of these solvents vary based on different starting materials employed. DESs, like ILs, can be chemically engineered by using various starting materials. DESs have certain physical properties in common with ILs, but they have a different chemical behaviour. Furthermore, the ability to customise the structural properties of HBDs and HBAs in DESs provide distinct and versatile control over their physicochemical properties such as freezing point/ melting point, density (ρ), viscosity (η), conductivity (κ), surface tension (γ), and refractive index (n_D) which are further discussed in this section.

5.3.1 Freezing Point:

The freezing point of DESs is the source of their appealing functionality and applications. The freezing point of a eutectic mixture is determined by a number of factors. These factors include lattice energy, the type and extent of interaction between HBD and the massive hydrogen bonding agent HBA, and the shift in liquid entropy after DESs creation.

As was previously stated, DESs are combinations that have lower freezing points than any of the components used to prepare them. For example, DES obtained by combining urea and ChCl in the molar ratio 2: 1 has a freezing point of 285.15 K, which is significantly lower than that of both urea (m.p. 575.15 K) and ChCl (m.p. 406.15 K). The freezing points of the majority of the DESs recorded so far are lower than 423.15 K. Conversely, DESs with freezing points smaller than 323.15 K are significantly more appealing due to their broader applications.

The freezing point decrease is determined by the degree of contact between the HBD and the anion, as well as the asymmetry of the quaternary ammonium salts. For instance, the freezing point of DES dependent on urea and choline salt decreases as $F > NO_3 > Cl > BF_4$, indicating an association between the freezing point and the degree of hydrogen-bonding. However, the molar composition of the components in DESs also plays a significant role in determining the freezing point.

A DES with a 1:1 molar ratio of ChCl and urea has a freezing point greater than 323.15 K, while a DES with a 1:2 molar ratio of ChCl and urea has a freezing point of 285.15 K. Similarly, the reaction of several carboxylic acids (malonic, levulinic acid) and sugar molecules (xylitol, sorbitol) with ChCl to create a eutectic mixture that can exist in the liquid state at room temperature implies that the freezing point of a DES is greatly altered by the choice of HBD with ChCl.

The essence of HBD determines its degree of contact and charge delocalization with the HBA, and hence is responsible for freezing point reduction. Nevertheless, the number of DESs with freezing points of 323.15 K is still very small, and on-going attempts are being made to produce room temperature DESs.

The most utilised and picked DES for various applications has been tabulated in Table 1 along with different HBA, HBDs and freezing point⁴.

5.3.2 Density (ρ):

It is essential to first consider the ρ of DESs in order to determine their potential usefulness in industries and chemical processes. DESs that are widely recorded have a higher ρ than vapour. Several research groups, including Mjalli *et. al.*, Pandey *et. al.*, Abbott *et. al.*, and others have suggested numerous methods for determining the ρ of DESs.

The molar ratio of the materials comprising the eutectic mixture also determine the ρ of DESs. Furthermore, the molecular structure of HBDs was found to have an impact on the total ρ of a DES.

For example, when the mole ratio of HBD glycerol in the ChCl-glycerol (glyceline) DES was increased from 1 to 3 moles, the ρ of the DES increased from 1.16 to 1.20 g cm⁻³. As a result, by varying the structural properties of their HBD and HBA, a variety of DESs with desired ρ can be developed⁴. Some reported ρ data are enlisted in Table 1.

5.3.3 Viscosity (η):

The determination of η offers a better understanding of the structural properties of DESs while also broadening their scope of application. At room temperature, DESs have high η levels (> 100 cP). The η of the eutectic composition is affected by a number of factors, including the form of ammonium salts and HBDs used, the organic salt/ HBD molar ratio, and temperature. The presence of a comprehensive hydrogen bonding network inside a DES, which, in essence, limits the mobility of constituted species and thus reduces the η of DESs, is the most significant explanation proposed for the extremely viscous nature of DESs among all aforementioned reasons. In addition to electrostatic and van der Waal interactions, other considerations such as ion size and voids play a part in determining the η of DESs.

It was noticed that the η of the DES varies with the nature of HBD. The increasing trend in η is caused by the creation of a significantly strong hydrogen-bonding network. However, one of the drawbacks of DESs is their high η , which makes them difficult liquids to work with in the lab and beyond². As a consequence, it is important to build a eutectic system with moderate or low η by conducting proper modulation in their components to optimise their use. Furthermore, numerous publications have published on the temperature-dependent η of DESs⁵. Table 5.1 depicted the reported η data from the available research.

5.3.4 Rheology:

The rheological behaviour of a fluid is a significant property that influences η based effects and applications such as mass transfer rates, pumping, and hydrodynamics. Rheology is a vital field of science that facilitates the transfer of substance and fluid elongation activities. Rheological tests help to characterise materials by recognising whose composition and flow properties, ensuring their effectiveness prior to deployment on wide scale operations.

The principle aspect of the significant drop in η with increasing temperature is structural collapse due to thermal expansion of the structure and shear stresses effect⁵.

5.3.5 Conductivity (κ):

The conducting properties of DESs are caused by the transport or motion of ionic species within them. Since a significant number of DESs have a strongly viscous nature, they have poor electrical conductivity ranging from 0.1 to 10 mS.cm⁻¹.

The existence and molar formulations of an ammonium salt and HBDs used throughout their preparation have a significant impact on the conductivity of DESs. Furthermore, Abbott and colleagues reported that increasing the salt concentration in DESs improved its ionic conductivity.

The authors observed that raising the concentration of ChCl in a mixture of glycerol resulted in a eutectic mixture with conductivity greater than 1 mS.cm⁻¹. Similarly, to η , the authors explored the thermal behaviour of conductivity and projected an Arrhenius equation for the understanding of the interaction. Cantered on the above-mentioned findings, a sequence of eutectic compositions with moderate conducting potential can be formulated by varying the type and concentration of inorganic salts within a DES.

5.3.6 Surface Tension (γ):

According to studies, DESs exhibit similar properties to ILs based on imidazolium and have a greater γ than organic solvents. One of the essential DES physical effects is γ . γ is also crucial for mass transfer and innovation processes including condensation, absorption split, and withdrawal. Comparing DESs to conventional ILs, the γ is greater in DESs.

This is an indication that salt and HBD produced stronger hydrogen bonds. According to research, ChCl-based DESs have higher γ due to strong hydrogen bonds, and the type of HBD also affects this γ . Additionally, it has been shown that γ reduces with increasing temperature.

The component interactions in DESs are weakened because at high temperatures, kinetic energy rises and cohesive forces between molecules diminish. The γ of DESs increases with an increase in the amount of salt (or a decrease in HBD content), and it is dependent on the salt/HBD molar ratio.

5.3.7 Refractive Index (η_D):

The η_D has been used to identify compounds, confirm and measure mixture concentrations, and evaluate the purity of substances. From a more fundamental perspective, the η_D may also be employed as an indication of a molecule's degree of electronic polarizability and can provide crucial details regarding intermolecular interactions or their behavior in solutions.

The experimental measurements of the η_D of DESs are time consuming and also expensive. η_D of materials often decrease with rising temperatures as a result of decreasing ρ values. The type of salt, molar ratio of HBD to HBA, temperature, and molecular weight of DES are only some of the variables that affect the η_D of DESs.

Table 5.1: Various physical properties (melting point (T_m), density (ρ), viscosity (η), conductivity (κ), surface tension (γ), and refractive index (η_D)) of DESs at 298.15 K³

HBA	HBD	Molar ratio	T_m (°C)	ρ (g·cm ⁻³)	η (mPa·s)	κ (mS·cm ⁻¹)	γ (mN·m ⁻¹)	η_D
ChCl	Urea	1:2	12.0	1.24	169.0	0.20	52.0	-
	Trifluoroacetamide	1:2	-	1.17	77.3	2.48	-	-
	Monoethanolamine	1:5	-3.8	1.08	48.5	-	48.2	1.4849
	Malonic acid	1:1	10.0	1.25	1124.0	0.88	65.7	1.5681
	Malic acid	1:1	-	1.24	541.1	1.13	-	1.4343
	Oxalic acid	1:1	34.0	1.259	8953.0	0.42	-	1.4864
	Levulinic acid	1:2	-	1.14	79.1	0.81	-	1.4610
	Glutaric acid	1:1	29.7	1.19	2015.0	-	-	1.4833
	Glycerol	1:2	-	1.20	318.1	1.75	56.0	1.4869
	Ethylene glycol	1:2	-66.0	1.19	40.0	7.33	48.9	1.4611
	Triethylene glycol	1:2	-	1.13	839.0	1.41	-	-
	Phenol	1:2	-	1.10	90.3	3.14	-	-
	d-fructose	2:1	10.0	1.27	11312.0	-	74.0	1.5198
	Glucose	2:1	15.0	1.24	-	-	71.6	1.5197
	Pyrogallol	1:2	-50.9	1.27	4850.0	0.11	-	1.5590
Tetraethylammonium chloride	Levulinic acid	1:2	-	1.10	69.8	1.05	-	1.4626
	Glycerol	1:3	-41.6	1.01	580.0	0.31	46.0	1.4774
	Ethylene glycol	1:2	-30.1	1.10	127.0	0.001	39.3	1.4672
	Triethylene glycol	1:1	17.1	1.02	289.4	0.29	40.6	1.4772
	Propanoic acid	1:2	-	0.97	154.0	0.42	-	1.4553
	Phenylacetic acid	1:2	-	1.04	288.0	0.16	-	1.5083
	Levulinic acid	1:2	-	1.03	65.6	0.45	-	1.4561
Tetrapropylammonium bromide	Glycerol	1:2	-15.0	1.19	712.5	0.37	51.0	1.4889
	Ethylene glycol	1:3	-13.3	1.13	56.02	3.37	46.2	1.4717
	Triethylene glycol	1:3	-19.2	1.14	71.9	1.05	46.2	1.4732
	Chloroacetic acid	1:2	-72.7	1.22	-	672.6	-	1.4828
	Benzilic acid	1:1	-7.54	1.78	11000.0	4.3 x 10 ⁻⁵	46.6	1.5508
Pyrogallol	1:1	-30.5	1.20	25000.0	0.03	50.3	1.5390	
Tetrabutylammonium bromide	Glycerol	1:4	-	1.15	869.0	0.12	36.6	-
	Ethanolamine	1:6	0.43	1.03	41.7	1.32	41.4	-
	Diethanol amine	1:6	-67.8	1.08	390.0	0.15	43.9	-
	Triethanol amine	1:3	-76.6	1.10	55.0	0.10	42.4	-
	Levulinic acid	1:2	-	1.10	175.1	0.22	-	1.4696
	Chloroacetic acid	1:1	-64.7	1.12	-	70.8	-	1.4840
	Imidazole	3:7	21.2	-	810.0	0.24	-	-
	Formic acid	1:1	-	1.06	455.0	0.11	37.2	-
	Acetic acid	1:1	-	1.18	528.0	0.08	34.5	-
	Propionic acid	1:1	-	1.13	636.0	0.09	32.4	-
	Oxalic acid	1:1	-	1.10	823.0	0.07	42.7	-
	Succinic acid	1:1	-	1.07	1075.0	0.03	38.2	-
	Pyrogallol	1:1	-40.4	1.13	18500.0	22.32	40.1	1.5230
	l-Nonanol	1:4	-11.2	0.89	43.7	117.1	23.7	1.4510
Methyl triphenyl-phosphonium bromide	Glycerol	1:3	-5.4	1.30	2190.0	0.10	58.9	1.4589
	Ethylene glycol	1:4	-49.3	1.23	109.8	0.79	51.3	1.5542
	Triethylene glycol	1:5	-48.4	1.19	-	1.94	49.9	1.5178
Lidocaine	Menthol	1:2	-	0.94	59.0	-	-	-
	Thymol	1:2	-	0.99	100.2	-	-	-
Menthol	decanoic acid	1:1	-	0.90	20.5	-	-	-
	Thymol	1:1	-	0.94	42.0	-	-	-
	l-tetradecanol	1:2	-	0.87	36.6	-	-	-
	l-naphthol	1:2	-	0.98	74.4	-	-	-
Thymol	Camphor	1:1	-44.0	0.99	25.8	-	-	-
	Decanoic acid	1:1	17.0	0.94	11.2	-	-	-

Note: The symbol “-” indicate the data not reported.

5.4 Applications of DESs:

DESs are seen as a more durable and cost-effective solution to the bulky solvents mentioned thus far. As a result, the flexible functions assigned to DES components allow for their complete use in a wide range of scientific and technological fields, including organic synthesis as solvent and catalyst, electrodeposition, inorganic chemical reactions, biomass, separation/extraction dissolution and in DESs⁶, polymer and nanoparticle formulation, and many others as depicted in Figure 5.3.

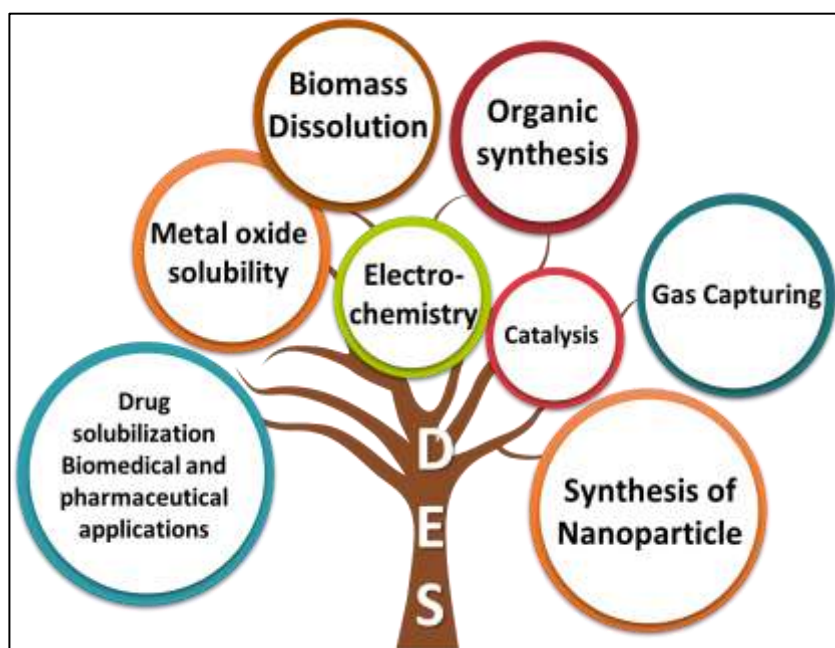


Figure 5.3: Application of DESs

5.4.1 Electrochemistry:

The spectrum of application of DESs in the field of electrochemistry is determined by a large electrode potential window (EPW). The use of DESs as a non-aqueous medium in the process of electrodeposition coatings is motivated by an extended spectrum of EPWs as well as inertness to any electron transfer reactions. As a result, in the electropolishing process, DESs have gained favour as a potential substitute for conventional solvents such as aqueous mixtures of phosphoric and sulfuric acid, as well as CrO_3 , which are highly corrosive, poisonous, and have poor effectiveness.

5.4.2 Catalysis:

Synthetic chemistry field is also concentrating on the use of DESs as catalyst. DESs composed with $\text{ChCl}:\text{ZnCl}_2$, exhibit Lewis acidic nature thus promising a role as a catalyst for various organic reactions *viz.*, esterification, Diels–Alder cycloaddition, O-acetylation of the sugar molecule, and protection of carbonyl group.

Furthermore, DESs serve as a catalyst in the synthesis of phenols, nitriles from aldehydes, pyran, and benzopyran derivatives. In the same way, scientists reported the catalytic properties of DES (ChCl-SnCl_2) in 1:2 molar ratio for the chemo selective ring-opening of epoxides with aromatic alcohols, amines, thiols, cyanide and azide.

5.4.3 Drug Solubilization Biomedical and Pharmaceuticals:

Drug solubility is an important characteristic attribute to look into for prescription formulations and processing design. The low water solubility of active pharmaceutical ingredients (APIs), which results in poor bioavailability and permeability, is one of the major problems with current APIs. Researchers have discovered several prescription eutectic combinations that comprise menthol/testosterone, ibuprofen/menthol, and lidocaine/procaine. However, these eutectic mixtures of local anaesthetics (EMLAs) appear to be sluggish in terms of absorption, water solubility, and thermal prosperity. Several research studies have documented significant enhancements in the solubility of diverse drugs using different deep eutectic solvents (DES) comprising ethylammonium chloride, tetrapropylammonium bromide, betaine, and choline bitartrate as hydrogen bond acceptors (HBAs), and ethylene glycol, 1,2-propanediol, glutaric acid, malonic acid, levulinic acid, lactic acid, and urea as hydrogen bond donors (HBDs). These DES show promise for nonaqueous liquid administration of drugs.

5.4.4 Metal Oxide Solubility:

Metals have traditionally been extracted from ores using pyrometallurgical and hydrometallurgical methods. In prior studies, it has been demonstrated that DES exhibited higher solubility towards metal oxides when compared to ILs and other organic/inorganic solvents. However, the notable drawback of these solvents was their toxicity issue. Therefore, from this point of view, DESs have also been recommended as alternate solvents for the solubilization of metal oxides in recent years.

It has been documented that particularly *ChCl-based* DESs have potential to solubilize a wide range of metal oxides which is significantly tuned by varying the nature and mole ratio of HBD used. A significant number of transition metals were generally discovered to be soluble in the various DESs, although the more covalent metal oxides (such as aluminates and silicates) were discovered to be insoluble in all DESs investigated to date. Furthermore, among all DES, malonic acid-based carboxylic acid (malonic acid and oxalic acid) has showed outstanding solubility.

5.4.5 Biomass Dissolution:

In general, biomass, an organic compound derived from natural sources such as plants, microorganisms, and animals, is biocompatible, green, low-cost, plentiful, and biodegradable material that has been used to manufacture fabrics, products, fuels and energy. Nevertheless, large number of biomass, specifically most biomass polymers have issue with the solubility in common solvent and thereby preventing their scope in terms of application. The favourable physicochemical properties of such non-aqueous DESs permit them for pre-treatment of biomass and their various useful transformation for particle uses.

5.4.6 Organic Synthesis:

DESs are being considered in organic reactions, such as Fischer indole annulation, Diels-Alder (ring forming and ring-opening), and many polymerizations reaction, was carried out in $\text{ChCl}:\text{ZnCl}_2$ -based DES. $\text{ChCl}:\text{urea}$ -based DES (reline) reported more promising role in inorganic reactions which involve the heteroaromatics transformation *via* carbonyl condensation reactions like Paal - Knorr synthesis of pyrroles and furans. Moreover, reline-based DES has been focused mainly on the organic reaction which involve the condensation-type mechanism such as Perkin, Knoevenagel, aldol, Henry and related reactions. In addition to this, the organic reaction wherein multicomponent coupling reaction (MCR) for example Knoevenagel condensation, followed by Michael addition was successfully achieved in reline.

5.4.7 CO₂ Capturing:

A significant problem attributed to excess greenhouse gases, particularly those produced on by humans, is climate change. In general, the burning of fossil fuels, transportation, and other businesses are the sources of CO₂ emissions. Currently, carbon capture and storage (CCS) is expected to be a successful method of causing the emission of large amounts of CO₂ into the environment in order to reduce pollution.

Several techniques were exposed for CO₂ separation *viz.*, organic solvent scrubbing, amine scrubbing, water scrubbing, adsorption, and membrane techniques. However, some techniques have several disadvantages such as energy, instability, corrosion, deterioration, large-scale operations, large volume requirement consumption and poor selectivity.

Previously, ILs have been suggested as possible media for CO₂ separation. But ILs exhibit numerous drawbacks such as limited solute solubility, unfavourable toxicity, complex synthesis route, high viscosity, poor biodegradability, and high cost and so the DESs are becoming a common subject of research where ChCl -based DESs are examined thoroughly⁷.

5.4.8 Nanoparticle Synthesis:

Due to the outstanding magnetic, electrochemical, and other special properties products of nanomaterials have grabbed a wide range of applications.

Furthermore, these nanoparticles hold a wide range of applications in fields such as catalysis, electronics, optical systems, magnetism, biology, and other sciences. DESs has open up exciting possibilities for creating sophisticated nanostructures in low-water or water free medium. The use of DESs to create practical, optimised nano-scale materials has made significant progress.

5.5 Self-Assembly of Amphiphiles In DES:

Lyophilic and lyophobic moieties are both present in surfactant molecules. When in solution, this amphiphilic structure drives a specific behaviour that causes aggregates to

self-assemble above a certain concentration, known as the critical micelle concentration (CMC). Surfactant is gathered into aggregates, which are frequently referred to as micelles, in order to lower the system's free energy. By generating aggregates where the tails are comparatively non-solvated by the surrounding medium, the energetically unfavourable lyophobic interaction between tail and solvent is circumvented since the solvated headgroups create a shell shielding the tails. The features of such aggregates are controlled by a delicate balance between the various components of the system, and the maximum size of the micelle is constrained by steric or electrostatic repulsion. In example, the repulsion between ionised headgroups regulates the shape of ionic surfactant micelles.

The presence of counterions in the vicinity of the headgroup area regulates the charge density and, depending on the counterion's properties, the effective charge and therefore, the micelle's structure. In the search of innovative solvents for self-assembly, the micelles assist the significant properties of solvents which make this self-aggregation facilitate and optimized for various applications.

The main difference is that each solvent has own driving force for the amphiphiles into micelles that leads to the change in CMC as well as aggregation number. Withstanding this, relatively few non-aqueous, "modern" molecular solvents like DESs that support such self-assembly have been established.

The majority of research on self-assembly in DES has so far been on ChCl-based systems with HBDs designed around amide, carboxylic acid, or alcohol functional groups. Surfactants that are completely insoluble in one DES can form strange aggregates in another system, indicating that surfactant self-assembly in DES varies significantly as a function of the DES composition.

Studying the behavior of surfactants throughout an appropriate compositional range of DESs is therefore quite interesting, especially for those DESs generated from natural products that have been appreciated for their favorable effects on the environment⁸.

In the absence of water, it has recently been shown that DES supports the self-assembly of new surfactants (such IL-based), cationic, anionic, and zwitterionic surfactants. Similar to the entropy-directed process that takes place in water, polar organic solvents, and ILs, it has been demonstrated that the self-assembly of surfactants in DES is supported by the solvophobic effect.

There are two basic approaches that can be distinguished: non-interactive and interacting systems. It has been demonstrated that the resultant micelle shape in DES depends on both the surfactant and solvent variables. One way to think about non-interacting systems is that they behave like water since there don't belong to any significant electrostatic connections between the ions of the surfactant and solvent.

On the other hand, the ionic components of the solvent as well as the native surfactant counterion have an influence on the charge density of the micelle in interacting systems. In this scenario, the formation of micelles exhibits distinct morphologies compared to those observed in water and other molecular solvents such as formamide or glycerol.

Therefore, alterations to the physicochemical characteristics of the solvent may be made to vary how a surfactant self-assembles, providing viable options for the synthesis of nanostructured materials and non-aqueous responsive materials. Additionally, it has been demonstrated that the presence of water affects the surfactant self-assembly in DES, providing an additional option for regulating the characteristics of the system. Some work related to self-assembly in DESs has been published recently and listed in Table 5.2.

Table 5.2: Self-assembly of various amphiphiles (Surfactant/ ILs)/ polymers) reported in DES.

HBA	HBD	Molar ratio	Amphiphile used for self-assembly	Ref.
<i>Surfactants in DES</i>				
ChCl	Malonic acid	1:1	Dodecyltrimethylammonium bromide (C ₁₂ TAB), Tetradecyltrimethylammonium bromide (C ₁₄ TAB), Hexadecyltrimethylammonium bromide (C ₁₆ TAB)	9
	Urea	1:2	Sodium Dodecylsulfate (SDS)	10, 11
	Glycerol	1:2	Cetyldimethylethanolammonium bromide, Cetyltributylphosphonium bromide	
	Glycerol	1:2	Hexadecyltrimethylammonium chloride,	
	Glycerol	1:2	Dodecyl-2-(trimethylammonio) ethylphosphate and N-alkyl-N, N-dimethyl-3-ammonio-1-propanesulfonate (alkyl = dodecyl, tetradecyl)	
	Glycerol	1:2	C ₁₂ TAB, C ₁₄ TAB, C ₁₆ TAB	
	Glycerol	1:2	Cetylpyridinium bromide (CPBr)	
	Ethylene glycol			
<i>ILs in DES</i>				
ChCl	Glycerol	1:2	1-butyl-3-methylimidazolium octylsulphate [Bmim][OS]	10
	Urea			

HBA	HBD	Molar ratio	Amphiphile used for self-assembly	Ref.
ChCl	Glycerol	1:2	N-alkyl-3-methylimidazolium bromide (C _n mimBr, n = 12, 14, 16)	
ChCl	Glycerol	1:2	N-alkyl-3-methylimidazolium chloride (C _n mimCl, n = 8, 10, 12, 14 and 16).	16
Polymers in DES				
Ethylammonium bromide (EABr)	Ethylene glycol	1:2	Poly (ethylene oxide) (PEO)	10
	Glycerol			
Butylammonium bromide (BABr)	Ethylene glycol	1:2	polyoxyethylene sorbitan monooleate (Tween-80), polyoxyethylene sorbitan laurate (Span-20)	13
	Glycerol			
	Urea	1:2	(VPGVG) ₂ -(VPGEG) -(VPGVG) ₂ , (VPAVG) ₂₀	14
	Urea	1:2	Star block (4-arm) ethylene oxide (EO)- propylene oxide (PO) block copolymer (Tetronic T1304)	15
	Ethylene glycol			
	Glycerol			
	Malonic acid	1:1		
	Glutaric acid			
Oxalic acid				

5.6 Conclusions and Future Prospective:

This book chapter explicitly indicates the presence of nanoscale assemblies as micelles in pure DES and demonstrate some distinct changes in solution behaviour between DES and that seen in water. The surfactant molecules get self-assembled greater in DES than observed in pure water. However, such behavior can modify as a function of solvent and surfactant concentration.

Furthermore, this chapter presents a consolidated an insight in tabular form into the micellar assembly formed in varies DESs that will inspire the readers for future applications in a variety of fields where fine control of aggregate size is a major concern such as inorganic material templating or novel technologies like drug delivery.

Thus, giving an account to the detailed literature survey, compressive fundamental research will improve our thoughtful of surfactant activity in numerous DES systems that will aid in the design and optimization of newer and interesting self-assembly using DESs for improved performance. Therefore, the creation of distinctive DESs with adjustable and recyclable abilities, as well as their molecular modes of action, including the amphiphile interaction in DESs, nature of interactions between amphiphiles with DESs are challenging and crucial for developing an environmentally benign and sustainable future.

5.7 References:

1. Abbott, A. P.; Boothby, D.; Capper, G.; Davies, D. L.; Rasheed, R. K., Deep eutectic solvents formed between choline chloride and carboxylic acids: versatile alternatives to ionic liquids. *Journal of the American Chemical Society*, **2004**, *126* (29), 9142-9147.
2. Zhang, Q.; Vigier, K. D. O. Royer, S.; Jerome, F., Deep eutectic solvents: syntheses, properties and applications. *Chemical Society Reviews*, **2012**, *41* (21), 7108-7146.
3. Omar, K. A.; Sadeghi, R. J. J. o. M. L., Database of Deep Eutectic Solvents and their Physical Properties: A Review. *Journal of Molecular Liquids*, **2023**, *384*, 121899.
4. Smith, E. L.; Abbott, A. P.; Ryder, K. S. J. C. r., Deep eutectic solvents (DESs) and their applications. *Chemical reviews*, **2014**, *114* (21), 11060-11082.
5. Jangir, A. K.; Sethy, P.; Verma, G.; Bahadur, P.; Kuperkar, K. J. J. o. M. L., An inclusive thermophysical and rheology portrayal of deep eutectic solvents (DES) for metal oxides dissolution enhancement. *Journal of Molecular Liquids*, **2021**, *332*, 115909.
6. Hansen, B. B.; Spittle, S.; Chen, B.; Poe, D.; Zhang, Y.; Klein, J. M.; Horton, A.; Adhikari, L.; Zelovich, T.; Doherty, B. W.; Gurkan, B.; Maginn, E. J.; Ragauskas, A.; Dadmun, M.; Zawodzinski, T. A.; Baker, G. A.; Tuckerman, M. E.; Savinell, R. F.; Sangoro, J. R., Deep Eutectic Solvents: A Review of Fundamentals and Applications. *Chemical Reviews*, **2021**, *121* (3), 1232-1285.
7. Zhang, Q.; Vigier, K. D. O.; Royer, S.; Jérôme, F., Deep eutectic solvents: syntheses, properties and applications. *Chemical Society Reviews*, **2012**, *41* (21), 7108-7146.
8. Pal, M.; Singh, R. K.; Pandey, S. J. C., Evidence of Self-Aggregation of Cationic Surfactants in a Choline Chloride+ Glycerol Deep Eutectic Solvent. *Chemphyschem*, **2015**, *16* (12), 2538-2542.
9. Sanchez-Fernandez, A.; Hammond, O. S.; Jackson, A. J.; Arnold, T.; Douch, J.; Edler, K. J., Surfactant–solvent interaction effects on the micellization of cationic surfactants in a carboxylic acid-based deep eutectic solvent. *Langmuir*, **2017**, *33* (50), 14304-14314.
10. Basu, M.; Hassan, P. A.; Shelar, S. B. J. J. o. M. L., Modulation of Surfactant Self-Assembly in Deep Eutectic Solvents and its relevance to Drug Delivery-A Review. *Journal of Molecular Liquids*, **2023**, *375*, 121301.
11. Hirpara, D.; Patel, B.; Chavda, V.; Desai, A.; Kumar, S. J. J. o. M. L., Micellization and clouding behaviour of an ionic surfactant in a deep eutectic solvent: A case of the reline-

- water mixture. Micellization and clouding behaviour of an ionic surfactant in a deep eutectic solvent: A case of the reline-water mixture, *Journal of Molecular Liquids*, **2022**, *364*, 119991.
12. Li, Q.; Wang, J.; Lei, N.; Yan, M.; Chen, X.; Yue, X., Phase behaviours of a cationic surfactant in deep eutectic solvents: from micelles to lyotropic liquid crystals. *Physical Chemistry Chemical Physics*, **2018**, *20* (17), 12175-12181.
 13. 13. Sakuragi, M.; Tsutsumi, S.; Kusakabe, K., Deep eutectic solvent-induced structural transition of microemulsions explored with small-angle X-ray scattering. *Langmuir*, **2018**, *34* (42), 12635-12641.
 14. 14. Nardecchia, S.; Gutiérrez, M. a. C.; Ferrer, M. L.; Alonso, M.; López, I. M.; Rodríguez-Cabello, J. C.; del Monte, F., Phase behavior of elastin-like synthetic recombinamers in deep eutectic solvents. *Biomacromolecules*, **2012**, *13* (7), 2029-2036.
 15. 15. Patidar, P.; Kanoje, B.; Bahadur, A.; Kuperkar, K.; Ray, D.; Aswal, V. K.; Wang, M.; Chen, L.-J.; Bahadur, P., Micellar characteristics of an amphiphilic star-block copolymer in DES-water mixture. *Colloid and Polymer Science*, **2021**, *299* (1), 117-128.
 16. 16. Tan, X.; Zhang, J.; Luo, T.; Sang, X.; Liu, C.; Zhang, B.; Peng, L.; Li, W.; Han, B., Micellization of long-chain ionic liquids in deep eutectic solvents. *Soft Matter*, **2016**, *12* (24), 5297-5303.

6. Basic Principles of Green Chemistry

Dr. Shubhendu Dhara

Department of Chemistry,
Bhairab Ganguly College,
Belgharia, Kolkata.

Abstract:

Ever increasing demand of modern civilization prompted monumental increase of small scale as well as industrial production of chemicals and chemical induced materials worldwide. All these production processes of materials generate large amount of toxic and hazardous chemical causing huge environmental crisis and health problems to the humans. To avoid the generation of chemical hazards alternative green approaches to the existing strategies have been adopted for the since last few decades. The principles and guidelines for these alternative environment friendly green approaches have been documented as the Principles of Green Chemistry.

Keywords:

Chemical syntheses, chemical hazards, environmental crisis, eco-friendly, green approaches, green principles.

6.1 Introduction:

Due to modernization and sophistication of human life global need for new consumable products multiplies continuously. And to meet this requirement there is a continuous increase of production processes in different industries and plants especially in chemicals and related industries. About all these production processes lead to the formation and or generation of hazardous and toxic materials either in the form of intermediate or by-products.

The wastes generated causing huge problems on the environment and society including global warming and extinction of living species from the ecosystem and disturbing the ecological balance on the earth. The chemistry community sorted out a remedy to this crisis in the form of alternative eco-friendly strategies over the existing productions processes of consumable products. These benign and eco-friendly methods of productions are emerged as a separate branch of chemistry namely 'Green Chemistry'.

The green chemistry is a specific branch of chemistry where eco-friendly and green approaches to chemical processes and chemical synthesis are studied for the benefit of the environment, we live in. By definition green chemistry is the design of chemical products and chemical processes that reduces or eliminates the use and generation of hazardous substances.

6.2 Background of Green Chemistry:

After the World War II, the green revolution made the use of pesticides in agriculture a common practice resulting in a great increase of global crop yields and agricultural production. But the consequences of pesticides on the environment and ecosystem were over looked for a long period of time. Later in 1962 Rachel Carson, a biologist and environmental activist first pointed out the harmful effect of use of pesticides on the environment in his scientific book the “**Silent Spring**” (Figure 6.1).¹



Figure 6.1: Harmful Effects of Pesticides Use in Agriculture

In 1970's some legal actions were taken by the US government by the formation of National Environmental Policy Acts (NEPA) and Environmental Protection Acts (EPA) which banned DDT to protect the environment from its adverse effect (Figure 6.2).

Later thirty industrialised countries together have formed the Organisation for Economic Co-operation and Development (OECD) and started mutual co-operation in chemical process and environmental pollution prevention strategies.

Many preventive measures and legal actions have been taken by different nations individually to handle problems of chemical pollutions.²

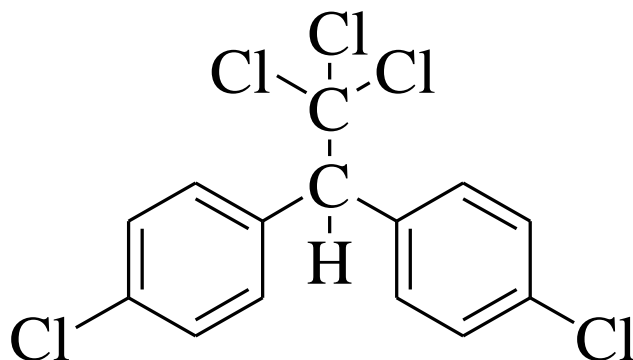


Figure 6.2: Dichlorodiphenyltrichloroethane (DDT)

Among the different scientific disciplines, chemistry and associated branches play a vital role in environment protection and public awareness. In recent years many new advanced chemical techniques and terminologies have been introduced in chemistry for example, atom economic processes, green or eco-friendly & renewable resources, E-factor *etc.* to understand and address the environmental issues out of chemical processes.

To address the environmental issues different names of chemical processes have been introduced such as **Clean Chemistry**, **Environmental Chemistry**, and **Sustainable Chemistry** *etc.* But the most widely accepted name of chemical study is “**Green chemistry**” coined by **Professor Paul Anastas** and after that a separate branch of chemistry was developed as “Green chemistry”.

6.3 Objective of Green Chemistry Approaches:

In today's world we are enormously dependent on chemicals and chemical induced products in our day life. Some of the essential chemicals include:

- Drug molecules like antibiotic and medicine to cure life threatening diseases
- Polymers *e.g.*, polymer-based materials are fulfilling our day-to-day needs such as plastic, nylon, Rayon, polyesters *etc.*
- Synthetic fuels, synthetic dies
- Agrochemical, fertilizers and many more.

All these essential chemicals have improved the quality of our life and on the other hand all these improvements have serious environmental effects either directly or indirectly. Almost all the chemicals used for generation of essential chemicals and the wastes generated during the manufacturing process have adverse effects on the environment and the ecosystem.

Today the situation is so frightening that the government has been forced to implement various measures to prevent and lessen generation of the environmental hazards at large. And new strategies of chemical productions evolved as **Green Chemistry**. The main objective of the green chemistry is to reduce or eliminate the pollution by preventing the use or generation of hazardous substances or products during production processes.

Chemists are continuously trying to develop benign and environmentally friendly Chemical syntheses of the existing product as well as for new value-added products. To encourage the green approaches by the scientific community and industries, the presidential green chemistry challenge award was introduced by US President Bill Clinton in 1995. In 5 different categories this award is given:

- Green synthetic pathway award
- Green reaction condition award
- Designing greener chemical award
- Small business award
- Academic Award

A. The first recipient of Green Chemistry award was

- The Monsanto's company for catalytic dehydrogenation of diethanolamine [(HOCH₂CH₂)₂NH]
- Dow chemical company for using 100% carbon dioxide as blowing agent for polyester foam seat packaging
- Rohm & Haas Company for designing environmentally friendly safe marine antifoulant.
- Donlar Corporation (Nanochem solution Inc.) for the production and use of thermal poly-aspartic acid

The **First Academy award** was given to Professor Mark Holtzapple from Texas A & M University for conversion of waste biomass into animal feed, usable chemicals and fuels.

6.4 Few Terminologies Used in Green Chemistry³

In designing eco-friendly and greener ways of production of value-added materials few new terminologies are commonly used in green chemistry.

6.4.1 Atom Economy (AE):

It is a measure of incorporation of atoms of the reactant molecules into the desired product in any chemical synthesis. It is also sometimes known as atom efficiency. The term was first introduced by Professor B. M. Trost of Stanford University in 1991. Atom economy of any chemical process can be represented as % atom economy (% AE).

$$\% \text{ Atom Economy} = \frac{\text{mass of the desired product in balanced equation}}{\text{total mass of the product formed in the balanced equation}} \times 100 \%$$

Here the total mass of the products formed in the balanced equation is equal to the number of reactants used in the reaction. The products include the desired product(s) as well as undesired products (by products). Later the by-products (*i.e.*, wastes) of the reaction were excluded from the equation of AE.

Therefore,

$$\% \text{ Atom Economy} = \frac{\text{mass of the desired product in balanced equation}}{\text{total mass of the reactant used in the balanced equation}} \times 100 \%$$

For example, the Wittig olefination reaction of carbonyl

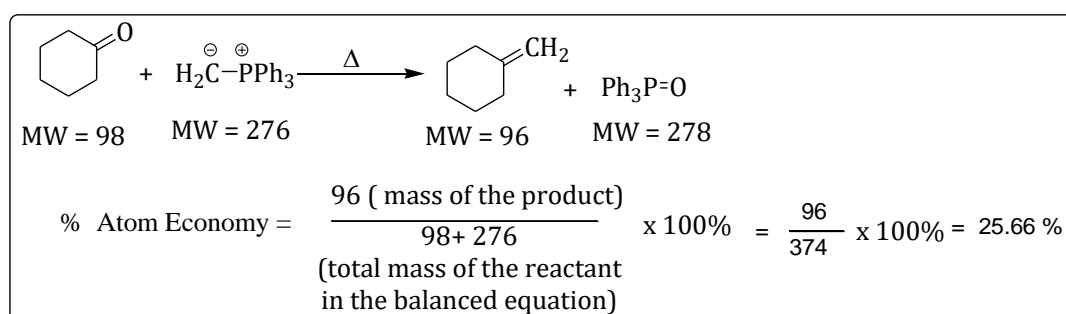


Figure 6.3: Calculation of Atom Economy

So, % atom economy of the **Wittig Olefination** reaction of cyclohexanone is only ~26%,

Therefore, it can be stated that Wittig reaction is not a good atomic economic reaction in respect of green chemistry (**Figure 6.3**). The atom economy also is a major factor in determining the efficiency of any chemical reaction in the course of a chemical synthesis.

6.4.2 Environmental factor (E-factor):

It is the indicator of waste products generated from a chemical reaction. Environmental factor is defined as the wastes formed per unit mass of the desired product. The term Environmental factor (E-factor) was introduced by Sheldon in 1992. It is expressed as:

$$\text{E-factor} = \frac{\text{Mass of the actual waste product}}{\text{Mass of the desired product}}$$

Though two concepts Atom Economy and Environment factors are seemed to be same but they are quite different. The calculation of atomic economy of any reaction can be done without carrying out the reaction in the lab. The atom economy of any reaction is calculated from the balanced stoichiometric chemical equation of the reaction. But for measurement of E-factor the whole experiment needs to be performed as it includes solvent used in the reaction, by-product, unreacted chemicals (reactants, catalyst, additive *etc.*) as waste product from the reaction. Therefore, the E-factor is an experimentally observed quantity but the atom economy (AE) is a theoretically calculated entity. For chemical reaction the ideal atom economy is 100% whereas the ideal E-factor for a chemical reaction is zero.

$$\text{E-factor} = \frac{[\text{Amount of the raw material (kg)} - \text{Amount of the desired product (kg)}]}{\text{Amount of the desired product (kg)}}$$

6.4.3 Life cycle assessment (LCA):

It is an alternative way of measuring the environmental impact of any product and its' process for generation. LCA considers the effects of all the inputs and outputs of a process to the environment.

For example, energy usage, extent of global warming, ozone layer depletion, acidification, eutrophication, smog formation and Eco-toxicity that can be generated from the inputs and outputs of any process.

LCA is the tool for assessment of potential harmful impact of a product or a process or system in all stages in their life cycle.

LCA assessment is done within some specific domains

- **Cradle to Gate-** It considers adverse effect beginning from raw materials to finished products.
- **Cradle to Grave-** It considers every impact starting from raw materials to the disposal of finished product after use.
- **Gate to Gate-** It considers the effects from the receiving point to starting materials to the shipping points of the end products.
- **Cradle to Cradle** – It is the most environment friendly concept among all. It is sustainable strategy which employs the concept of recycling of the used products as raw materials in some other production process or in the same product synthesis after degradation to the monomer unit (small molecules).

6.5 Limitations in Pursuing Strategies of Green Chemistry:

To combat emergent environmental crisis out of the hazardous chemicals from different chemical processes, 12 principles (guidelines) of green chemistry have been postulated by Dr. P Anastas John C. Warner. But to implement these green strategies in reality there are some limitations as follows:

- A. **Very high cost and complex nature of most of the green strategies** make it to implement in small scale or medium scale chemical organisations.
- B. **Lack of proper information (such as toxic limit) about hazards of chemical pollutants** is major difficulty to implementation green principles.
- C. Unavailability of enough chemistry-based technology or solution for many chemical processes is another obstacle in pursuing green approaches.
- D. Lack of knowledge about alternative feedstock and the basic principles of Green Chemistry by the person developing the new chemicals in most of the chemical organisations.
- E. There is a huge communication gap between the chemical Industry and the Green chemistry solution provided to us. The absence of knowledge transfer strategies is one of the hurdles to implement the Green Chemistry approaches in chemical industries.
- F. **Strict regulatory restrictions of different government bodies is the one the major obstacles** green chemistry approaches.

6.6 Principles of Green Chemistry:

Green synthesis can be conveniently carried out by following 12 principles of green chemistry suggested by Paul Anastas and J. C. Warner.^{3,4}

➤ Principle 1:

Statement: Prevention of pollution: it is always better to prevent generation of waste than to clean up the waste.

Explanation:

The chemical synthesis should be designed in such a manner so that there would be minimum waste production or no waste generation. The overall cost of any product from a chemical process increases with added cost for the treatment and disposal of the host generated not only in the form of by-product but also in the form of unreacted starting materials, reagents and solvent. Therefore, it is suitable to think of designing chemical process minimising the chemical waste. It is also better to follow the principle “prevention is better than cure” (**Figure 6.4**).



Figure 6.4: Industrial Wastes

A. Principle 2:

Statement:

Chemical process should be designed to maximize the incorporation of all the starting materials used in the process into the final product.

Explanation:

This is also known as atom efficiency of any organic synthesis. It is commonly observed that in any organic synthesis 1 equivalent (1mole) of starting material leads to the formation of 1 equivalent (1mole) of the desired end product and these reactions are considered as 100% efficient and yield is 100%. But in reality, these are not 100 % atom economic reactions as wastes generated in this process are not taken into account for calculation of AE of the reaction.

Therefore, these reactions may or may not be the greener way of synthesis depending upon whether wastes are generated or not. Such as very well known the Grignard addition reaction is not an atom economic reaction whereas Diels-Alder cyclo-addition reaction is 100 % atom economic (**Figure 6.5**).

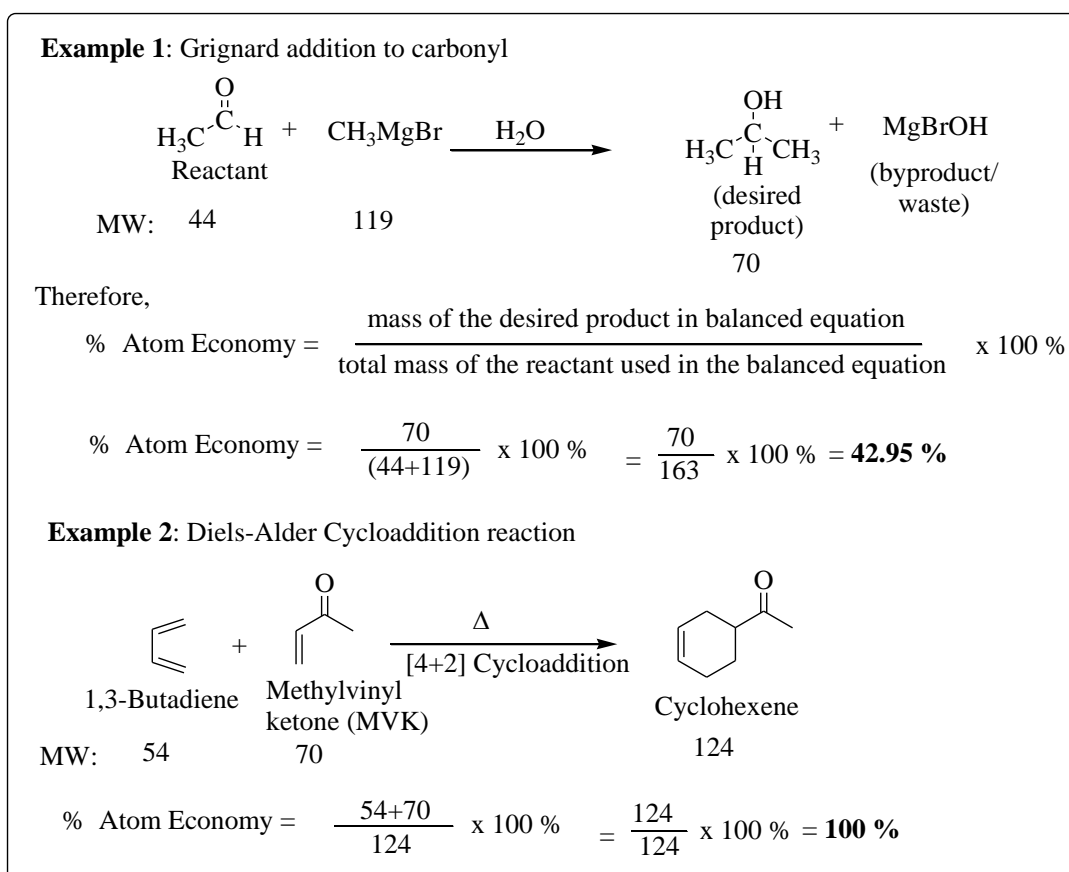


Figure 6.5: Examples Atom Economy (AE)

B. Principle 3:

Statement:

Whenever practicable, synthetic methodologies should be designed to use and generate substances that possess little or no toxicity to human health and the environment.

Explanation:

In the context of green chemistry, it is very important not to use any harmful or hazardous starting materials and also not to generate any toxic by-product or end-product. These chemicals are not only harmful to the worker in the chemical industry but also harmful to the environment.

For example, Synthesis of Adipic acid [$\text{HOOC}(\text{CH}_2)_4\text{COOH}$]

Conventional synthesis of Adipic acid:

- Uses benzene, a known carcinogen, as a starting material.
- Involves oxidation with an excess of HNO_3 , and production of greenhouse gas nitrous oxide (N_2O), the latter accounting for approximately 5–8% of the worldwide anthropogenic N_2O emissions (**Figure 6.6**).

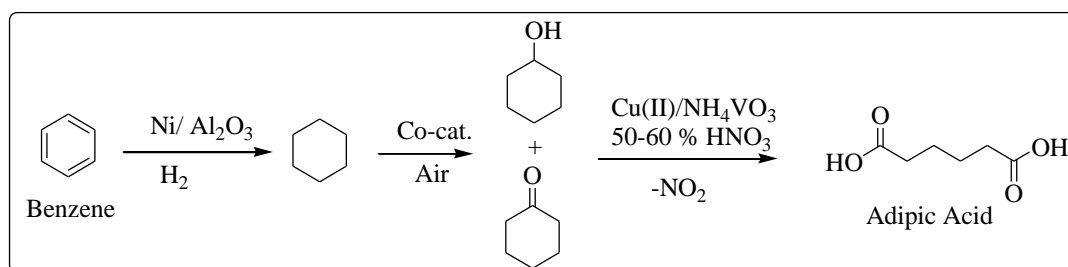


Figure 6.6: Industrial synthesis of Adipic acid

Alternative synthesis of adipic acid:

- Uses biocatalytic (*E. coli*) processes for producing adipic acid from sugars (**Figure 6.7**).
- Biocatalytic process using yeast converts sugars to *cis,cis*-muconic acid, and this intermediate stage allows ready access to adipic acid.
- Uses water as solvent at ambient temperature and pressure.

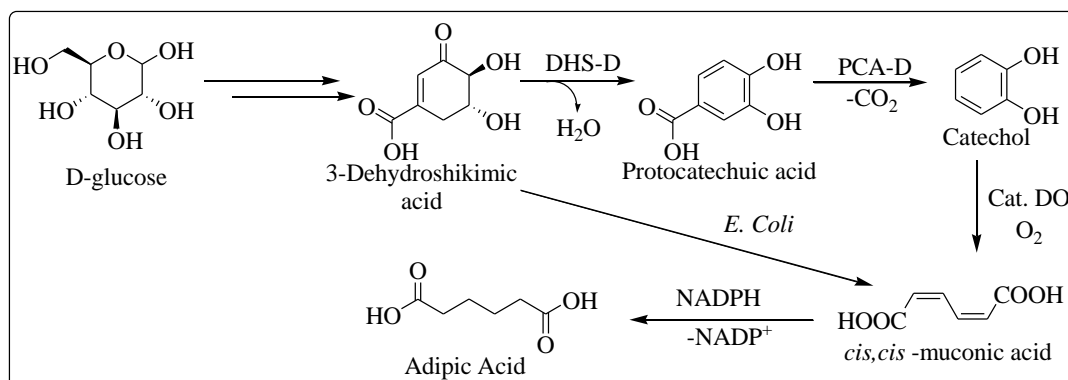


Figure 6.7: Green synthesis of adipic acid

C. Principle 4

Statement: Designing safe chemicals: Chemical products should be designed to preserve efficacy of the function while reducing toxicity.

Explanation:

The end product of a chemical synthesis not only should be safe and have particular effect but also should not have any toxic effect. For example, the drug Thalidomide was found to have a toxic effect when used to reduce morning sickness during pregnancy. It was also found that Thalidomide (**Figure 6.8**) was causing serious birth defects in the newborn child and subsequently the drug was banned. After intense investigation, it was found that the drug was administered as racemic mixture as it was obtained from synthesis. But only one enantiomer acts as effective drug candidate and the other enantiomer is toxic to the patient causing serious birth defects (**Figure 6.8**).

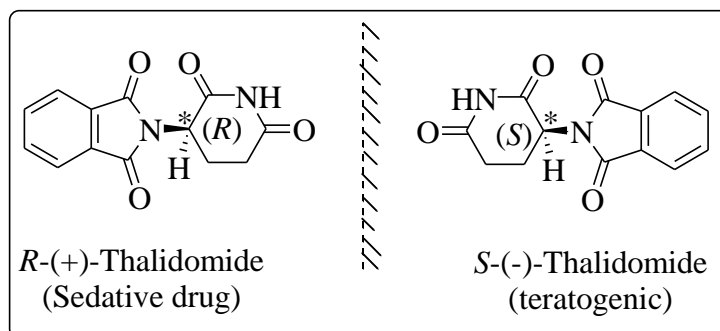


Figure 6.8: Chemical Structure of Thalidomide

D. Principle 5:

Statement:

The use of auxiliary substances (solvents, separating agents, *etc.*) should be made unnecessary whenever possible and, when used, innocuous.

Explanation: One of the most commonly used auxiliary substances in chemical synthesis is solvent in reactions and separating agent. In most of the cases volatile organic compounds like, methylene chloride (CH_2Cl_2), chloroform (CHCl_3), perchloroethylene ($\text{Cl}_2\text{C}=\text{CCl}_2$), carbon tetrachloride (CCl_4), benzene, toluene *etc.* are used as solvent.

And it has been reported that the halogenated solvent and the hydrocarbons show carcinogenic effects. Some of the compounds also have hazardous effect on the environment such as chlorofluorocarbons (CFCs), used as cleaning solvent or blowing agent in the refrigerator. These CFCs are known to be the main cause of depletion in the ozone layer above the earth.

The CFCs also have some serious health hazards to human beings. Some less harmful benign compounds are recently used as an alternative solvent to the above like water, supercritical Carbon Dioxide (scCO₂), ionic liquid (ILs), Polyethylene glycol (PEGs), Fluorous compounds *etc.* These benign compounds are known as **green solvents**.

Apart from that reaction should be design such a way that there is no need of any solvent (*i.e.*, solvent free reactions) or separation technique after the completion of reaction. For example, reaction involving Polymers supported reagent or substrates (e.g., Merrifield Synthesis of amino peptide).

E. Principle 6

Statement:

Energy requirements should be recognized for their environmental and economic impacts and should be minimized. Synthetic methods should be conducted at ambient temperature and pressure.

Explanation:

For any chemical reactions energy is required and this energy requirement should be minimised. For example, beginning from dissolving the starting material to the completion of the reaction energy is required. It should be ascertained that for a reaction to completion heating should be done for a minimum period of time and by continuous monitoring progress of the reaction like using TLC or online monitoring.

On the other hand, alternative source of energy *e.g.*, microwave heating, sonication, photochemical irradiation *etc.* can be used instead of thermal energy for carrying out Chemical synthesis (**Figure 6.9**)

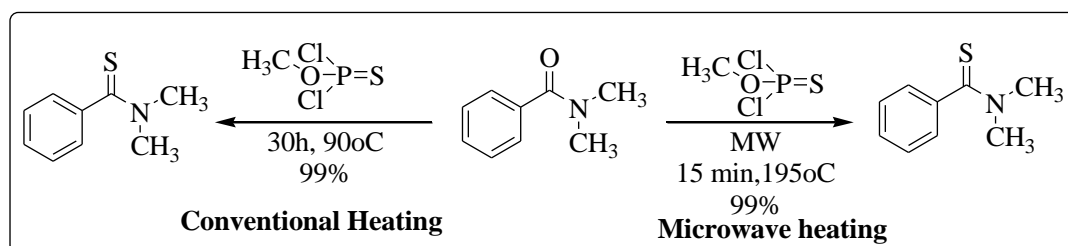


Figure 6.9: Comparison of Conventional Heating and Alternative Energy

F. Principle 7:

Statement:

A raw material or feedstock should be renewable rather than depleting whenever technically and economically practical.

Explanation:

Raw materials for any chemical process are obtained either from renewable sources or non-renewable sources. Like petroleum oil still now is the major source of energy production worldwide and it is a non-renewable resource for petrochemical industries as it is depleting sharply. And it is well known that replenishment of petroleum oil takes millions of years from animal and vegetable sources. On the other hand, agricultural wastes, biomass *etc.* can be a renewable feedstock for some petrochemical industry as it is cycling every year.

Biofuels, bioethanol and biogas can be generated from vegetable oils or domestic wastes which are renewable resources. National and international policies are being framed to promote use of alternative fuels for energy production. Production of levulinic acid from municipal wastes, agricultural wastes, paper mill wastes *etc.* by simple dilute acid hydrolysis at high temperature is one of the most important examples of use of renewable feedstock (**Figure 6.10**).

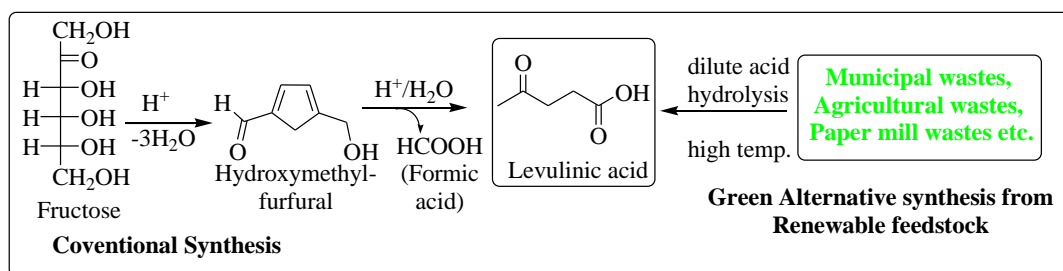


Figure 6.10: Synthesis of Levulinic acid from renewable feedstock

G. Principle 8:

Statement:

Unnecessary derivatization (blocking group, protection/deprotection, temporary modification of physical/chemical processes) should be avoided whenever possible.

Explanation:

Unnecessary derivatization (Protection-Deprotection & Temporary notification of physical and chemical processes) should be avoided whenever possible. The protection and deprotection is sometimes necessary to solve the chemo-selectivity problems in a chemical synthesis. But the protection-deprotection protocol increase the number of chemical steps as well as number of by-products (*i.e.* wastes), consequently increases the cost of production of a particular product. Therefore, our synthetic design for desired compound should be without protection- deprotection techniques or minimum numbers of it.

For example, conventional synthesis of 6-aminopenicillanic acid, core unit of penicillin uses 3 steps and intermediate products. Whereas these conversions can be carried out enzymatically in a single step with better efficiency (**Figure 6.11**).

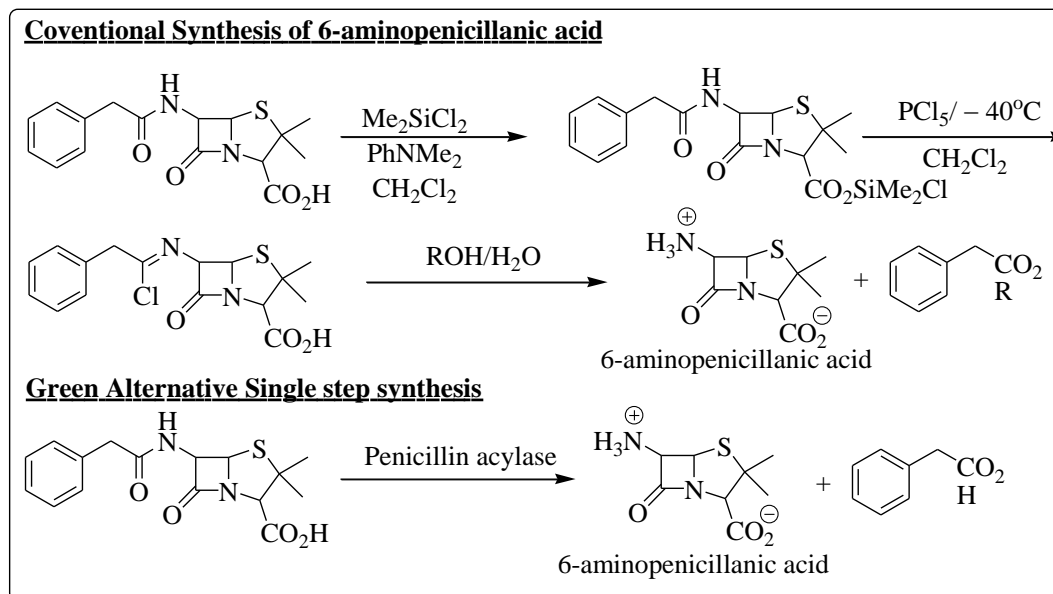


Figure 6.11: Fewer Step Synthesis 6-aminopenicillanic acid

H. Principle 9:

Statement:

Catalytic reagents (as selective as possible) are superior to stoichiometric reagents.

Explanation:

In most of the stoichiometric reactions all the starting materials are not consumed and the reaction does not go to completion. Stoichiometric reactions always generate large number of wastes in the form of unreacted starting material and by-products.

On the other hand, use of catalysts which are very selective in their action, increases the reaction efficiency and reduces the overall waste production by converting more numbers of reactant molecules into products in a chemical reaction.

Therefore, catalytic reactions are always preferable over the non-catalytic ones in the context of green of chemistry. It is environment friendly and cost effective for any industry.

For example, conventional synthesis of Disodium iminodiacetate (DSIDA) is carried out applying Strecker synthesis with HCHO, NH₃ and HCN (gas). It uses toxic HCN gas as well as produces large number of wastes.

On the other hand, Cu or ZrO₂ catalytic Monsanto method uses less harmful diethanolamine with less amount of waste generation (**Figure 6.12**).

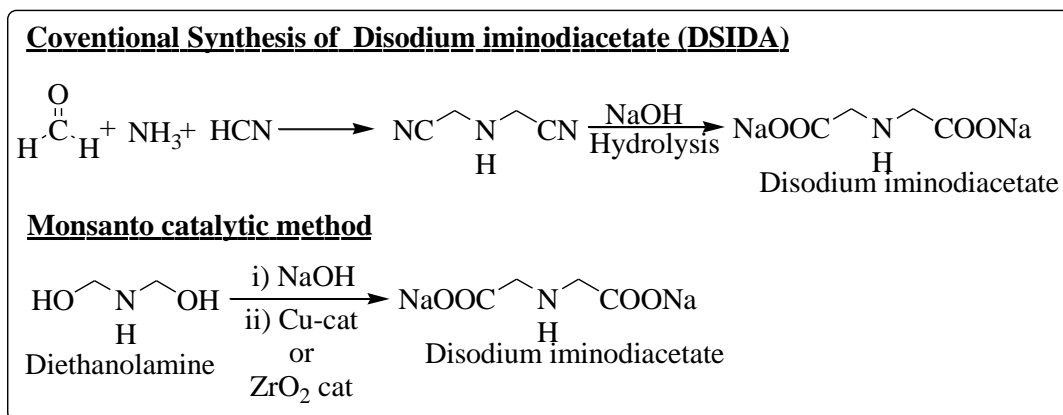


Figure 6.12: Catalytic Synthesis of Disodium Iminodiacetate (DSIDA)

I. Principle 10:

Statement:

A chemical product should be designed so that at the end of its practical particular function it does not persist in the environment rather will break down into an innocuous (less harmful) degradation product.

Explanation:

One of the most important aspects of green chemistry is that the end product of a chemical reaction should not be persisted but should be biodegradable. The persistent chemicals are not biodegradable and remain in the environment for a long period of time.

The accumulation of persistence chemicals by the living organism causes serious health problems to their existence on the earth. For example, plastics and pesticides like DDT, are the persistent chemical in the environment. DDT and plastics do not degrade to less harmful units rather remain in the environment year after years and causes serious health issues to the living organisms. So, an alternative to non-biodegradable polymer like plastic, polythene, terylene & Nylons, a biodegradable polymer (polypropylene carbonate) has been designed which degrades to innocuous products after its usual lifetime (**Figure 6.13**).

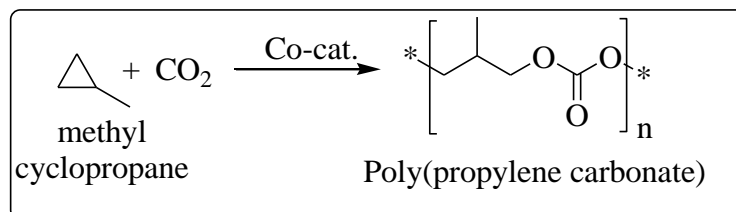


Figure 6.13: Synthesis of Biodegradable Polymer

J. Principle 11:

Statement:

Analytical methodologies need to be further developed to allow for real-time in-process monitoring and control prior to the formation of hazardous substances.

Explanation: Advanced analytical techniques need to be developed and applied online monitoring and control prior to the formation of hazardous substances. With the advancement of analytical tools, it is possible to find out the generation of hazardous intermediate chemicals or by-products in due course of a reaction. It is necessary to have reliable sensors, monitors and analytical techniques in a process stream to detect and characterise the harmful chemical entities during progress of a reaction. It is thus possible to monitor a chemical process and generation of hazardous by-products to prevent any chemical accident which may occur.

K. Principle 12:

Statement:

Substances and the form of substances used in a Chemical synthesis process should be chosen so as to minimise the potential for chemical accidents including release, explosion, and fire.

Explanation:

The episode of Bhopal gas tragedy in India, Seveso in Italy, Flixbourogh and many other causes deaths and disabilities in thousands of peoples. The use of volatile reagents and like (MIC in Bhopal gas tragedy) results in fires and explosion in some of the chemical industry.

Tragedy of Bhopal-1984:

Arguably the most tragic industrial accident in history is the Bhopal Gas Tragedy. Over 40 tons of methyl isocyanate (CH_3NC) was accidentally released while a reservoir tank overheated at a Union Carbide pesticide plant, located in the heart of the city of Bhopal. December 3, 1984 –toxic gas was leaked from a Union Carbide factory, killing thousands instantly and injuring many more (many of who died later of exposure). Up to 20,000 people have reported to be died as a result of exposure methyl isocyanate (3-8,000 instantly). More than 120,000 still suffer from ailments caused by exposure.

6.7 Conclusion:

Continuous growth of production of materials and subsequent waste formation is leading to a great threat to the environment and ecosystem. But the necessity of the materials in today's modern world urges the development of alternative less harmful and eco-friendly methods of production process over the existing ones.

Therefore, benign and environment friendly greener approaches to conventional production processes to the value-added consumable materials have been emerged as the best remedy to the uprising tremendous crisis to the environment and civilization. The guidelines to be followed for greener production processes causing less harm to environment and human civilization have been emerged as Twelve Principles of Green Chemistry postulated by P. Anastas & J. C. Warner.

6.8 Reference:

1. Carson, R. (2002). *Silent Spring* (First Mariner Books edition 2002). Mariner Books. ISBN 0-618-2 5305-x
2. Bandyopadhyay, C. K. (2019). *An Insight into Green Chemistry* (1st edition). Books and Allied (P) Ltd. ISBN:- 978-81-939848-7-1
3. Dey, S.P. & Sepay, N. (2022). *A Text Book of Green Chemistry* (1st edition). Techno World Publishers. ISBN 978-93-92145-03-2
4. Ahluwalia, V. K. (2013). *Green Chemistry A Text Book* (Fifth Reprint) Narosa Publishing House; ISBN : 978-81-8487-201-9

7. Green Chemistry: A Sustainable Approach to Chemistry

Jhinuk De

Degination,
Department of Chemistry,
National Institute of Technology,
Agartala, Tripura, India.

Abstract:

Green chemistry is a scientific outline and approach that intends to develop and design chemical approaches as well as products that are eco-friendly, financially practical, and also socially answerable. It includes the application of a collection of concepts, consisting of the plan of less harmful syntheses, the application of renewable feedstocks, energy efficiency, unused reduction, and the promotion of safer chemical items as well as procedures.

By following these concepts, environment-friendly chemistry pursues to reduce the adverse effect of chemical activities on human health as well as the environment, while also enhancing the efficiency as well as effectiveness of chemical process.

This book chapter provides an overview of the principles of green chemistry, its significance in assisting sustainability, as well as its applications in various areas such as syntheses, solvent selection, waste minimization, and life process valuation. It also highpoints the difficulties as well as future directions of green chemistry, consisting of the requirement for interdisciplinary collaborations, government plans, as well as public understanding. Ultimately, green chemistry provides a path towards a much better sustainable future, where chemistry plays an essential job underway economic growth, caring human wellness, and conserving the stability of our world.

Keywords:

pollution prevention, waste management, solvent less reaction, atom economy, catalysis.

7.1 Introduction:

In modern synthesis and industrial processes development of a clean technology for environmentally benign methodology for academia as well as the industry is a great challenge. Efforts are being made to design and discover synthetic protocols so that minimum or no hazardous and toxic materials are released in the environment due to the tight governmental legislation concerning impact of the released materials in human health and environment. Thus, design of environmentally friendly reaction has received tremendous attention in the area of green synthesis. The term Green Chemistry is coined by Prof. P. Anastas and Prof. John C. Warner.

7.2 Definition of the Green Chemistry by These 12 Principles:

7.2.1 Pollution Prevention:

It is better to prevent waste than to manage or clean up waste after it is formed. Respect less of the scale, using benign and also secure materials and techniques is regularly likely going to be useful.

7.2.2 Atom Economy:

Synthetic approaches need to be designed to maximize the incorporation of all building materials utilized while doing so into the end product. If an existing reaction provides a 75% yield with moderate byproducts, as well as an alternate synthesis accomplishes a significantly higher yield yet also minimizes the atom economic situation by a bigger quantity, after that the preliminary reaction might show more eco-friendly responsible.

7.2.3 Less Hazardous Chemical Synthesis:

Wherever practicable, synthetic methodologies ought to be designed to utilize as well as produce substances that possess little or no toxicity to human health and wellness and the environment.

7.2.4 Designing Safer Chemicals:

Chemical materials must be designed to protect effectiveness of function while minimizing toxicity.

7.2.5 Used Safer Solvents and Auxiliaries:

Using auxiliary substances (e.g., solvents, separation technique, etc) should be made attainable and also, harmless when made use of.

7.2.6 Design A Chemical Process for Energy Efficiency:

Energy needs to be recognized for their environmental as well as economic influences as well as must be minimized. Synthetic methods need to be carried out at ambient temperature and also pressure.

7.2.7 Use of Renewable Feed Stocks:

A raw material of feedstock must be sustainable rather than diminishing any place technically and also financially possible. The chemical sector's reliance on petroleum-based feedstocks must be dealt with. The timeline for depletion may be arguable; nonetheless, long term sustainable options need to be determined. Agricultural-based feedstocks offer guarantee as the isolation as well as purification technologies enhance.

7.2.8 Reduce Derivatives:

Unnecessary derivatization (blocking group, protection/deprotection, and temporary modification of physical/chemical processes) should be avoided whenever possible.

7.2.9 Catalysis of a Chemical Reaction:

Catalytic reagents (as selective as possible) are superior to stoichiometric reagents. In order to make transition state energies more accessible in a chemical transformation, the use of catalysts can be quite beneficial. There are countless examples of stoichiometric reactions that might have catalytic alternatives.

7.2.10 Design for Degradation - While Designing a New Chemical:

Chemical products should be designed so that at the end of their reaction they do not persist in the environment and break down into innocuous degradation products.

7.2.11 Real-Time Analysis for Pollution Avoidance:

Analytical methodologies need to be further developed to allow for real-time, in-process monitoring and control prior to the formation of hazardous substances.

7.2.12 Essentially Safer Chemistry for Accident Prevention:

Substances used in a chemical process should be chosen so as to minimize the potential for chemical accidents, including releases, explosions, and fires.

By adhering to these principles, chemists can minimize the negative impact of chemical activities on human health and the environment, while also improving the efficiency and profitability of chemical processes.

Green chemistry is not a solution to all environmental problems; but the most fundamental approach to preventing pollution. This means, Green Chemistry is safe, conserves raw materials and energy; more cost effective than conventional methods.

There are three main ways to make chemical processes 'greener':

- a. Re-design chemical process to use different, less hazardous starting materials,
- b. Use milder reaction conditions, better catalysts and less hazardous solvents;
- c. Follow production methods with fewer steps and higher atom economy;
- d. Use of catalysis wherever is possible.

However, it has been observed that catalysts employed are not always ecofriendly, some of them are costly or they may contain toxic heavy or transition metals. Therefore, not only volatile organic solvent but also the toxicity of reagents/catalysts also creates severe environmental damage during the process of waste disposal.

This prompted scientific community around the globe to develop new synthetic protocol of solvent free and ecofriendly catalytic reactions and industrial processes under modified experimental conditions towards development of real green methodology. In the national context, many National Institutes and University have taken initiatives to develop green protocols to save our mother earth.

7.3 Sustainable Synthesis and Manufacturing:

One of the key objectives of green chemistry is to develop efficient and sustainable synthetic routes for the production of chemicals and materials. This involves the use of innovative catalytic processes, such as bio-catalyst and organo catalyst, which can minimize energy requirements and reduce waste generation. Additionally, the utilization of renewable feedstocks, such as biomass-derived compounds, can help reduce the dependence on fossil fuels and promote a more sustainable chemical industry.

7.4 Solvent Selection and Design:

Solvents play a crucial role in chemical processes, but many traditional solvents are hazardous, volatile, and pose significant risks to human health and the environment. Green chemistry emphasizes the development and use of safer, non-toxic solvents, including water and bio-based solvents, which can offer comparable performance while minimizing environmental impacts. Furthermore, the concept of solvent less reactions, such as mechanochemistry and solid-state synthesis, can eliminate the need for solvents altogether, leading to greener and more sustainable processes.

7.5 What Is Solvent Free Reaction?

A solvent-free reaction may be carried out using the reactants alone or incorporating them in like clays, zeolite, silica, alumina and ionic liquid, solid support or other matrices.⁵ Thermal process or irradiation with UV, microwave or ultrasound can also be employed to bring about the reaction. Solvent-free reactions obviously reduce pollution and bring down handling costs due to simplification of experimental procedure, work up technique and saving in labor. These would be especially important during industrial production. Considering these advantages, reactions without use of conventional organic solvents have attracted the much attention to synthetic organic chemists.² Although a number of modern so-called green solvents, fluoruous media, ionic liquids and water have been extensively studied recently and considered as magical chemical due their unique properties, have a large variety of applications in all areas of the chemical industries.

7.6 Waste Minimization and Valorisation:

Traditional chemical processes often generate substantial amounts of waste, including harmful by-products and pollutants. Green chemistry focuses on waste minimization through process intensification, where reactions are conducted under milder conditions and with higher selectivity, leading to reduced waste generation. Additionally, waste valorisation techniques, such as recycling, reusing, and converting waste into valuable products or feedstocks, can help close the loop and transform waste into a resource.

7.7 Life Cycle Assessment and Sustainability Metrics:

Assessing the environmental impact of chemical products and processes is essential for ensuring their sustainability. Life Cycle Assessment (LCA) is a tool commonly used in green chemistry to evaluate the environmental performance of a product or process throughout its entire life cycle.

LCA considers all stages, from raw material extraction and production to product use and disposal, enabling scientists and engineers to identify areas for improvement and make informed decisions towards greener alternatives.

7.8 Green Chemistry in Industry and Academia:

Green chemistry has gained significant traction in both industrial and academic settings. Many companies have recognized the importance of integrating sustainable practices into their operations to reduce costs, enhance their public image, and comply with environmental regulations.

Academic institutions play a crucial role in advancing green chemistry through research, education, and the development of new methodologies. Collaboration between academia and industry is vital for the successful implementation of green chemistry principles and the translation of scientific discoveries into practical solutions.

7.9 Challenges and Future Directions:

While green chemistry has made substantial progress, several challenges remain. Developing sustainable alternatives for complex chemical processes, scaling up green technologies, and addressing the global nature of chemical production are ongoing endeavors.

Additionally, interdisciplinary collaborations, government policies, and public awareness are crucial for accelerating the adoption of green chemistry on a larger scale. Future directions in green chemistry include the exploration of emerging technologies, such as artificial intelligence and machine learning, to facilitate the design and discovery of sustainable chemicals and materials.

7.10 Conclusion:

Green chemistry offers a comprehensive and systematic approach to address the environmental and societal issues associated with chemical processes and products. By embracing the principles of green chemistry, we can pave the way for a more sustainable future, where chemistry plays a central role in advancing economic prosperity, protecting human health, and preserving the integrity of our planet.

Through continued research, innovation, and collaboration, we can transform the chemical industry and achieve a harmonious balance between human activities and the natural world.

7.11 References:

1. Anastas, P. T., & Warner, J. C. (1998). *Green chemistry: Theory and practice*. Oxford University Press.
2. Sheldon, R. A. (2007). *Green chemistry: Innovations and applications*. Wiley.
3. Trost, B. M. (2009). Green and sustainable chemistry: The first decade. *Angewandte Chemie International Edition*, 48(31), 5074-5080.
4. Worth, A. (2011). Green chemistry: Challenges and opportunities. *Chemical Society Reviews*, 40(12), 5623-5632.
5. Sheldon, R. A. *Green Chem.*, 2005, 7, 267.
6. Tanaka, K.; Toda, F. *Chem. Rev.*, 2000, 100, 1025.

8. Ceric Ammonium Nitrate: An Alternative Over Metal Catalysts for Multicomponent Synthesis

Vishwa Deepak Tripathi

Department of Chemistry,
C. M. Science College Darbhanga
(A Constituent unit of L. N. Mithilal University Darbhanga),
Bihar, India.

Sanjeev Kumar Jha

Department of Chemistry,
M. L. T. College Saharsa
(A Constituent unit of B. N. Mandal University Madhepura),
Bihar, India.

Abstract:

Libraries of benzoxanthenes as well as benzochromenes were efficiently synthesized via one-pot, three-component reactions of 2-naphthol, aldehydes, and cyclic 1,3-diketones/malononitrile/ethyl cyanoacetate in the presence of catalytic amount of ceric ammonium nitrate (CAN) under solvent free conditions. The protocol offers rapid synthesis of structurally diverse benzoxanthenes and benzochromenes for biologically screening. All the synthesized compounds were evaluated for their anti-proliferative activity and several compounds were exhibiting promising anti-proliferative activity.

Keywords:

Benzoxanthene; Benzochromene; CAN; Multi-component reactions; Anticancer.

8.1 Introduction:

Design of highly efficient chemical reaction sequences that provide maximum structural complexity and diversity with a minimum number of synthetic steps to assemble compounds with interesting properties is a major challenge of modern drug discovery¹. Recently multi-component reactions have emerged as a highly valuable synthetic tool in the context of modern drug discovery. The atom economy and convergent character, the simplicity of a one-pot procedure, the possible structural variations, the accessible complexity of the molecules, and the very large number of accessible compounds are among the described advantages of multi-component reactions². Thus, they are perfectly amenable to automation for combinatorial synthesis³⁻⁶. Benzoxanthenes and benzochromenes are important classes of biologically active heterocycles⁷. These compounds are being utilized as in photodynamic therapy as well as benzoxanthenes find application in laser technology⁸. Benzoxanthenes have also been employed as dyes⁹, pH sensitive fluorescent materials for visualization of biomolecules¹⁰⁻¹¹.

Many benzoxanthene derivatives are potent nonpeptidic inhibitors of recombinant human calpain I¹², and novel CCR1 receptor antagonists¹³. Benzochromenes are widely employed as pigments, cosmetics, potential agrochemicals, and also as components of many natural products¹⁴. Due to enormous biological and industrial importance associated with benzo(xanthenes)chromenes, various methods of their preparation have been reported. In our continuing efforts towards the developments of improved synthetic routes for biologically important heterocycles¹⁵ we report here a rapid and efficient synthesis of structurally diverse libraries of benzo(xanthenes)chromenes.

8.2 General Information:

Unless otherwise specified all the reagents and catalysts were purchased from Sigma-Aldrich and were used without further any purification. The common organic solvents were purchased from Ranbaxy. Organic solutions were concentrated under reduced pressure on a Büchi rotary evaporator. Chromatographic purification of products was accomplished using flash chromatography on 230-400 mesh silica gel. Reactions were monitored by thin-layer chromatography (TLC) on 0.25mm silica gel plates visualized under UV light, iodine or KMnO₄ staining. ¹H and ¹³C NMR spectra were recorded on a Bruker DRX -200 & 300 Mhz Spectrometer.

Chemical shifts (δ) are given in ppm relative to TMS and coupling constants (J) in Hz. IR spectra were recorded on a FT IR spectrophotometer Shimadzu 8201 PC and are reported in terms of frequency of absorption (cm⁻¹). Mass spectra (ESI MS) were obtained by Micromass Quattro II instrument.

A. General procedure for the synthesis of 12-substituted-9,10-dihydro-8H-benzo[a]xanthen-11(12H)-ones (4a-o): In a 25 ml round bottom flask, 2-naphthol (1 mmol), cyclic 1,3-diketone (1 mmol), aldehyde (1 mmol) and CAN (5 mol %) were taken. The reaction mixture was heated at 120 °C for 30 minutes under solvent free conditions. The reaction was followed by TLC monitoring. After completion, ethyl acetate was added to the reaction mixture and was shaken well to dissolve all organic compounds. Then it was filtered to remove CAN. The filtrate was concentrated and the crude obtained was purified by silica-gel column chromatography to yield pure compounds.

B. General procedure for the synthesis of 14-substituted-14H-dibenzo [a, j]xanthenes (5a-n): In a 25 ml round bottom flask, aldehyde (1 mmol), 2-naphthol (2 mmol), and CAN (5 mol %) were taken. The reaction mixture was stirred at 120 °C under solvent-free conditions for 30 minutes. After completion, the reaction mixture was cooled to room temperature and ethyl acetate was added and shaken well to dissolve all organic components then filtered to remove CAN. The filtrate was concentrated to yield crude which was purified by silica gel column chromatography.

C. General procedure for the synthesis of 3-amino-1-substituted-1H-benzo[f]chromenes (7a-k): In a 25 ml round bottom flask, aldehyde (1 mmol), 2-naphthol (1 mmol), malononitrile/ethyl cyanoacetate (1 mmol), and CAN (5 mol %) were taken. The reaction mixture was stirred at 120 °C under solvent-free conditions for 30 minutes. After completion, the reaction mixture was cooled to room temperature and ethyl acetate was

added and shaken well to dissolve all organic components then filtered to remove CAN. The filtrate was concentrated to yield crude which was purified by silica gel column chromatography.

8.3 Characterization Data for Synthesized Compounds:

9,9-dimethyl-12-phenyl-9,10-dihydro-8H-benzo[a]xanthen-11(12H)-one (4a). Mp 154-155 °C; ESI MS (m/z) = 355 [M+H]. IR (KBr, cm^{-1}): 3125, 2954, 1651, 1595, 1398, 1375, 1228, 1176, 1025, 808, 743, 699, 510. ^1H NMR (CDCl_3 , 300 MHz) δ = 0.96 (s, 3H), 1.11 (s, 3H), 2.27 (dd, J = 7.0 & 16.0 Hz, 2H), 2.57 (s, 2H), 5.71 (s, 1H), 7.03-7.06 (m, 1H), 7.15-7.18 (m, 2H), 7.31-7.44 (m, 5H), 7.75-7.78 (m, 2H), 7.99 (d, J = 8.5 Hz, 1H). ^{13}C NMR (CDCl_3 , 75 MHz) δ = 27.2, 29.3, 32.3, 34.7, 41.4, 50.9, 114.3, 117.0, 117.7, 123.7147.8, 124.9, 126.3, 127.0, 128.3, 128.4, 128.5, 128.9, 131.4, 131.5, 144.7, 163.9, 196.9. Elemental Analysis Calculated for $\text{C}_{25}\text{H}_{22}\text{O}_2$: C, 84.72; H, 6.26. Found: C, 84.75; H, 6.28.

12-(4-methoxyphenyl)-9,9-dimethyl-9,10-dihydro-8H-benzo[a]xanthen-11(12H)-one (4b). Mp 205-206 °C; ESI MS (m/z) = 385 [M+H]. IR (KBr, cm^{-1}): 3121, 2958, 1652, 1607, 1507, 1462, 1382, 1218, 1143, 1028, 834, 747, 661, 539. ^1H NMR (CDCl_3 , 300 MHz) δ = 0.97 (s, 3H), 1.11 (s, 3H), 2.27 (dd, J = 6.0 & 16.0 Hz, 2H), 2.56 (s, 2H), 3.68 (s, 3H), 5.65 (s, 1H), 6.69-6.71 (m, 2H), 7.24-7.45 (m, 5H), 7.74-7.78 (m, 2H), 7.98 (d, J = 8.5 Hz, 1H). ^{13}C NMR (75 MHz, CDCl_3) δ = 27.2, 29.3, 32.3, 33.9, 41.4, 50.9, 55.1, 113.6, 114.4, 117.1, 117.9, 123.7, 124.9, 127.0, 128.4, 128.7, 129.4, 131.4, 131.5, 137.2, 147.7, 157.8, 163.7, 197.0. Elemental Analysis Calculated for $\text{C}_{26}\text{H}_{24}\text{O}_3$: C, 81.22; H, 6.29. Found: C, 81.15; H, 6.20.

12-(4-chlorophenyl)-9,9-dimethyl-9,10-dihydro-8H-benzo[a]xanthen-11(12H)-one (4c). Mp 181-182 °C; ESI MS (m/z) = 389 [M+H]. IR (KBr, cm^{-1}): 3133, 2958, 1648, 1596, 1483, 1400, 1375, 1224, 1139, 1009, 841, 747, 535. ^1H NMR (CDCl_3 , 300 MHz) δ = 0.96 (s, 3H), 1.12 (s, 3H), 2.28 (dd, J = 8.5 & 16.0 Hz, 2H), 2.56 (s, 2H), 5.68 (s, 1H), 7.12-7.14 (m, 2H), 7.25-7.45 (m, 5H), 7.76-7.79 (m, 2H), 7.90 (d, J = 8.5 Hz, 1H). ^{13}C NMR (CDCl_3 , 75 MHz) δ = 27.1, 29.3, 32.3, 34.2, 41.4, 50.9, 113.9, 117.1, 123.5, 125.0, 127.2, 128.4, 128.5, 129.1, 129.8, 131.2, 131.5, 131.9, 143.3, 147.7, 164.1, 196.9. Elemental Analysis Calculated for $\text{C}_{25}\text{H}_{21}\text{ClO}_2$: C, 77.21; H, 5.44. Found: C, 77.12; H, 5.33.

12-(3,4-dimethylphenyl)-9,9-dimethyl-9,10-dihydro-8H-benzo[a]xanthen-11(12H)-one (4d). Mp 181-182 °C; ESI MS (m/z) = 383 [M+H]. IR (KBr, cm^{-1}): 3125, 2958, 1650, 1593, 1398, 1371, 1237, 1226, 1172, 819, 747, 478. ^1H NMR (CDCl_3 , 300 MHz) δ = 0.99 (s, 3H), 1.11 (s, 3H), 2.09 (s, 3H), 2.13 (s, 3H), 2.27 (dd, J = 4.0 & 16.0 Hz, 2H), 2.56 (dd, J = 2.5 & 17.5 Hz, 2H), 5.63 (s, 1H), 6.91 (d, J = 8.0 Hz, 1H), 7.03-7.10 (m, 2H), 7.25-7.43 (m, 3H), 7.72-7.77 (m, 2H), 8.04 (d, J = 8.5 Hz, 1H). ^{13}C NMR (CDCl_3 , 75 MHz) δ = 19.4, 20.0, 27.4, 29.2, 32.4, 34.3, 41.4, 51.0, 114.5, 117.1, 118.1, 123.8, 124.9, 125.9, 127.0, 128.4, 128.7, 129.5, 129.7, 131.5, 134.4, 136.2, 142.3, 147.7, 163.8, 196.2. Elemental Analysis Calculated for $\text{C}_{27}\text{H}_{26}\text{O}_2$: C, 84.78; H, 6.85. Found: C, 84.71; H, 6.80.

9,9-dimethyl-12-(3-nitrophenyl)-9,10-dihydro-8H-benzo[a]xanthen-11(12H)-one (4e). Mp 169-170 °C; ESI MS (m/z) = 400 [M+H]. IR (KBr cm^{-1}): 3125, 2954, 2864, 1649, 1596, 1529, 1375, 1344, 1225, 1025, 812, 748, 683, 510. ^1H NMR (CDCl_3 , 300 MHz) δ = 0.95 (s,

3H), 1.13 (s, 3H), 2.29 (dd, $J_1 = 13.0$ & 16.0 Hz, 2H), 2.61 (s, 2H), 5.82 (s, 1H), 7.35-7.47 (m, 4H), 7.79-8.12 (m, 6H). ^{13}C NMR (CDCl_3 , 75 MHz) $\delta = 27.1, 29.3, 32.3, 34.8, 41.4, 50.8, 113.1, 116.0, 117.3, 121.6, 123.1, 123.3, 125.2, 127.4, 128.7, 129.1, 129.7, 131.0, 131.6, 134.9, 146.8, 147.8, 148.4, 164.6, 196.8$. Elemental Analysis Calculated for $\text{C}_{25}\text{H}_{21}\text{NO}_4$: C, 75.17; H, 5.30; N, 3.51. Found: C, 75.08; H, 5.20; N, 3.38.

9,9-dimethyl-12-(thiophen-2-yl)-9,10-dihydro-8H-benzo[a]xanthen-11(12H)-one (4f). Mp 180-181 $^{\circ}\text{C}$; ESI MS (m/z) = 361 [M+H]. IR (KBr, cm^{-1}): 3105, 2958, 1651, 1593, 1376, 1224, 1177, 1147, 1009, 813, 746, 700, 661, 507. ^1H NMR (CDCl_3 , 300 MHz) $\delta = 1.05$ (s, 3H), 1.14 (s, 3H), 2.35 (s, 2H), 2.57 (s, 2H), 6.04 (s, 1H), 6.74-6.77 (m, 2H), 7.00-7.01 (m, 1H), 7.30-7.51 (m, 3H), 7.78-7.82 (m, 2H), 8.04 (d, $J = 8.5$ Hz, 1H). ^{13}C NMR (CDCl_3 , 75 MHz) $\delta = 27.2, 29.3, 29.4, 32.3, 41.4, 50.9, 113.8, 117.1, 117.2, 123.5, 124.0, 125.0, 125.1, 126.3, 127.2, 128.4, 129.1, 131.4, 147.8, 148.6, 164.6, 196.8$. Elemental Analysis Calculated for $\text{C}_{23}\text{H}_{20}\text{O}_2\text{S}$: C, 76.64; H, 5.59. Found: C, 76.55; H, 5.50.

12-tert-butyl-9,9-dimethyl-9,10-dihydro-8H-benzo[a]xanthen-11(12H)-one (4g). Mp 110-111 $^{\circ}\text{C}$; ESI MS (m/z) = 335 [M+H]. IR (KBr, cm^{-1}): 3125, 2962, 1642, 1592, 1394, 1220, 1176, 1005, 812, 750, 616, 490. ^1H NMR (CDCl_3 , 300 MHz) $\delta = 0.78$ (s, 9H), 1.14 (s, 3H), 1.27 (s, 3H), 2.28 (d, $J = 16.5$ Hz, 1H), 2.42 (d, $J = 16.5$ Hz, 1H), 2.52 (d, $J = 18.0$ Hz, 1H), 2.65 (d, $J = 18.0$ Hz, 1H), 4.62 (s, 1H), 7.28 (d, $J = 9.0$ Hz, 1H), 7.40-7.43 (m, 1H), 7.49-7.52 (m, 1H), 7.72 (d, $J = 9.0$ Hz, 1H), 7.80 (d, $J = 8.0$ Hz, 1H), 8.21 (d, $J = 9.0$ Hz, 1H). ^{13}C NMR (CDCl_3 , 75 MHz) $\delta = 27.4, 27.8, 30.1, 31.7, 35.9, 40.0, 41.6, 51.0, 113.9, 116.8, 118.4, 124.6, 126.0, 127.8, 128.2, 131.3, 132.7, 150.6, 167.6, 197.2$. Elemental Analysis Calculated for $\text{C}_{23}\text{H}_{26}\text{O}_2$: C, 82.60; H, 7.84. Found: C, 82.51; H, 7.71.

12-ethyl-9,9-dimethyl-9,10-dihydro-8H-benzo[a]xanthen-11(12H)-one (4h). Yellow oil; ESI MS (m/z) = 307 [M+H]. IR (Neat, cm^{-1}): 3130, 2960, 1651, 1595, 1394, 1225, 1177, 1145, 813, 748, 649, 480. ^1H NMR (CDCl_3 , 300 MHz) $\delta = 0.61$ (t, $J = 7.5$ Hz, 3H), 1.16 (s, 3H), 1.20 (s, 3H), 1.83-1.86 (m, 2H), 2.37 (d, $J = 4.5$ Hz, 2H), 2.55 (d, $J = 3.5$ Hz, 2H), 4.74 (t, $J = 4.0$ Hz, 1H), 7.20 (d, $J = 8.5$ Hz, 1H), 7.42-7.45 (m, 1H), 7.56-7.53 (m, 1H), 7.70 (d, $J = 9.0$ Hz, 1H), 7.82 (d, $J = 8.0$ Hz, 1H), 8.10 (d, $J = 8.0$ Hz, 1H). ^{13}C NMR (CDCl_3 , 75 MHz) $\delta = 9.0, 27.3, 27.4, 28.7, 29.7, 32.2, 41.4, 51.1, 112.1, 116.8, 117.7, 123.3, 124.8, 126.7, 128.0, 128.6, 131.2, 131.5, 148.7, 166.3, 197.6$. Elemental Analysis Calculated for $\text{C}_{21}\text{H}_{22}\text{O}_2$: C, 82.32; H, 7.24. Found: C, 82.22; H, 7.30.

12-(4-hydroxyphenyl)-9,9-dimethyl-9,10-dihydro-8H-benzo[a]xanthen-11(12H)-one (4i) Mp 210 $^{\circ}\text{C}$. ESI MS (m/z) = 371 (M+H). IR (KBr, cm^{-1}): 3223, 3071, 2957, 2870, 1631, 1590, 1511, 1449, 1380. ^1H NMR (CDCl_3 , 300 MHz) $\delta = 0.97$ (s, 3H), 1.11 (s, 3H), 2.18-2.36 (m, 2H), 2.57 (s, 2H), 5.65 (s, 1H), 6.61 (d, $J = 8.5$ Hz, 2H), 6.98 (s, 1H), 7.17 (d, $J = 9.0$ Hz, 2H), 7.31-7.44 (m, 3H), 7.75-7.80 (m, 2H), 7.99 (d, $J = 8.3$ Hz, 1H). ^{13}C NMR (CDCl_3 , 75 MHz) $\delta = 27.1, 29.2, 32.3, 33.9, 41.4, 50.8, 114.5, 115.4, 116.9, 117.9, 123.8, 124.9, 126.9, 128.3, 128.7, 129.5, 131.4, 131.5, 136.4, 147.5, 154.5, 164.5, 198.2$. Elemental Analysis calculated for $\text{C}_{25}\text{H}_{22}\text{O}_3$: C, 81.06; H, 5.99. Found C, 80.96; H, 5.90.

12-phenyl-9,10-dihydro-8H-benzo[a]xanthen-11(12H)-one (4j). Mp 202-203 $^{\circ}\text{C}$; ESI MS (m/z) = 327 (M+H). IR (KBr, cm^{-1}): 3129, 3052, 2954, 1645, 1594, 1453, 1373, 1229, 1189, 999, 955, 816, 758, 701, 531. ^1H NMR (CDCl_3 , 300 MHz) $\delta = 1.96$ -2.06 (m, 2H),

2.34-2.47 (m, 2H), 2.66-2.75 (m, 2H), 5.74 (s, 1H), 7.04-7.08 (m, 1H), 7.15-7.18 (m, 2H), 7.32-7.43 (m, 5H), 7.75-7.78 (m, 2H), 7.96 (d, $J = 8.5$ Hz, 1H). ^{13}C NMR (CDCl_3 , 75 MHz) $\delta = 20.3, 27.8, 34.7, 37.1, 115.6, 117.0, 117.7, 123.7, 124.9, 126.3, 127.0, 128.3, 128.4, 128.5, 128.9, 131.4, 131.5, 145.1, 147.8, 165.6, 197.1$. Elemental Analysis Calculated for $\text{C}_{23}\text{H}_{18}\text{O}_2$: C, 84.64; H, 5.56. Found: C, 84.50; H, 5.48.

12-(4-chlorophenyl)-9,10-dihydro-8H-benzo[a]xanthen-11(12H)-one (4k). Mp 208-209 $^{\circ}\text{C}$; ESI MS (m/z) = 313 (M+H). IR (KBr, cm^{-1}): 3130, 3052, 2962, 1647, 1593, 1488, 1368, 1228, 1189, 1139, 1089, 1000, 954, 818, 753, 530. ^1H NMR (CDCl_3 , 300 MHz) $\delta = 1.93$ -2.08 (m, 2H), 2.35-2.48 (m, 2H), 2.63-2.76 (m, 2H), 5.72 (s, 1H), 7.12-7.16 (m, 2H), 7.25-7.44 (m, 5H), 7.76-7.79 (m, 2H), 7.88 (d, $J = 8.5$ Hz, 1H). ^{13}C NMR (CDCl_3 , 75 MHz) $\delta = 20.3, 27.8, 34.2, 37.0, 115.1, 117.0, 117.1, 123.5, 125.1, 127.1, 128.5, 129.1, 129.9, 131.2, 131.5, 132.0, 143.6, 147.8, 165.8, 197.1$. Elemental Analysis Calculated for $\text{C}_{23}\text{H}_{17}\text{ClO}_2$: C, 76.56; H, 4.75. Found: C, 76.42; H, 4.68.

12-(3,4-dimethylphenyl)-9,10-dihydro-8H-benzo[a]xanthen-11(12H)-one (4l). Mp 174-175 $^{\circ}\text{C}$; ESI MS (m/z) = 355 [M+H]. IR (KBr, cm^{-1}): 3121, 2962, 2933, 1651, 1594, 1373, 1225, 1190, 1140, 997, 955, 821, 747, 617, 495, 459. ^1H NMR (CDCl_3 , 300 MHz) $\delta = 1.97$ -2.07 (m, 2H), 2.11 (s, 3H), 2.14 (s, 3H), 2.34-2.48 (m, 2H), 2.62-2.77 (m, 2H), 5.67 (s, 1H), 6.92 (d, $J = 7.5$ Hz, 1H), 7.03-7.09 (m, 2H), 7.32-7.44 (m, 3H), 7.74-7.78 (m, 2H), 7.99 (d, $J = 8.5$ Hz, 1H). ^{13}C NMR (CDCl_3 , 75 MHz) $\delta = 19.3, 19.9, 20.3, 27.8, 34.2, 37.1, 115.9, 117.0, 118.1, 123.8, 124.8, 125.9, 127.0, 128.3, 128.6, 129.5, 129.7, 131.4, 131.5, 134.4, 136.3, 142.6, 147.8, 165.5, 197.0$. Elemental Analysis Calculated for $\text{C}_{25}\text{H}_{22}\text{O}_2$: C, 84.72; H, 6.26. Found: C, 84.60; H, 6.15.

11-phenyl-8,9-dihydrobenzo[f]cyclopenta[b]chromen-10(11H)-one (4m). Mp 237-238 $^{\circ}\text{C}$; ESI MS (m/z) = 313 (M+H). IR (KBr, cm^{-1}): 3391, 3125, 1705, 1667, 1596, 1377, 1232, 1101, 1011, 942, 811, 747, 696, 528, 509. ^1H NMR (CDCl_3 , 300 MHz) $\delta = 2.45$ -2.55 (m, 2H), 2.73-2.84 (m, 2H), 5.58 (s, 1H), 7.09-7.12 (m, 1H), 7.18-7.21 (m, 2H), 7.26-7.28 (m, 2H), 7.38-7.40 (m, 3H), 7.77-7.84 (m, 3H). ^{13}C NMR (CDCl_3 , 75 MHz) $\delta = 25.4, 33.8, 36.0, 116.1, 117.4, 118.9, 124.2, 125.2, 126.6, 127.2, 128.2, 128.4, 128.5, 129.6, 131.7, 131.8, 143.6, 149.2, 177.1, 202.5$. Elemental Analysis Calculated for $\text{C}_{22}\text{H}_{16}\text{O}_2$: C, 84.59; H, 5.16. Found: C, 84.48; H, 5.09.

11-(4-chlorophenyl)-8,9-dihydrobenzo[f]cyclopenta[b]chromen-10(11H)-one (4n). Mp 233-234 $^{\circ}\text{C}$; ESI MS (m/z) = 347 (M+H). IR (KBr, cm^{-1}): 3426, 3131, 1699, 1658, 1396, 1233, 1088, 1013, 9445, 819, 744, 527. ^1H NMR (CDCl_3 , 300 MHz) $\delta = 2.45$ -2.56 (m, 2H), 2.75-2.84 (m, 2H), 5.55 (s, 7.82-7.85 (m, 2H), 1H), 7.15-7.21 (m, 4H), 7.38-7.41 (m, 3H), 7.69-7.71 (m, 1H). ^{13}C NMR (100 MHz, CDCl_3) $\delta = 25.4, 33.8, 35.5, 115.5, 117.4, 118.3, 124.0, 125.3, 127.3, 128.6, 128.7, 129.5, 129.9, 131.6, 131.8, 132.4, 142.0, 149.2, 177.2, 202.4$. Elemental Analysis Calculated for $\text{C}_{22}\text{H}_{15}\text{ClO}_2$: C, 76.19; H, 4.36. Found: C, 76.07; H, 4.28.

11-(3,4-dimethylphenyl)-8,9-dihydrobenzo[f]cyclopenta[b]chromen-10(11H)-one (4o). Mp 223-224 $^{\circ}\text{C}$; ESI MS (m/z) = 313 (M+H). IR (KBr, cm^{-1}): 3407, 3131, 1709, 1670, 1591, 1396, 1237, 943, 825, 746, 498. ^1H NMR (CDCl_3 , 300 MHz) $\delta = 2.12$ (s, 3H), 2.13 (s, 3H), 2.47-2.50 (m, 2H), 2.75-2.79 (m, 2H), 5.50 (s, 1H), 6.93-7.03 (m, 3H), 7.36-7.40 (m, 3H), 7.79-7.83 (m, 3H). ^{13}C NMR (CDCl_3 , 75 MHz) $\delta = 19.4, 19.9, 25.3, 33.8, 35.5, 116.5, 117.4,$

119.2, 124.2, 125.1, 125.5, 127.1, 128.4, 129.3, 129.4, 129.7, 131.8, 131.9, 134.8, 136.6, 141.2, 149.2, 177.1, 202.5. Elemental Analysis Calculated for C₂₄H₂₀O₂: C, 84.68; H, 5.92. Found: C, 84.56; H, 5.85.

14-phenyl-14H-dibenzo[a,j]xanthene (5a). Mp 181 °C; ESI MS (*m/z*) = 359 (M+H). IR (KBr, cm⁻¹): 3024, 1590, 1410, 1245. ¹H NMR (CDCl₃, 300 MHz) δ = 6.49 (s, 1H), 6.98 (t, *J* = 7.6 Hz, 1H), 7.12 (t, *J* = 7.6 Hz, 2H), 7.38 (t, *J* = 7.6 Hz, 2H), 7.48 (d, *J* = 8.8 Hz, 2H), 7.52 (d, *J* = 7.6 Hz, 2H), 7.55 (t, *J* = 7.6 Hz, 2H), 7.77 (d, *J* = 8.8 Hz, 2H), 7.83 (d, *J* = 8.0 Hz, 2H), 8.40 (d, *J* = 8.4 Hz, 2H). Elemental Analysis Calculated for C₂₇H₁₈O: C, 90.47; H, 5.06. Found: C, 90.35; H, 4.94.

14-(3-Hydroxyphenyl)-14H-dibenzo [a,j] xanthene (5b). Mp 261-263 °C; ESI MS (*m/z*) = 375 (M+H). IR (KBr, cm⁻¹): 3446, 1620, 1588, 1247, 961, 816, 745, 694. ¹H NMR (DMSO-d₆, 200 MHz) δ = 6.41 (s, 1H), 6.79-7.11 (m, 3H), 7.35-7.86 (m, 12H), 8.44 (d, *J* = 9.6 Hz, 2H), 8.84 (bs, 1H). ¹³C NMR (DMSO-d₆, 75 MHz) δ = 36.40, 113.32, 114.89, 117.53, 117.60, 118.90, 123.36, 124.36, 126.73, 128.43, 128.77, 129.00, 130.86, 131.12, 146.70, 147.88, 157.31. Elemental Analysis Calculated for C₂₇H₁₈O₂: C, 86.61; H, 4.85. Found: C, 86.55; H, 4.88.

14-(4-Methoxyphenyl)-14H-dibenzo [a,j] xanthene (5c). Mp 213-215 °C; ESI MS (*m/z*) = 389 (M+H). IR (KBr, cm⁻¹): 2999, 2833, 1734, 1591, 1508, 1457, 1430, 1399, 1247, 1027, 958, 829, 807, 740. ¹H NMR (CDCl₃, 200 MHz) δ = 3.58 (s, 3H), 6.40 (s, 1H), 6.65 (d, *J* = 9.7 Hz, 2H), 7.32-7.85 (m, 12H), 8.35 (d, *J* = 9.6 Hz, 2H). ¹³C NMR (CDCl₃, 50 MHz) δ = 36.9, 53.2, 114.3, 117.2, 118.3, 123.5, 124.1, 127.4, , 129.1, 129.4, 131.4, 133.7, 137.2, 149.3, 158.2. Elemental Analysis Calculated for C₂₈H₂₀O₂: C, 86.57; H, 5.19. Found: C, 86.41; H, 5.20.

14-(4-Methylphenyl)-14H-dibenzo [a,j] xanthene (5d). Mp 238-240 °C; ESI MS (*m/z*) = 373 (M+H). IR (KBr, cm⁻¹): 3020, 2908, 1620, 1591, 1509, 1457, 1430, 1247, 959, 837, 810, 739. ¹H NMR (CDCl₃, 200 MHz) δ = 2.18 (s, 3H), 6.39 (s, 1H), 6.90 (d, *J* = 9.6 Hz, 2H), 7.32-7.80 (m, 12H), 8.36 (d, *J* = 9.4 Hz, 2H). ¹³C NMR (CDCl₃, 50 MHz) δ = 19.1, 35.4, 115.7, 116.2, 121.3, 122.7, 125.2, 126.4, 127.4, 129.2, 129.5, 134.0, 140.8, 146.6. Elemental Analysis Calculated for C₂₈H₂₀O: C, 90.29; H, 5.41. Found: C, 90.32; H, 5.44.

14-(2-chlorophenyl)-14H-dibenzo[a,j]xanthene (5e). Mp 213–215 °C; ESI MS (*m/z*) = 393 (M+H). IR (KBr, cm⁻¹): 3059, 1625, 1594, 1516, 1462, 1404, 1248. ¹H NMR (CDCl₃, 300 MHz): d 6.82 (s, 1H), 6.92 (m, 2H), 7.25-7.27 (m, 1H), 7.37–7.65 (m, 8H), 7.79-7.84 (m, 4H), 8.75 (d, *J* = 8.5 Hz, 1H). Elemental Analysis Calculated for C₂₇H₁₇ClO: C, 82.54; H, 4.36. Found: C, 82.44; H, 4.25.

14-(4-(3-chloropropoxy) phenyl)-14H-dibenzo[a,j]xanthene (5f). Mp 158 °C; ESI MS (*m/z*) = 451 (M+H). IR (KBr, cm⁻¹): 3065, 2912, 2846, 1590, 1509, 1399, 1378, 1250, 1182. ¹H NMR (CDCl₃, 300 MHz) δ = 1.98-2.17 (m, 2H), 3.42 (t, *J* = 6.4 Hz, 1H), 3.57 (t, *J* = 6.4Hz, 1H), 3.79-3.87 (m, 2H), 6.46 (s, 1H), 6.64 (d, *J* = 8.7 Hz, 2H), 7.41-7.59 (m, 8H), 7.62-7.83 (m, 4H), 8.39 (d, *J* = 8.5 Hz, 2H). ¹³C NMR (CDCl₃, 75 MHz) δ = 32.6, 37.5, 41.9, 64.4, 114.8, 117.9, 118.4, 123.1, 124.6, 127.2, 129.2, 129.2, 129.6, 131.5, 131.8,

138.0, 149.1, 157.4. Elemental Analysis Calculated for C₃₀H₂₃ClO₂: C, 79.90; H, 5.14. Found: C, 79.82; H, 5.05.

14-(4-chlorophenyl)-14H-dibenzo[a,j]xanthene (5g). Mp 286-288 °C; ESI MS (*m/z*) = 393 (M+H). IR (KBr, cm⁻¹): 3026, 2914, 1621, 1590, 1241. ¹H NMR (CDCl₃, 300 MHz) δ = 6.42 (s, 1H), 7.10 (d, *J* = 9.6 Hz, 2H), 7.62–7.30 (m, 12H), 8.30 (d, *J* = 9.4 Hz, 2H). ¹³C NMR (CDCl₃, 75 MHz) δ = 35.4, 116.5, 117.2, 122.8, 124.1, 126.6, 127.9, 128.2, 128.8, 129.2, 130.2, 147.5. Elemental Analysis Calculated for C₂₇H₁₇ClO: C, 82.54; H, 4.36. Found: C, 82.44; H, 4.25.

14-(2,4-dichlorophenyl)-14H-dibenzo[a,j]xanthene (5h). Mp 252 °C; ESI MS (*m/z*) = 427 (M+H). IR (KBr, cm⁻¹): 3066, 2933, 1619, 1592, 1248. ¹H NMR (CDCl₃, 300 MHz) δ = 6.71 (s, 1H), 6.90 (d, *J* = 9.5 Hz, 1H), 7.23-7.82 (m, 12H), 8.60 (d, *J* = 9.5 Hz, 2H). ¹³C NMR (CDCl₃, 75 MHz) δ = 42.8, 125.8, 126.8, 131.6, 132.9, 133.3, 135.4, 135.8, 137.0, 137.6, 138.9, 139.6, 140.1, 141.4, 150, 157.5. Elemental Analysis Calculated for C₂₇H₁₆Cl₂O: C, 75.89; H, 3.77. Found: C, 75.78; H, 3.68.

14-(3-Fluorophenyl)-14H-dibenzo [a,j] xanthene (5i). Mp 259 °C; ESI MS (*m/z*) = 377 (M+H). IR (KBr, cm⁻¹): 3154, 1594, 1403, 1240, 1207, 1069, 817, 747; ¹H NMR (CDCl₃, 300 MHz) δ = 6.51 (s, 1H) 6.72–8.38 (m, 16H); ¹³C NMR (CDCl₃, 75 MHz) δ = 38.1, 113.8 and 114.0 (J_{C-F} 21.5 Hz), 115.6 and 115.9 (J_{C-F} 21.5 Hz), 117.1, 118.2, 122.9, 124.31 and 124.34 (J_{C-F} 2.8 Hz), 124.8, 127.4, 129.3, 129.5, 130.1 and 130.2 (J_{C-F} 8.3 Hz), 131.5, 131.7 (J_{C-F} 19.4 Hz), 147.8, 147.9 (J_{C-F} 6.2 Hz), 149.2, 161.7, 165.0; Elemental Analysis Calculated for C₂₇H₁₇FO: C, 86.15; H, 4.55; F, 5.05. Found: C, 86.11; H, 4.54, F, 5.07.

14-(2-Nitrophenyl)-14H-dibenzo[a,j]xanthene (5j). Mp 293 °C; ESI MS (*m/z*) = 404 (M+H). IR (KBr, cm⁻¹): 3400, 3058, 1593, 1523, 1350, 1240, 1142, 810, 748; ¹H NMR (CDCl₃, 300 MHz) δ = 7.52 (s, 1H) 7.10-8.56 (m, 16H); ¹³C NMR (CDCl₃, 75 MHz) δ = 32.9, 118.0, 118.4, 123.0, 124.6, 125.0, 125.3, 127.8, 128.0, 129.4, 129.5, 129.9, 130.8, 132.1, 132.6, 134.5, 141.3, 147.5, 149.8; Elemental Analysis Calculated for C₂₇H₁₇NO₃: C, 80.38; H, 4.25; N, 3.47. Found: C, 80.25; H, 4.24, N, 3.57.

14-(3-trifluoromethylphenyl)-14-H-3,11-dibromodibenzo[a,j]xanthene (5k). Mp 202-204 °C; ESI MS (*m/z*) = 582 (M+H). ¹H NMR (CDCl₃, 300 MHz) δ = 6.41 (s, 1H), 7.25-7.30 (m, 2H), 7.50 (d, *J* = 8.8 Hz, 2H), 7.61-7.73 (m, 6H), 7.99 (d, 2H, *J* = 1.8 Hz), 8.14 (d, *J* = 8.8 Hz, 2H). ¹³C NMR (CDCl₃, 75MHz) δ = 37.9, 116.4, 118.5, 119.2, 123.8, 123.9, 124.4, 124.5, 125.2, 128.6, 129.3, 129.7, 130.3, 130.8, 131.0, 131.1, 131.4, 132.3, 145.3, 148.8. Elemental Analysis Calculated for C₂₈H₁₅Br₂F₃O: C, 57.56; H, 2.59. Found: C, 57.47; H, 2.65.

14-isopropyl-14H-dibenzo[a,j]xanthene (5l). Mp 155 °C; ESI MS (*m/z*) = 325 (M+H). IR (KBr, cm⁻¹): 1622, 1591, 1515, 1457, 1240. ¹H NMR (CDCl₃, 200 MHz) δ = 8.26 (d, *J* = 8.0 Hz, 2H), 7.90-7.72 (m, 4H), 7.61-7.49 (m, 2H), 7.43-7.32 (m, 4H), 5.42 (d, *J* = 7.0 Hz, 1H), 2.28 (m, 1H), 0.81 (d, *J* = 7.0 Hz, 6H). Elemental Analysis Calculated for C₂₄H₂₀O: C, 88.85; H 6.21. Found: C, 88.78; H, 6.15.

14-benzyl-14H-dibenzo[a,j]xanthene (5m). Mp 178 °C; ESI MS (m/z) = 373 (M+H). IR (KBr, cm^{-1}): 3061, 3019, 1617, 1587, 1511, 1488, 1451, 1397, 1241. ^1H NMR (CDCl_3 , 300 MHz) δ = 3.27 (d, J = 4.7 Hz, 2H), 5.80 (t, J = 4.7 Hz, 1H), 6.12 (d, J = 9.0 Hz, 2H), 6.84-7.20 (m, 5H), 7.45-7.91 (m, 8H), 8.25 (d, J = 9.0 Hz, 2H); ^{13}C NMR (CDCl_3 , 75 MHz) δ = 33.0, 41.33, 115.27, 117.39, 122.18, 124.10, 126.10, 126.68, 127.18, 128.35, 128.88, 129.76, 130.84, 131.30, 137.55, 150.11; Elemental Analysis Calculated for $\text{C}_{28}\text{H}_{20}\text{O}$: C, 90.33; H, 5.37; found: C, 90.27; H, 5.37

14-propyl-14H-dibenzo[a,j]xanthene (5n). Mp 152 °C; ESI MS (m/z) = 325 (M+H). IR (KBr): 3066, 2961, 2874, 1623, 1591, 1518, 1488, 1461, 1434, 1400, 1245 cm^{-1} ; ^1H NMR (CDCl_3 , 300 MHz) δ = 0.62 (t, J = 7.2 Hz, 3H), 1.04 (m, 2H), 2.03 (m, 2H), 5.58 (t, J = 4.6 Hz, 1H), 7.40 (d, J = 8.8 Hz, 2H), 7.45-7.66 (m, 4H), 7.79 (d, J = 8.8 Hz, 2H), 7.89 (d, J = 7.7 Hz, 2H), 8.27 (d, J = 8.5 Hz, 2H); ^{13}C NMR (CDCl_3 , 75 MHz) δ = 14.8, 20.20, 42.0, 43.10, 115.40, 118.60, 122.48, 123.40, 126.24, 128.3, 128.48, 128.80, 133.60, 150.3; Elemental Analysis Calculated for $\text{C}_{24}\text{H}_{20}\text{O}$: C, 88.85; H, 6.21; found: C, 88.90; H, 6.12.

3-amino-1-(4-nitrophenyl)-1H-benzo[f]chromene-2-carbonitrile (7a). Mp 190 °C; ESI MS (m/z) = 344 (M+H). IR (KBr, cm^{-1}): 3429, 3331, 2190. ^1H NMR (DMSO-d_6 , 300 MHz) δ = 5.56 (s, 1H), 7.16 (bs, 2H), 7.37 (d, J = 9.0 Hz, 1H), 7.40-7.50 (m, 2H), 7.47 (d, J = 8.5 Hz, 2H), 7.71-8.00 (m, 2H), 7.98 (d, J = 9.0 Hz, 1H), 8.15 (d, J = 8.5 Hz, 2H); Elemental Analysis Calculated for $\text{C}_{28}\text{H}_{20}\text{O}$: C, 69.96; H, 3.82; N, 12.24. Found: C, 69.89; H, 3.71; N, 12.10.

3-amino-1-(1H-indol-3-yl)-1H-benzo[f]chromene-2-carbonitrile (7b). Mp 220 °C; ESI MS (m/z) = 336 (M+H). IR (KBr, cm^{-1}): 3420, 3215, 2155, 1648, 1538. ^1H NMR (CDCl_3 , 200 MHz) δ = 3.82 (s, 1H), 7.01 (bs, 2H), 7.40-7.81 (m, 11H), 10.30 (s, 1H). Elemental Analysis Calculated for $\text{C}_{27}\text{H}_{17}\text{NO}_3$: C, 78.32; H, 4.48; N, 12.46. Found: C, 78.25; H, 4.34, N, 12.59.

3-Amino-1-(4-fluorophenyl)-9-methoxy-1H-benzo[f]-chromene-2-carbonitrile (7c). Mp 238–239 °C; ESI MS (m/z) = 347 (M+H). IR (KBr, cm^{-1}): 3465, 3359, 2183, 1662, 1654, 1592, 1509, 1408, 1239, 1218, 827. ^1H NMR (CDCl_3 , 300 MHz) δ = 3.69 (s, 3H), 4.52 (s, 2H), 5.12 (s, 1H), 6.85 (s, 1H), 6.96 (t, J = 8.2 Hz, 2H), 7.02-7.19 (m, 4H), 7.70 (t, J = 8.2 Hz, 2H); ^{13}C NMR (CDCl_3 , 75 MHz) δ = 37.8, 55.5, 58.3, 103.6, 114.5, 115.1, 115.7, 116.0, 117.3, 121.0, 126.5, 129.5, 129.6, 130.5, 132.1, 142.5, 147.7, 158.5, 159.6, 160.1, 162.9. Elemental Analysis Calculated for $\text{C}_{21}\text{H}_{15}\text{FN}_2\text{O}_2$: C, 72.82; H, 4.37; N, 8.09. Found: C, 72.70; H, 4.40; N, 8.10;

3-Amino-1-(4-fluorophenyl)-1H-benzo[f]chromene-2-carbonitrile (7d). Mp 237–238 °C; ESI MS (m/z) = 317 (M+H). ^1H NMR (CDCl_3 , 300 MHz) δ = 4.62 (s, 2H), 5.24 (s, 1H), 6.94 (t, J = 8.6 Hz, 2H), 7.12-7.17 (m, 2H), 7.25 (d, J = 6.8 Hz, 1H), 7.40 (dd, J = 2.8 Hz, 2H), 7.63-7.65 (m, 1H), 7.80-7.83 (m, 2H). Elemental Analysis Calculated for $\text{C}_{20}\text{H}_{13}\text{FN}_2\text{O}$: C, 75.94; H, 4.14; N, 8.86. Found: C, 76.00; H, 4.02; N, 8.72.

3-Amino-1-(furan-2-yl)-1H-benzo[f]chromene-2-carbonitrile (7e). Mp 225–226 °C; ESI MS (m/z) = 289 (M+H). ^1H NMR (CDCl_3 , 300 MHz) δ = 5.48 (s, 1H), 6.22-6.30 (m, 2H), 7.08 (s, 2H), 7.27 (d, J = 9.2 Hz, 1H), 7.42-7.54 (m, 3H), 7.91 (d, J = 8.9 Hz, 2H), 8.03 (d,

$J = 8.5$ Hz, 1H). Elemental Analysis Calculated for $C_{18}H_{12}N_2O_2$: C, 74.99; H, 4.20; N, 9.72. Found: C, 75.05; H, 4.12; N, 9.60.

3-Amino-1-pentyl-1H-benzo[f]chromene-2-carbonitrile (7f). Colourless oil. ESI MS (m/z) = 293 (M+H). 1H NMR ($CDCl_3$, 300 MHz) $\delta = 0.79-0.83$ (t, $J = 6.1$ Hz, 3H), 1.21-1.46 (m, 6H), 7.44-7.59 (m, 2H), 1.79-1.82 (m, 2H), 4.25 (t, $J = 8.7$ Hz, 1H), 4.68 (s, 2H), 7.14 (d, $J = 9.2$ Hz, 1H), 7.71 (d, $J = 8.6$ Hz, 1H), 7.81-7.91 (m, 2H). Elemental Analysis Calculated for $C_{19}H_{20}N_2O$: C, 78.05; H, 6.89; N, 9.58. Found: C, 77.92; H, 6.82; N, 9.45.

3-Amino-1-phenyl-1H-benzo[f]chromene-2-carbonitrile (7g). Mp 278–279 °C; ESI MS (m/z) = 299 (M+H). IR (KBr, cm^{-1}): 3435, 3208, 2185, 1669, 1560. 1H NMR ($DMSO-d_6$, 300 MHz) $\delta = 5.30$ (s, 1H), 7.00 (s, 1H), 7.13-7.47 (m, 8H), 7.85 (d, $J = 4.5$ Hz, 1H), 7.90-7.96 (m, 2H). Elemental Analysis Calculated for $C_{20}H_{14}N_2O$: C, 80.52; H, 4.73; N, 9.39. Found: C, 80.40; H, 4.60; N, 9.25.

3-Amino-1-(2-chlorophenyl)-1H-benzo[f]chromene-2-carbonitrile (7h). Mp 265-267 °C; ESI MS (m/z) = 333 (M+H). 1H NMR ($CDCl_3$, 300 MHz) $\delta = 4.54$ (s, 2H), 5.89 (s, 1H), 6.91 (d, $J = 8.8$ Hz, 1H), 7.02-7.12 (m, 2H), 7.24-7.26 (m, 1H), 7.37-7.45 (m, 3H), 7.67 (d, $J = 7.7$ Hz, 1H); 7.78-7.82 (m, 2H). Elemental Analysis Calculated for $C_{20}H_{13}ClN_2O$: C, 72.18; H, 3.94; N, 8.42. Found: C, 72.10; H, 4.00; N, 8.30.

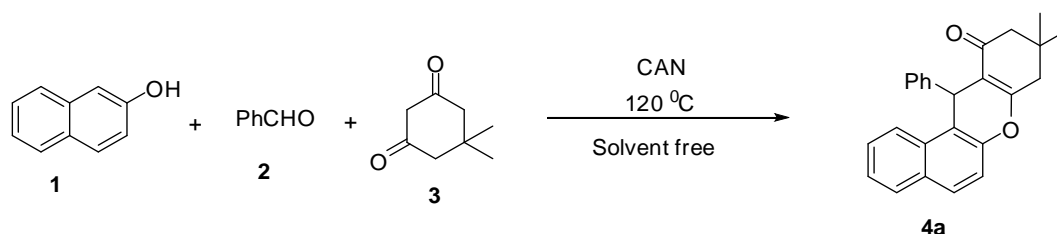
3-Amino-1-(4-methoxyphenyl)-1H-benzo[f]chromene-2-carbonitrile (7i). Mp 194 °C; ESI MS (m/z) = 329 (M+H). 1H NMR ($CDCl_3$, 300 MHz) $\delta = 3.72$ (s, 3H), 4.60 (s, 2H), 5.19 (s, 1H), 6.78 (d, $J = 7.5$ Hz, 2H), 7.09 (d, $J = 7.6$ Hz, 2H), 7.22 (d, $J = 10$ Hz, 1H), 7.39-7.36 (m, 2H), 7.69-7.66 (m, 1H), 7.78 (d, $J = 8.6$ Hz, 2H). Elemental Analysis Calculated for $C_{21}H_{16}N_2O_2$: C, 76.81; H, 4.91; N, 8.53. Found: C, 76.86; H, 4.98; N, 8.65.

3-Amino-1-p-tolyl-1H-benzo[f]chromene-2-carbonitrile (7j). Mp 253-254 °C; ESI MS (m/z) = 313 (M+H). 1H NMR ($CDCl_3$, 300 MHz) $\delta = 4.57$ (s, 2H), 5.21 (s, 1H), 7.02-7.12 (m, 4H), 7.25 (d, $J = 8.6$ Hz, 1H), 7.37-7.40 (m, 2H), 7.68-7.71 (m, 1H), 7.78-7.81 (m, 2H). Elemental Analysis Calculated for $C_{21}H_{16}N_2O$: C, 80.75; H, 5.16; N, 8.97. Found: C, 80.84; H, 5.05; N, 9.15.

Ethyl 3-amino-1-(4-chlorophenyl)-1H-benzo[f]chromene-2-carboxylate (7k). Mp 190–191 °C; ESI MS (m/z) = 380 (M+H). 1H NMR ($CDCl_3$, 300 MHz) $\delta = 1.36$ (t, $J = 5.9$ Hz, 3H), 4.21 (q, $J = 5.1$ Hz, 2H), 6.31 (s, 2H), 5.56 (s, 1H), 7.13 (d, $J = 7.1$ Hz, 2H), 7.25-7.27 (m, 3H), 7.35-7.47 (m, 2H), 7.76 (t, $J = 8.4$ Hz, 2H), 7.94 (d, $J = 8.7$ Hz, 1H). Elemental Analysis Calculated for $C_{22}H_{18}ClNO_3$: C, 69.57; H, 4.78; N, 3.69. Found: C, 69.45; H, 4.80; N, 3.58.

8.4 Results and Discussion:

Our initial experiments were focused on one-pot, three-component reaction of 2-naphthol, benzaldehyde, and dimedone using different catalysts under solvent free conditions, and the results are listed in Table 8.1 (Scheme 1).



8.4.1 Scheme 1:

It was found that ceric ammonium nitrate (CAN) showed better catalytic activity among other catalysts such as FeCl_3 , SnCl_4 , ZnCl_2 , and AlCl_3 . Although Ce (IV) derivatives are normally employed as single-electron oxidants, the use of the commercially available, inexpensive, and easily handled CAN in carbon-carbon and carbon-heteroatom bond forming reactions has recently attracted much attention [31-34], although these studies are still in their early stages. The main current goal in this area is the development of reactions that allow the use of catalytic amounts of CAN [35-41]. When 5 mol % CAN was used, the reaction proceeded smoothly and gave the product **4a** in 94% yield (Table 8.1, entry 6). Moreover, we found that the yields were obviously affected by the amount of CAN loaded. When 0.5 mol %, 2 mol % and 10 mol % of CAN were used, the yields were 39%, 70%, and 93% respectively (Table 8.1, entries 7-9). Therefore, 5 mol % of CAN was sufficient to push the reaction forward and further increasing the amount of CAN did not increase the yields. The catalytic activity of the recycled CAN was also examined. CAN was reused five times for the reaction without noticeable loss of activity (Table 8.1, entry 10).

In addition, no product was detected in the absence of the catalyst (Table 8.1, entry 1). The above results showed that CAN was essential in the reaction, and the best results were obtained when the reaction was carried out with 5 mol % of CAN under solvent free conditions at 120 °C.

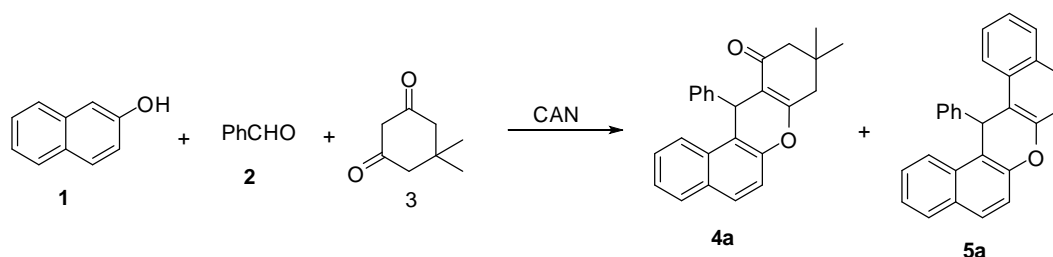
Table 8.1: Screening of catalysts for one-pot condensation of 2-naphthol, benzaldehyde, and dimedone ^a

Entry	Catalyst	Catalyst (mol %)	Time (min)	Yield (%) ^b
1	None	-	120	<5
2	FeCl_3	5	30	25
3	SnCl_4	5	30	37
4	ZnCl_2	5	30	32
5	AlCl_3 .	5	30	35
6	CAN	5	30	94
7	CAN	0.5	30	39
8	CAN	2	30	70
9	CAN	10	30	93
10 ^c	CAN	5	30	94, 93, 94, 93, 92

^aReaction conditions: 2-naphthol (1.0 mmol), benzaldehyde (1.0 mmol), and 5,5-dimethylcyclohexane-1,3-dione (1.0 mmol), solvent free, 120 °C. ^b Isolated yield. ^c Catalyst was reused five times.

Then, we examined the effect solvents over the above reaction. The results of table 8.2 indicate that solvents affected the efficiency of the reaction. Yields were poor in acetonitrile, dichloromethane and tetrahydrofuran (Table 8.2, entries 1-3). Better yields were obtained in more polar solvents like methanol and ethanol (Table 8.2, entry 4 & 5).

However, the best results were obtained under solvent free conditions (Table 8.2, entry 6). In addition, 14-phenyl-14H-dibenzo[a,j]xanthene **5a** was obtained as a side product in all solution phase reactions (Scheme 2). On the other hand, **5a** were not isolated under solvent free conditions.



8.4.2 Scheme 2:

Table 8.2: Solvent effect on the reaction of 2-naphthol, benzaldehyde, and dione catalyzed by CAN

Entry	Solvent	Temp (°C)	Time (min)	Yield (%)	
1	Acetonitrile	Reflux	120	38	10
2	Dichloromethane	Reflux	120	32	5
3	Tetrahydrofuran	Reflux	120	25	13
4	Methanol	Reflux	120	46	12
5	Ethanol	Reflux	120	50	10
6	None	120	30	94	Not isolated

In order to study the generality of this protocol, a library of 12-substituted-9,10-dihydro-8H-benzo[a]xanthene-11(12H)-ones were built using 2-naphthol, aldehydes and cyclic 1,3-dicarbonyl compounds (Figure 8.1).

The diversity in benzo xanthene library was generated using aliphatic, electron rich as well as electron deficient aromatic aldehydes, cyclohexane-1,3-dione, 5,5-dimethylcyclohexane-1,3-dione and cyclopentane-1,3-dione.

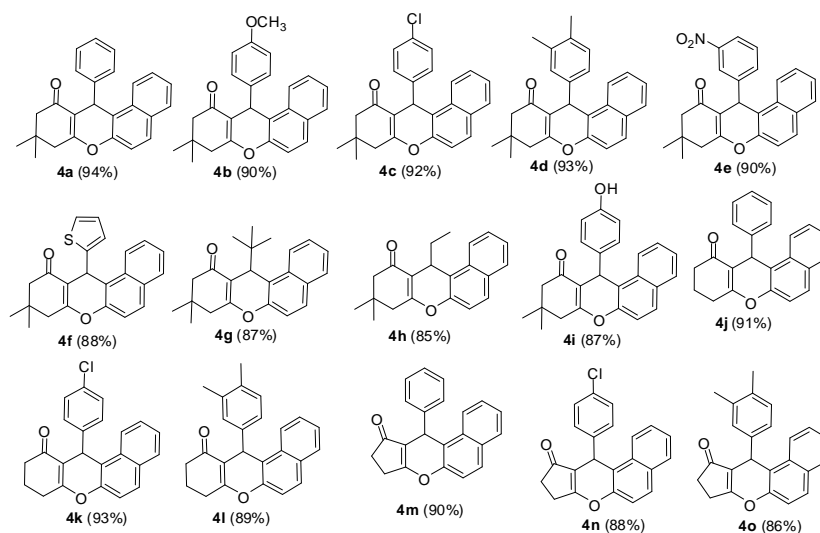
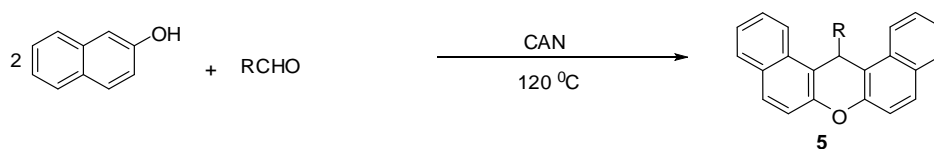


Figure 8.1: Synthesized Library of Compounds

It was observed that in the absence of cyclic 1,3-diketone, the CAN catalyzed reaction of 2-naphthol and aldehyde under solvent free conditions resulted to the formation of compound **5** in almost quantitative yield (Scheme 3, Figure 8.2).



8.4.3 Scheme 3:

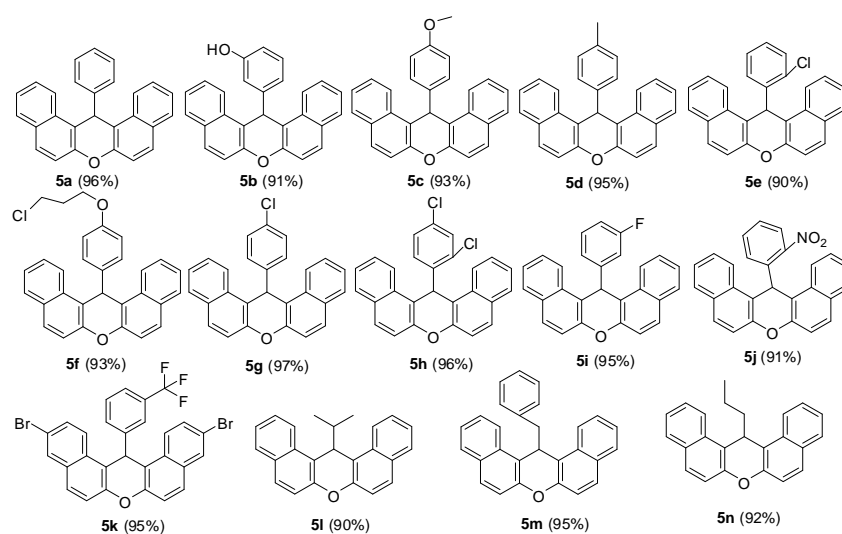


Figure 8.2: 14-substituted-14H-dibenzo [a, j] xanthenes

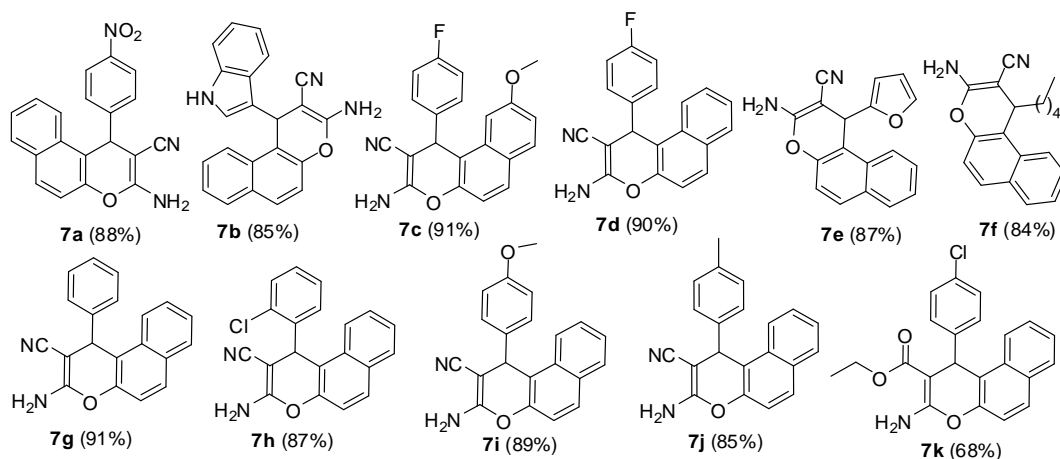
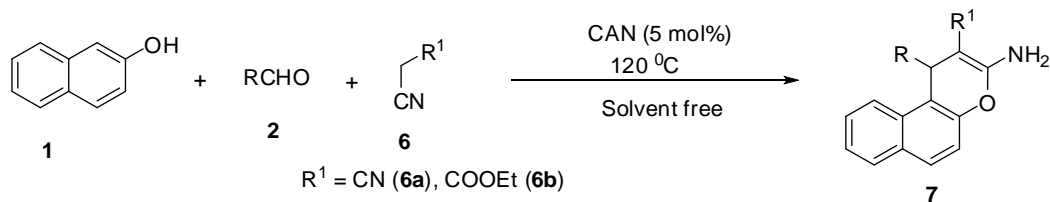


Figure 8.3: 3-amino-1-substituted-1H-benzo[f]chromenes

Using malononitrile or ethyl cyanoacetate as third component in the CAN mediated multi-component reaction of 2-naphthol and aldehydes, we synthesized a library of benzochromenes (Scheme 4, Figure 8.3).

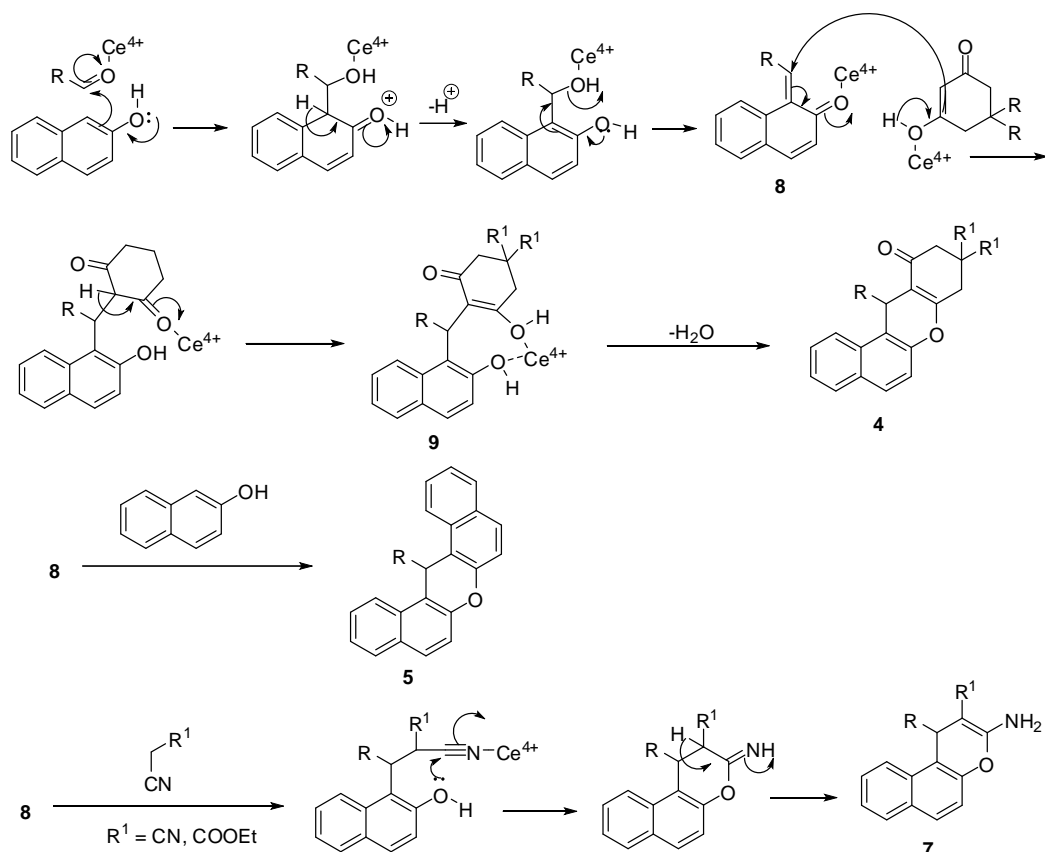


8.4.4 Scheme 4:

The formation of benzoxanthenes and benzochromenes could be explained by a proposed tentative mechanism (Scheme 5).

It was supposed that the reaction occurred via the ortho-quinone methides intermediate **8**, which was formed by the nucleophilic addition of β -naphthol to aldehyde catalyzed with CAN.

Subsequent attack of cyclic 1,3-dicarbonyl compounds to the intermediate **8**, afforded **9**. Then compounds **9** eliminated one molecule of H₂O and afforded compound **4**.



8.4.5 Scheme 5.

In the absence of cyclic 1,3-dicarbonyls the second molecules of β -naphthol attacks to intermediate **8** leading to the formation compound **5**. Reaction of malononitrile (**6a**) or ethyl cyanoacetates (**6b**) with intermediate **8** yields benzochromenes **7**. All the synthesized compounds were screened for their anti-proliferative activity in human prostate cancer (DU-145), breast cancer (MCF-7), cervical carcinoma (C-33A), lung carcinoma (A 549), oral squamous cell carcinoma (KB), control for general cytotoxicity (Vero) cancer cell lines. The compounds which were showing activity below 50 $\mu\text{g/ml}$ were summarised in table 9.3. Benzochromenes (**4b**, **4c**, **4f**, **4i**, **4n**, **7a**, **7b**, **7c**, **7e**, **7i** and **7k**) were found more active than comparison to benzoxanthenes (**5b**, **5f** and **5j**). Compounds **4i** (6.7 $\mu\text{g/ml}$) and **7a** (8.9 $\mu\text{g/ml}$) was most potent in MCF-7, showed more activity than anti breast cancer drug tamoxifen (10 $\mu\text{g/ml}$).

Table 8.3: Inhibition of proliferation of the compounds

Compounds	IC ₅₀ ($\mu\text{g/ml}$)					
	DU 145	MCF-7	C-33A	A 549	KB	Vero
4b	12.5	18.1	8.2	13.7	4.0	8.9
4c	14.3	19.8	14.7	12.6	17.6	5.2

Compounds	IC ₅₀ (µg/ml)					
	DU 145	MCF-7	C-33A	A 549	KB	Vero
4f	8.0	11.7	9.9	6.1	6.7	18.2
4i	11.3	6.7	17.7	27.7	21.8	5.7
4n	26.7	23.3	19.2	32.8	16.9	13.3
5b	19.0	21.1	36.6	16.3	18.5	38.6
5f	21.7	37.8	38.6	36.8	11.7	41.9
5j	25.6	21.9	28.6	23.2	16.3	29.7
7a	13.3	8.9	14.6	8.3	7.6	12.5
7b	10.0	12.2	10.5	5.4	15.2	8.1
7c	16.7	22.1	19.7	18.9	21.6	14.0
7e	18.6	15.7	15.0	22.5	14.2	11.7
7i	12.4	14.2	27.1	10.2	19.6	18.9
7k	17.4	16.7	11.9	12.9	12.9	19.6

8.5 Conclusion:

In conclusion, we have efficiently synthesized structurally diverse libraries of benzoxanthenes, and benzochromenes via CAN catalyzed three-component reactions under solvent free conditions. The advantages of this method include the use of recyclable catalyst, high yields, simple workup procedure, and easy isolation. Anti-proliferative activities were evaluated for all the synthesized compounds, some of the synthesized compounds exhibited significant activity in various cell lines.

Acknowledgments: R. A. Maurya and S. Sharma are thankful to CSIR, New Delhi for financial support. Authors also acknowledge SAIF-CDRI for providing spectral and analytical data.

8.6 References:

- Schreiber S L (2000) Target-Oriented and diversity-oriented organic synthesis in drug discovery. *Science* 287: 1964-1969
- Trost B M (1995) Atom economy-A challenge for organic synthesis: Homogeneous catalysis leads the way. *Angew Chem Int Ed Engl* 34: 259-281
- Weber L, Illgen K, Almstetter M (1999) Discovery of new multi component reactions with combinatorial methods. *Synlett* 366-374
- Bienayme H, Hulme C, Oddon G, Schmitt P (2000) Maximizing synthetic efficiency: multi-Component transformations lead the way. *Chem A Eur J* 6: 3321-3329
- Terrett N K *Combinatorial Chemistry*. Oxford University Press New York 1998
- Domling A (2006) Recent developments in isocyanide based multicomponent reactions in applied *chemistry*. *Chem Rev* 106: 17-89
- Hafez H N, Hegab M I, Ahmed-Farag I S, El-Gazzar A B A (2008) A facile regioselective synthesis of novel *spiro*-thioxanthene and *spiro*-xanthene-9',2-

- [1,3,4]thiadiazole derivatives as potential analgesic and anti-inflammatory agents. *Bioorg Med Chem Lett* 18: 4538-4543
8. Banerjee A, Mukherjee A K (1981) Chemical aspects of santalin as a histological stain *Stain Technol* 56: 83
 9. Menchen S M, Benson S C, Lam J Y L, Zhen W, Sun D, Rosenblum B B, Khan S H, Taing M (2003) Sulfonated diarylrhodamine dyes. US Patent 6583168
 10. Knight C G, Stephens T (1989) Xanthene-dye-labelled phosphatidylethanolamines as probes of interfacial pH. *Studies in phospholipid vesicles. Biochem J* 258: 683-687
 11. Ahmad M, King T A, Ko D -K, Cha B H, Lee J (2002) Performance and photostability of xanthene and pyrromethene laser dyes in sol-gel phase, *J Phys D Appl Phys* 35: 1473
 12. Chatterjee S, Iqbal M, Kauer J C, Mallamo J P, Senadhi S, Mallya S, Bozyczko-Coyne D, Siman R (1996) Xanthene derived potent nonpeptidic inhibitors of recombinant human calpain I. *Bioorg Med Chem Lett* 6: 1619-1622
 13. Naya A, Ishikawa M, Matsuda K, Ohwaki K, Saeki T, Noguchi K Ohtake N (2003) Structure–activity relationships of xanthene carboxamides, novel CCR1 receptor antagonists. *Bioorg Med Chem* 11: 875-884
 14. Ellis G P (1977) In the Chemistry of Heterocyclic Compounds. Chromenes, Chromanes and Chromones; Weissberger A Taylor E C Eds John Wiley: New York p 11: Chapter 11
 15. Abdel Galil F M, Riad B Y, Sherif S M, Elnagdi M H (1982) Activity nitriles in heterocycle synthesis: A novel synthesis of 4-azoloyl-2-aminoquinolines. *Chem Lett* 1123

9. Natural Product in Research and Drug Discovery

Vishwa Deepak Tripathi

Department of Chemistry,
C. M. Science College Darbhanga
(A Constituent unit of L. N. Mithila University Darbhanga),
Bihar, India.

Anand Mohan Jha

Department of Chemistry,
M. L. S. M. College Darbhanga
(A Constituent unit of L. N. Mithila University Darbhanga),
Bihar, India.

9.1 Natural Product in Research and Drug Discovery:

The therapeutic use of plants is as old as human civilisation. Even today plants remain the primary sources of health care for most people in the world. It is estimated that around 80% of the world's population rely mainly on traditional medicine for their primary health care. Over the centuries, natural products have provided a tremendous number of substances that serve as medicine or as lead structure for drug development. Around one third of the currently marketed drugs have structures that are related or derived from natural products. Some natural product-derived drugs that are a hallmark of modern pharmaceutical care include quinine, theophylline, penicillin G, morphine, paclitaxel, digoxin, vincristine, doxorubicin, cyclosporine and vitamin A among many other examples.

Ancient Egyptians practiced medicine from as far back as 2900 BC. The "Ebers Papyrus", the best known first record of Egyptian pharmaceutical practice has been dated to as far back as 1500 BC. The papyrus, which describes over 700 drugs, mostly of plant origin, details different drug formulations including gargles, snuffs, poultices, infusions, pills and ointments, with beer, milk, wine and honey being commonly used as vehicles. Dioscorides first documented the medicinal use of natural substances as far back as 78 AD. Until now, thousands of medicinal plants described then remain relevant today in modern medicine.

Although such plant materials are no longer used as crude drug preparations, they remain important sources of purified active principles that have become cornerstones of modern therapy. Apart from covering a wide spectrum of disease indications—anti-cancer, anti-infective, anti-diabetic among others, they also show an exceptional diversity of chemical structures. Analysis of the chemical the therapeutic use of plants is as old as human civilisation. Even today plants remain the primary sources of health care for most people in the world. It is estimated that around 80% of the world's population rely mainly on traditional medicine for their primary health care. Over the centuries, natural products have provided a tremendous number of substances that serve as medicine or as lead structure for drug development. Around one third of the currently marketed drugs have structures that are related or derived from natural products.

Some natural product-derived drugs that are a hallmark of modern pharmaceutical care include quinine, theophylline, penicillin G, morphine, paclitaxel, digoxin, vincristine, doxorubicin, cyclosporine and vitamin A among many other examples. Ancient Egyptians practiced medicine from as far back as 2900 BC.

The “Ebers Papyrus”, the best known first record of Egyptian pharmaceutical practice has been dated to as far back as 1500 BC. The papyrus, which describes over 700 drugs, mostly of plant origin, details different drug formulations including gargles, snuffs, poultices, infusions, pills and ointments, with beer, milk, wine and honey being commonly used as vehicles. Dioscorides first documented the medicinal use of natural substances as far back as 78 AD. Until now, thousands of medicinal plants described then remain relevant today in modern medicine.

Although such plant materials are no longer used as crude drug preparations, they remain important sources of purified active principles that have become cornerstones of modern therapy. Apart from covering a wide spectrum of disease indications—anti-cancer, anti-infective, anti-diabetic among others, they also show an exceptional diversity of chemical structures. Analysis of the chemical properties of recently developed small molecule natural-product-derived drugs has revealed that half of them were in conformity with Lipinski’s Rule of 5 for orally available drugs.

Despite such advantages and a proven track record of successes, many big pharmaceutical companies have been discouraged from pursuing natural product-based drug discovery due to perceived disadvantages of natural products. These include challenges in ensuring access and adequate supply, the complexities of natural product chemistry with associated slowness of working with natural products, and intellectual property rights concerns.

Furthermore, the use of combinatorial chemistry to generate large libraries of synthetic compounds gave hope to pharmaceutical companies much to the detriment of natural products-based drug discovery research.

9.2 History:

Natural products also called secondary metabolites are the only substances to be used as medicines in all over the world. They have been the first and, for a long time, sole source of curative agents. Since less than 10% of the world’s biodiversity has been evaluated for potential biological activity, many more useful natural lead compounds await discovery with the challenge being how to access this natural chemical diversity.

One of the earliest records of natural products were depicted on clay tablets in cuneiform from Mesopotamia (2600 B.C.) which documented oils from *Cupressus sempervirens* (Cypress) and *Commiphora* species (myrrh) which are still used today to treat coughs, colds and inflammation. The Ebers Papyrus (2900 B.C.) is an Egyptian pharmaceutical record, which documents over 700 plant-based drugs ranging from gargles, pills, infusions, to ointments. The Chinese Materia Medica (1100 B.C.) (Wu Shi Er Bing Fang, contains 52 prescriptions), Shennong Herbal (~100 B.C., 365 drugs) and the Tang Herbal (659 A.D., 850 drugs) are documented records of the uses of natural products.

The Greek physician, Dioscorides, (100 A.D.), recorded the collection, storage and the uses of medicinal herbs, whilst the Greek philosopher and natural scientist, Theophrastus (~300 B.C.) dealt with medicinal herbs. During the Dark and Middle Ages, the monasteries in England, Ireland, France and Germany preserved this Western knowledge whilst the Arabs preserved the Greco-Roman knowledge and expanded the uses of their own resources, together with Chinese and Indian herbs unfamiliar to the Greco-Roman world.

It was the Arabs who were the first to privately own pharmacies (8th century) with Avicenna, a Persian pharmacist, physician, philosopher and poet, contributing much to the sciences of pharmacy and medicine through works such as the *Canon Medicinæ*. The use of natural products as medicines has been described throughout history in the form of traditional medicines, remedies, potions and oils with many of these bioactive natural products still being unidentified.

The dominant source of knowledge of natural product uses from medicinal plants is a result of man experimenting by trial and error for hundreds of centuries through palatability trials or untimely deaths, searching for available foods for the treatment of diseases.

One example involves the plant genus *Salvia* which grows throughout the southwestern region of the United States as well as northwestern Mexico and which was used by Indian tribes of southern California as an aid in childbirth. Male newborn babies were “cooked” in the hot *Salvia* ashes as it was believed that these babies consistently grew to be the strongest and healthiest members of their respective tribes and are claimed to have been immune from all respiratory ailments for life.

The plant, *Alhagi maurorum* Medik (Camel’s thorn) secretes a sweet, gummy material from the stems and leaves during hot days. This gummy sap is called “manna” and consists mostly of melezitose, sucrose and invert sugar and it has been documented and claimed by the Ayurvedic people that the plant aids in the treatment of anorexia, constipation, dermatosis, epistaxis, fever, leprosy, and obesity. It was also used by the Israelis who boiled the roots and drank the extract as it stopped bloody diarrhea.

The Konkani people smoked the plant for the treatment of asthma, whilst the Romans used the plant for nasal polyps. The plant *Ligusticum scoticum* Linnaeus found in Northern Europe and Eastern North America was eaten raw first thing in the morning and was believed to protect a person from daily infection.

The exploitation of traditional medicines for the development of modern drugs produced the first commercially available pure drug substances. The isolation of morphine from the opium latex by the German Pharmacist Sertürner in 1805 could be seen as the start of pharmaceutical natural product research. Shortly thereafter the isolation of many other substances followed atropine in 1819, quinine and caffeine in 1820, and digitoxin in 1841.

Quinine was isolated in 1820 from the bark of several *Cinchona* species that have been used by Peruvian Indians to treat shivering and malarial fevers. In 1826, quinine and morphine became the first commercially available pure natural compounds produced by Caventou and Merck, respectively.

The progression of the role of natural products in drug discovery (Figure 1) proceeded from the traditional use of whole plants and plant extracts to the isolation and identification of the active principle pure compounds, to the application of derivatised, optimised molecules, and finally to the use of natural products as leads for medicinal chemistry.

9.3 Today:

After decades of very successful drug discovery and development, the pharmaceutical industry down scaled natural product research in the late 1990s in favour of automated high throughput screening (HTS) of compound libraries. Compound libraries assembled with the aid of combinatorial chemistry were thought to produce more hits than ‘old fashioned’ natural products.

Despite this decline in the use of natural products in drug discovery, newly marketed drugs derived from natural compounds hold about the same share as before.

The numerous and successful discoveries of compounds in the early times of modern drug discovery were quite exclusively based on the traditional use of the plant. Of all known organic molecules, only 1% is natural products, 99% are synthetic, but more than one third of all drug sales are based on natural products.

The reason behind this fact is the evolutionary selection? Evolutionary selection is the answer; nature’s own high-throughput screening has optimized these biologically active compounds.

Especially the numerous compounds with antibacterial activity do not surprise, as fighting for space and resources, and against other organisms, plays a pivotal role in survival.

Early attempts to apply HTS to botanical extracts were faced with many difficulties. With the introduction of biochemical assays in the 90s, the screening process had shifted from functional cellular assays to cell-free biochemical assay formats, which are very sensitive and prone to artefacts.

The typically coloured plant extracts are not compatible with such screening assays due to interference with detection caused by colour, fluorescence, or quenching effects of components in the extract.

Moreover, the complexity of extracts potentially induces aggregation of components, chemical reactions within the assay or difficulties of solubility in assay buffer⁸. Pre-fractionation or purification to reduce the chemical complexity of the extracts needs to be implemented before HTS can be performed.

This is time-consuming and laborious and generally reduces the attractiveness of screening of natural compounds. Another approach is to use the power of combinatorial chemistry in combination with knowledge on active natural products and create a library that extends upon the structural properties of known natural compounds. This strategy generates libraries with enhanced specificity and selectivity

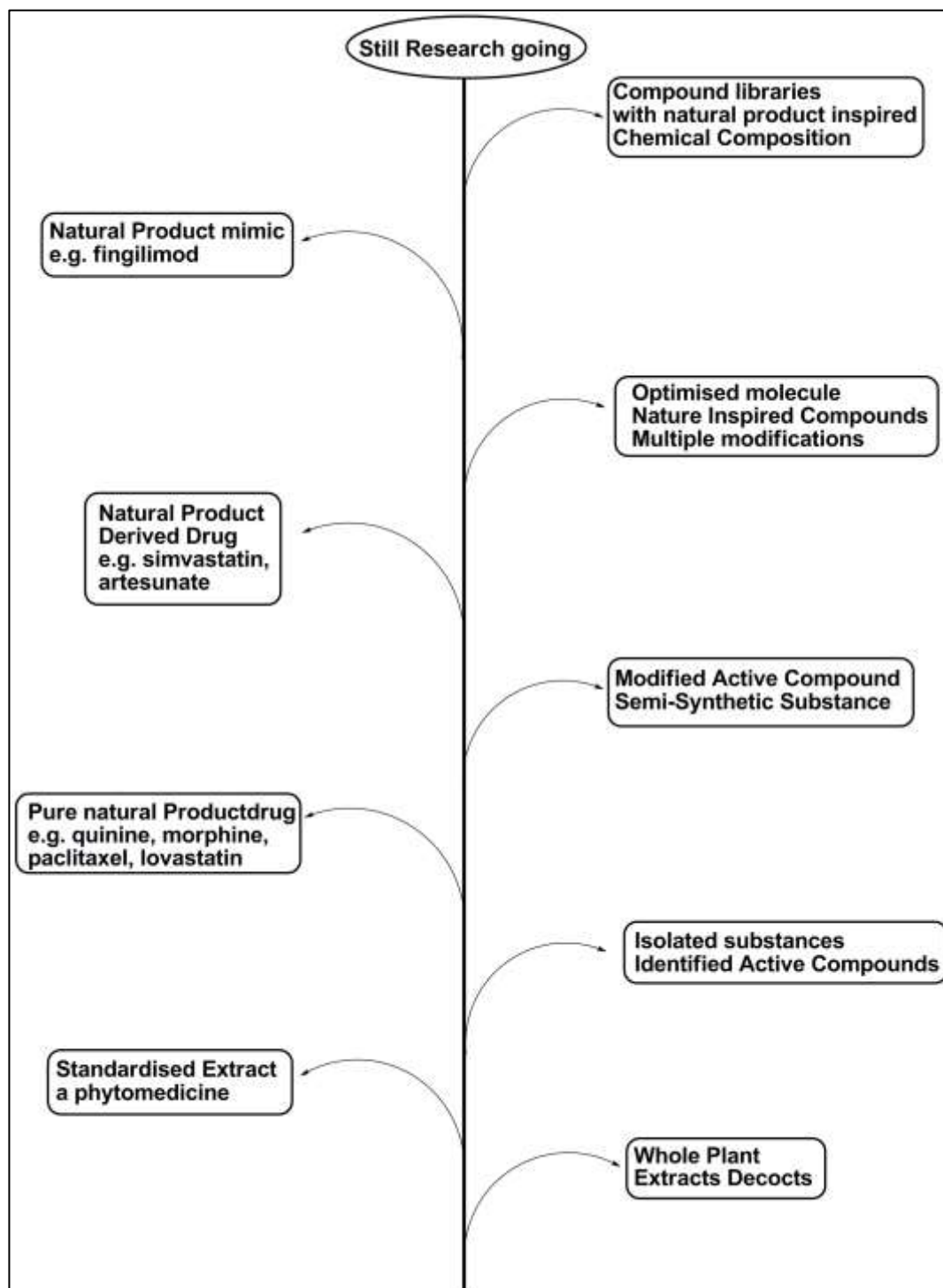


Figure 9.1: Diagram Describing the Various Roles of Natural Products in Drug Discovery and Development

9.4 Natural Product Inspired Synthesis:

We have seen in previous section that how natural resources have made the life possible on the earth by contributing in every aspect of life from medicine to food, shelter and cloths. Apart from their direct use as therapeutic agents' natural products are great source of inspiration for synthetic chemists due to their fascinating structure and structural complexity. Various structural variations and attracting pharmacophores inspire medicinal chemists to design the synthetic pathways to derivatize the natural product nucleus to get desired properties. The chemistry involving derivatization of natural molecules in desired way to enhance the properties of molecule is known as natural product inspired synthesis. Many of the naturally occurring alkaloids are very interesting form medicinal perspective, but their structural features render these molecules to become a drug. Like structural features are responsible for poor solubility, low bioavailability and less receptor bonding affinity. These properties of molecules can be enhancing if certain groups or nucleus is modified in the molecules.



Figure 9.2: Schematic Representation of Natural Product Inspired Synthesis to Convert Natural Molecules into Drug Molecules

As shown in figure the natural products can be modified different ways to get the desired properties better solubility, high potency, more stability and high selectivity in natural molecules. Natural product inspired synthesis serves as efficient toll to bring these changes in the molecules. In the next upcoming sections we will see that how this contributed in miraculous ways for the development of compounds of therapeutic importance.

9.5 Marketed Drugs Based on Natural Molecules:

Some of the frontline examples of successfully marketed drugs that are natural compounds, derivatives of natural compounds, or synthetic molecules for which the lead was a natural product. The focus here is on some more recent drugs that had a major impact on human lives, while the more historical and well-known examples such as morphine, penicillin, quinine, streptomycin and others are left out.

9.6 Lovastatin:

Since the discovery of a correlation between high cholesterol levels and coronary heart disease in the 1950s, the lowering of high cholesterol levels with drugs has been pursued. The cholesterol biosynthesis is a complex process involving more than 30 enzymes and was discovered during the 1950s and 60s. HMG-CoA (3-hydroxy-3-methylglutaryl-coenzyme A) reductase is the rate-limiting enzyme of the biosynthetic pathway and hence most suitable for inhibition. Furthermore, when HMG-CoA reductase is inhibited an alternative pathway for degradation of the substrate is available which prevents accumulation of HMG-CoA. Soon after, in 1978, another HMG-CoA reductase inhibitor was discovered in the Merck laboratories from *Aspergillus terreus* and named mevilonin (lovastatin) (Figure 10.2).

Compactin was highly effective in lowering plasma cholesterol in animal models as well as patients with hypercholesterolaemia. However, compactin was withdrawn from clinical trials in 1980 due to unpublished reasons. Because of the structural similarity between compactin and lovastatin, clinical studies with lovastatin had to be stopped as well.

After additional animal studies and some investigation in small-scale high-risk patient studies, clinical development was re-launched in 1983 until, finally, in 1987 the FDA approval for lovastatin was obtained. Soon after, other statins from microbial sources were released. Simvastatin entered the market in 1988, it is semi-synthetically derived from lovastatin introducing a minor side chain modification.

In 1991 pravastatin followed, with a modification in the side chain ring. Later synthetically designed products with different chemical structures followed fluvastatin in 1994, atorvastatin in 1997, cerivastatin in 1998 and rosuvastatin in 2003.

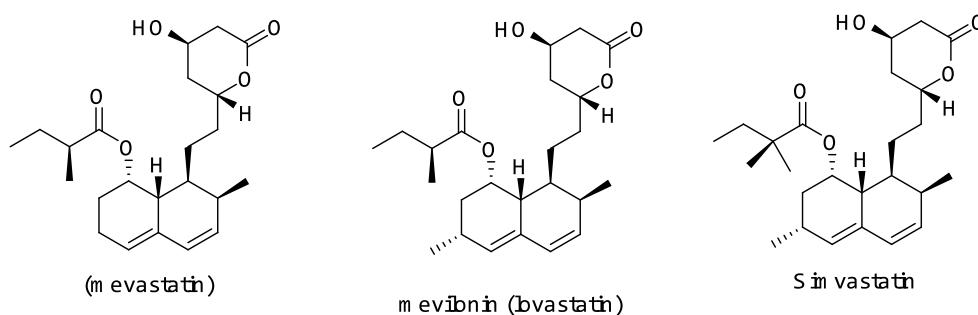


Figure 9.3: Structures of Campthecin, Mevilonin and Simvastatin

The mechanism of action of statins goes beyond blocking cholesterol biosynthesis. Inhibition of HMG-CoA reductase reduces levels of mevalonate, which in turn leads to upregulation of low-density lipoprotein (LDL) receptors on hepatocytes. The upregulation of LDL receptors increases the uptake of LDL from blood, the major marker of elevated cholesterol levels. With the discovery of lovastatin, it was for the first time possible to achieve large reductions in plasma cholesterol of up to 40%. The treatments formerly available were all of limited efficacy or tolerability.

The bile acid sequestrants are moderately effective and poorly tolerated due to gastrointestinal side effects whereas fibrates produce a rather small reduction in LDL-cholesterol but are well tolerated and widely used. In 2001, however, cerivastatin, only introduced in 1998, had to be withdrawn from the market due to severe side effects of rhabdomyolysis which occurred in concomitant use with gemfibrozil. The mechanism for this side effect still remains elusive but further studies demonstrated the safety of other statins. Nevertheless, myalgia as a side effect under statin therapy occurs but seldom develops into severe myolysis. The statins became the most effective drugs so far for preventing and halting arteriosclerosis. Despite the wide use of these drugs, it is believed that they are underutilised in patients who are free of symptoms with only moderately elevated cholesterol levels.

9.7 Paclitaxel:

Plants have a long history in the use of cancer treatment. The first plant derived drug to treat cancer was the Vinca alkaloid vincristine, which was approved for clinical use in 1963. A more recent discovery of a plant-derived chemotherapeutic agent was paclitaxel (Figure 3) from *Taxus brevifolia* bark. Paclitaxel was shown to stabilize microtubule assembly, whereas Vinca alkaloids and colchicin prevent the assembly of microtubules. Even in absence of essential GTP, paclitaxel promotes microtubule assembly. Although paclitaxel shows no structural resemblance to GTP, it is able to interact specifically with the β - subunit of microtubules, a region that is associated with GTP binding and hydrolysis. The stabilisation of microtubules by paclitaxel forces the tumour cell into multiple DNA replication cycles that eventually initiate apoptosis

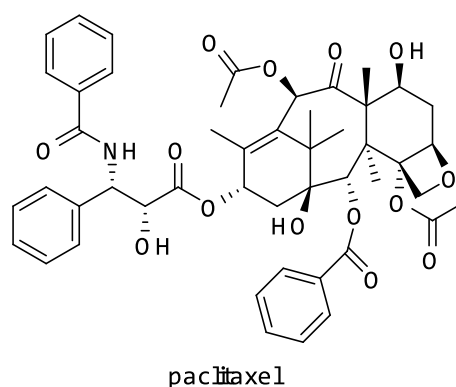


Figure 9.4: Structure of Paclitaxel

Clinical trials with paclitaxel were started in the early 1980s, and FDA approval for treatment of refractory ovarian cancer was granted in 1992. Since the introduction of paclitaxel to the treatment of ovarian cancer the survival rate has more than doubled and further applications have been approved. Today, paclitaxel is also used in the treatment of breast and colon cancers as well as Kaposi's sarcomas of HIV infected patients. Preparation of sufficient amounts of paclitaxel to launch clinical studies was nearly impossible, as isolation from the bark results in very low yields and excoriation causes the trees to die. In 1986, the precursor deacetyl baccatin III was isolated from the needles of *Taxus baccata*,

and the semi-synthetic approach led to the production of sufficient amount of paclitaxel from renewable sources. From the perspective of both basic science and clinics, paclitaxel has led to significant progress in understanding and treating cancer.

9.8 Sirolimus, Rapamycin:

Rapamycin (Figure 4) was discovered in the 1970s as a potent antifungal metabolite of the bacterial strain *Streptomyces hygroscopicus* and was named after the origin of the sample, the Easter Island Rapa Nui. Its clinical development as an antifungal drug was stopped when its strong antiproliferative and immunosuppressive effects were detected. The substance fell into oblivion until studies on the mechanism of action led to the identification of its target (target of rapamycin, TOR) in 1992.

Later, the compound was also named sirolimus due to its structural similarities with tacrolimus, which was discovered in 1987. The immunosuppressive activity of rapamycin is due to its blocking of interleukin 2 (IL2) mediated T-cell proliferation and activation thereby preventing allograft rejection after organ transplantation.

The combination of rapamycin with calcineurin inhibitors such as cyclosporine A or tacrolimus results in significant synergistic effects that improve the prevention of organ rejection (Kahan, 1998). In 1997 rapamycin/sirolimus obtained FDA approval for preventing host-rejection of kidney-transplants. Further studies address the use of rapamycin in autoimmune diseases such as psoriasis, multiple sclerosis or rheumatoid arthritis and are still ongoing.

The additional inhibitory effects of rapamycin on the proliferation of vascular smooth muscle cells led to the development of rapamycin as antirestenosis drug, and coronary-artery stents releasing rapamycin are approved in surgery since 2003.

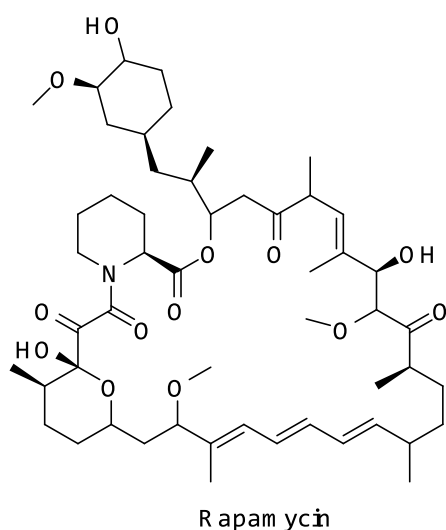


Figure 9.5: Structure of Rapamycin

9.9 Artemisin:

The Chinese medicinal herb qing hao (*Artemisia annua*) was traditionally used to reduce fever and, in 1596, was mentioned for the first time to treat malaria. In 1972, Chinese scientists managed to isolate the active principle of the herb and called it qinghaosu, meaning ‘the active principle of qing hao’, named artemisinin (Figure 5) for the Western world. The structure was elucidated in 1980 and revealed to be a sesquiterpene structure with an unusual endoperoxide group. The high lipophilicity of artemisinin made administration as a drug difficult; therefore, various derivatives were synthesised, including arthemether, arteether and artesunate (Figure 5). The biological activity of the artemisinins depends on the cleavage of the peroxide bond after contact with iron-II-hem within the parasite.

The generated free radical alkylates the heme molecule or parasite proteins. Inhibition of the sarco/endoplasmic reticulum Ca^{2+} -ATPase (SERCA) has been proposed as an additional target. The active metabolite dihydroartemisinin kills nearly all asexual stages of parasite lifecycle in the blood, and also affects the gametocytes, which are responsible for the infection of the *Anopheles* mosquito and transmit the disease. Furthermore, the artemisinins act faster than any other antimalarial drug with a fever and parasite clearance time of less than two days.

However, due to the short plasma half-life of these drugs therapy needs to be continued for 5-7 days, or needs to be combined with other antimalarial drugs. The combination usually applied is artesunate-lumefantrine. In 2000 Swissmedic approved the drug for sale under the name Riamet; in other countries it is sold as Coartem.

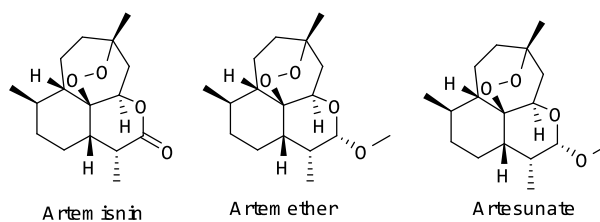


Figure 9.6: Structures of Artemisinin, Artemether and Artesunate

9.10 Vincristine:

Vincristine, also known as leurocristine and marketed under the brand name Oncovin among others, is a chemotherapy medication used to treat a number of types of cancer. Vincristine was approved by the US Food and Drug Administration (FDA) in July 1963 as Oncovin, a major chemotherapeutic agent. The drug was initially discovered by a team led by Dr. J.G. Armstrong, then marketed by Eli Lilly and Company. Studies in the 1950s revealed that the rosy periwinkle *Catharanthus roseus* contained over 120 alkaloids, many of which are biologically active, the two most significant being vincristine and vinblastine. Vincristine belongs to a class of chemotherapy drugs called plant alkaloids. Plant alkaloids are made from plants.

The vinca alkaloids are made from the periwinkle plant (*Catharanthus rosea*). The taxanes are made from the bark of the Pacific Yew tree (*Taxus*). The vinca alkaloids and taxanes are also known as antimicrotubule agents. The podophyllotoxins are derived from the May Apple plant. Camptothecan analogs are derived from the Asian "Happy Tree" (*Camptotheca acuminata*).

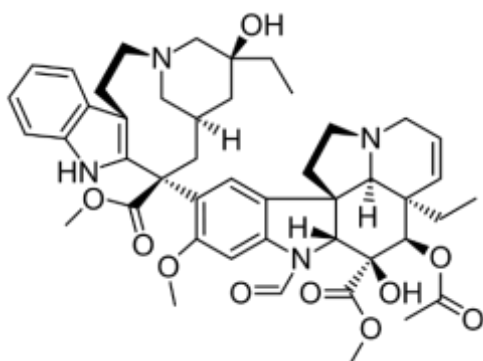


Figure 9.7: Structure of Vincristine

9.11 Penicillin:

Penicillin (PCN or pen) is a group of antibiotics, derived originally from common moulds known as *Penicillium* moulds; which includes penicillin G (intravenous use), penicillin V (use by mouth), procaine penicillin, and benzathine penicillin (intramuscular use). Penicillin antibiotics were among the first medications to be effective against many bacterial infections caused by staphylococci and streptococci. Penicillin was discovered in 1928 by Scottish scientist Alexander Fleming. People began using it to treat infections in 1942.

There are several enhanced penicillin families which are effective against additional bacteria; these include the antistaphylococcal penicillins, aminopenicillins and the antipseudomonal penicillins. They are derived from *Penicillium* fungi. Fleming shared the 1945 Nobel Prize in Physiology or Medicine for his discovery, along with Oxford University scientists Howard Florey and Ernst Boris Chain (who developed improved ways to produce and concentrate the drug and prove its antibacterial effects).

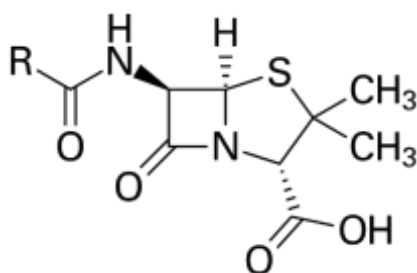


Figure 9.8: Structure of Penicilline

Penicillin belongs to the beta-lactam family of antibiotics, the members of which use a similar mechanism of action to inhibit bacterial cell growth that eventually kills the bacteria. Bacteria cells are surrounded by a protective envelope called the cell wall.

One of the primary components of the bacterial cell wall is peptidoglycan, a structural macromolecule with a net-like composition that provides rigidity and support to the outer cell wall. In order to form the cell wall, a single peptidoglycan chain is cross-linked to other peptidoglycan chains through the action of the enzyme DD-transpeptidase (also called a penicillin binding protein—PBP). Throughout a bacterial lifecycle, the cell wall (and thus the peptidoglycan crosslinks) is continuously remodeled in order to accommodate for repeated cycles of cell growth and replication. Penicillins and other antibiotics in the beta-lactam family contain a characteristic four-membered beta-lactam ring.

Penicillin kills bacteria through binding of the beta-lactam ring to DD-transpeptidase, inhibiting its cross-linking activity and preventing new cell wall formation. Without a cell wall, a bacterial cell is vulnerable to outside water and molecular pressures, and quickly dies. Since human cells do not contain a cell wall, penicillin treatment results in bacterial cell death without affecting human cells.

9.12 Vancomycin:

Vancomycin is an antibiotic used to treat a number of bacterial infections. It is recommended intravenously as a treatment for complicated skin infections, bloodstream infections, endocarditis, bone and joint infections, and meningitis caused by methicillin-resistant *Staphylococcus aureus*. Vancomycin was first isolated in 1953 by Edmund Kornfeld (working at Eli Lilly) from a soil sample collected from the interior jungles of Borneo by a missionary, Rev. William M. Bouw (1918-2006). The organism that produced it was eventually named *Amycolatopsis orientalis*. The original indication for vancomycin was for the treatment of penicillin-resistant *Staphylococcus aureus*.

The rapid development of penicillin resistance by staphylococci led to its being fast-tracked for approval by the Food and Drug Administration in 1958. Vancomycin was first sold in 1954. It is on the World Health Organization's List of Essential Medicines. The World Health Organization classifies vancomycin as critically important for human medicine.

Vancomycin is a glycopeptide antibiotic with a history that can be traced back to the 1950s when it was discovered in soil produced by the organism *Streptomyces orientalis*. The bacterial cell wall is an extremely important barrier that bacteria use to stay alive. This cell wall is made mostly of peptidoglycan, which is a mesh-like structure made of proteins (peptides) and sugars (glycan). In order for a bacterium to replicate, it must build a new peptidoglycan cell wall. Vancomycin protected the nutrient supply needed by *Streptomyces orientalis* by creating and dispersing the antimicrobial, resulting in the inhibition of many of the other bacteria species that may enter its territory.

Vancomycin binds to the acyl-D-ala-D-ala portion of the growing peptidoglycan cell wall, which is a group of amino acids. By binding, multiple mechanisms of action begin to take place resulting in bacterial inhibition.

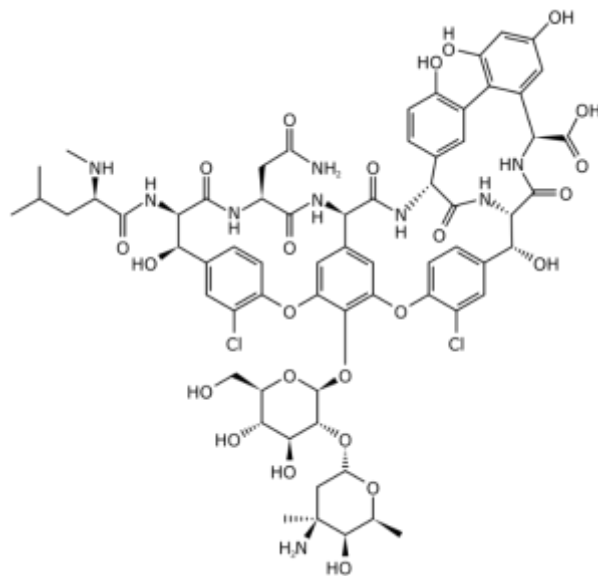


Figure 9.9: Structure of Vancomycine

9.13 Erythromycin:

Erythromycin is an antibiotic used for the treatment of a number of bacterial infections. This includes respiratory tract infections, skin infections, chlamydia infections, pelvic inflammatory disease, and syphilis. Erythromycin was first isolated in 1952 from the bacteria *Saccharopolyspora erythraea*. It is on the World Health Organization's List of Essential Medicines, the safest and most effective medicines needed in a health system. Eli Lilly's research team, led by J. M. McGuire, managed to isolate erythromycin from the metabolic products of a strain of *Streptomyces erythreus* (designation changed to *Saccharopolyspora erythraea*) found in the samples. In 1981, Nobel laureate (1965 in chemistry) and professor of chemistry at Harvard University Robert B. Woodward (posthumously), along with a large number of members from his research group, reported the first stereocontrolled asymmetric chemical synthesis of erythromycin A.

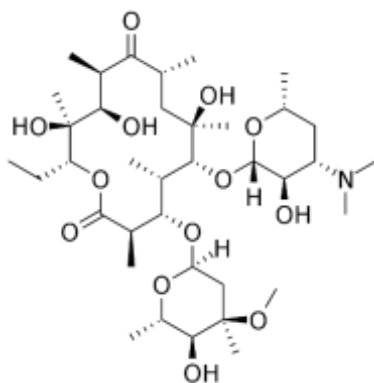


Figure 9.10: Structure of Erythromycine

In order to replicate, bacteria require a specific process of protein synthesis, enabled by ribosomal proteins. Erythromycin acts by inhibition of protein synthesis by binding to the 23S ribosomal RNA molecule in the 50S subunit of ribosomes in susceptible bacterial organisms.

It stops bacterial protein synthesis by inhibiting the transpeptidation/translocation step of protein synthesis and by inhibiting the assembly of the 50S ribosomal subunit. This results in the control of various bacterial infections. The strong affinity of macrolides, including erythromycin, for bacterial ribosomes, supports their broad-spectrum antibacterial activities.

9.14 Doxorubicin:

Doxorubicin is a chemotherapy medication used to treat cancer including breast cancer, bladder cancer, Kaposi's sarcoma, lymphoma, and acute lymphocytic leukemia. Doxorubicin was approved for medical use in the United States in 1974. It is on the World Health Organization's List of Essential Medicines. Versions that are pegylated and in liposomes are also available however, are more expensive. Doxorubicin was originally made from the bacteria *Streptomyces peucetius*. Doxorubicin interacts with DNA by intercalation and inhibition of macromolecular biosynthesis. This inhibits the progression of topoisomerase II, an enzyme which relaxes supercoils in DNA for transcription. Doxorubicin stabilizes the topoisomerase II complex after it has broken the DNA chain for replication, preventing the DNA double helix from being resealed and thereby stopping the process of replication. Doxorubicin and daunorubicin together can be thought of as prototype compounds for the anthracyclines. Subsequent research has led to many other anthracycline antibiotics, or analogs, and there are now over 2,000 known analogs of doxorubicin. Doxorubicin is also known to be fluorescent. This has often been used to characterize doxorubicin concentrations, and has opened the possibility of using the molecule as a theranostic agent.

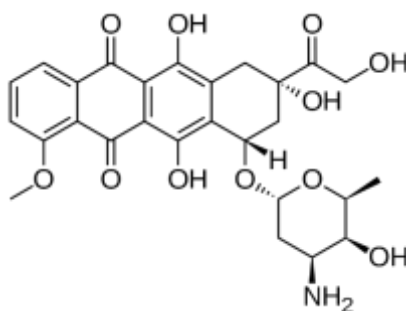


Figure 9.11: Structure of Doxorubicin

Doxorubicin has antimitotic and cytotoxic activity through a number of proposed mechanisms of action: Doxorubicin forms complexes with DNA by intercalation between base pairs, and it inhibits topoisomerase II activity by stabilizing the DNA-topoisomerase II complex, preventing the religation portion of the ligation-religation reaction that topoisomerase II catalyzes.

9.15 Calanolide A:

Calanolide A is an experimental non-nucleoside reverse transcriptase inhibitor (NNRTI). This compound was extracted from the *Calophyllum lanigerum*, of variety *austrocoriaceum*, trees in Lundu, Malaysian state of Sarawak in 1992 by United States National Cancer Institute (NCI). Calanolide A is unique among non-nucleoside reverse transcriptase inhibitor (NNRTIs) in that it may bind two distinct sites in reverse transcriptase, namely active site and Foscarnet binding site of the enzyme. The drug also acts in synergistic fashion with nevirapine in inhibiting HIV-1 virus. In 2003, the Calanolide A compound was found to have anti-tuberculosis activity.

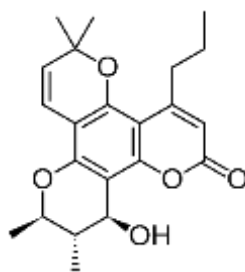


Figure 9.12: Structure of Calanolide A

Calanolide A is unique among non-nucleoside reverse transcriptase inhibitor (NNRTIs) in that it may bind two distinct sites in reverse transcriptase, namely active site and Foscarnet binding site of the enzyme. The drug also acts in synergistic fashion with nevirapine in inhibiting HIV-1 virus. In 2003, the Calanolide A compound was found to have anti-tuberculosis activity.

9.16 Morphine:

Morphine is a pain medication of the opiate family that is found naturally in a number of plants and animals, including humans. It acts directly on the central nervous system (CNS) to decrease the feeling of pain. Morphine was first isolated between 1803 and 1805 by German pharmacist Friedrich Sertürner. Sertürner originally named the substance morphium after the Greek god of dreams, Morpheus, as it has a tendency to cause sleep. This is generally believed to be the first isolation of an active ingredient from a plant. The primary source of morphine is isolation from poppy straw of the opium poppy. Morphine is the most abundant opiate found in opium; the dried latex extracted by shallowly scoring the unripe seedpods of the *Papaver somniferum* poppy. Morphine is generally 8–14% of the dry weight of opium, although specially bred cultivars reach 26% or produce little morphine at all (under 1%, perhaps down to 0.04%). About 70 percent of morphine is used to make other opioids such as hydromorphone, oxycodone, and heroin. It is also on the World Health Organization's List of Essential Medicines. In 2017, it was the 155th-most commonly prescribed medication in the United States, with more than four million prescriptions. Morphine is used primarily to treat both acute and chronic severe pain. Its duration of analgesia is about three to seven hours. Side-effects of nausea and constipation are rarely severe enough to warrant stopping treatment.

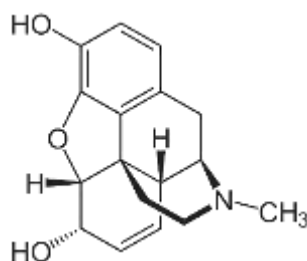


Figure 9.13: Structure of Morphine

Morphine is a highly addictive substance. Morphine is beneficial in reducing the symptom of shortness of breath due to both cancer and noncancer causes. In the setting of breathlessness at rest or on minimal exertion from conditions such as advanced cancer or end-stage cardiorespiratory diseases. Morphine is the prototypical opioid and is the standard against which other opioids are tested. It interacts predominantly with the μ - δ -opioid receptor heteromer. The μ -binding sites are discretely distributed in the human brain, with high densities in the posterior amygdala, hypothalamus, thalamus, nucleus caudatus, putamen, and certain cortical areas. They are also found on the terminal axons of primary afferents within laminae I and II (substantia gelatinosa) of the spinal cord and in the spinal nucleus of the trigeminal nerve. Morphine is a phenanthrene opioid receptor agonist. Its main effect is binding to and activating the μ -opioid receptor (MOR) in the central nervous system.

9.17 Streptomycin:

Streptomycin is an antibiotic used to treat a number of bacterial infections. This includes tuberculosis, *Mycobacterium avium* complex, endocarditis, brucellosis, Burkholderia infection, plague, tularemia, and rat bite fever. Streptomycin was discovered in 1943 from *Streptomyces griseus*. It is on the World Health Organization's List of Essential Medicines, the safest and most effective medicines needed in a health system. Streptomycin is a protein synthesis inhibitor. It binds to the small 16S rRNA of the 30S subunit of the bacterial ribosome, interfering with the binding of formyl-methionyl-tRNA to the 30S subunit. This leads to codon misreading, eventual inhibition of protein synthesis and ultimately death of microbial cells through mechanisms that are still not understood.

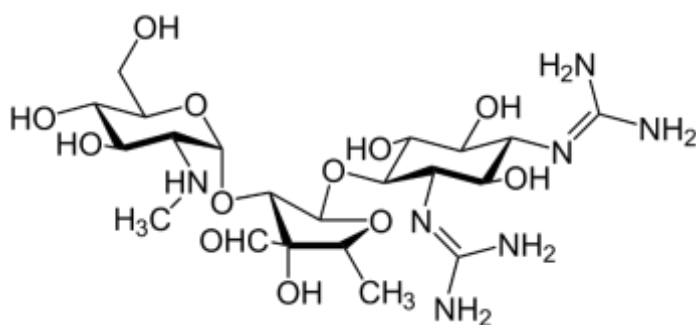


Figure 9.14: Structure of Streptomycin

Streptomycin was first isolated on October 19, 1943, by Albert Schatz, a PhD student in the laboratory of Selman Abraham Waksman at Rutgers University in a research project funded by Merck and Co. Of these, streptomycin and neomycin found extensive application in the treatment of numerous infectious diseases. Streptomycin was the first antibiotic cure for tuberculosis (TB). In 1952 Waksman was the recipient of the Nobel Prize in Physiology or Medicine in recognition "for his discovery of streptomycin, the first antibiotic active against tuberculosis".

Streptomycin is a protein synthesis inhibitor. It binds to the small 16S rRNA of the 30S subunit of the bacterial ribosome irreversibly, interfering with the binding of formyl-methionyl-tRNA to the 30S subunit. This leads to codon misreading, eventual inhibition of protein synthesis and ultimately death of microbial cells through mechanisms that are still not understood. Speculation on this mechanism indicates that the binding of the molecule to the 30S subunit interferes with 50S subunit association with the mRNA strand. This results in an unstable ribosomal-mRNA complex, leading to a frameshift mutation and defective protein synthesis; leading to cell death.

9.18 Quinine:

Quinine is a medication used to treat malaria and babesiosis. This includes the treatment of malaria due to *Plasmodium falciparum* that is resistant to chloroquine when artesunate is not available. Quinine was first isolated in 1820 from the bark of a cinchona tree, which is native to Peru. Bark extracts had been used to treat malaria since at least 1632 and it was introduced to Spain as early as 1636 by Jesuit missionaries from the New World. It is on the World Health Organization's List of Essential Medicines. Quinine is used for its toxicity to the malarial pathogen, *Plasmodium falciparum*, by interfering with the parasite's ability to dissolve and metabolize haemoglobin. It was first used to treat malaria in Rome in 1631. Quinine remained the antimalarial drug of choice until after World War II. Since then, other drugs that have fewer side effects, such as chloroquine, have largely replaced it.

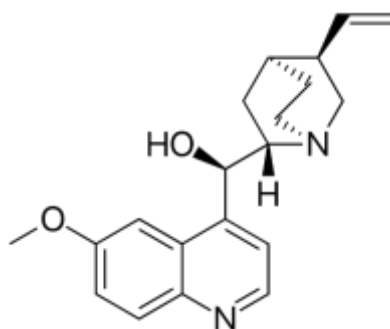


Figure 9.15: Structure of Quinine

Quinine is used for its toxicity to the malarial pathogen, *Plasmodium falciparum*, by interfering with the parasite's ability to dissolve and metabolize haemoglobin. As with other quinoline antimalarial drugs, the precise mechanism of action of quinine has not been fully resolved, although in vitro studies indicate it inhibits nucleic acid and protein synthesis, and

inhibits glycolysis in *P. falciparum*. This model involves the inhibition of hemozoin biocrystallization in the heme detoxification pathway, which facilitates the aggregation of cytotoxic heme. Free cytotoxic heme accumulates in the parasites, causing their deaths. Quinine may target the malaria purine nucleoside phosphorylase enzyme.

9.19 Reference:

1. Wang, Y. *Phytochemistry Reviews* 2008, 7, 395-406.
2. Onaga, L. *EMBO Rep* 2001, 2, 263-265.
3. Cheuka P. M., Mayoka G., Mutai P., Chibal K., *Molecules*, 2017, 22, 58.
4. Cragg, G.M.; Newman, D.J. *Biodiversity: A continuing source of novel drug leads. Pure Appl. Chem.* 2005, 77, 7–24.
5. Hicks, S. *Desert Plants and People*, 1st ed.; Naylor Co.: San Antonio, TX, USA, p. 75.
6. Duke, J.A.; Duke, P.A.K.; du Cellier, J.L. *Duke's Handbook of Medicinal Plants of the Bible*; CRC Press Taylor and Francis Group: Boca Raton, FL, USA, 2008; p. 552.
7. Potterat, O., and Hamburger, M. *Prog Drug Res* 65, 2008, 45, 47-118.
8. Corson, T. W., and Crews, C.M. *Cell*, 2007, 130, 769-774. Greenwood, D. *J Antimicrob Chemother*, 1992, 30, 417-427.
9. Newman, D. J., Cragg, G. M., and Snader, K. M. The influence of natural products upon drug discovery. *Nat Prod Rep* 2000, 17, 215-234.
10. Baker, D. D., Chu, M., Oza, U., and Rajgarhia, V. *Nat Prod Rep* 2007, 24, 1225-1244.
11. Butler, M. S., and Newman, D.J. *Prog Drug Res* 2008, 65, 1, 3-44.
12. Rishton, G. M. *Am J. Cardiol* 2008, 101, 43D-49D.
13. Nussbaum, F., Brands, M., Hinzen, B., Weigand, S., and Häbich, D. *Angew. Chem. Int. Ed.* 2006, 45, 5072-5129.
14. Newman, D. J., Cragg, G. M., and Snader, K.M. *J Nat Prod* 2003, 66, 1022-1037.
15. Paterson, I., and Anderson, E.A. *Chemistry. Science* 2005, 310, 451-453.
16. Koehn, F. E., and Carter, G. T.). *Nat Rev Drug Discov.* 2005, 4, 206-220.
17. Kannel, W. B. *Am J. Cardiol* 1995, 76, 69C-77C.
18. Russell, D. W. *Cardiovasc Drugs Ther* 1992, 6, 103-110. Sabers, C. J., Martin, M. M., Brunn, G. J., Williams, J. M., Dumont, F. J., Wiederrecht, G., and Abraham, R. T. *J Biol Chem* 1995, 270, 815-822.
19. Alberts, A. W., Chen, J., Kuron, G., Hunt, V., Huff, J., Hoffman, C., Rothrock, J., Lopez, M., Joshua, H., Harris, E., et al. *Proc. Natl. Acad. Sci.* 1980. 77, 3957-3961.
20. Kuroda, M., Tsujita, Y., Tanzawa, K., and Endo, A. *Lipids* 1979, 14, 585-589. Mabuchi, H., Haba, T., Tatami, R., Miyamoto, S., Sakai, Y., Wakasugi, T., Watanabe, A., Koizumi, J., and Takeda, R. *N Engl J Med* 1981, 305, 478-482. Mabuchi, H., Sakai, T., Sakai, Y., Yoshimura, A., Watanabe, A., Wakasugi, T., Koizumi, J., and Takeda, R. *N Engl J. Med.* 1983, 308, 609-613. Kuroda, M., Tsujita, Y., Tanzawa, K., and Endo, A. *Lipids* 1979, 14, 585-589.
21. Tobert, J. A. *Nat Rev Drug Discov* 2003, 2, 517-526.
22. Illingworth, D. R., and Sexton, G. J. *J Clin Invest* 1984, 74, 1972-1978.
23. Brown, M. S., and Goldstein, J. L. *J Lipid Res.* 1980, 21, 505-517.
24. Tobert, J.A. *Nat Rev Drug Discov.* 2003, 2, 517-526.
25. Furberg, C. D., and Pitt, B. *Cardiovasc Med* 2001, 2, 205-207.
26. Wani, M. C., Taylor, H. L., Wall, M. E., Coggon, P., and McPhail, A.T. *J. Am. Chem. Soc.* 1971, 93, 2325-2327.

27. Schiff, P. B., Fant, J., and Horwitz, S. B. *Nature* 1979, 277, 665-667. Schiff, P. B., and Horwitz, S. B. *Biochemistry* 1981, 20, 3247-3252.
28. Snyder, J. P., Nettles, J. H., Cornett, B., Downing, K. H., and Nogales, E. *Proc Natl Acad Sci U S A* 2001, 98, 5312-5316.
29. Stewart, Z. A., Mays, D., and Pietenpol, J. A. *Cancer Res* 1999, 59, 3831-3837.
30. Crown, J., and O'Leary, M. *Lancet* 2000, 355, 1176-1178
31. Oberlies, N. H., and Kroll, D. J., *J. Nat. Prod.* 2004, 67, 129-135.
32. Bissery, M. C., Guenard, D., Gueritte-Voegelein, F., and Lavelle, F. *Cancer Res* 1991, 51, 4845-4852.
33. Vezina, C., Kudelski, A., and Sehgal, S. N. *J Antibiot* 1975, 28, 721-726.
34. Heitman, J., Movva, N. R., and Hall, M. N. *New Biol* 1992, 4, 448-460.
35. Dumont, F. J., Staruch, M. J., Koprak, S. L., Melino, M. R., and Sigal, N. H. *J Immunol* 1990, 144, 251-258.
36. Kahan, B. D., Podbielski, J., Napoli, K. L., Katz, S. M., Meier-Kriesche, H. U., and Van Buren, C.T. *Transplantation* 1998, 66, 1040-1046.
37. Foronczewicz, B., Mucha, K., Paczek, L., Chmura, A., and Rowinski, W. *Transpl Int* 2005, 18, 366-368.
38. Morice, M.C., Serruys, P.W., Sousa, J.E., Fajadet, J., Ban Hayashi, E., Perin, M., Colombo, A., Schuler, G., Barragan, P., Guagliumi, G., et al. *N Engl J Med* 2002, 346, 1773-1780.
39. Acton, N., and Klayman, D. L. *Planta Med* 1985, 51, 441-442.
40. Bhisutthibhan, J., Pan, X. Q., Hossler, P. A., Walker, D. J., Yowell, C. A., Carlton, J., Dame, J. B., and Meshnick, S. R. *J Biol Chem* 1998, 273, 16192-16198.
41. Eckstein-Ludwig, U., Webb, R. J., Van Goethem, I. D., East, J. M., Lee, A. G., Kimura, M., O'Neill, P. M., Bray, P. G., Ward, S. A., and Krishna, S. *Nature* 2003, 424, 957-961.
42. Wiesner, J., Ortmann, R., Jomaa, H., and Schlitzer, M. *Angew Chem Int Ed Engl* 2003, 42, 5274-5293.
43. White, N. J. *Science* 2008, 320, 330-334.

10. A Summarized Study of Recent Advances in Biologically Active Quinazolines

Vishwa Deepak Tripathi

Department of Chemistry,
C. M. Science College Darbhanga
(A Constituent Unit of L. N. Mithila University Darbhanga),
Bihar, India.

Abstract:

Quinazolinones and Quinazolines are considered to be most important heterocyclic molecules in the pool of biologically active heterocyclic molecules synthesized in literature. The importance is reflected by the large number of biological potentials related with the same molecule. The present review is focused on the compilation of the reported by researchers in the area of synthesis of biologically active quinazoline based heterocyclic molecules. This review is compiled by authors with the intention of summarizing the biological potential of quinazolines in the order of their targets, which is believed to be very beneficial for readers and researchers actively involved in research. Anti-inflammatory, Analgesic, Antibacterial, Antitubercular, Anticancer and anticancer properties have been included and structures of the synthesized molecules are represented in each section the figures. The level of biological activity and the active functional moiety or pharmacophores are pointed out and the best active compound of each series is discussed sequentially. Authors believe that this review will be very beneficial for readers and covers the important study related to the quinazolines based heterocyclic molecules.

Keywords:

Quinazolines, Quinazolinones, Anticancer, Antitubercular, Antiinflammatory, Analgesic, Anti-convulsant.

10.1 Introduction:

Nitrogen based heterocycles are constituting the most massive group of organic molecules in the field of medicinal chemistry and drug discovery. More than 80% of the bioactive natural and synthetic molecules are the nitrogen containing heterocycles. Among all the nitrogen-based heterocycles the quinazoline group-based heterocycles are even most omnipresent whether synthetic or natural molecules. The three types of heterocycles belonging to same class one is Quinazoline and other two types of Quinazolinone structures lies in the present category. These structures are very closely related in structures, only difference is the presence of the ketonic group and its position in the molecule.

The structures are shown the figure 11.1. The figure one clearly shows that the quianzoline does not possess the ketonic group and Quinazolin-2(1H)-one contains ketonic group at position 2 and Quinazolin-4(3H)-one contains ketonic group at 4th position.

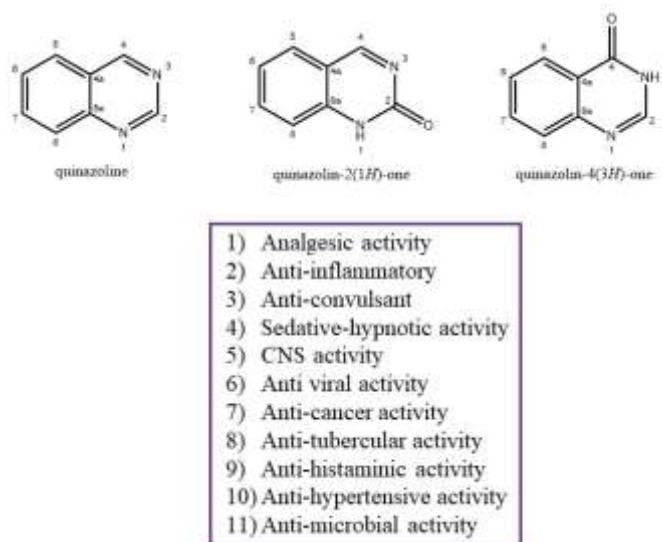


Figure 10.1: Structure of Quinazolines and Biological Activities Associated with them.

A careful survey of literature reveals the fact that these three structures are omnipresent in the most of the drugs and bioactive molecules. The Quinazoline molecule lies in category of fused heterocycle in which a benzene ring is fused with a pyrimidine ring as illustrated in figure 10.1. The oxoquinazoline analogue which is considered to be first synthetic molecules of this class was first synthesized from group of Griess et al., in 1869, by condensation process. Similar analogues were prepared by Bischler and Lang by a decarboxylative reaction of 2-carboxy compound.

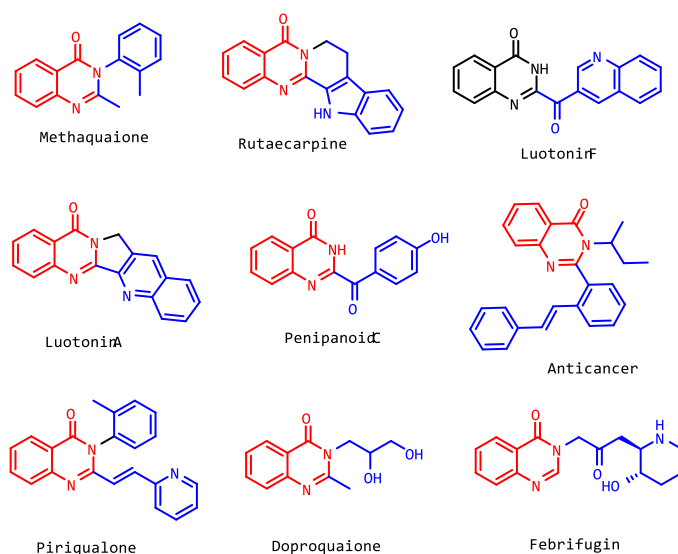


Figure 10.2: Biologically Active Quinazoline Based Natural and Drug Molecules

Quinazolines and its related compounds are well reported in literature for their excellent biological properties against various biological targets. Quinazoline based molecules and natural products are known for their analgesic, anti-oxidant, anti-inflammatory and other. We collected the molecules from various sources and categorized them according to their pharmacological significance. We covered the Analgesic, Anticancer, Anticonvulsant, Antimicrobial, Antitubercular and anti-inflammatory properties of these molecules.

10.2 Summary of Quinazolines with Biological Potential Against Different Targets:

10.2.1 Analgesic Activity:

2-phenyl quinazoline and its derivatives were prepared by Alagarsamy research group and they evaluated their synthesized molecules for their analgesic properties.¹⁷ They converted the quinazoline nucleus into various derivatives and established a proper Structure Activity Relationship (SAR). They introduced methyl, thiomethyl, butyl and benzyl substitution on the heterocyclic ring.¹⁸⁻¹⁹

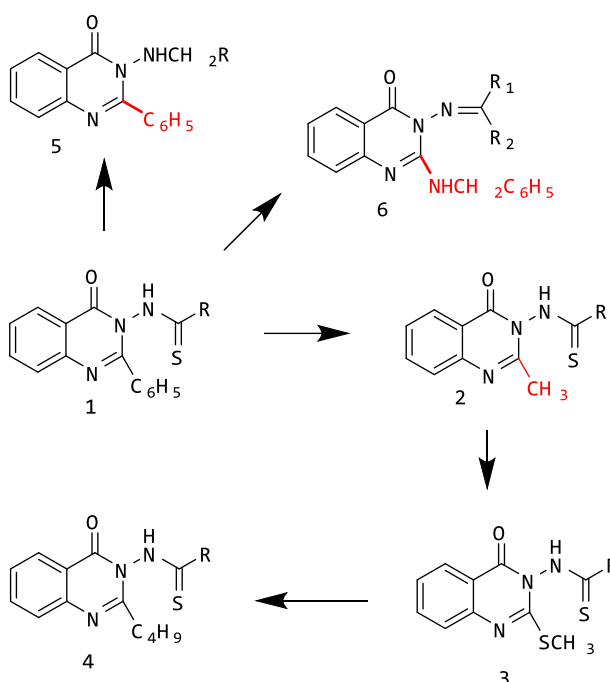


Figure 10.3: Structures of Quinazoline Derivatives Exhibited Analgesic Activities.

They reported that the introduction of alkyl groups as shown in structure 2, 3 and 5 results in increase in analgesic activity of molecules. An increase in the lipophilic character by introducing the alkyl group is believed to be responsible for better biological activity. While any heteroatom in the alkyl group shows the decrease in the activity of molecule which may be due to the increase in the polarity of molecules. They have shown that the introduction of amino derivatives in place of alky groups further lowers the activity of quinazoline

analogues. The most active compound was found to be structure **3** with activity of around 58% potential within 2.5 h in vivo evaluation. The thiourea substituted analogue **2** and **3** were also prepared by them through changing the aromatic phenyl ring in structure **1** with methyl group and further it converted to corresponding thomethyl analogues.²⁰⁻²² (Figure 10.3)

Further in continuation of their work they have prepared methoxy substituted quinazolines (**7**) as shown in the figure 10.3. Among the analogues prepared by them the methylpropylidene derivative have shown the enhanced potential with activity of 65% analgesic potential within 3 h.²³ They also reported the synthesis of 3-phenylquinazolinone (**8**) which exhibited the activity of (74 % analgesic potential at 3 h at 20 miligram per Kg,). They reported the further synthesis of (1,3,4)-thiadiazolo quinazolinones **9** which shows moderate biological activity.

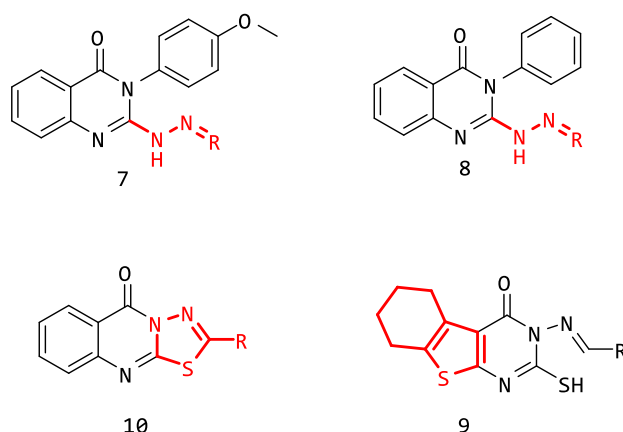


Figure 10.4: Structures of Few Potent Analgesic Molecules

From their study they identified that introduction of alkyl group or lipophilicity at at N-3 position increases the pharmacological property of the molecules. They also shown the preparation of isosteric analogue of theses molecues by synthesizing the mercapto substituted amino derives of quinazolines which does not exhibit enhancement in activity. The best active compound of this series was butylideneamino analogue with activity of (74 % analgesic potential at 3 h at 20 miligram per kg body weight).²⁴⁻²⁶

In another report Kumar and coworkers have shown the preparation of 3 substituted phenyl halogen analogues **11** and its analogues.²⁷ After biological evaluation they found that 11 was showing moderate biological activity at 50 mg/kg dose. They also prepared hydrazine analogues compound **12** which were exhibiting decreased biological activity.

Pyrazino derivative compound **13** of the main compounds was also been prepared and evaluated for activity, which shown potent pharmacological activity. The derivative having 4-chloro substitution at the phenyl ring was reported as the derivatives with highest level of biological activity within the series. These molecules have also shown th COX (Cyclo oxygenase) inhibitor activity. In extension of this work, they made efforts for introduction of indolyl moiety at C-3 postion nad prepared 2,3,6-trisubstituted quinazolinones **14**.

Substitution of Amino-acetyl methylene group also introduced at 2nd place of the heterocyclic ring to increase the biological activity of this series.²⁸ On biological evaluation they found that trisubstituted quinazolinone shown moderate biological activity while introduction of phenylamino-acetyl-methylene chain increased the pharmacological potential.

The thiazolyl moiety in quinazolinones at C-2 position known to trigger the biological activity in these molecules. *o*-methoxyphenylthiazolidine analogue was the most active compound prepared by them in this series with more than 80% of analgesic activity.

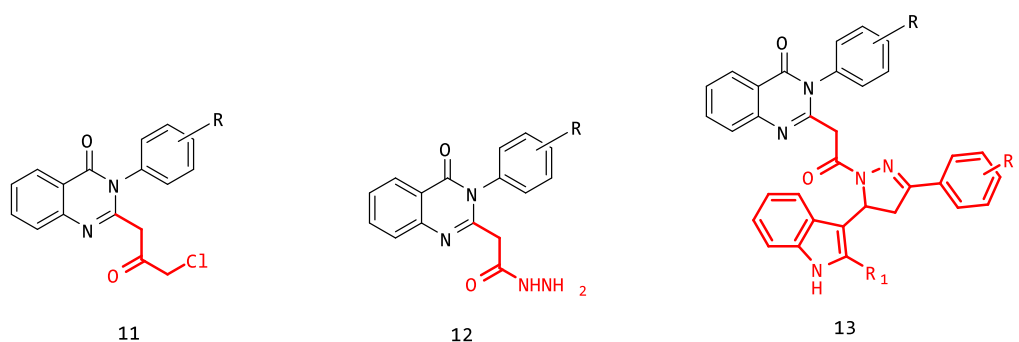


Figure 10.5: Structures Showing the Quinazolinones with Analgesic Activity.

Further the Indolyl moiety at C-3 position is replaced by thiazolyl group **16** in the series. Thiazolyl quinazolinones show moderate analgesic activity at 50mg/kg dose. In place of thiazolyl group the azomethane linkage and azetidione moieties **17** were introduced at position C-3 and evaluated for activity which showed increased activity.²⁹ On placing thiazolinone in place of azetidione compound **18** exhibited better pharmacological activity.

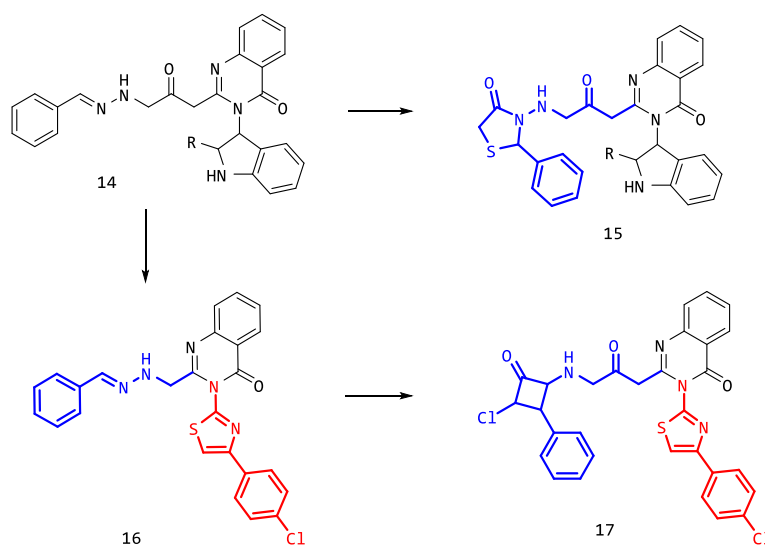


Figure 10.6: Structure of Few Quinazolinone Analogues Having Analgesic Activity

Several pyrazoles based quinazolinone derivatives (compound 19) were synthesized as shown in the figure 7. The 2-phenyl analogue have shown the activity of (65% inhibition) while 2-ethyl substitution compound have shown the activity of (45% potential) whereas methyl substitution at the aromatic ring shown (50% analgesic property). The derivative with 2 methyl substitution was reported to be the best molecule of the series of was, which have shown 24% inhibition in acetic acid.³⁰⁻³¹ Isatin being a very interesting heterocycle from biological perspective, attracted synthetic medicinal chemists to work on this specific moiety. In a work reported isatin based hydrazine derivatives of quinazolinones have been prepared by attaching heteroaryl groups such as 2 substituted hydrazide derivative of quinazolinone moiety and hydrazide derivative of benzoxazinonyl by using hydrazine followed by condensation involving isatin analogues.

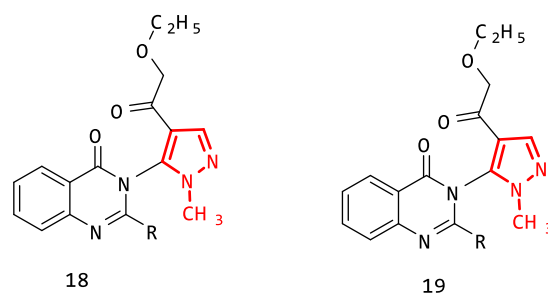


Figure 10.7: Structures of Some Pyrazole Derivatives of Quinazolinone Analogues.

SAR study shows that the 2-phenyl analogues of quinazolinone shown increased activity than 2-methyl derivative. The amino substitution on phenyl ring at the nitrogen at N-1 position have not affect biological potential of quinazolinone instead the methyl substituted quinazolinone as indicated by molecules 23. derivative showed only mid activity. The bicyclic heteroaromatic pharmacophores 24 were synthesized by the enhanced biological properties, good aqueous solubility made this molecule a potential drug candidate to test in higher animal models after its in vivo activity.³²⁻³⁵

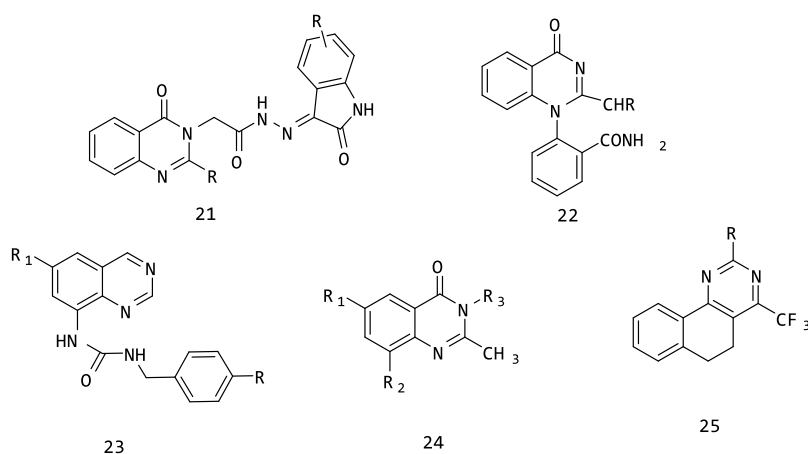


Figure 10.8: Structures Of Isatin Analogues of Quinazolinones.

10.2.2 Anti-Inflammatory Activity:

Quinazolinones are well reported in literature for its pharmacological property against inflammation. All the structures discussed above have also been evaluated for their potential against inflammation in literature and were found to be potentially useful. In this section we will discuss the structures of molecules bearing the quinazoline and quinazolinone nucleus and showing the anti-inflammatory property. The quinazolinone nucleus have been derivatized in various ways to improve its biological activity, and few of them are explained in this section. In one of the report 12 methyl analogue of quinazolinone **27** and 6 methyl derivative of quinazolinone **28** compounds have been prepared as novel ring systems and after anti-inflammatory biological evaluation they were found to be good molecules against inflammation and inflammatory disease. The isopropyl analogue of quinazolinone (**26**) derivative was showing moderate anti-inflammatory activity. In this series compounds 27 and 28 were found to be better anti-inflammatory agent than 26.³⁶⁻³⁷

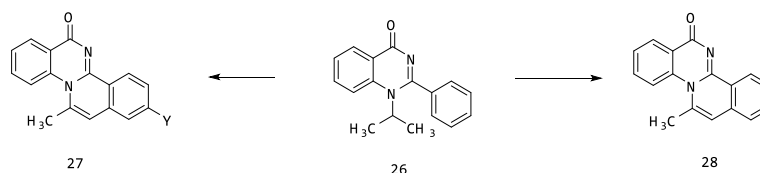


Figure 10.9. Structure of molecules having anti-inflammatory activity

In an attempt to screen the biological activity of 6 aminoarylmethyl derivatives of quinazolinone **31** dihydro analogue **32** these molecules have been synthesized and evaluated for biological potential. The screened molecules have shown varying activity (from 12.7% to 58.24%). The iodo derivative at position 10 in the compound 31 exhibit remarkable increase in biological activity as anti-inflammatory molecule. Instead, the phenylaminoethyl group and p-methoxyphenylaminoethyl at position 6 also shown to increase the biological activity of compound. With help of QSAR it was established that 4-(1H)-quinazolinones **33** increase the anti-inflammatory property in the quinazolinone nucleus. In this report the entire series have shown potential anti-inflammatory property, but 2-piperdinomethyl derivatives were found to be best active molecules.³⁸⁻⁴¹

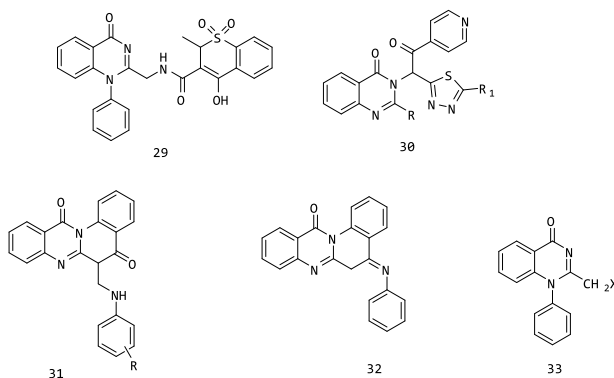


Figure 10.10: Structure showing anti-inflammatory quinazolinone molecules

In an attempt to access the trisubstituted quinazolinones another series of quinazolinones were prepared as shown in Figure 10.10. These synthesized compounds were evaluated for in vivo potential activity in rat paw edema at 50 milligram per kilogram body weight dose.

Results of screening explained that the synthesized compounds **34-38** shown broad range of biological activity ranging from 10.28% to 53.33%. The methoxy group at the 3rd place and dimethylamino substitution at the second place were found to increase the biological activity.

These molecules have also exhibited the ulcerogenic activity, while the phenylbutazone was the best ulcerogenic compound.⁴²

The benzothiazole substituted 2-phenyl quinazolinones as shown in figure **39** and **40** were prepared to evaluate their anti-inflammatory property by using the standard indomethacin as reference.

After evaluation it was established that the synthesized series displayed varying range of biological activity ranging from 21.3% to 27% protection in carrageenan induced edema method.⁴³

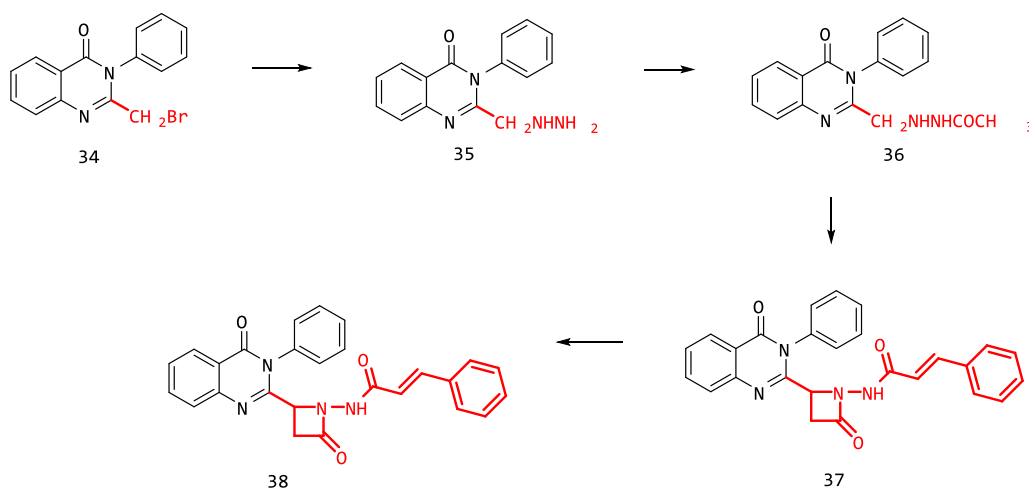


Figure 10.11: Scheme showing synthesis of azitidine based quinazolinone analogues

In extension of this work the bromo derivative **40** also prepared and evaluated for activity which displayed the less biological potential than the parent molecule.

The SAR established in this study was that the electron withdrawing groups (like p-nitro and halogen) tends to decrease the biological activity while electron donating groups (like alkyl and alkoxy) tends to increase the biological activity of compounds. The mild activity as COX-I enzyme inhibitor have shown by these molecules.⁴⁴⁻⁴⁵

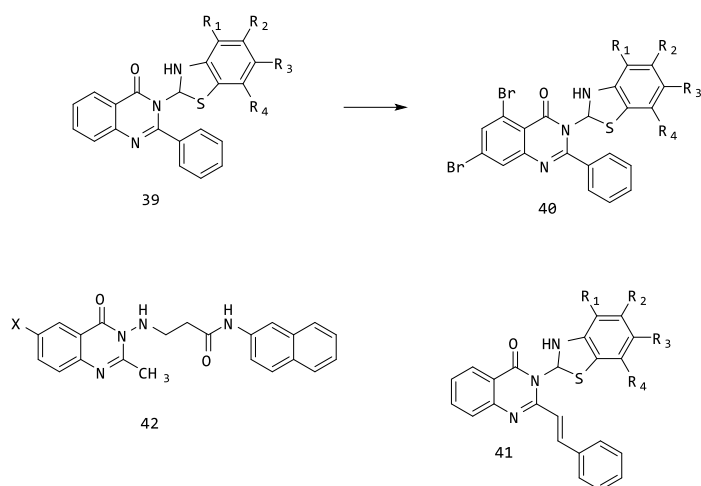


Figure 10.12: Structures of some thiazole based anti-inflammatory quinazolines

In one of the reports few novel quinazolinones were prepared with thiazolidinone and azetidinone in order to study their anti-inflammatory activity. The studied compounds (**43-45**) were found to be substantiative active against the screened target with activity ranging from (16.3-36.3%) compared to reference phenylbutazone.⁴⁶ The authors have reported that biological potential of molecule increase effectively on cyclasation of arylidene compound **43** into azetidinone **44** and thiazolidinones **45**. Whereas thiazolidinone nucleus was found to be better than corresponding azetidinone analogues. The compound 46 Leniolisib is a potent phosphoinositide-3-kinase inhibitor synthesized from compound 46 is a selective inhibitor with more active as anti-inflammatory agent.

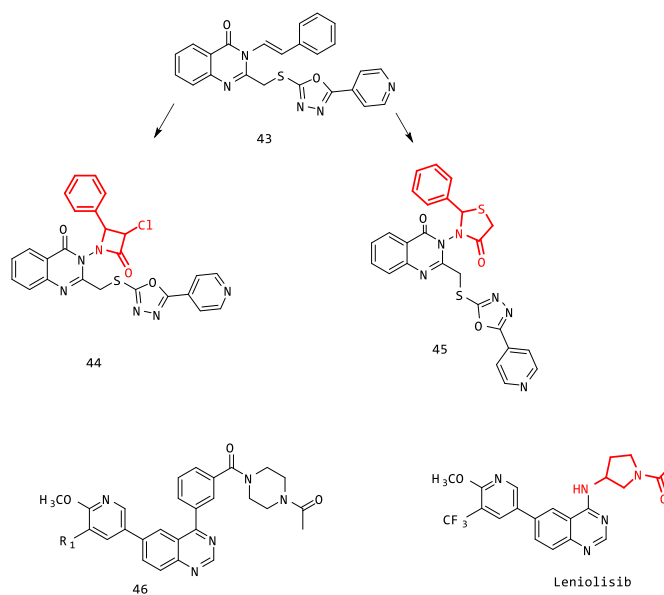


Figure 10.13: Some thiazolidinone and azetidinone analogues with anti-inflammatory activity.

This is reported to inhibit the large spectrum of immune cell functions for B cells at IC₅₀ value of 0.007 micromolar to 0.2020 μ M, nutrophils, mast cells, plasmocytidic dendritic cells, basophiles, monocytes, neutrophils. It is also reported to inhibit antigen specific antibody production and shows excellent results by reducing the disease behavior.⁴⁷

10.2.3 Anticonvulsant Activity:

The compounds bearing quinazolinone moiety quinazolinonyl pyrazolines **49** and quinazolinyl isoxazolines **50** have been screened for their anti-convulsant activity. These molecules were prepared from compound 47 through the formation of the compound **48**.

The compounds screened have exhibited diverse range of biological potential. As shown the figure 13 the molecules exhibited higher anti-convulsant poential.

The resean behind this activity is reported to be the presence of pyrazole and isoxazole based heterocycles. A total of 30 compound shave been synthesized in this report out of which eight showed significant inhibition.⁴⁸

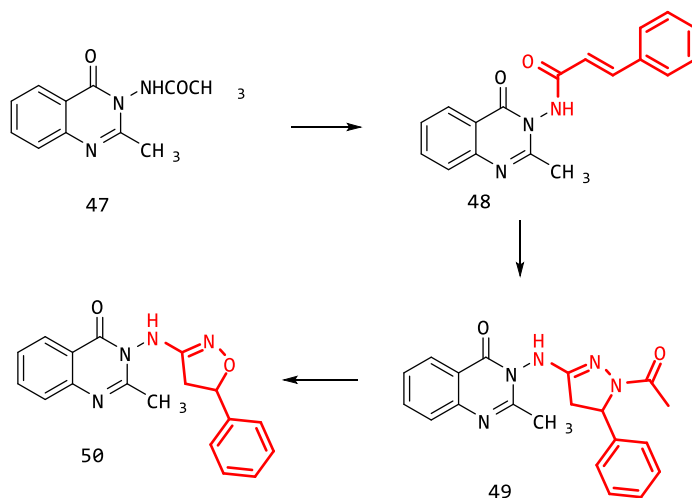


Figure 10.14: Structures showing pyrazolines and quinazolinyl isoxazolines analogues with anti-convulsant activities.

A small group of quinazolin-4(3H)-one based molecules (**51-55**) have been prepared to investigate their anti-convulsant activity as shown in figure 14. These molecules were tested in vivo by applying MES (maximal electro schok) method. The increased activity was shown by the molecule 53 having thiadiazole at C-3 position was (40-50%).

The compounds **51** and **52** were found to be less potential by showing inhibition (20-30%) and (30-50%) respectively. These activities were found to be less than the standard used phenytoin, for which the inhibition was 80%. The alkyl benzylidenyl group in the structure **54** is reported to be crucial for biological activities of these molecules. Results shown that the phenyl group substituted molecules showed less activity.⁴⁹

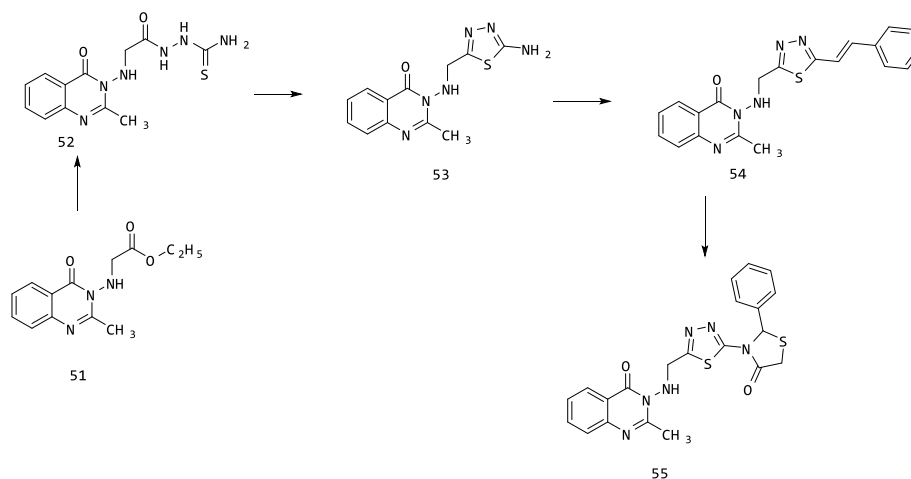


Figure 10.15: Quinazolinone based compounds having anti-convulsant activity

Medicinal Chemists around the globe are making efforts towards development of new molecules for anti-convulsant activity in order to reduce the side effect of existing drugs. In this effort 2 substituted heterocyclic nucleus like 2-thiobarbituric acid and quinazolinone based single molecular framework have been synthesized. After the screening of compound aminoethyl substitution at 3rd position showed average biological potential as anti-convulsant agent, while the compound **57** thiosemicarbazone analogue exhibited more anti-convulsant property. The activity of molecule was increased to some extent on incorporating oxothiosemicarbazone substitution in quinazolinone system results in higher potential for convulsant disorder. The molecule **58** having oxobarbituric acid substitution was found to be more potent. The compound **59** thiazole analogue was achieved by cyclisation of **57** by sulfuric acid and liquid ammonia. These analogues were found to be more potent anti-convulsant agents. In another modification of this nucleus the quinazolinone nucleus was converted into thiazolo acid substituted quinazolinone **60**. Compound **60** has shown excellent anti-convulsant activity with 60-90% protection in both models. The best active molecule was found to be 6,8-dibromo quinazolinone and thiobarbituric acid.⁵⁰⁻⁵²

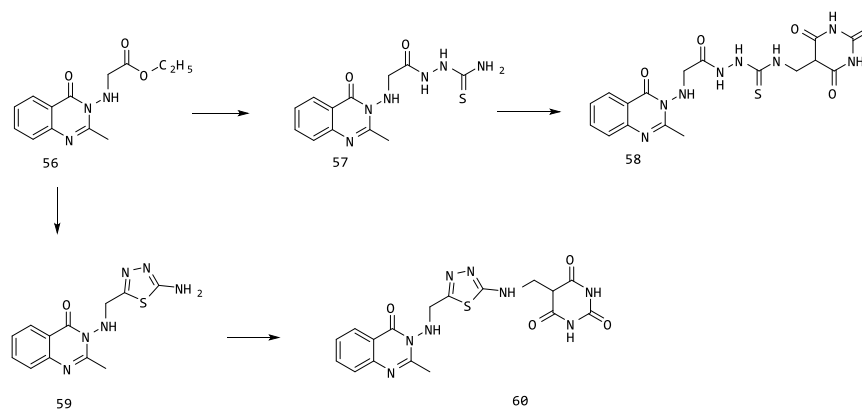


Figure 10.16: Few quinazolinone analogues with anti-convulsant activity

In one of the reports published 4-(3*H*)-quinazolinethiones were found to be very less active as CNS active agent in 4-(3*H*)-quinazolinethione **61**. Author has reported that if sygen is replaced by sulphur, then it leads to reduce the biological activity. Authors did the modification in quinazoline moiety havin fluoromethyl substitution in the parent quinazoline based heterocyclic system **62**, **63**, **64** and tested all the prepared analogues for their CNS depressant activity.

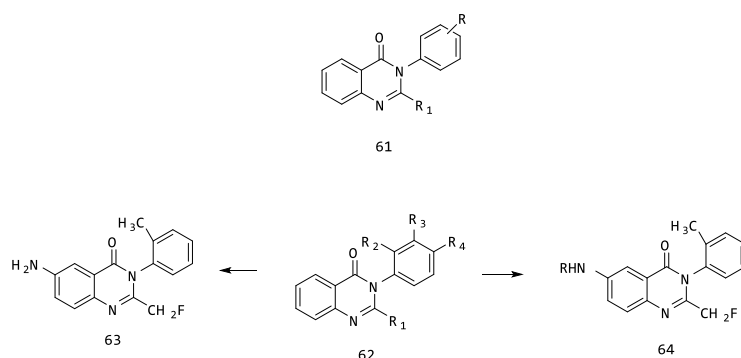


Figure 10.17: Structures of few quinazolinones shoeing CNS depressant activity.

It was noted by the result of biological evaluation that 2-fluoromethyl moiety with fluorine in place of hydrogen exhibits very nominal decrease in activity, but 2-trifluoromethyl analogueshoed greater activity. But it was reported that 3-phenyl substitution in hydroxyl group decreases the biological activity.⁵³ Quinazolinone ring system is also part of some metabolites of molecule afloqualone as depicted in figure 10.17. These metabolites were synthesized in laboratory in an attempt and exhibited significant potential as CNS active agentat 100 mg/kg dose with LD50 of >100 mg/kg. But the activity was lost in case of 6-amino derivative. This result shows that free 6-amino group is not active biologically so the protection of this group is required first to convert it into active analogue. Authors Also reported the the size of the substitution is also very important for the activity. While analyzing the toxic nature of these molecules the substituted quinazolin-4-one **67** and 1,8-naphthyridines were found to be least toxic in nature.⁵⁴⁻⁵⁷

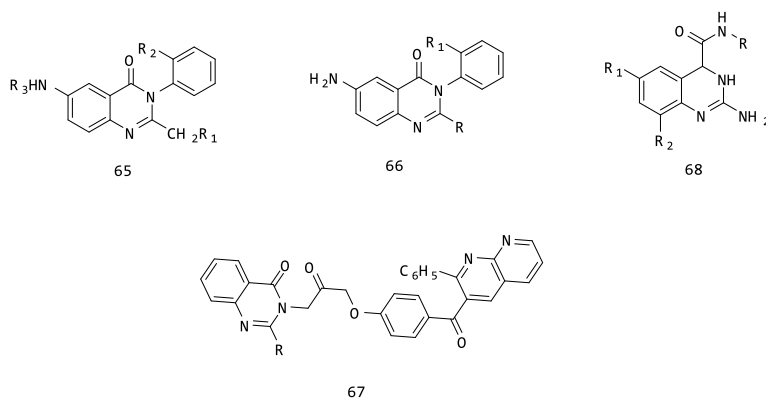


Figure 10.18: Quinazolinone derivatives as CNS depressant activity

11.2.4 Antiviral Activity:

Quinazolinones and quinazoline molecules are also reported to possess antiviral properties. Many quinazolinone based nucleus and its derivatives have been synthesized and evaluated for their antiviral properties. Few of the reports are included in this section regarding antiviral effects of quinazoline and quinazolinone molecules.

In this regard 2-substituted thiadiazolo quinazoline derivatives have been prepared and evaluated for their property against Human immunodeficiency virus. Observation of biological evaluation reveals that 4-methoxy substitution in the phenylamino ring derivative exhibited 15% inhibition but 2-propene amino substitution derivative exhibited decreased level of biological activity. The disubstitution of quinazoline followed by the biological evaluation against the antiviral target 31-25% defense.⁵⁸

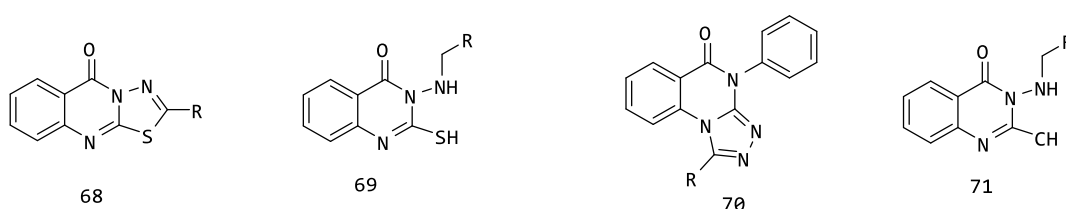


Figure 10.19: Quinazolinone derivatives with anti-HIV activity.

The new sulphonamido quinazolin-4-(3H)-one's derivatives also reported for their mild anti-HIV activity. These molecules were synthesized and evaluated for anti-HIV properties, but the evaluated compounds of this series were not very good inhibitor of HIV. While these molecules were showing cytotoxic effects in the evaluated cell lines.⁵⁹⁻⁶¹

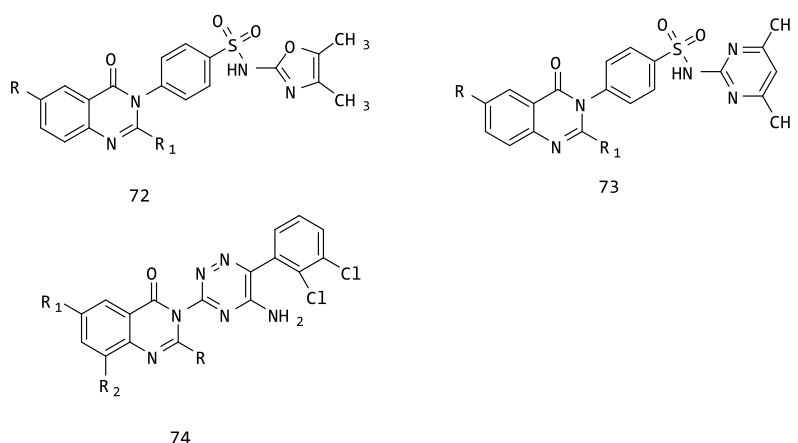


Figure 10.20: Quinazolinone sulfonamide analogues evaluated for anti-HIV property.

In an attempt few novel disubstituted quinazolinone analogues have been prepared and were screened for their inhibitory property against HIV-1. The results showed that the analogue with imidazole ring was better as anti-HIV molecule.⁶²⁻⁶³

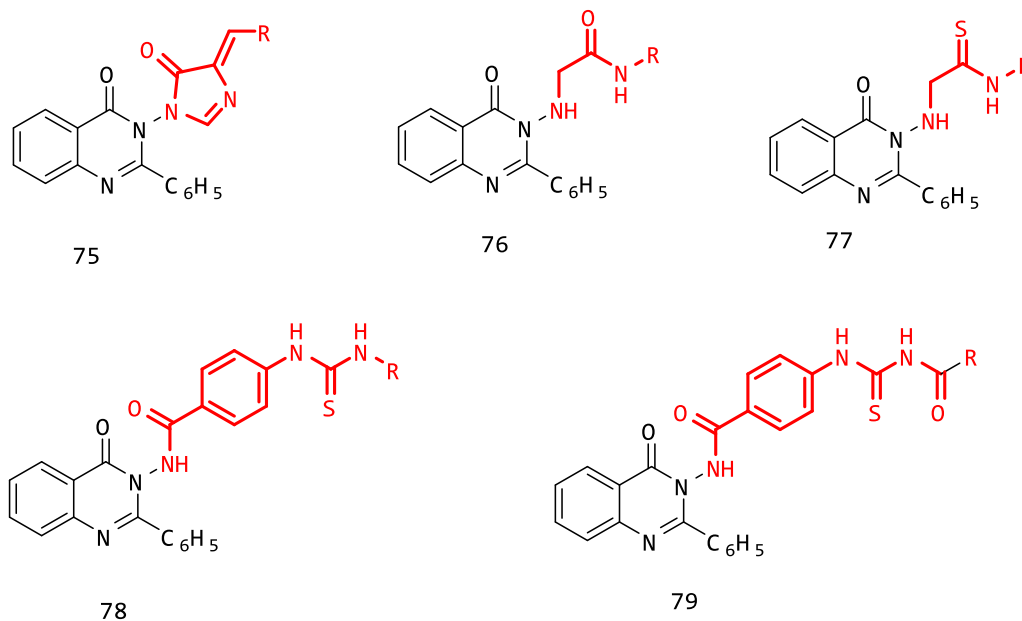


Figure 10.21: Quinazolinone analogues highlighting the pharmacophoric moiety.

Whereas arylacetamide substitution at the 3rd place in the parent heterocyclic system were found to be enhancing in terms of anti-HIV potential. The best molecule of this series was the 4-hydroxybenzylidino imidazoline derivatives with 48% inhibition. Surprisingly the molecules with phenyl thiourea moiety were found to be least active.⁶⁴

The 2-methyl-3-(arylthiocarbamido)-quinazol-4-one's series derivatives as depicted in figure 10.21 were synthesized and evaluated for their biological potential against Gomphrena mosaic virus. They exhibited the viral inhibition in varying range in between 15-80 %. A careful evaluation of biological activity shows that the dichlorophenyl thiocarbamido and hydroxyl substitution at the 4th position derivatives have shown maximum reduction of the viral colonies.

This proves that the chloro and hydroxyl substitution in phenyl ring enhances the biological activity of compound. Halogen substitution specifically the chloro substitution have reported to alter the biological potential upto significant extent of molecule.⁶⁵

In another work the bromo derivative of the 2,3 disubstituted quinazolinone analogues were designed and prepared to evaluate the cytotoxic and anti-viral activity. It was found in the investigation that the phenyl substitution at 2nd place and chlorophenyl analogue at 3rd position of aminoquinazolinone enhances the virus inhibiting potential to a great extent with MIC value of 1.92 µg/ml.

These compounds showed cytotoxic property in HeLa cells too. But the analogues with methyl and phenyl groups were found to be least active for their cytotoxic activity.⁶⁶ In an attempt to study the effect of inserting fused heterocyclic system in molecule on anti-viral property a series of 1,2,3-trisubstituted pyrrolidine analogues

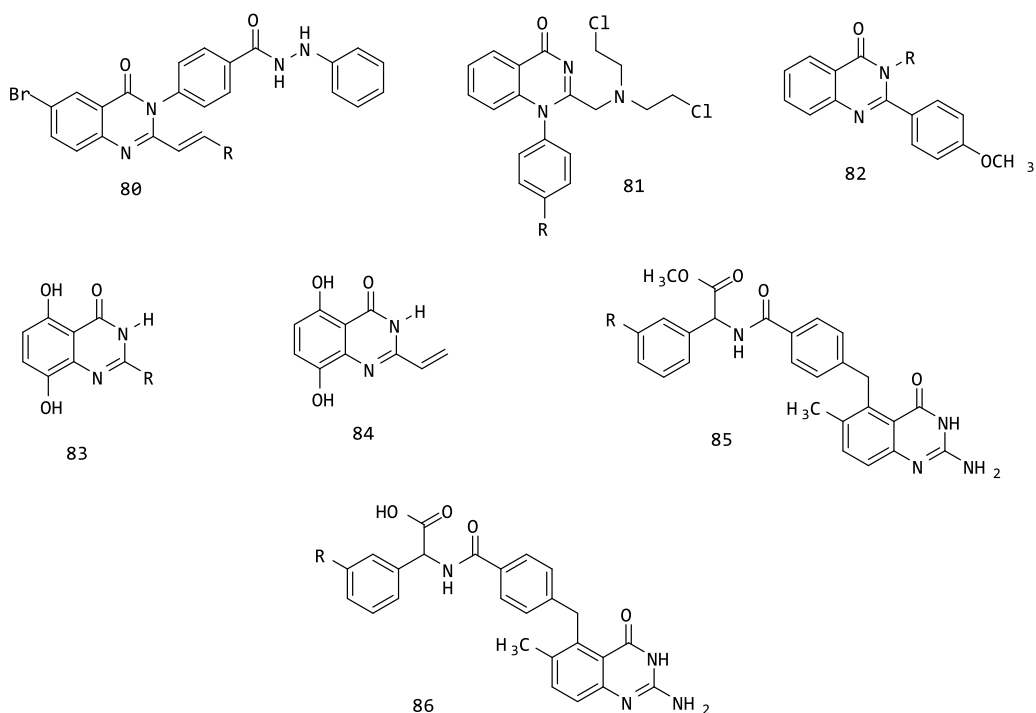


Figure 10.22: Quinazolinones with fused heterocyclic systems showing anti-viral activity

among all the analogues synthesized the imidazo-[4,5-b]-pyridine analogue showed a comparable anti-viral potential as shown by benzimidazole. Imidazopyridine derivatives with IC_{50} value of 2.8 nM have shown the maximum anti-viral activity.

Interestingly the oxo/thiono triazolo isoquinolinyl quinazolones derivatives were screened for viral inhibition and among the tested compounds the phenyl substituted analogue has been found to possess adequate inhibition for influenza virus whereas the other members of the series were found to be mild active as antiviral agents.⁶⁷⁻⁶⁸

10.2.5 Anticancer Activity:

Quinazolinone heterocyclic moiety is reported in literature for anticancer activity against various cell lines as breast cancer cells, prostate cancer, lung cancer, Ovarian cancer, blood cancer etc. Due to its pharmacophoric nature this moiety has attracted considerable interest of medicinal chemists worldwide.

Some quinazolinones were planned for their synthesis, cancer inhibiting potential evaluation and docking studies. This series of molecules were tested for DHF reductase inhibition potential by applying DHFR inhibition assay methodology and using methotrexate as positive control. Interestingly the evaluated compounds showed a lower range of IC_{50} values from 0.4 to 70 μ M. The benzyl, phenyl and methyl substitution in the parent nucleus was found to increase the anti-cancer potential.

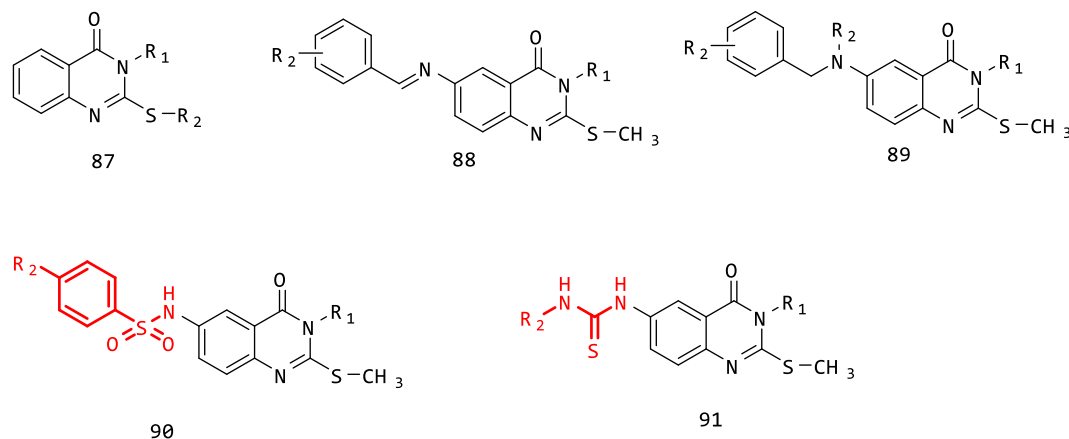


Figure 10.23: Quinazolinones with anticancer activity.

In an attempt several novel analogues were prepared and screened for their inhibitory property against cyclin dependent kinases (CDKs). The evaluated molecules showed satisfactory potential as cyclin dependent kinase inhibitors and their less selective nature against serine-threonine and tyrosine kinases. The most potent molecule of the series was optimized to more stable analogue, good solubility and more stable plasma protein binding. In vivo evaluation was carried out in healthy nude mouse (10 mg/kg) showed the half-life of 2.6 h. This molecule was given orally in a dose of 10mg/kg body weight and displayed highest level of oral bioavailability (85%).⁷²⁻⁷⁴

A new series of pyrido substituted analogues have been synthesized and evaluated against irreversible pan-erbB inhibitor. A detailed SAR study reveals that in case of 3 chloro derivative and 5 amino benzyl derivative, 5 amino benzyl indazole analogue, substitutions researchers found excellent potency for pan-erbB isolated enzyme inhibition with IC₅₀ value of 500 nM range. The molecules bearing cyclic amine substitutions were found to be rapid inhibitors of cellular erbB1 target. Interestingly the 4-anilino substitution was found to be the enhancer for pan-erbB inhibition potential. The pyrido[3,4-*d*] pyrimidine analogue was found better inhibitor than the standard canertinib. Author considered the presence of piperidiny crotonamide Michael acceptor and a 3 chloro substituted analogue the main source for generating inhibitory property in the molecule.⁷⁵⁻⁷⁶

Baria and coworkers reported the synthesis and SAR study in pyrazolo substituted quinazolinone analogues. They found that this class of compounds work as good P1k1 inhibitors with the inhibitory concentration of value of 0.005 micromolar. They found that dioxolane, dioxane, and dioxepine quinazolinone analogues emerged as good EGFR inhibitors. The evaluated derivatives have exhibited IC₅₀ values of 0.067 to 10 μM.⁷⁷⁻⁷⁸

A small library of quinazolinone based molecules have been prepared to investigate the effective and selective BCRP inhibitors. Substitution at 2, 4, 6 and 7 position of the parent quinazolinone nucleus was introduced in order to develop a detailed structure activity relationship. A careful analysis of SAR in this work showed that the phenyl substitution at 2nd and 4th position in parent anilinoquinazolinone moiety were having more

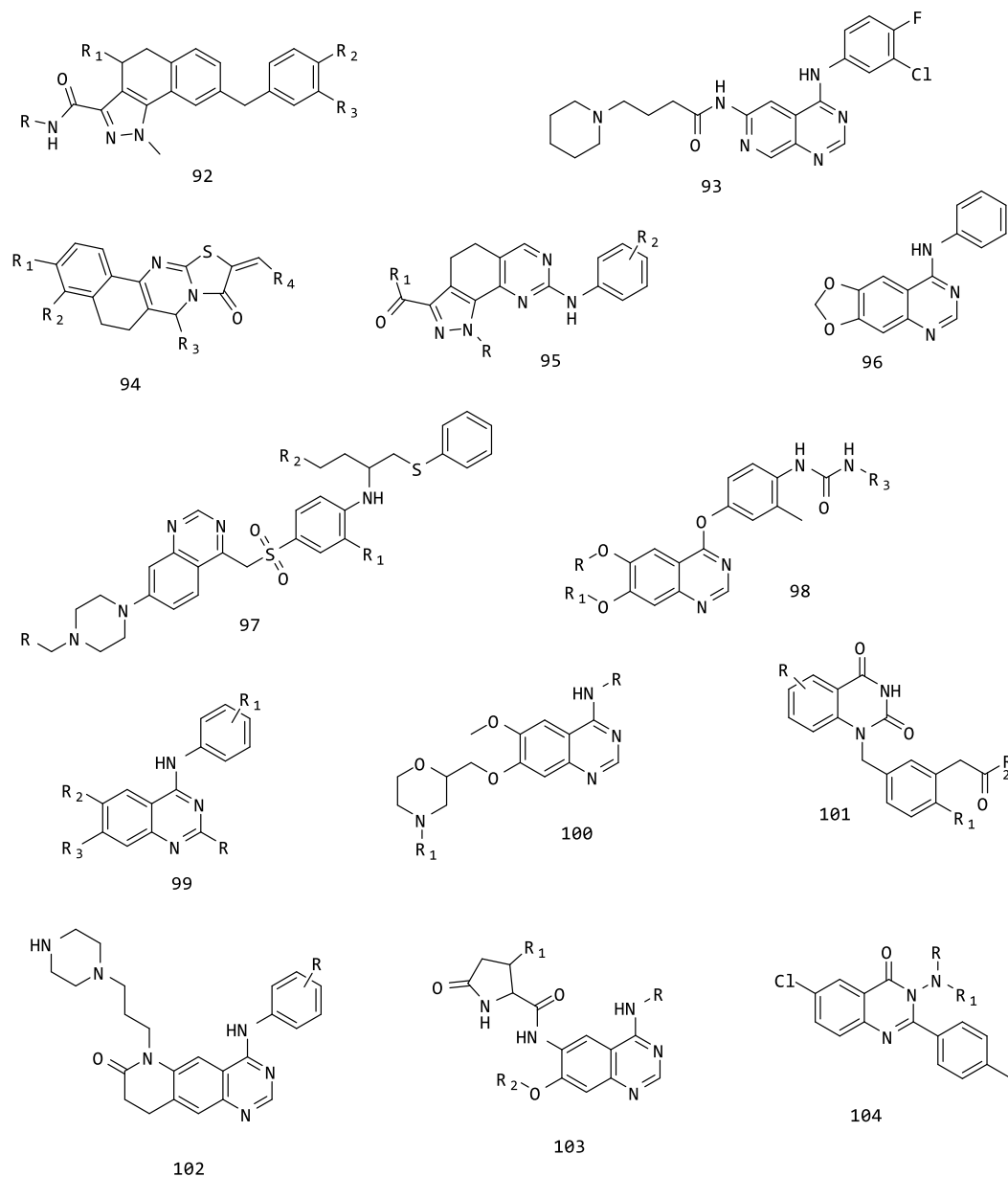


Figure 10.24: Quinazolinone based molecules bearing anticancer activity

potential than the other analogues of the series. The NO₂, Cn and CF₃ substitutions were found to be pharmacophoric substituents and enhances the BCRP inhibition potencies.⁷⁹⁻⁸⁰ The dihydro dioxino analogues have been prepared in an attempt to evaluate the anticancer properties of synthesized molecules. Evaluated derivatives were found to be active against EGFRwt and exhibited very good inhibition. The inhibitory potential of these molecules was as low as 50 nM and for few analogues upto 10 nM. 11 molecules of the series have shown IC₅₀ values of 100 nM. Docking studies of these compounds against EGFR active pocket have supported the inhibitory potential as shown in the figure.⁸¹

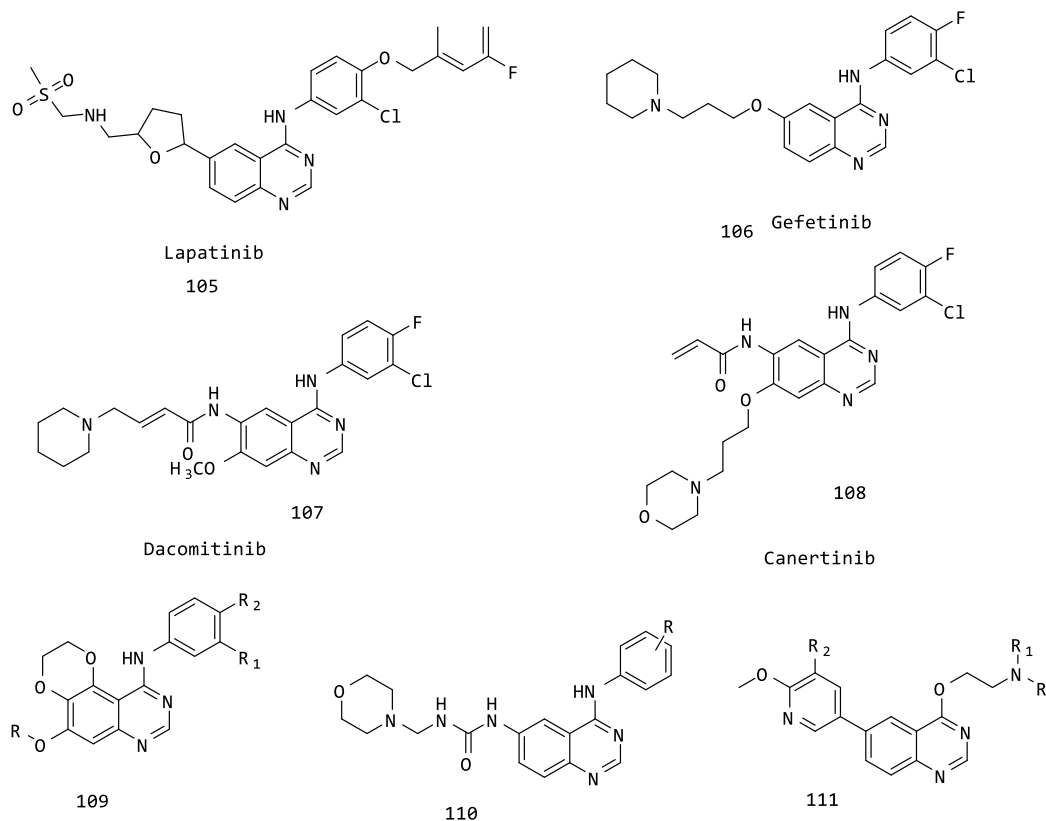


Figure 10.25: 4-anilinoquinazolines based anticancer quinazolines.

The molecules based on aniline substitution at the 4th place of quinazoline with ureido at the 6th place and and thioureido analogues have been synthesized as shown in the figure for investigating their inhibitory effect against wide type mutant EGFR.

The screened compounds have shown the inhibition of EGFR targets with IC₅₀ values of 0.4 to 9.5 nM range. These molecules exhibited good inhibition with IC₅₀ value of (1.76-2.38 nM). The binding mode of the molecules were further supported by docking studies.⁸²

The library of compounds contacting 4,6-disubstituted quinazoline derivatives have been synthesized and screened against PI3K target. The evaluated molecules were showing very good inhibition of lung cancer and breast cancer cell lines with IC₅₀ values in the range of 0.5-38 nM. The most active molecule of the series was 2-morpholinoethylamino analogue which was showing inhibition with inhibitory concentration value of 0.4 micromolar for lung cancer and inhibitory concentration value 0.11 micromolar whereas dimethyl amino derivatives have also shown inhibition against evaluated cell lines.

This analogue was not efficient as MCF-7 inhibitor but the IC₅₀ value was found to be 8.6 μM. The substitutions at position 4 of quinazoline is considered to play important role in determining the biological potency of molecule.⁸³

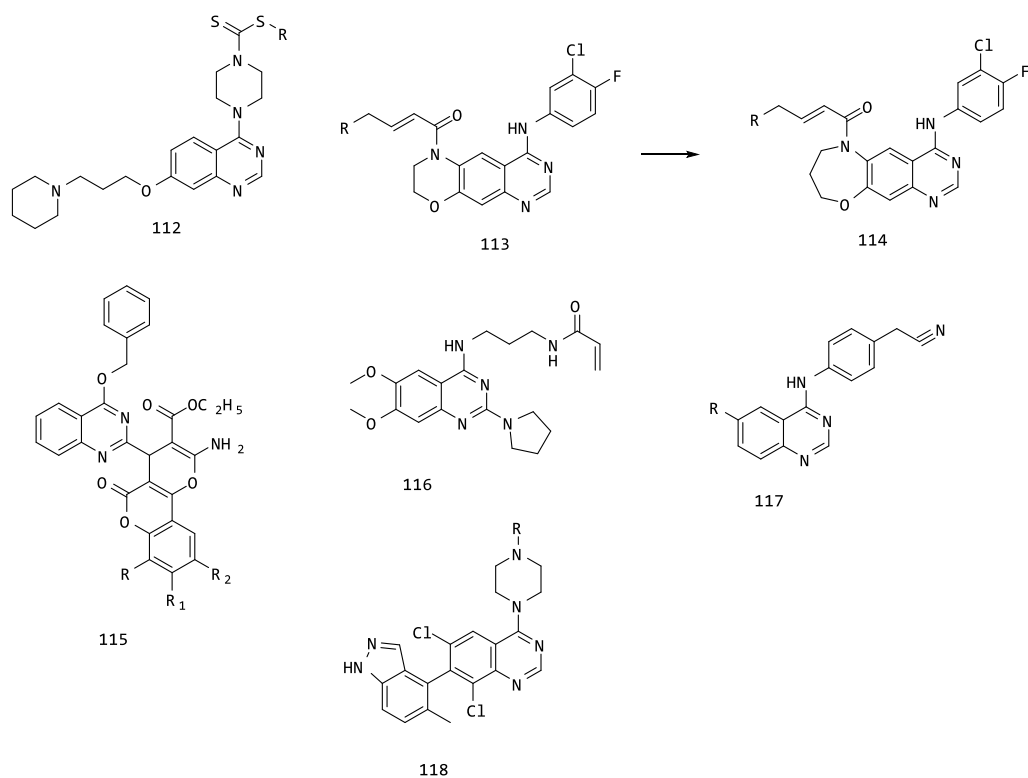


Figure 10.26: 4,6-disubstituted quinazoline molecules as anticancer agents.

It is also evident from the report that 6-methoxypyridin-3-yl group at position 6th showed poor antiproliferative inhibition against both lung cancer and breast cancer cell lines. The active molecules have also shown very good inhibition of cancer growth in animal model during in vivo evaluation.

The alicyclic and alkyl halide derivatives of quinazolines have also been synthesized via multistep synthesis from starting compounds having piperazine-1-carbodithioate moiety.

These synthesized molecules were then screened for lung cancer breast cancer, and colorectal cancer targets. Molecules exhibited moderate inhibitory potential against all the three anticancer targets with inhibitory concentration values under 9 micromolar concentration.

The detailed analysis between the structure and biological activity in these compounds have shown that the electron withdrawing substitution at phenyl ring enhancing the inhibitory potential of synthesized analogues.

Whereas replacement of phenyl ring from open chain alkyl group or cyclohexyl group does not much change the biological activity of screened molecules. The oxazine and oxazepine derivatives of quinazolines were designed and prepared to evaluate the antitumor property. These molecules are found to be more efficient than the known inhibitors⁸⁴⁻⁸⁵

10.2.6 Anti-tubercular Activity:

Tuberculosis is one of the biggest threats for public health which reflects from the increasing number of deaths every year due to tuberculosis. Quinazoline based molecules are widely known for antitubercular properties. Thiazolidinone, hydrazide and thiosemicarbazide derivatives are reported for antitubercular activities against H₃₇Rv strain in *Mycobacterium tuberculosis*. The MIC for these compounds were 0.02 microgram per millilitre and the area of inhibition were lower from 20mm.⁸⁶

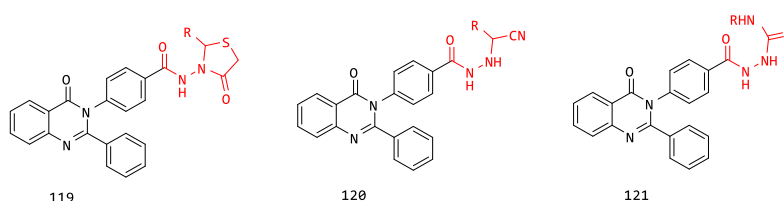


Figure 10.27: Quinazoline with antitubercular activities

In a quest to design antitubercular quinazoline molecule bromo substitution at the 3rd place in parent heterocyclic molecules was prepared and evaluated for inhibitory potential at concentration 200, 100, 50, 25 µg/ml for H₃₇Rv strain the results obtained clearly reveals that the synthesized compounds showed anti-tubercular activity with MIC value of 6025-100 µg/ml. The nitro substituted molecule was found to possess better inhibitory property than the halogen substituted analogue.⁸⁷

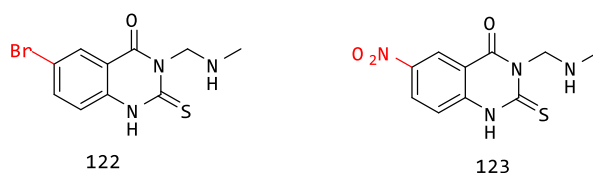


Figure 10.28: Quinazoline based small heterocyclic molecules.

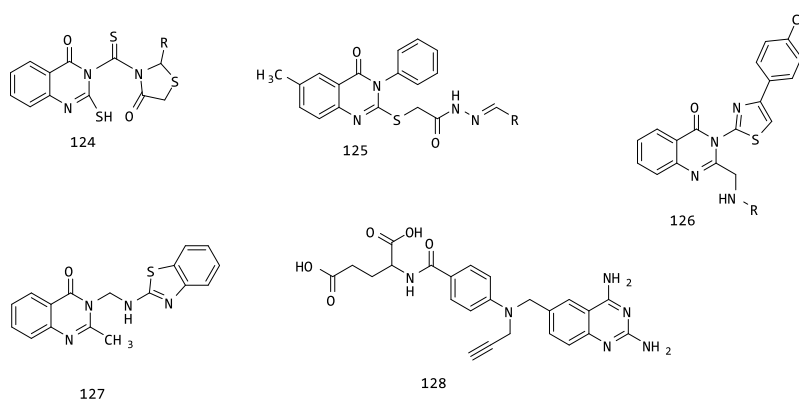


Figure 10.29: Structures showing antitubercular quinazolines

In another report synthesis of 4-thiazolidinone derivatives has been reported, which further evaluated for their antitubercular activity against H37Rv strain of *M. tuberculosis*. The screening was performed at 12.5 µg/ml concentration. The 6-methyl mercapto analogue was evaluated for biological activity but the screened compound does not exhibited significant inhibition of H37Rv strain.

On changing the molecule to the thiazoline derivative of the quinazolinone and their analogues screened at various concentrations for their biological activity (10, 50 and 100 µg/ml) and streptomycin was used as control to test the anti-tubercular activity. All the tested compounds have been proved to possess better antituber activity.⁸⁸⁻⁸⁹

10.2.7 Anti-Histaminic Activity:

Quinazolines are reported to have anti-histaminic activity in literature which prompt medicinal chemists to prepare quinazolinone analogues with anti-histaminic property. Different analogies of triazole based quinazolinones have been prepared and evaluated for antihistaminic activity. The methyl substitution was showing enhanced activity than other counterparts.⁹⁰

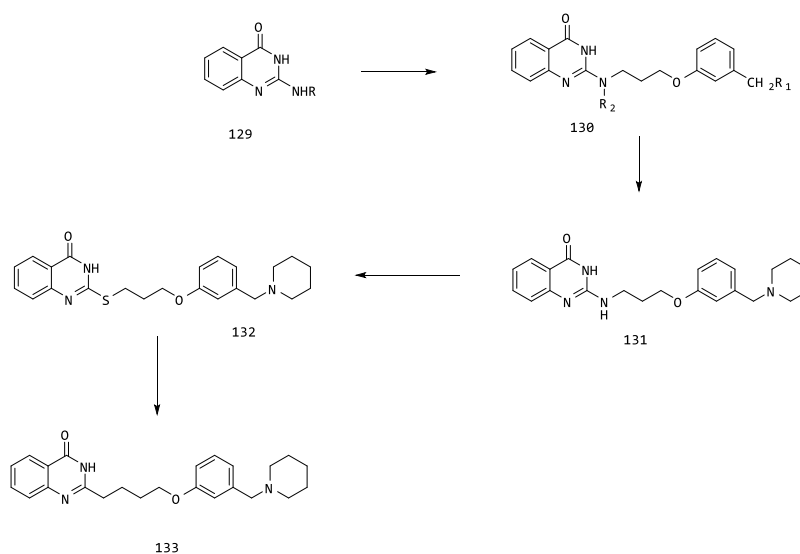


Figure 10.30: Structures showing anti-histaminic quinazolines

It was reported that the increasing the lipophilicity in molecular structure was tends to decrease the biological activity of molecule. In another work 4-quinazolinone derivatives have been synthesized and evaluated for H₂-antagonist Activity.

It was concluded from the results that molecules with stromatic system substitution resulted in the best value of (-log K_B) which was more convincing in comparison to the standard the standard used in biological testing. The thiazole and furan substitution were showing comparable activity whereas the imidazole analogue has shown the decrease the antihistaminic property.⁹¹

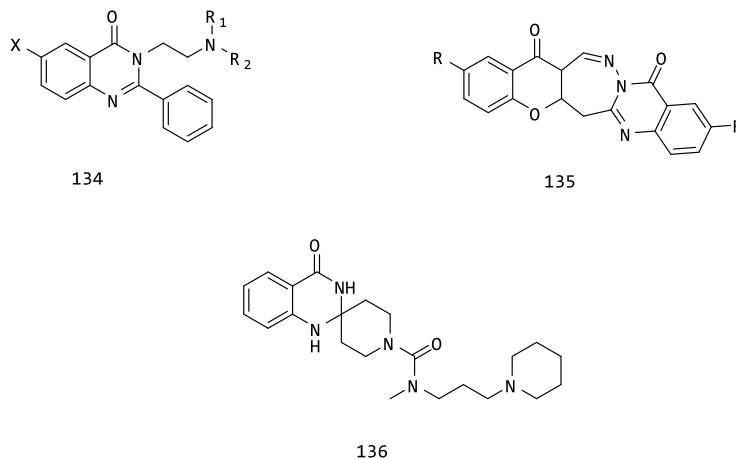


Figure 10.31: Spiro-isobenzofuranones derivatives having anti-histaminic activity

The better activity of molecule prompt to synthesize more analogues of the similar class of compounds. Later the pyrrolidinyl or 3-methylpiperidino groups were introduced in place of piperidino group which was proved to be more potent as antihistaminic molecule. The any of the amino substitution was going to decrease the biological activity.⁹²

In an attempt to investigate the anti-histaminic activity dialkyl amino substitution of dihydro quinazolinones have been synthesized and evaluated for H₁-anti-histaminic activity. These analogues were showing good inhibition potential.

Almost all the molecules of series were showing 100% blockade of agonistic influence. In SAR study it was established that the molecules with three methylene groups was more potent than the other members of synthesized molecules.

This result proved that increasing lipophilicity by increasing the chain length tends to enhance the biological activity of molecule. Whereas the halogen substitution in aromatic ring were not showing any promising biological activity. Among the evaluated analogues dibutyl amino derivative and iodo substitution at the 6th place in dibutyl amino quinazoline were the two most potent molecules.⁹³⁻⁹⁴

In another report the thiadiazepin derivative at the 6th place in parent heterocycle analogue have been synthesized to test the *in vitro* anti-histaminic activity in guinea pig ileum. The bromo substitution at the quinazolinone ring system at 6th position was tending to increase the activity as it was the best active compound of the series, whereas the methyl substitution at the same position decreases the activity as methyl analogue was the least active compound of the series.

Even the unsubstituted analogue was more potent than the methyl substitution. Increasing the number of bromo substitution as in the case of 6-substituted thiadiazepin derivative at the 6th place in quinazolinone does not exhibit any significant increase in the biological activity.⁹⁵⁻⁹⁶

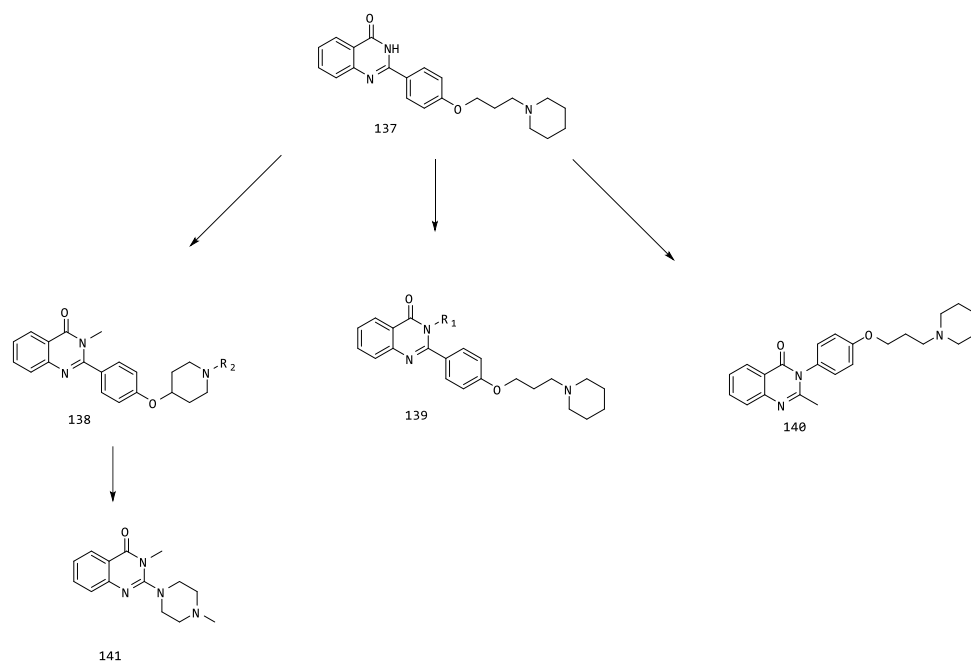


Figure 10.32: Quinazoline derivatives having anti-histaminic activity.

Several Spiro-isobenzofuranones derivatives were found to be very selective antihistaminic molecules with capability of brain permeability. These classes of molecules have been evaluated against Human H₃ targets which reveals that substitution at the nitrogen atom of quinazoline was responsible to alter the biological activity. To check the more potent substitution molecule was derivatized to get several analogues. Among the synthesized molecules Spiro-isobenzofuranone analogue was the most potent one.

It was again converted into amide derivative which was much more potent than the original Spiro-isobenzofuranone with IC₅₀ value of 0.72 nM. Another methoxy substitution at the 5th place has shown the inhibitory concentration value in the range of 0.51 to 0.54 nanomolar. In this sequence aminoalkoxy derivatives of quinazolinone have been prepared and evaluated and they found to be even more selective and more potent. To establish clearer SAR other regioisomeric analogues were synthesized and examined as shown in the figure 32.⁹⁷⁻¹⁰⁰

10.3 References:

1. Griess P., Ueber die einwirkung des cyans auf anthranilsaure, Berichte 2 (1869) 415-418.
2. P. Griess, Ueber die einwirkung von cyan auf amidobenzoesaure und anthranilsaure in wasseriger losung, Berichte 11 (1878) 1985-1988.
3. 40. Hangarge, R. V.; Sonwane, S. A.; Jarikote, D. V.; Shingare, M. S.; Green Chem., 2001, 3, 310-312.
4. Bindra, J. S. In The Alkaloids; Manske, R. H. F., Ed.; Academic Press: New York, 1973; Vol. 14, pp 84-121.

5. Wang L., Gao D., Chem. Cent. J. 2013, 7, 95-110.
6. Asif L., Int. Journal Med. Chem., 2014, 18, 395-397.
7. Rakesh K. P., Manukumar H. M., Gowda D. C., Bioorganic and Medicinal Chemistry Letters, 2015, 25, 1072-1077.
8. Hu P., Zhang T., Dong L., Wang X., Chen T., Liang E., Shi H., Shan X., Liang P., Chem. Biol. Drug Des. 85 (2015) 672-684.
9. Ugale V. G., Bari S. B., Eur. Jouram of Med. Chem., 2014, 80, 447-501.
10. Selvam T. K., Sivakumar A., Prabhu P. H., J. Pharm. Bioallied Sci. 6 (2014) 278-284.
11. Ji Q., Yang D., Wang X., Chen C., Deng Q., Ge Z., Yuan L., Yang X., Liao F., Bioorganic and Medicinal Chemistry, 2014 22, 3405-3413.
12. Jafari E., Khajouei M. S., Hassanzadeh F., Hakimelahi G. H., Khodarahmi G. A., Res. Pharm. Sci. 11 (2016) 1-14.
13. Al-Salahi R., Abuelizz H. A., Ghabbour H. A., El-Dib R., Marzouk M., Chemistry Cent. J., 2016, 19, 10-21.
14. Wan P., Hu S., Li S., Xie D., Gan X., Molecules 20 (2015) 11861- 11874.
15. Ravez S., Castillo-Aguilera O., Depreux P., Goossens L., Expert Opin. Ther. Pat. 25 (2015) 789-804.
16. Mehndiratta S., Sapra S., Singh G., Singh M., Nepali K., Anticancer Drug Discov. 11 (2016) 2-66.
17. Alagarsamy V., Solomon V. R., Vanikavitha G., Paluchamy V., Chandran M. R., Sujin A. A., Thangathiruppathy A., Amuthalakshmi S., Revathi R., Biological Pharma Bull., 2002, 25, 1432-1435.
18. Alagarsamy V., Muruganantham G., Venkateshaperumal R., Biological Pharma Bull., 2003, 26, 1711-1714.
19. Alagarsamy V., Rajesh S., Ramaseshu M., Vijaykumar S., Ramseshu K. V., Duraianandakumar T., Biological Pharma Bull., 2004, 27, 652-656.
20. Alagarsamy S., Solomon S. P., Meena R., S. Ramseshu V., Biological Pharma Bull. 2005, 28, 1091-1094.
21. Alagarsamy V., Muthukumar V., Pavalarani N., Vasanthanathan P., Revathi R., Biological Pharma Bull., 2003, 26, 557-559.
22. Newman, D.; Cragg, G. J. Nat. Prod. 2007, 70, 461-477.
23. Koch, M. A.; Schuffenhauer, A.; Scheck, M.; Wetzel, S.; Casaulta, M.; Odermatt, A.; Ertl, P.; Waldmann, H.; Proc. Natl. Acad. Sci. USA 2005, 102, 17272-17277.
24. Wetzel, S.; Schuffenhauer, A.; Roggo, S.; Ertl, P.; Waldmann, H.; Chimia 2007, 61, 355-360.
25. Schuffenhauer, A.; Ertl, P.; Roggo, S.; Wetzel, S.; Koch, M. A.; Waldmann, H.; J. Chem. Inf. Model. 2007, 47, 47-58.
26. Moeller, G.; Adamski, J. Mol. Cell. Endocrinol. 2006, 248, 47-55.
27. Kumar A., Sharma S., Bajaj K., Indian Journal of Chemistry 42B, 2003, 1979-1984.
28. Kumar A., Sharma S., Sharma S., Panwar H., Singh T., V. K. Srivastava, Bio. Medicinal Chemistry, 2003, 11, 5293-5299.
29. Kumar A., Singh R. C., Kumar B. S., Bio. Medicinal Chemistry, 2007, 15, 3089-3096.
30. Daidone G., , Raffa D., Plescia S., Mantione L., Catena Cutuli V. M., Mangano N. G., Caruso A., Eur. J. Med. Chem. 29(1994) 707-711.
31. Daidone G., Maggio B., Raffa D., Plescia S., Mantione L., Catena Cutuli V. M., Mangano N. G., Caruso A., European Journal of Medicinal Chemistry, 2001, 36, 737-742.
32. Adamski, J.; Jakob, F. J. Mol. Cell. Endocrinol. 2001, 171, 1-4.

33. Lukacik, P.; Keller, B.; Bunkoczi, G.; Kavanagh, K. L.; Lee, W. H.; Adamski, J.; Oppermann, U. *Biochem. J.* 2007, 204, 419–427.
34. Pannerselvam P., Pradeepchandran R., Sridhar S. R., *Indian Journal Pharm. Science*, 2003), 65, 268–273.
35. Gomtsyan P., Bayburt E., Schmidt, Zheng H., Perner R., Didomenico S., Koenig P., Turner S., Hannick S. M., Macri B. S., McDonald H. A., Honore P., Wismer C. T., Marsh K. C., Wetter J., Stewart K. D., Oie T., Jarvis M. F., Surowy C. S., Faltynek C. R., Lee C. H., *J. Med. Chem.* 48 (2005) 744–752.
36. Luu-The, V. J. *Steroid Biochem. Mol. Biol.* 2001, 76, 143.
37. Mindnich, R.; Moller, G.; Adamski, J. *Mol. Cell. Endocrinol.* 2004, 218, 7.
38. Bothara P., Kadam S. S., Shivram V. S., *Indian Drugs*, 1998, 35, 372–376.
39. Thomas P., Murugan V., Elango K., *Indian Journal of Heterocyclic Chemistry*, 1999, 9, 151–152.
40. Saxena S., Verma M., Saxena A. K., *Indian Journal of Chemistry* 30-B, 1991, 453–456.
41. Gangwal N., Narasimhan B., Mourya V. K., Dhake A. S., *Indian Journal of Heterocyclic Chemistry*, 2003, 12, 201–204.
42. Rani S., Srivastava P., Kumar P., *Indian Journal of Chemistry* 41B, 2002, 2642–2646.
43. Sachin S. L., Sudhir G. W., Sharad K. M., *ARKIVOC* XI, 2006, 21–26.
44. Jessy, Sambantham A., *Indian Journal of Pharmaceutical Sciences*, 2007, 69, 476–478.
45. Bansal P., Srivastava P., Kumar A., *Eur Journal of Medicinal Chemistry*, 2001, 36, 81–92.
46. Kumar P., Rajput, *Eur J. Med. Chem.* 2007, 44, 83–90.
47. Hoegenauer K., Soldermann N., Zécri F., Strang R. S., Graveleau N., Wolf R. M., Cooke N. G., Smith A. B., Hollingworth G. J., Blanz J., Gutmann S., Rummel G., Littlewood-Evans A., Burkhart C., *ACS Medicinal Chemistry Letters*, 2017, 89, 75–980.
48. Archana, Srivastava V. K., Chandra S., Kumar P., *Indian Journal of Chemistry* 41B, 2002, 2371–2375.
49. Archana, Kumar A., *European Journal of Chemistry*, 2002, 37, 873–882.
50. Archana Srivastava, Kumar A., *Bioorganic and Medicinal Chemistry*, 2004, 12, 1257–1264.
51. Jatav V., Mishra P., Kashaw S., Stables J. P., *Eur. J. Med. Chem.* 43 (2008) 135–141.
52. Jatav V., Mishra A., *European Journal of Medicinal Chemistry*, 2008, 43, 1945–1954.
53. Hisano T., Ichikawa P., Kito G., Nishi S., *Chem. Pharm. Bull.* 20 (1972) 2575–2584.
54. Zappala M., Grasso S., Micale N., Zuccalà G., Menniti F. S., Ferreri G., De Sarro G., De Micheli C., *Bioorganic and Medicinal Chemistry Letters*, 2003, 13, 4427–4430.
55. Gursoy A., Terzioglu N., *Turkish Journal of Chem.*, 2005, 29, 247–254.
56. Kulkarni P, Bishnoi A., *Journal of Indian Chemical Society*, 1990, 67, 852–854.
57. Patel C. K., Khedekar P. B., Bhusari K. S., *Indian Journal of Heterocyclic Chemistry*, 2006, 15, 217–220.
58. Henderson, B. E.; Ross, R.; Bernstein, L. *Cancer Res.* 1988, 48, 246.
59. Selvam S., Vanitha R., Chandramohan C., *Indian Journal of Pharmaceutical Sciences*, 2004, 66, 82–86.
60. Santner, S. J.; Feil, P. D.; Santen, R. J. *J. Clin. Endocr. Metab.* 1984, 59, 29–33.
61. Selvam P., Abileshini B., Alagarsamy V., Pannecouque C., De Clercq E., *Indian Journal of Heterocyclic Chemistry*, 2006, 16, 73–74.
62. Pandey V. P., Shukla P. S., *Indian Drugs*, 1999, 36, 37–40.
63. Pandey M. S., Tusi S., *Indian Journal of Chemistry* 43B, 2004, 180–183.

64. Pandey C. P., Pathak L. K., Mishra S. P., *Indian J. Chem.* 44B (2005) 1940–1943.
65. Pandey V. P., Kumar J., *Indian Journal of Heterocyclic Chemistry*, 2006, 16, 65–66.
66. 11. Pasqualini, J. R.; Chetrite, G. S. J. *Steroid Biochem. Molec. Biol.* 2005, 93, 221–236.
67. Varma P. K., Prakash P., Ali Khan A., *Indian drugs*, 1986, 23, 345–349.
68. Kulkarni Y. D., Rowhani A., *Journal of Indian Chemical Society*, 1990, 67, 46–47.
69. 12. Santner, S. J.; Feil, P. D.; Santen, R. J. J. *Clin. Endocr. Metab.* 1984, 59, 29–33.
70. Piotrowska D. G., Andrei G., Schols D., Snoeck R., Lysakowska M., *Eur. J. Med. Chem.* 126 (2017) 84–100.
71. Gursoy A., Karali N., *European Journal of Medicinal Chemistry*, 2003, 38, 633–643.
72. Murgan V., Caroline C. T., Rama Sarma G. V. S., Kumar E. P., *Indian Journal of Pharmaceutical Sciences*, 2003, 65, 386–389.
73. Forsch R. A., Wright J. E., Rosowsky A., *Bioorg. Med. Chem.* 10 (2002) 2067–2076.
74. Raffa D., Edler M. C., Daidone G., Maggio B., Merikech M., Plescia S., Schillaci D., Bai R., Hamel E., *European Journal of Medicinal Chemistry*, 2004, 39, 299–304.
75. Baek D. A., Kang T. P., Kim H. S., *Bulletin of Korean Chemical Society*, 2004, 25, 1898–1906.
76. Girija K., Selvam P., Nagarajan R., De Clercq E., Gopal V., *Indian Journal of Heterocyclic Chemistry*, 2005, 14, 255–256.
77. Cao S. L., Feng Y. P., Jiang Y. Y., Liu S. Y., Ding G. Y., Li R. T., *Bioorg. Med. Chem. Lett.* 15 (2005) 1915–1917.
78. Jin Y., Zhou Z. Y., Tian W., Yu Q., Long Y. Q., *Bioorganic and Medicinal Chemistry*, 2006, 16, 5864–5869.
79. De Jonge M. J. A., Dumez H., Verweij J., Yarkoni S., Snyder D., Lacombe D., Marréaud S., Yamaguchi T., Punt C. J., *Eur. J. Cancer* 42 (2006) 1768–1774.
80. Al-Rashood S. T., Aboldahb I. A., Nagi M. N., Abouzeid L. A., Abdel-Aziz A. A., Abdel-Hamide S. G., Youssef K. M., Al-Obaid A. M., El-Subbagh H. I., *Bioorganic and Medicinal Chemistry*, 2006, 14, 8608–8621.
81. Krapf M. K., Gallus J., Wiese M., *Journal of Medicinal Chemistry*, 2017, 60, 4474–4495.
82. McGregol L. P., Jenkins M. S., Kerwin C., *Biochemistry* 56 (2017) 3178–3183.
83. Tu Y., Wang C., Xu S., Lan Z., Li W., Han J., Zhou Y., Zheng P., Zhu W., *Bioorganic and Medicinal Chemistry*, 2017, 25, 3148–3157.
84. Zhang Y., Gao H., Liu R., Liu J., Chen L., Li X., Zhao L., Wang W., Li B., *Bioorganic and Medicinal Chemistry Letters*, 2017, 18, 4309–4313.
85. Zhang Y., Zhang Y., Liu J., *Bioorganic and Medicinal Chemistry Letters*, 2017, 27, 1584–1587.
86. Henderson, B. E.; Ross, R.; Bernstein, L. *Cancer Res.* 1988, 48, 246.
87. Maestri V., Tarozzi A., Simoni E., Cilia A., Poggesi E., Naldi M., Nicolini B., Pruccoli L., Rosini M., Minarini A., *European Journal of Medicinal Chemistry*, 2017, 136, 259–269.
88. Lundquist, J. J.; Toone, E. J. *Chem. Rev.* 2002, 102, 555.
89. Shirodkar P. S., Meghana M. T., *Indian Drugs*, 1998, 35, 597–599.
90. Langenhan, J. M.; Griffith, B. R., Thorson, J. S. J. *Nat. Prod.* 2005, 68, 1696–1711.
91. Trivedi V. S., Undavia N. P., Trivedi P. K., *Journal of Indian Chemical Society*, 2004, 81, 506–508.
92. Luu-The, V.; Tremblay, P.; Labrie, F. *Mol. Endocrinol.* 2006, 20, 437–443.

93. Pattan S., Krishna Reddy, Manvi F., Desai B. T., Bhat A. R., Indian Journal of Chemistry, 45B, 2006, 1778–1781.
94. Nandy P., Vishalakshi M. T., Bhat A. R., Indian J. Heterocycl. Chem. 15 (2006) 293–294.
95. Jr. Santa Maria J. P., Park Y., Yang L., Murgolo N., Altman M. D., Zuck P., Adam G., Chamberlin C., Saradjian P., Dandliker P., Boshoff H. I. M., C. Garlisi C., Olsen D. B., Young K., Glick M., Nickbarg E., Kutchukian P. S., ACS Chem. Biol. 12 (2017) 2448–2456.
96. Jitsuoka M., Tsukahara D., Ito S., Tanaka T., Tokita S., Sato N., Bioorg. Med. Chem. Lett. 18 (2008) 5101–5106.
97. Mizutani T., Nagase T., Ito S., Miyamoto Y., Tanaka T., Takenaga N., Tokita S., Sato N., Bioorg. Med. Chem. Lett. 18 (2008) 6041–6045.
98. Smits R. A., Adami M., Istyastono E. P., Zuiderveld O. P., Van Dam C. M., de Kanter F. J., Jongejan A., Coruzzi G., Leurs R., de Esch I. J., J. Med. Chem. 53 (2010) 2390–2400.
99. Allen E. E., de Laszlo S. E., Huang S. X., Quagliato C. S., Greenlee W. J., Chang R. S., Chen T. B., K. Faust A., Lotti V. J., Bioorg. Med. Chem. Lett. 3 (1993) 1293–1298.
100. de Laszlo S. E., Allen E. E., Quagliato C. S., Greenlee W. J., Patchett A. A., Nachbar R. B., Sieg P. K. S., Chang R. S., Kivlighn S. D., Schornb T. S., Faust K. A., Bioorg. Med. Chem. Lett. 3 (1993) 1299–1304

11. Photocatalytic Investigations of Organic Dyes Using Phosphate and Tungstate Based Nanomaterials

**Indumukhi B. C., Vinayaka S., Ishwarya S., Harini H. V.,
Nagaswarupa H. P.**

Department of Studies in Chemistry,
Davangere University,
Davangere, India.

Abstract:

In present days photocatalysis is widely employed in different field of applications involving decontaminating surfaces, air and water by sterilization, hydrogen evolution, and photo electrochemical reactions of dyes. By employing the alkaline-earth metal phosphate, tungsten -based photocatalysts concentrated on the abatement of water pollutants, and water splitting treatment. The innovation of new materials is necessary to increase the performances of photocatalytic properties. The synthesized phosphates and tungstates characterized by using different spectroscopic technique like XRD, SEM, TEM, FTIR etc. The main approach is to synthesize nano hybrid phosphates, tungstates and their applications to photocatalytic decomposition.

Keywords:

Phosphates, Tungstate's, Methods, Photocatalytic degradation.

11.1 Introduction:

Today, industrial revolution put very bad impact on globe. A variety of harmful compounds in wastewater ejected by various printing, dyes, textile, leather and other toxic chemicals into the environment. These chemicals directly effect on the photosynthesis process of aquatic plants and animals make a serious problem to ecosystem [1,2]. Now a days organic dyes become dangerous to the environment. To overcome from these problems photocatalytic decomposition of toxic organic complexes presents in industrial wastewater before entering into fresh waterbody [3].

Additionally, a variety of chemical and physical techniques are used to break down textile waste, but they produce contaminants that cannot be broken down by nature and require external expensive treatment. creation of a highly reactive hydroxyl radical to help with these issues. the high oxidative strength of hydroxyl ($\bullet\text{OH}$) radicals, which is further enhanced by UV light's ability to produce hydroxyl radicals, causes dye to degrade more quickly. Nanotechnology is regarded as the most inevitable technology of the twenty-first century [10].

An explanation of nanotechnology is that it is the control of matter as it exists on an atomic and molecular scale with at least one characteristic dimension measured in nanometers. In addition to that, it can also be described as the design, manufacture and application of construction of devices and systems by controlling conditions for synthesized material at the nanometer scale in order to achieve desired size and shape of the particles [11]. It is imperative that support basic and essential research in the field of environmental curatives, which is carried out to address environmental difficulties related to organic pollutants along with harmful chemicals. It has been proposed that photocatalysis could achieve the purpose of eliminating all toxic chemicals by virtue of its efficiency and potential for broad application [12].

In addition to its appealing qualities, tungsten oxide nanostructures have been studied in a number of electrochromic, photochromic, and photocatalytic domains also in sensors and energy storage devices. A transition metal tungsten oxide having wide range of applications with band gap of 2.6 to 3.7 eV with definite size and shape engrossed the marvelous interest of researchers. Band gap energy sometimes varied than the reported values. Tungsten atom displacement and oxygen atom rotation cause the ideal ReO_3 cubic structure to tilt in bulk tungsten oxide, which has a perovskite-like structure. The WO_3 -modified corners of octahedral WO_6 are shared by the stoichiometric tungsten oxide structures. The sub-stoichiometric structure shares the WO_6 octahedral edges. Self-doped oxygen vacancies are present in the WO_x composition with $\text{O} \times 3$ that is sub-stoichiometry. Since the investigation of the materials is largely determined by the nano-sized structure production method and the original precursors, the phase transition behavior in nanostructured WO_3 can be highly complex [13].

11.2 Mechanism of Photocatalysis Using Phosphate and Tungstate Nanomaterials:

The light radiation contains energy in the form of Photons. Each photon carries an energy of $E=h\nu$. When an electron absorbs energy from the photon, the holes (h^+) in the valency band (VB) are left behind as the electrons are excited from the valency band to the conduction band (CB)

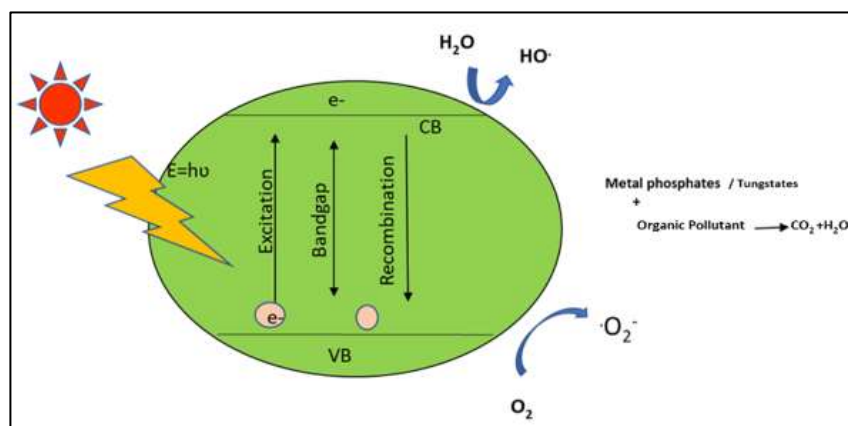


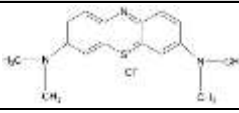
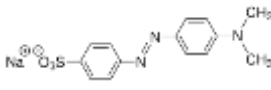
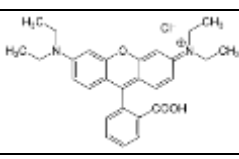
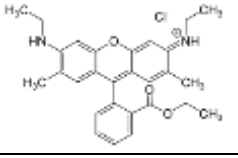
Figure 11.1: Photocatalytic Degradation of Organic Dyes

In photocatalysis, electron absorbs energy of certain wavelength from electromagnetic radiation, and the excitation take place from valence band (VB) to conduction band (CB) leaving behind holes in the valence band and forms electron-hole pair. The electron-hole pair make a strong redox system. The energy difference between the two bands is called band gap. Both electrons and holes are located in the same band. The water molecule that causes the holes on the phosphates or tungstate surfaces produces hydroxyl radicals through the oxidation of OH. The O₂ molecule that is present in the absorbed air on the surfaces of PO₄ or WO₄ is simultaneously reduced by electrons in the conduction band, eventually forming peroxy radicals. These photochemical processes are utilized to oxidise and degrade both organic and inorganic materials [7]. Metal phosphonates are inorganic compounds in which metal sites are bounded with phosphoric acid and metal phosphates are hybrid of organo-inorganic porous nano-phosphates employed as a source of phosphates [8]. Cationic/anionic or non-ionic surfactants may be the source of meso-porosity in these porous-hybrid nanomaterials, metal-ligand coordination is used in voids on the micropore length scale [8]. Doping rare earth metals boosts photocatalytic activity and the proportion of dye degradation because they contain 4f vacant orbitals [9].

The liberation of active oxygen species like superoxide free radicals (O₂⁻) and hydroxyl free radicals (OH), donated towards the decomposition of organic dye molecule, is typically linked to the electrons and holes produced by photons. Consider an example in which oxygen vacancies fabricated on the surface or sub-surface initiates the liberation of CO₂ with the involvement of oxygen and electrons. Doping of noble metal nano-phosphates and tungstate like Au, Ag, and Pt on the surface enhances the photocatalysis. The Bismuth nano-phosphates acts as electron acceptor involves interaction of electron with the metallic Bi and the CB, which promotes the separation of photo generated pairs of electron-holes [8,9].

11.3 Dye and Their Structure:

Table 11.1: Various dyes used for photocatalytic degradation.

Dyes Used	Structure	Molecular Formula	Molar mass	Boiling Point
Methylene Blue (MB)		C ₁₆ H ₁₈ ClN ₃ S	319.85 g/mol	---
Methyl Orange (MO)		C ₁₄ H ₁₄ N ₃ NaO ₃ S	327.33 g/mol	100°C
Rhodamine B (RhB)		C ₂₈ H ₃₁ ClN ₂ O ₃	479.02 g/mol	---
Rhodamine 6G (R6G)		C ₂₈ H ₃₁ N ₂ O ₃ Cl	479.02 g/mol	<200°C

Dyes Used	Structure	Molecular Formula	Molar mass	Boiling Point
Coomassie Brilliant Blue (CBB)		$C_{45}H_{44}N_3NaO_7S_2$	854.04 g/mol	---
Brilliant Green (BG)		$C_{27}H_{34}N_2O_4S$	475.6 g/mol	---
Malachite Green (MG)		$C_{23}H_{25}ClN$	364.91 g/mol	520.91°C
Eriochrome Black T (EBT)		$C_{20}H_{12}N_3O_7SNa$	461.381 g/mol	102°C
Crystal Violet (CV)		$C_{25}H_{30}ClN_3$	407.979 g/mol	118°C
Eosin Y		$C_{20}H_6Br_4Na_2O_5$	691.86 g/mol	682.3°C

11.4 Methods of Synthesis:

Chemically or biologically, nanoparticles can be created. The presence of some poisonous substances deposited on the surface has resulted in several negative effects connected to chemical production techniques. The manufacture of nanoparticles via biological processes that involve the use of microbes, enzymes, fungi, plants, or plant extracts provides an environmentally benign alternative to physical as well as chemical approaches [14].

A. Top-down synthesis: The presence of some poisonous substances deposited on the surface has resulted in several negative effects connected to chemical production techniques. The manufacture of nanoparticles via biological processes that involve the use of microbes, enzymes, fungi, plants, or plant extracts provides an environmentally benign alternative to physical as well as chemical approaches.

B. Bottom-up method: - The constructive method is another name for bottom-up approach. It is top-down approach inverted. With this technique, significantly less-complex chemicals are used to create nanoparticles. Spinning, Sol-gel, pyrolysis, Chemical vapour deposition (CVD) and biological synthesis are all components of the Bottom-up approach [15].

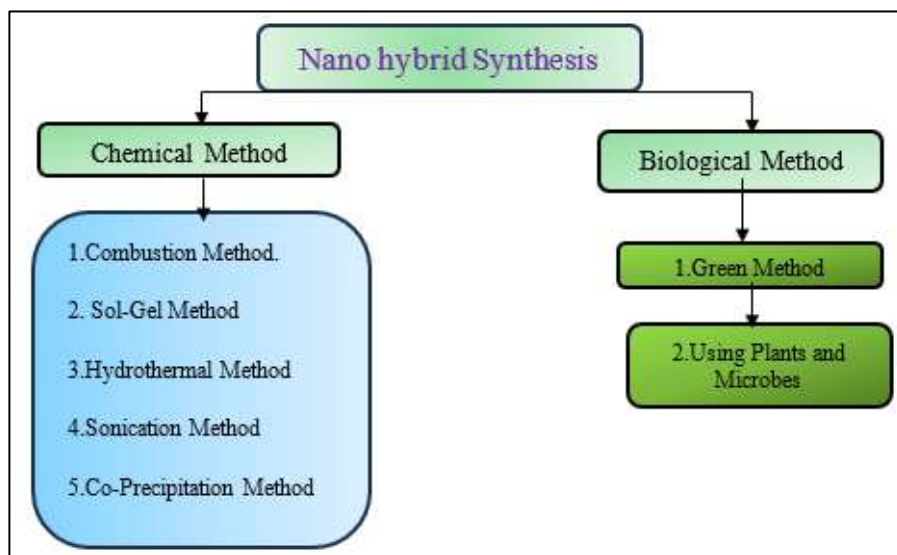


Figure 11.2: Synthesis Methods of Nano-Phosphates and Tungstate's,

Table 11.2: Reaction Parameters for Synthesis Of Phosphates

Sr. No	Name of the phosphates	Method of synthesis	Reaction conditions	Degradation of dye/ chemical	References
1	Silver-phosphates (Z-scheme)	Sonication	AgNO ₃ , Na ₂ HPO ₄ , dried at 70 ^o c	Photocatalytic degradation of Rhodamine-B	16
2	Carbon modified Bismuth phosphate	Hydrothermal method	D-glucose, Bi (NO ₃) ₃ , NaH ₂ PO ₄ , HNO ₃	Perfluoro octanoic acid	17
3	Zirconium phosphate, gelatin composite	Sol-gel method	Gelatin-gel, zirconium nitrate	Methylene blue, Fast green	18
4	Titania-pillared Zirconium phosphate, Titanium phosphate	Sol-gel method	Titanium isopropoxide, HCl, Sodium phosphate, calcination at 500 ^o C for 5hrs	Complete degradation of hexavalent chromium, 4-nitrophenol in acidic medium, phenol and methylene blue in neutral medium	19
5	Boron nitride modified Bismuth Phosphate	Solvothermal Combustion method	Bi (NO ₃) ₂ , H ₃ PO ₄ , boric-acid, urea, autoclave at	Enrofloxacin	20

Sr. No	Name of the phosphates	Method of synthesis	Reaction conditions	Degradation of dye/ chemical	References
			160°C for 24 hours, calcination at 900°C for 5hrs		
6	Zirconium phosphate/Silver chloride composite	Sol-gel method	Zirconyl propionate, propanol, phosphoric acid	Rhodamine-B	21
7	Calcium phosphate	---	Calcium chloride, titanium sulphate, ammonium hydroxide, pH-9	Methylene blue	22
8	Silver/Silver phosphate composite	---	Silver nitrate, phosphoric acid, 65-70°C stirring for 24hrs, calcination at 650°C/1000°C for 1hr	Methylene blue	23
9	Silver-Tin oxide quantum dots on Silver-phosphate	Precipitation method	AgNO ₃ , NaH ₂ PO ₄	Carbamazepine	24
10	Effects of salts on Silver-phosphates	Precipitation method	AgNO ₃ , Na ₂ HPO ₄	Methylene blue	25

Table 11.3: Synthesis of Tungstate's, Calcination Temperature, Dyes Used For Decomposition

Sr. No	Tungstate NPs	Methods	Calcinated temp(°C)	Dye	Reference
1	α -SnWO ₄	Hydrothermal	200	MB	26
2	CuWO ₄	Hydrothermal	600	4-Nitrophenol	27
3	Bi ₂ WO ₆	Facile Microwave Hydrothermal	400	RhB	28
4	NiWO ₄	Molten Salts Process	500	MB	29
5	FeWO ₄ /ZnO Composite	Co-precipitation	500	MB	30

Photocatalytic Investigations of Organic Dyes Using Phosphate and Tungstate Based Nanomaterials

Sr. No	Tungstate NPs	Methods	Calcinated temp(^o C)	Dye	Reference
6	NiCoWO ₄	Hydrothermal	600	MB	31
7	Bi ₂ WO ₆	Facile Hydrothermal	180	RhB	32
8	ZnWO ₄	Co-precipitation	500	MB	33
9	NiWO ₄	Precipitation	500	MB	34
10	La ₂ (WO ₄) ₃	Chemical Precipitation	800	MB & RhB	35
11	Bi ₂ WO ₆	Hydrothermal	220	R6G	36
12	CaWO ₄	Combustion	500	MB	37
13	NiWO ₄	Simple salt solution addition, Co-precipitation, Sol-Gel	400	MB	38
14	BaWO ₄ -MoS ₂	Co-Precipitation	200	RhB	39
15	Pr ₂ (WO ₄) ₃	Precipitation	70	MB	40
16	NiWO ₄	Electrochemical	700	MO	41
17	Bi ₂ WO ₆	Hydrothermal	110	RhB	42
18	PbWO ₄	Co-Precipitation	100	MB & Thiazine	43
19	ZnWO ₄ /AgCl Composite	Hydrothermal	180		44
20	Bi ₂ WO ₆	Hydrothermal	180	CBB	45
21	CdWO ₄	Hydrothermal	180	Cr & MO	46
22	Bi ₂ WO ₆	Hydrothermal	180	RhB	47
23	CoWO ₄	Hydrothermal	450	BG	48
24	ZnWO ₄ /CuWO ₄ /Ag ₂ WO ₄	Combustion		MO	49
25	ZnWO ₄	Combustion	400-1000	MB	50
26	CuWO ₄	Solvothermal	700	MO & MB	51
27	Bi ₂ WO ₆	Hydrothermal	120	RhB	52
28	MnWO ₄ / TmVO ₄	Sonochemical	500	RhB 2-Naphthol PR EY	53
29	CuWO ₄ -RGO	Hydrothermal	170	BG & MG	54
30	CoWO ₄	Sonochemical	550	MO	55
31	BaWO ₄	Chemical solution	200	MB	56

Sr. No	Tungstate NPs	Methods	Calcinated temp(⁰ C)	Dye	Reference
32	BaWO ₄ /MoS ₂	Co-Precipitation	400	EBT	57
33	CoNiWO ₄	Microemulsion	600	MB	58
34	CaWO ₄	Simple chemical	500	MB	59
35	SrWO ₄	Co-Precipitation	60-70	RhB	60
36	BaWO ₄	Sonochemical	500	MO	61
37	Ag-AgBr/ CaWO ₄	Deposition- Precipitation & Photo reduction	500	Acid Red 18	62
38	ZrWMoO ₈ /Ag	Hydrothermal & Reduction	550	RhB	63
39	ZrW ₂ O ₈	Sol-Gel	390-650	RhB	64
40	Pr ³⁺ : CaWO ₄	Ultrasound assisted precipitation	600	RhB	65
41	Co ²⁺ : Bi ₂ WO ₆	Hydrothermal	100	RhB	66
42	CoWO ₄	Precipitation	500	MV, MB, EY, PR	67
43	CuWO ₄	Hydrothermal	600	TR	68
44	Fe ₂ O ₃ /WO ₃ / FeWO ₄	Simple Precipitation, Acid Precipitation, Hydrothermal	150 150-200 100	MO	69
45	CaWO ₄	Hydrothermal	160	RhB	70
46	BaWO ₄	Simple Soft Chemical	400 & 800	RhB	71
47	N: MnWO ₄	Hydrothermal	60	MB	72
48	SrWO ₄	Sono chemical	500	MO	73
49	BaWO ₄	Hydrothermal	60	CV	74
50	CoWO ₄	Co-precipitation	500	MO	75
51	CuWO ₄	Solvo thermal	700	MO & MB	76
52	β-Ag ₂ WO ₄	Facile precipitation	80	MO & Phenol	77
53	Ag ₂ WO ₄	Ion exchanged Hydrothermal	180	RhB & MB	78

(MO-methyl orange, RhB -rhodamine B, MB- methylene blue, EBT-eriochrome black-T, EY- eosin Y, CV-crystal violet, PR- para red, MV-methyl violet, TR-teracycline)

11.5 Characterization:

By evaluating the manner in which X-rays interact with a material, a method called X-ray diffraction (XRD) can be employed to examine its atomic and molecular structure. By scanning a sample with a narrowly focused electron beam, scanning electron microscopy (SEM) creates pictures of the material. A thin sample is used in transmission electron microscopy, another type of electron microscopy, to obtain images. By using adsorption and desorption of nitrogen isotherms were collected, also the plots of pore size distribution studied. UV-Vis spectrophotometry is a method for calculating how much of an object's ultraviolet and visible light is absorbed or reflected. [52].

11.5.1 XRD:

X-Ray Diffraction analysis was employed for the determination of crystallographic structures of nano-phosphates. When materials are irradiated by X-rays, the scattering angle and intensities were measured. The d-spacing can be determined by using Bragg's equation:

$$2d\sin\Theta=n\lambda$$

Where, n- is an integer,

Θ - an angle of incidence,

λ - wavelength of X-ray radiation,

d- spacing between two diffracting planes.

By using Scherrer equation one can identified the structure as well as particle size of the nano-phosphate. The equation is

$$T = K\lambda/\beta \cos\Theta$$

Where T- the mean particle size, K- a dimensionless shape factor (≈ 0.9), λ - a wavelength of X-rays, β - instrumental line broadening, Θ - is Bragg's angle.

XRD analysis reveals the structure of nano-phosphate as well as effect of doping on the host material. For example, the effect of doping of Al^{3+} ion on the Ag_3PO_4 . The Al doped Ag_3PO_4 does not shows any effect on the crystal structure of the phosphate. It provides the information about complete dispersion of Al^{3+} ions in the crystal lattice of Ag_3PO_4 (9). The cobalt phosphate modified graphitic carbon nitride shows two diffraction peaks at 27.5° and 13.2° , which are agreeable with graphitic nitride (0 0 2) and (1 0 0). The diffraction peaks explain the fine deposition of graphitic carbon nitride on the cobalt phosphate [21].

The synthesized nanomaterials crystal structure and phase purity were investigated using XRD. The JCPDS File No. 82-2068, which corresponds to a mono-clinic structure with the space group C2/c, displays the diffraction peaks found for each surface.

When compared to the standard sample, it is possible to see that the diffraction peaks have widened, proving that the final output is a crystal with a nanometer-sized dimension. Three adjacent peaks that match to the material's JCPDS file's planes (-221), (-132), and (023) are located at 27.1830, 28.0830, and 28.6080, respectively, and form a primary peak at 28.20 in all samples owing to the peak merger. More peaks form when the calcination temperature rises, as can be seen in the sample of S3 when compared to those of S1 and S2. The additional peak in the S3 pattern generated at 19.5360 is referenced to the $\text{La}_2(\text{WO}_4)$ JCPDS no: 19-0669.3. The Scherer equation formula was used to determine the lattice parameters of the samples from the distance d for the vertices with the Miller index.

11.5.2 FTIR:

FTIR was employed to obtain IR-spectrum of absorption as well as emission of solid, liquid and gaseous compounds, it gives high resolution spectral data. For TiO pillared ZrP (Zirconium phosphate) and TiP (Titanium phosphate), the FTIR shows IR bands in the region of $1300\text{-}900\text{cm}^{-1}$ for ZrP and for TiP the band region was $1300\text{-}1000\text{cm}^{-1}$ which may contain (PO_3) asymmetric, (PO_3) symmetric and deformed (PO_3) at 650cm^{-1} . The peak for P-O-P bridge was observed at 970cm^{-1} . In case of bending vibration, the peaks observed at 1619cm^{-1} for ZrP, 1617cm^{-1} for TiP, and strong peaks were observed at 3148cm^{-1} for ZrP and 3406cm^{-1} for TiP stretching vibrations of -OH group and band broadening arises due to the presence of Hydrogen bonding. For TiO_2 the peak observed at lower wave number region i.e., $480\text{-}450\text{cm}^{-1}$ [16]. FTIR spectroscopic examination was done to analyze the nature of chemical bonds and functional groups in the material. The spectra of the calcinated NCW-NPs and the smooth peaks observed in the range $3000\text{-}3420\text{cm}^{-1}$ can be attributed to the O-H stretching frequency of the adsorbed aqua molecules. The peak observed at 2310cm^{-1} is referred to CO_2 , whereas a strong peak is obtained at 1632cm^{-1} for aqua molecule. The low-frequency IR-bands (between 400 and 1000cm^{-1}) associated with Co-O, Ni-O, W- and W-O-W bridges. The O-W-O and W-O oscillation modes observed at 824cm^{-1} and 659cm^{-1} , while the two absorption peaks observed at 525cm^{-1} and 461cm^{-1} refers to the vibrational modes of the Co-O and Ni-O bonds, respectively [31].

11.5.3 SEM:

In SEM the focused beam of electrons was employed for the scanning of a sample surface. When electrons in a beam interacts with atoms of the sample, produces variety of signals which contain the information of physical features of atoms on the surface of a molecule. For example, in case of carbon modified Bismuth phosphate, the carbon sphere showed the perfect spherical shape, irregular shaped flower like structures and their size ranging from 100nm to $9\mu\text{m}$. The carbon sphere and bismuth hydroxy phosphate inhibit one another for their growth into full sphere due to friction exerted and mass transfer of the precursors [19]. According to the SEM pictures, MoS_2 nanoparticles have a spherical structure while BaWO_4 nanoparticles have an octahedral-like morphology. The composite has a flower-like appearance, indicating strong photocatalytic activity. According to SEM findings, particle size has appreciable impact on the morphology of BaWO_4 , MoS_2 , and $\text{BaWO}_4\text{-MoS}_2$.

The presence of a larger molecules in the specimen may be the result of particle agglomeration at high processing temperatures. [39].

11.5.4 TEM:

The synthesized hybrid phosphates and tungstate's nano-particles size and their diameter was examined by transmission electron microscopy (TEM). The grain size of the synthesized particles measured by TEM compared with the crystal size evaluated by the Scherer equation.

The average size of synthesized particles diameter was around 10 to 35 nm, and it was confirmed by Bright-field TEM micrographs, while the smallest visible separation point could be determined by agglomeration of crystalline/ nanocrystalline particles. In addition, the tungstate Ni morphology is shown as small nanocrystals, while $\text{CO}_{0.5}\text{Ni}_{0.5}\text{WO}_4$ appears as an oval. The interplanetary distances calculated from ring diameters are compared with the JCPDS standard. Cobalt tungstate showed an average diameter of 13 nm which was calcinated at 600°C for 10 h. NiWO_4 having planes at (010) and (100) showed maximum photocatalysis [58].

11.5.5 EDAX:

EDS or EDAX is an analytical technique used to characterize a sample's chemical makeup or ascertain its elemental composition. It is a sort of X-ray fluorescence spectroscopy that analyses a sample by electromagnetic radiation interactions with the material, detecting X-rays that the material releases in reaction to interacting with charged particles. To determine the components of $\text{BaWO}_4\text{-MoS}_2$ particles, Energy Dispersive X-ray Diffraction analysis (EDAX) was carried out.

This demonstrates how pure the synthesized Nanocomposite is. The EDAX readings provided proof that the Nanocomposite Barium, Tungsten, Oxygen, Molybdenum, and Sulphur elements were present. They showed conspicuous peaks at 4.5 eV, 2.0 eV, 0.5 eV, 2.0 eV, and 2.5 eV, respectively. The $\text{BaWO}_4\text{-MoS}_2$ Nanocomposite that was created is made up of what elements. The findings demonstrate that the sample contained enough levels of Ba, W, O, Mo, and S [39].

11.5.6 UV-Visible:

The electrical structure and optical characteristics of materials are investigated using the UV-Vis spectroscopy technique. ZrWMoO_8 bars' absorption spectrum and spectral characteristics are typical of metal oxides. The near-UV area of the absorption spectrum has a trailing edge.

The absorption of light increases and the band gap transition 1 is thought to be the cause of the spectrum's steep form. By applying $(h\nu) = A(hEg)_{1/2}$ to the Tauc relationship, the band gap may be calculated directly. Here, $h\nu$ is energy of a photon, A is the direct transition absorption constant, and the absorption coefficient can be determined using the scattering spectra as well as reflectance spectra. In contrast to pure ZrWMoO_8 , the composite $\text{ZrWMoO}_8/\text{Ag}$ material has a distinct absorption spectrum. The metallic silver particles' surface plasmonic resonance, which is positioned at a wavelength of 360 nm, is responsible for the significant absorption peak.

Additionally, it is evident that ZrWMoO₈/Ag's adsorption edge has moved to a higher wavelength compared with ZrWMoO₈ alone. Due to the presence of different visible light absorption the red shift can be observed for ZrWMoO₈ and also for ZrWMoO₈/Ag composites as well as the quantum and plasmonic internment effects of silver clusters on the ZrWMoO₈ surfaces.

11.5.7 BET:

The analysis of specific pore volume and distribution of pore size on the outer surface was independent, the BJH analysis (Barrett-Joyner-Halenda) was employed for the measurement of pore size and surface area distribution. The synthesized -SnWO₄N₂ nanoparticles size was determined by adsorption-desorption isotherm. The materials increased porosity and surface area boost the adsorption capacity, which boosts the effectiveness of photocatalytic breakdown when exposed to light. The total pore volume and pore diameter was found to be 0.26 cm³g⁻¹, 13.2 nm respectively and the BET surface area of the NP-SnWO₄s is 29.2 m²g⁻¹ [26].

11.5.8 Raman Spectroscopy

The rotational spectra, vibrational spectra and others were examined in the low frequency region by employing Raman scattering spectroscopy. Light is scattered by matter in this process, as a result of the interaction with the system's vibrational modes, the frequency of the dispersed light is altered. In Raman spectra, CuWO₄ showed 36 vibrational modes, out of which 18 modes are Raman active. Internal and external vibrational modes have been distinguished between the active Raman modes.

The first one referred to vibrations of the clusters, and next one is a part of the phonon lattice vibrations. The WO₆ octahedron deforms as it comes into contact with Cu in the lattice. CuWO₄ micro-Raman spectra were captured at ambient temperature.

The deformed octahedral cluster 3's symmetrical stretching oscillation mode of the O-W-O is responsible for the sharp and prominent peak seen at roughly 906 cm⁻¹ [51].

11.6 Photocatalytic Application:

Photocatalysis is a promising technology for various applications such as environmental cleaning, clean energy generation, CO₂ reduction, and more. The principle involves the decomposition of harmful organic pollutants generally discussed. In short, by applying a light having higher energy than the band gap energy, excitation of electron can take place from valence band to conduction band (e⁻ cb) leaving a "hole" in the valence band (h⁺ vb). If the absorbed energy remains higher than the electrons and holes can move towards the surface area of the nano-catalyst, where the decomposition of the toxic dye molecule take place, simultaneously hydroxide free radical and superoxide free radicals involve in the redox reactions. The highly reactive free radicals are reason for the photodecomposition of organic complex molecules. Despite the presence of these efficient radicals, the capacity of a catalyst employed in degradation is still low, which is enhanced by doping of the catalyst with rare-earth metals [42].

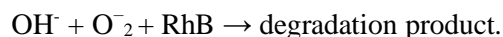
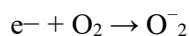
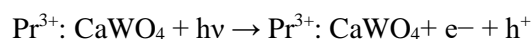
11.6.1 Photocatalysis of RhB:

The method by which RhB dye is photo catalytically degraded. The two processes that make up photocatalytic degradation-a photocatalysis and photosensitized processes. The direct decomposition of RhB was the potent oxidizing hole of Ag_3PO_4 . The intermolecular transition, allow RhB dye to be activated by incident of light radiation, after producing O_2 RhB was mineralized.

After UV light absorption, the photocatalytic activity of Pr^{3+} : CaWO_4 nanostructures synthesized with carbohydrates and without a hairstyling agent were compared.

After 90 minutes under a UV lamp, the photocatalytic calculation indicates that the percentage of RhB decomposition is around 65.2% in denominator 1, 79.4% in denominator 2, 86.8% in denominator 3, 93.1 in denominator 4, and 98.7% in denominator 5. The outcomes showed that utilizing maltose as a greening agent (lower particle size) increased the photocatalytic activity. Therefore, the photocatalytic performance of Pr^{3+} : CaWO_4 nanostructures produced with maltose is superior to that of other enclosing agents [65].

Mechanism for the photocatalysis of RhB may be explained as:



11.6.2 Photocatalysis of MO:

In order to evaluate the NPs' photocatalytic activity, UV-Vis spectra were used to track how well NiWO_4 NPs performed as photocatalysts for MO. The variation in MO solution concentration when exposed to UV light and NiWO_4 NPs. The C/C0 levels and decomposition efficiency are presented with a parameter of the irradiation time. According to the findings, MO is attenuated when NiWO_4 NPs are present, and a maximum attenuation of roughly 87% is seen after 100 minutes of UV exposure.

The slope reveals the kinetics of the MO decomposition process in the presence of NiWO₄ NPs is of pseudo-first order kinetics. These findings, together with the photo catalysis rate constant and maximal conversion of NiWO₄ NPs are reliable and useful photocatalysts for removal of organic pollutants [41].

11.6.3 Photocatalysis of EBT:

The study of photocatalytic degradation showed that the BaWO₄/MoS₂ mixture exhibited higher photocatalytic activity for EBT degradation compared with BaWO₄. The oxidation of EBT was found to be 99.20% using the BaWO₄/MoS₂ photosynthetic catalyst [63].

11.6.4 Photocatalysis of 2,4-DNP:

The decomposition of 2,4-DNP, showed decreased photocatalytic degradation when isopropanol added into the reaction solution, which indicates that hydroxide free radical ($\bullet\text{OH}$) is the active specie for decomposition of 2,4-DNP. It also explains the role of superoxide ($\bullet\text{O}_2^-$) and a hole (h^+) is negligible [16].

11.7 Future Prospects:

Phosphates & Tungstate nanoparticles are produced using direct calcination, which is based on electrochemical, Sol-gel, Solution combustion and co-precipitation techniques. Using FT-IR, XRD, SEM, and EDS, the researchers were able to test the properties of the newly synthesized nanoparticles. This study offers a quick and easy method that uses direct sunlight to degrade toxic chemicals in wastewater. More importantly, photocatalysts can be used on interior walls illuminated with fluorescent lamps to render the bacteria inside inactive. The example gives suggestions for creating new photocatalysts that can be used in real-life situations. For the applications of pharmaceutical waste decomposition, dye contamination, and photocatalytic antibacterial, nanomaterials with attractive photocatalytic performance have been extensively studied. Their crystalline phase, band gap and particle size all affect their photocatalytic activity. In particular, the pH level, shape and crystal phase need to be further investigated as they have a notable effect on the photocatalytic activities of phosphate & tungstate nanomaterials.

11.8 Reference:

1. Solmaz, S. K. A., Birgül, A., Üstün, G. E., & Yonar, T. (2006). Colour and COD removal from textile effluent by coagulation and advanced oxidation processes. *Coloration Technology*, 122(2), 102-109.
2. Alam, M. Z., Ahmad, S., Malik, A., & Ahmad, M. (2010). Mutagenicity and genotoxicity of tannery effluents used for irrigation at Kanpur, India. *Ecotoxicology and Environmental Safety*, 73(7), 1620-1628.
3. Akbar Hosseini, S. (2016). Nanocrystalline EuVO₄: Synthesis, characterization, optical and photocatalytic properties. *Journal of Materials Science: Materials in Electronics*, 27, 10775-10779.
4. Jain, A., & Vaya, D. (2017). Photocatalytic activity of TiO₂ nanomaterial. *Journal of the Chilean Chemical Society*, 62(4), 3683-3690.

- Santos, A. P., Souza, B. M., Silva, T. F., Cavalcante, R. P., Oliveira, S. C., Machulek, A., ... & Vilar, V. J. (2018). Mineralization of humic acids (HAs) by a solar photo-Fenton reaction mediated by ferrioxalate complexes: commercial HAs vs extracted from leachates. *Environmental Science and Pollution Research*, 25, 27783-27795.
- Huang, C. P., Dong, C., & Tang, Z. (1993). Advanced chemical oxidation: its present role and potential future in hazardous waste treatment. *Waste management*, 13(5-7), 361-377.
- Cai, T., Liu, Y., Wang, L., Zhang, S., Zeng, Y., Yuan, J., ... & Luo, S. (2017). Silver phosphate-based Z-Scheme photocatalytic system with superior sunlight photocatalytic activities and anti-photocorrosion performance. *Applied Catalysis B: Environmental*, 208, 1-13.
- Xu, T., Zhu, Y., Duan, J., Xia, Y., Tong, T., Zhang, L., & Zhao, D. (2020). Enhanced photocatalytic degradation of perfluorooctanoic acid using carbon-modified bismuth phosphate composite: Effectiveness, material synergy and roles of carbon. *Chemical Engineering Journal*, 395, 124991.
- Thakur, M., Sharma, G., Ahamad, T., Ghfar, A. A., Pathania, D., & Naushad, M. (2017). Efficient photocatalytic degradation of toxic dyes from aqueous environment using gelatin-Zr (IV) phosphate nanocomposite and its antimicrobial activity. *Colloids and Surfaces B: Biointerfaces*, 157, 456-463.
- Das, D. P., & Parida, K. M. (2008). Solar light induced photocatalytic degradation of pollutants over titania pillared zirconium phosphate and titanium phosphate. *Catalysis surveys from Asia*, 12, 203-213.
- Chen, Z., Chen, X., Di, J., Liu, Y., Yin, S., Xia, J., & Li, H. (2017). Graphene-like boron nitride modified bismuth phosphate materials for boosting photocatalytic degradation of enrofloxacin. *Journal of colloid and interface science*, 492, 51-60.
- Pica, M., Nocchetti, M., Ridolfi, B., Donnadio, A., Costantino, F., Gentili, P. L., & Casciola, M. (2015). Nanosized zirconium phosphate/AgCl composite materials: A new synergy for efficient photocatalytic degradation of organic dye pollutants. *Journal of Materials Chemistry A*, 3(10), 5525-5534.
- Piccirillo, C., Dunnill, C. W., Pullar, R. C., Tobaldi, D. M., Labrincha, J. A., Parkin, I. P., ... & Castro, P. M. (2013). Calcium phosphate-based materials of natural origin showing photocatalytic activity. *Journal of Materials Chemistry A*, 1(21), 6452-6461.
- El-Gendy, N. S., & Nassar, H. N. (2020). Sustainable Photo-and Bio-Catalysts for Wastewater Treatment. *Photocatalysts in Advanced Oxidation Processes for Wastewater Treatment*, 139-165.
- Monfort, O., Dworniczek, E., & Plesch, G. (2016). Photocatalytic and Antimicrobial Properties of Silver Phosphate, Hydroxyapatite and Their Composites. In *Electrically Active Materials for Medical Devices* (pp. 177-192).
- Duan, Z., Deng, L., Shi, Z., Zhang, H., Zeng, H., & Crittenden, J. (2019). In situ growth of Ag-SnO₂ quantum dots on silver phosphate for photocatalytic degradation of carbamazepine: performance, mechanism and intermediates toxicity assessment. *Journal of colloid and interface science*, 534, 270-278.
- Amornpitoksuk, P., Intarasuwan, K., Suwanboon, S., & Baltrusaitis, J. (2013). Effect of phosphate salts (Na₃PO₄, Na₂HPO₄, and NaH₂PO₄) on Ag₃PO₄ morphology for photocatalytic dye degradation under visible light and toxicity of the degraded dye products. *Industrial & Engineering Chemistry Research*, 52(49), 17369-17375.
- Alharthi, F. A., Shashank, M., Shashikanth, J., Viswantha, R., Alghamdi, A. A., Alghamdi, J., ... & Ganganagappa, N. (2021). Hydrothermal synthesis of α -SnWO₄:

- Application to lithium-ion battery and photocatalytic activity. *Ceramics International*, 47(7), 10242-10249.
19. Cai, Y., Yang, F., Wu, L., Shu, Y., Qu, G., Fakhri, A., & Gupta, V. K. (2021). Hydrothermal-ultrasonic synthesis of CuO nanorods and CuWO₄ nanoparticles for catalytic reduction, photocatalysis activity, and antibacterial properties. *Materials Chemistry and Physics*, 258, 123919.
 20. Adhikari, R., Trital, H. M., Rajbhandari, A., Won, J., & Lee, S. W. (2015). Microwave induced morphology evolution of bismuth tungstate photocatalyst: Evaluation of photocatalytic activity under visible light. *Journal of Nanoscience and Nanotechnology*, 15(9), 7249-7253.
 21. AlShehri, S. M., Ahmed, J., Alzahrani, A. M., & Ahamad, T. (2017). Synthesis, characterization, and enhanced photocatalytic properties of NiWO₄ nanobricks. *New Journal of Chemistry*, 41(16), 8178-8186.
 22. Buvaneswari, K., Karthiga, R., Kavitha, B., Rajarajan, M., & Suganthi, A. (2015). Effect of FeWO₄ doping on the photocatalytic activity of ZnO under visible light irradiation. *Applied Surface Science*, 356, 333-340.
 23. Alharthi, F. A., Alanazi, H. S., Alsyaahi, A. A., & Ahmad, N. (2021). Hydrothermal synthesis, characterization and exploration of photocatalytic activities of polyoxometalate: Ni-CoWO₄ nanoparticles. *Crystals*, 11(5), 456.
 24. Dai, X. J., Luo, Y. S., Zhang, W. D., & Fu, S. Y. (2010). Facile hydrothermal synthesis and photocatalytic activity of bismuth tungstate hierarchical hollow spheres with an ultrahigh surface area. *Dalton Transactions*, 39(14), 3426-3432.
 25. Geetha, G. V., Keerthana, S. P., Madhuri, K., & Sivakumar, R. (2021). Effect of solvent volume on the properties of ZnWO₄ nanoparticles and their photocatalytic activity for the degradation of cationic dye. *Inorganic Chemistry Communications*, 132, 108810.
 26. Karthiga, R., Kavitha, B., Rajarajan, M., & Suganthi, A. (2015). Photocatalytic and antimicrobial activity of NiWO₄ nanoparticles stabilized by the plant extract. *Materials Science in Semiconductor Processing*, 40, 123-129.
 27. Kuriakose, S., Hitha, H., Jose, A., John, M., & Varghese, T. (2020). Structural and optical characterization of lanthanum tungstate nanoparticles synthesized by chemical precipitation route and their photocatalytic activity. *Optical Materials*, 99, 109571.
 28. Lu, S. Y., Yu, Y. N., Bao, S. J., & Liao, S. H. (2015). In situ synthesis and excellent photocatalytic activity of tiny Bi decorated bismuth tungstate nanorods. *RSC advances*, 5(104), 85500-85505.
 29. Manjunath, K., & Thimmanna, C. G. (2018). Effect of organic fuels on surface area and photocatalytic activity of scheelite CaWO₄ nanoparticles. *Materials Research Express*, 5(3), 035030.
 30. Mohamed, M. M., Ahmed, S. A., & Khairou, K. S. (2014). Unprecedented high photocatalytic activity of nanocrystalline WO₃/NiWO₄ hetero-junction towards dye degradation: effect of template and synthesis conditions. *Applied Catalysis B: Environmental*, 150, 63-73.
 31. Nivetha, P., Kavitha, B., & Kalanithi, M. (2021). Investigation of photocatalytic and antimicrobial activities of BaWO₄-MoS₂ nanoflowers. *Journal of Science: Advanced Materials and Devices*, 6(1), 65-74.
 32. Pourmortazavi, S. M., Rahimi-Nasrabadi, M., Ganjali, M. R., Karimi, M. S., Norouzi, P., & Faridbod, F. (2017). Facile and effective synthesis of praseodymium tungstate nanoparticles through an optimized procedure and investigation of photocatalytic activity. *Open Chemistry*, 15(1), 129-138.

33. Pourmortazavi, S. M., Rahimi-Nasrabadi, M., Karimi, M. S., & Mirsadeghi, S. (2018). Evaluation of photocatalytic and supercapacitor potential of nickel tungstate nanoparticles synthesized by electrochemical method. *New Journal of Chemistry*, 42(24), 19934-19944.
34. Qamar, M., & Khan, A. (2014). Mesoporous hierarchical bismuth tungstate as a highly efficient visible-light-driven photocatalyst. *RSC Advances*, 4(19), 9542-9550.
35. Asha, S., Hentry, C., Bindhu, M. R., Al-Mohaimeed, A. M., AbdelGawwad, M. R., & Elshikh, M. S. (2021). Improved photocatalytic activity for degradation of textile dyeing waste water and thiazine dyes using $PbWO_4$ nanoparticles synthesized by co-precipitation method. *Environmental Research*, 200, 111721.
36. He, H., Luo, Z., & Yu, C. (2021). Embellish zinc tungstate nanorods with silver chloride nanoparticles for enhanced photocatalytic, antibacterial and antifouling performance. *Colloids and Surfaces A: Physicochemical and Engineering Aspects*, 613, 126099.
37. Shad, N. A., Sajid, M. M., Amin, N., Javed, Y., Akhtar, K., Ahmad, G., ... & Ikram, M. (2019). Photocatalytic degradation performance of cadmium tungstate ($CdWO_4$) nanosheets-assembly and their hydrogen storage features. *Ceramics International*, 45(15), 19015-19021.
38. Shang, Y., Cui, Y., Shi, R., & Yang, P. (2019). Effect of acetic acid on morphology of Bi_2WO_6 with enhanced photocatalytic activity. *Materials Science in Semiconductor Processing*, 89, 240-249.
39. Taneja, P., Sharma, S., Umar, A., Mehta, S. K., Ibhaddon, A. O., & Kansal, S. K. (2018). Visible-light driven photocatalytic degradation of brilliant green dye based on cobalt tungstate ($CoWO_4$) nanoparticles. *Materials Chemistry and Physics*, 211, 335-342.
40. Thomas, A., Janáky, C., Samu, G. F., Huda, M. N., Sarker, P., Liu, J. P., ... & Rajeshwar, K. (2015). Time-and energy-efficient solution combustion synthesis of binary metal tungstate nanoparticles with enhanced photocatalytic activity. *ChemSusChem*, 8(10), 1652-1663.
41. Grabis, J., Jankovica, D., Kodols, M., & Rasmene, D. (2012). Photocatalytic activity of $ZnWO_4$ nanoparticles prepared by combustion synthesis. *Latvian Journal of Chemistry*, 51(1-2), 93.
42. Waimbo, M., Anduwan, G., Renagi, O., Badhula, S., Michael, K., Park, J., ... & Kim, Y. S. (2020). Improved charge separation through H_2O_2 assisted copper tungstate for enhanced photocatalytic efficiency for the degradation of organic dyes under simulated sun light. *Journal of Photochemistry and Photobiology B: Biology*, 204, 111781.
43. Zhang, L., & Zhu, Y. (2012). A review of controllable synthesis and enhancement of performances of bismuth tungstate visible-light-driven photocatalysts. *Catalysis Science & Technology*, 2(4), 694-706.
44. Sobhani-Nasab, A., Pourmasoud, S., Ahmadi, F., Wysokowski, M., Jesionowski, T., Ehrlich, H., & Rahimi-Nasrabadi, M. (2019). Synthesis and characterization of $MnWO_4/TmVO_4$ ternary nano-hybrids by an ultrasonic method for enhanced photocatalytic activity in the degradation of organic dyes. *Materials Letters*, 238, 159-162.
45. Babu, M. J., Botsa, S. M., Rani, S. J., Venkateswararao, B., & Muralikrishna, R. (2020). Enhanced photocatalytic degradation of cationic dyes under visible light irradiation by $CuWO_4$ -RGO nanocomposite. *Advanced Composites and Hybrid Materials*, 3, 205-212.

46. Alborzi, A., & Abedini, A. (2016). Synthesis, characterization, and investigation of magnetic and photocatalytic property of cobalt tungstate nanoparticles. *Journal of Materials Science: Materials in Electronics*, 27, 4057-4061.
47. Barzgari, Z., Askari, S. Z., & Ghazizadeh, A. (2015). Solar photocatalytic activity of chemical solution-prepared barium tungstate nanostructures. *Materials Science in Semiconductor Processing*, 33, 36-41.
48. El-Sheikh, S. M., & Rashad, M. M. (2015). Novel synthesis of cobalt nickel tungstate nanopowders and its photocatalytic application. *Journal of Cluster Science*, 26, 743-757.
49. Farsi, H., Barzgari, Z., & Askari, S. Z. (2015). Sunlight-induced photocatalytic activity of nanostructured calcium tungstate for methylene blue degradation. *Research on Chemical Intermediates*, 41, 5463-5474.
50. Hossainian, H., Salavati-Niasari, M., & Bazarganipour, M. (2016). Photodegradation of organic dye using strontium tungstate spherical-like nanostructures; synthesis and characterization. *Journal of Molecular Liquids*, 220, 747-754.
51. Khademolhoseini, S., & Ali Zarkar, S. (2016). Preparation and characterization of barium tungstate nanoparticles via a new simple surfactant-free route. *Journal of Materials Science: Materials in Electronics*, 27, 9605-9609.
52. Li, K., Dong, C., Zhang, Y., Wei, H., Zhao, F., & Wang, Q. (2014). Ag-AgBr/CaWO₄ composite microsphere as an efficient photocatalyst for degradation of Acid Red 18 under visible light irradiation: Affecting factors, kinetics and mechanism. *Journal of Molecular Catalysis A: Chemical*, 394, 105-113.
53. Liu, Q. Q., Fan, C. Y., Sun, X. J., Cheng, X. N., Yang, J., & Tang, H. (2016). Influence of doping and solid solution formation on photocatalytic activity of ZrW₂O₈ with cubic structure. *Materials Technology*, 31(3), 153-159.
54. Mohammadi-Aghdam, S. (2017). Green synthesis and characterization of Pr³⁺: CaWO₄ nanostructures in the presence of maltose as a capping agent for photocatalytic degradation of rhodamine B. *Journal of Materials Science: Materials in Electronics*, 28, 17161-17167.
55. Monisha, K., Kavipriya, S., Silambarasan, A., Arulmozhi, R., Abirami, N., & Ramesh, R. (2020). Hydrothermal synthesis of hierarchically structured cobalt doped bismuth tungstate with improved photocatalytic activity. *Optik*, 206, 164366.
56. Mosleh, M. (2018). Application of new method for the synthesis of cobalt tungstate nanostructures and cobalt tungstate/calcium carbonate nanocomposites and removal of organic pollutants. *Journal of Materials Science: Materials in Electronics*, 29, 4855-4861.
57. Hang, T. T. M., Vy, N. H. T., Hanh, N. T., & Pham, T. D. (2021). Facile synthesis of copper tungstate (CuWO₄) for novel photocatalytic degradation of tetracycline under visible light. *Sustainable Chemistry and Pharmacy*, 21, 100407.
58. Narendhran, S., Shakila, P. B., Manikandan, M., Vinoth, V., & Rajiv, P. (2020). Spectroscopic investigation on photocatalytic degradation of methyl orange using Fe₂O₃/WO₃/FeWO₄ nanomaterials. *Spectrochimica Acta Part A: Molecular and Biomolecular Spectroscopy*, 232, 118164.
59. Nobre, F. X., Muniz, R., do Nascimento, E. R., Amorim, R. S., Silva, R. S., Almeida, A., ... & Leyet, Y. (2022). Correction to: Hydrothermal temperature dependence of CaWO₄ nanoparticles: structural, optical, morphology and photocatalytic activity. *Journal of Materials Science: Materials in Electronics*, 1-2.

60. Mohamed Jaffer Sadiq, M., & Samson Nesaraj, A. (2015). Soft chemical synthesis and characterization of BaWO₄ nanoparticles for photocatalytic removal of Rhodamine B present in water sample. *Journal of Nanostructure in Chemistry*, 5, 45-54.
61. Li, Q., Yue, B., Iwai, H., Kako, T., & Ye, J. (2010). Carbon nitride polymers sensitized with N-doped tantalum acid for visible light-induced photocatalytic hydrogen evolution. *The Journal of Physical Chemistry C*, 114(9), 4100-4105.
62. Talebi, R., & Safari, A. (2016). Synthesis, characterization, and investigation of magnetic and photocatalytic property of SrWO₄ nanoparticles. *Journal of Materials Science: Materials in Electronics*, 27, 9842-9846.
63. Talebi, R., & Safari, A. (2016). Synthesis, characterization, and investigation of magnetic and photocatalytic property of SrWO₄ nanoparticles. *Journal of Materials Science: Materials in Electronics*, 27, 9842-9846.
64. Vosoughifar, M. (2017). Simple route for preparation of cobalt tungstate nanoparticles with different amino acids and its photocatalyst application. *Journal of Materials Science: Materials in Electronics*, 28, 8011-8016.
65. Waimbo, M., Anduwan, G., Renagi, O., Badhula, S., Michael, K., Park, J., ... & Kim, Y. S. (2020). Improved charge separation through H₂O₂ assisted copper tungstate for enhanced photocatalytic efficiency for the degradation of organic dyes under simulated sunlight. *Journal of Photochemistry and Photobiology B: Biology*, 204, 111781.
66. Wang, X., Fu, C., Wang, P., Yu, H., & Yu, J. (2013). Hierarchically porous metastable β-Ag₂WO₄ hollow nanospheres: controlled synthesis and high photocatalytic activity. *Nanotechnology*, 24(16), 165602.
67. Gregory, P. (1990). Classification of dyes by chemical structure. *The chemistry and application of dyes*, 17-47.
68. Engel, R. (1977). Phosphonates as analogues of natural phosphates. *Chemical Reviews*, 77(3), 349-367.
69. De Santana, Y. V., Gomes, J. E. C., Matos, L., Cruvinel, G. H., Perrin, A., Perrin, C., ... & Longo, E. (2014). Silver molybdate and silver tungstate nanocomposites with enhanced photoluminescence. *Nanomaterials and Nanotechnology*, 4(Godište 2014), 4-22.
70. George, T., Joseph, S., & Mathew, S. (2005). Synthesis and characterization of nanophased silver tungstate. *Pramana*, 65, 793-799.

12. Functional Materials for Energy Storage Applications

V. V. Deshmukh

Department of Physics,
Shri Shivaji Science College, Amravati,
Maharashtra 444603, India.

H. P. Nagaswarupa

Department of Studies in Chemistry,
Shivagangothri,
Davangere University,
Davangere 577007, India.

Abstract:

The rapid growth in global energy demands, coupled with the need for sustainable and clean energy sources, has propelled the development of contemporary materials for energy storage applications. Energy storage is essential for tackling the erratic and variable nature of renewable energy sources, enhancing grid stability, and enabling the transition towards a more sustainable energy future. The area of innovative materials for energy storage applications is introduced in this book chapter. It discusses the underlying ideas and specifications governing energy storage systems and emphasises the vital role that materials science and engineering have played in the development of energy storage technologies. Breakthroughs in energy storage and the acceleration of the shift to a more sustainable energy system depend on our ability to comprehend the special characteristics and design issues of these materials.

Keywords:

nanomaterial, fuel cell, energy storage, batteries, supercapacitors

12.1 Introduction:

Energy is indeed among the most critical topics in the 21st century, given the challenges we face with depleting fossil fuels and environmental issues associated with their use. The increasing demand for energy, coupled with the need for sustainable development, has driven the focus on efficient energy utilization and the exploration of renewable and clean energy sources. Energy cannot be generated or destroyed; it can only be changed or moved from one form to another, according to the principle of conservation of energy. By allowing for the storage and preservation of energy, energy storage systems support the idea of energy conservation while also enhancing overall energy efficiency, flexibility, and sustainability. Energy storage plays an essential role in the transition to a sustainable energy future.

By storing extra energy during times of low demand and releasing it during times of high need, it facilitates the efficient integration and use of intermittent renewable energy sources, such as solar and wind power. In addition to providing grid stability, boosting power quality, and offering backup power during outages, energy storage technologies also increase the dependability and resilience of energy systems.

The variety of research being done on energy storage has significantly increased during the past several years on a worldwide level. Modern battery technologies, such lithium-ion batteries, have revolutionized electric cars and portable devices while also facilitating the grid integration of renewable energy sources.

Energy storage system performance, longevity, and cost-effectiveness are always being improved by researchers. The material selection for energy storage systems is crucial because it affects the systems' energy capacity, power delivery, cycle life, safety, environmental effect, cost, and applicability for certain applications.

These materials include carbon-based, polymer-based, and metal-based substances, each with its own unique properties and possible advantages of energy storage technologies.

12.2 Classification of Energy Storages:

Energy storage systems are usually categorized into numerous groups based on a range of variables. The following list of typical energy storage technology categories.

12.2.1 Thermal Energy Storage:

Another strategy for addressing the timing discrepancy between power supply and consumer demand is thermal energy storage. It entails storing extra thermal energy as sensible heat or latent heat in a substance and using it when needed later.

- ***Sensible Heat Storage:*** Sensible heat storage devices regulate the temperature of a substance, like water or rock, to store and release thermal energy.
- ***Latent Heat Storage:*** Latent heat storage systems use phase change materials (PCMs) to store and release energy during the process of melting and solidifying.
- ***Thermochemical Storage:*** Thermochemical storage systems utilize chemical reactions to store and release heat energy.

12.2.2 Mechanical Energy Storage:

Mechanical energy storage typically used to store energy during periods of low demand or when electricity is available at lower costs, such as during off-peak hours. The process involves converting electrical energy into mechanical energy to store it, and then converting the stored mechanical energy back into electrical energy when needed.

It offers a technique to optimize renewable energy sources, balance power supply and demand, and strengthen grid stability. It is a process used in energy storage systems to provide a dependable and affordable energy source.

- ***Pumped Hydroelectric Storage (PHS)***: PHS involves pumping water to a higher elevation during times of low energy demand and releasing it to generate electricity during peak demand.
- ***Compressed Air Energy Storage (CAES)***: In subterranean caverns, compressed and stored air from CAES systems is later expanded to provide energy using a turbine.
- ***Flywheel Energy Storage (FES)***: Flywheels have a rotating rotor that stores energy that gets later transformed into electricity if necessary.

12.2.3 Chemical Energy Storage:

- ***Hydrogen Storage***: Fuel cells or combustion may be used to create and store hydrogen as a chemical fuel, which can then be turned into power.
- ***Synthetic Fuels***: Energy can be stored in the form of synthetic fuels, such as synthetic natural gas (SNG), methanol, or dimethyl ether (DME), which can be used in various applications including transportation.

12.2.4 Electrochemical Energy Storage:

Electrochemical energy storage/release is indeed achieved through the movement of electrons and ions. Batteries and Supercapacitors are two common types of electrochemical energy storage devices.

- ***Batteries***: Batteries store energy through electrochemical reactions. They are classified into various types, including lithium-ion, lead-acid, nickel-cadmium, and sodium-ion batteries, among others.
- ***Supercapacitors***: Through the physical separation of charges at the electrode-electrolyte interface, supercapacitors store electrical energy. They work in pseudo-capacitive charge-storage and electric double layer modes. These two mechanisms contribute to the energy storage capabilities of supercapacitors.
- ***Fuel Cells***: Through chemical processes involving fuel and an oxidising agent, such as hydrogen and oxygen, fuel cells produce electricity. They are usually divided into proton exchange membrane fuel cells (PEMFC), solid oxide fuel cells (SOFC), and alkaline fuel cells (AFC) based on the electrolyte utilised.

12.2.5 Electromagnetic Energy Storage:

Superconducting Magnetic Energy Storage (SMES):

SMES uses the process of charging and discharging the superconducting coil to store and release energy. The coil receives electrical energy during charging, which produces a magnetic field that stores energy within the superconducting material of the coil.

As a result of the coil's powerful magnetic field, the energy is stored as magnetic field energy. It is essential to recollect that some energy storage technologies may fall into multiple categories depending on their operational characteristics and underlying principles.

Furthermore, there are several emerging and innovative energy storage technologies like organic flow batteries, advanced capacitors that do not fit neatly into these classifications but offer unique solutions for specific applications.

12.3 Types of Materials Used for Energy Storages:

Depending on their unique usage and the kind of energy they store, materials used in energy storage can be divided into a variety of categories.

12.3.1 Common Materials:

A. Carbon-Based Materials:

Carbon materials play a crucial role in energy storage applications owing to their unique properties, such as high surface area, excellent conductivity, and chemical stability [Table 13.1]. Here is a classification of carbon materials commonly used for energy storage:

Activated Carbon:

A very porous kind of carbon with a sizable interior surface area is activated carbon. Charcoal is treated physically or chemically during the activation process, such as by heating it to high temperatures while being exposed to an activator like steam or chemicals like potassium hydroxide or zinc chloride. This treatment creates small pores and fissures on the exterior of the carbon, significantly increasing its surface area. The large surface area and porous structure of activated carbon make it a valuable material for energy storage applications.

Carbon Nanotubes (CNTs):

CNTs have a notable impact on the electrochemical performance of batteries and supercapacitors. Their open structure, high chirality, and excellent electrical conductivity make them versatile additives. CNTs contribute to increased energy storage capacities, improved charge-discharge rates, and overall higher performance in energy storage systems whether they are used as an active anode component or as a way to improve electrical conductivity in cathode materials. There are two main types of carbon nanotubes:

- ***Single-walled nanotubes (SWNTs):*** SWNTs consist of a single cylindrical tube formed by seamlessly wrapping a single graphite sheet.
- ***Multiwalled nanotubes (MWNTs):*** MWNTs are composed of multiple concentrically nested nanotubes, resembling rings of a tree trunk. MWNTs can have several layers of carbon sheets, providing additional pathways for charge transport.

Carbon Aerogels and Xerogels:

Carbon aerogels are three-dimensional, highly porous structures composed of interconnected carbon nanoparticles. In a sol-gel technique, organic aerogels based on resorcinol-formaldehyde or phenol-furfural precursors are pyrolyzed to create carbon

aerogels. A monolithic three-dimensional mesoporous network of carbon nanoparticles is created as a result of this procedure. The aerogels are typically dried using supercritical drying techniques, such as using liquid carbon dioxide (CO₂) as a solvent, to maintain their porous structure.

On the other hand, carbon xerogels are obtained by conventional drying methods, which involve removing the solvent from the gel without using supercritical conditions. This drying process results the more compact and denser structure compared to aerogels. Carbon aerogels and xerogels are appealing possibilities for batteries and supercapacitors due to their self-supporting structure, high surface area, low density, and superior electrical conductivity.

Carbon Fibers:

Carbon fibers are composed of thin carbon filaments with high strength and stiffness. Carbon fibers are commonly used as a reinforcement material in composite electrodes for high-performance energy storage systems like lithium-sulfur batteries and fuel cells.

Carbon Nanofibers:

Carbon nanofibers are like carbon fibers but with smaller diameters and a more disordered structure. Due to the extent of their surface and electrical conductivity, carbon nanofibers have potential uses in energy storage systems including supercapacitors, lithium-ion batteries, and hydrogen storage.

Carbon Black:

Carbon black is a fine powder composed of carbon particles with a small size and high surface area. To improve the electrical conductivity of electrodes for batteries and supercapacitors, carbon black is frequently utilised as a conductive addition.

Graphene:

A single layer of carbon atoms set up in a two-dimensional honeycomb lattice make up graphene. Due to its excellent mechanical strength and strong electrical conductivity, graphene is used in energy storage applications. It could potentially be utilised as an electrode material in supercapacitors and batteries.

Table 12.1: Carbon Material for Energy Storages

Sr. No	Material	Synthesis Method	Structure	Morphology	Application	Ref.
1.	AC air cathode (NH ₂ -PVDF membrane with carbon catalyst)	low-pressure rolling phase inversion method	membrane	microporous	Fuel Cell	[1]

Sr. No	Material	Synthesis Method	Structure	Morphology	Application	Ref.
2.	AC from (Wisteria sinensis seeds biomass)	chemical activation	crystalline	lump morphology	Energy storage	[2]
3.	AC (Litchi shells)	melt-diffusion	amorphous	Channel-like macropores	Lithium–sulfur batteries	[3]
4.	AC (American ginseng waste)	precarbonization and KOH activation	amorphous	macropores	Coin cell Supercap	[4]
5.	TiO ₂ nanoribbons + MWCNT	hydrothermal	one-dimensional	Nanotube network-like	Supercap	[5]
6.	CNT@MnO ₂ composite	One step hydrothermal precipitation	hexagonal	porous nanofloret	zinc-ion batteries	[6]
7.	CuO@MnO ₂ /N-MWCNT	sonication-supported hydrothermal	monoclinic	nanotubes	supercap	[7]
8.	Carbon aerogel	sol-gel polymerization		nanoparticle	Proton Exchange Membrane Fuel Cell	[8]
9.	Carbon aerogel (rGO@SnO ₂)	In-situ		Nanosheet 2D morphology	lithium-ion batteries	[9]
10.	Graphene aerogel	two-step activation	microporous	Nanosheets	supercap	[10]
11.	Carbon fibres rGO/Fe ₃ O ₄	electrospinning		Nanofibers 350 nm	lithium-ion batteries	[11]
12.	rGO/Ni _x Co _y S	Hydrothermal		High density porous	quasi-solid supercapacitor	[12]

B. Polymer-Based Materials:

a. Conducting polymers:

High electrical conductivity polymers, such polyaniline and polypyrrole, have the potential to be used in energy storage technology. They can be utilised in the creation of flexible batteries or as electrode materials. [Table 12.2].

b. Polymer electrolytes:

With solid or gel-like polymers that transport ions in place of liquid electrolytes, these materials can improve the performance and safety of batteries. They provide more stability and can promote the advancement of solid-state batteries. [13, 14].

Table 12.2: Polymer Material for Energy Storage.

Sr. No.	Material	Synthesis Method	Structure	Morphology	SC/ Capacity	Cyclic Stability	Application	Ref.
1.	PPy@Cdots	in-situ chemical oxidative polymerization	polycrystalline	flexible chain	676 F/g	97.5%	Supercapacitor	[15]
2.	Chitosan/polyaniline film	In situ chemical polymerization	polycrystalline	coral-like nanowire	111 mF cm ⁻²	74%	Supercapacitor	[16]
3.	PEDOT	electropolymerization	polycrystalline		31.8 mA h g ⁻¹	78%	Rechargeable Zn batteries	[17]
4.	(SCNT-NH ₂ -L)	esterification and amidation	3D	polymeric	3861.4 mAh g ⁻¹	74.3%	Lithium-ion batteries.	[18]
5.	PEDOT/V ₂ O ₅	conducting polymer intercalation	2D		154 mA h g ⁻¹	80%	Zinc-ion batteries	[19]

C. Metal-Based Materials:

a. *Lithium metal:*

Lithium metal is a potential energy storage material due to its high specific capacity. It is being explored for use in advanced energy storage systems such as lithium-metal batteries, which have the potential to significantly increase energy density compared to traditional lithium-ion batteries.

b. *Transition metal oxides:*

Lithium-ion batteries frequently employ transition metal oxides as cathode materials. This includes lithium cobalt oxide (LiCoO₂), lithium nickel cobalt manganese oxide (NCM), and lithium iron phosphate (LiFePO₄). These materials offer good cycle stability and high energy density. [Table 3].

c. *Metal-organic frameworks (MOFs):*

A type of porous materials known as MOFs is made up of metal ions and organic ligands. They are appealing for uses in gas storage and electrochemical energy storage due to their huge surface area and customizable pore topologies. Some MOFs are being explored for use as electrode materials in supercapacitors and lithium-ion batteries.

d. *Metal Chalcogenides:*

Metal chalcogenides, such as metal sulfides (e.g., iron sulfide, cobalt sulfide) and metal selenides (e.g., copper selenide, nickel selenide), have gained attention as electrode materials for energy storage devices. These materials exhibit high electrical conductivity and can undergo reversible electrochemical reactions, making them suitable for applications in batteries and supercapacitors. Researchers are actively investigating novel combinations and modifications of these materials to improve their properties, increase energy storage

capacity, enhance cycling stability, and address issues like expense and influence on the ecosystem. The field of energy storage materials is evolving rapidly, driven by the demand for efficient and sustainable energy storage solutions.

Table 12.3: Transition Metal for Energy Storage.

Sr. No	Material	Synthesis Method	Structure	Morphology	Application	Ref.
1.	transition metal ferrite	Sol-gel	single-phase spinel	macroporous	Supercapacitor	[20]
2.	Manganese dioxide (MnO ₂)/CNT	scale up immersion	amorphous	flasky	Supercapacitor	[21]
3	NiSe ₂ @Fe ₃ Se ₄	chemical bath deposition	cubic	octahedral-like crystal	Supercapacitor	[22]
4	Transition metal nitride	synthetic route	3D		lithium-sulfur batteries	[23]
5	TiNbCT _x /Nb-doped	Hydrothermal		grain	lithium-ion batteries	[24]

D. Hybrid Materials:

which combine multiple components or material types, are being explored for energy storage applications to leverage the advantages of each component. Here are some examples of hybrid materials for energy storage:

- a. **Hybrid Organic-Inorganic Composites:** These materials combine organic and inorganic components to take advantage of their respective properties. For example, combining conductive polymers with metal oxides or carbon-based materials can result in hybrid electrodes with improved electrochemical performance in batteries and supercapacitors.
- b. **Metal-Organic Framework/Carbon Composites:** Metal-organic frameworks (MOFs) can be integrated with carbon-based materials, such as carbon nanotubes or graphene, to form hybrid composites. These materials are useful for energy storage applications due to their large surface area, better electrical conductivity, and improved ion transport.
- c. **Core-Shell Structures:** Core-shell structures involve encapsulating one material within another, creating hybrid materials with unique properties. For instance, coating metal nanoparticles with a conductive polymer shell can enhance stability and electrochemical performance in energy storage devices like batteries and supercapacitors.
- d. **Nanocomposites:** Nanocomposites are materials composed of nanoscale components dispersed within a matrix material. For energy storage, hybrid nanocomposites can be created by combining nanoparticles or nanowires of different materials within a conductive matrix. These nanocomposites can exhibit improved properties, such as enhanced capacitance or higher charge/discharge rates, for use in batteries and supercapacitors.

- e. **Organic-Inorganic Hybrid Perovskites:** In the realm of solar cells, hybrid perovskites, which contain both organic and inorganic components, have attracted a lot of interest. They are also being investigated for uses in energy storage. High-capacity and inexpensive energy storage devices could be possible with hybrid perovskite-based materials.

Table 12.4: Hybrid Material for Energy Storage.

Sr. No	Material	Method	Morphology	Capacity	Capacity retention	Application	Ref.
1.	Zn-Co MOF nanospheres/rGO	Hydrothermal	nano sphere	2925 F g ⁻¹	96%	asymmetric supercapacitor	[25]
2.	rGO-PPy-jute	electrochemical polymerization	wrinkled and kinked veil	117 F g ⁻¹	90%	low-cost and eco-friendly supercapacitors	[26]
3	Zn-deposited carbon cloth: Cathode and RuO ₂ /CNT: Anode	flexible battery based on a gel electrolyte		800 mAh gZn ⁻¹	100%	Zn-Ag battery and a Zn-air battery	[27]
4	Mg metal anode and Li Cathode	electrochemical deposition and stripping processes	Dendritic	105 mAh/g	83%	Magnesium and Lithium battery	[28]
5	Cellulose fiber/multi-walled carbon nanotube (MWCNT)/reduced graphene oxide (rGO)/Cobalt oxide (Co ₃ O ₄)/tin oxide (SnO ₂)	hydrothermal method	Fiber	215 F g ⁻¹	88%	supercapacitor	[29]

12.3.2 Advanced Materials for Energy Storage:

A. Batteries:

A lithium-ion battery is composed of several key components, including the anode, cathode, electrolyte, and separator. Here is a breakdown of each component's material:

Anode (Negative Electrode) material: The anode is the electrode where lithium ions are stored during battery charging. Common anode materials include carbon (graphite) and insertion-type materials like Li₄Ti₅O₁₂ and TiO₂. From the anode to the cathode, lithium ions travel during discharge. Since lithium-ion batteries (LIBs) were first commercialised by Sony in 1991, graphite has been extensively utilised as the primary anode material. However, graphite does have some limitations.

Another of the main issues is its low theoretical capacity, which restricts its suitability for high-power applications. Furthermore, at low operating voltages, the graphite electrode can react with the electrolyte, resulting in the deposition of metallic lithium. Given these challenges, alternative like intercalation, conversion and alloying type anode materials have been discovered and improved.

Cathode (Positive Electrode) material: The cathode is the electrode that receives and stores lithium ions during battery discharging. Li-containing metal oxides having layered structures, like lithium cobalt oxide (LiCoO₂), or materials with tunnel structures, like lithium manganese oxide (LiMn₂O₄), are common cathode components. Lithium ions flow from the cathode to the anode during charging.

Electrolyte: The electrolyte serves as an electronic insulator and conducts lithium ions between the anode and cathode. It is typically a solution of inorganic lithium salts, such as lithium hexafluorophosphate (LiPF₆), dissolved in a mixture of two or more organic solvents. The electrolyte allows for the movement of lithium ions during charging and discharging.

Separator: The separator physically separates the anode and cathode to prevent short circuits. It is a permeable membrane that lets lithium ions pass through but prevents electrons from doing the same. During the charging and discharging operations, the separator also offers routes for the movement of lithium ions between the electrodes.

Table 12.5: Advanced Material for Energy Storage.

Material	Method	Temp (°C)	Capacity (mAh/g)	Voltage	Application	Ref
Ni-containing Si-C silicon carbide	carbonization of nanodispersed silicon with carbon monofluoride	500–1100	100	2V	Anode LIB	[30]
Ni _x Co _{1-x} (OH) ₂	co-precipitation	700	227	4.3V	Cathode LIB	[31]
Fe ₂ VO ₄ /rGO	Solvothermal		1013.7		SIB & LIB	[32]
SeP Selenium Phosphide with Graphene	ball milling		855		Anode SIB	[33]
Sn-MOF	Hydrothermal	400	982.8	1.5V	Flow Batteries	[34]
MnCo ₂ O ₄ /N-GQD/MXene	Hydrothermal		753	1.54 V	Metal-Air	[35]

B. Supercapacitors:

Supercapacitors (SCs) known for their high-power density, which enables rapid charging and discharging. Unlike primary and secondary batteries, which store energy through chemical reactions, supercapacitors store energy through electrostatic charge separation.

A supercapacitor has two electrodes immersed in an electrolyte with a separator between the electrodes. Electrode materials for supercapacitors can be categorized into carbon-based materials, metal oxides, and conducting polymers. Each material category has its advantages and limitations. Metal oxides offer larger capacitance compared to carbon materials owing to their capacity to undergo multielectron transfer during fast Faradaic reactions.

However, cheaper metal oxides often suffer from poor electrical conductivity and cycling stability, which affects their overall performance. Conducting polymers offer pseudo capacitance through redox reactions, but their relatively low electrical conductivity and higher cost compared to carbon materials can be drawbacks.

Therefore, to overcome these problems, tailored porous carbon materials like Carbon aerogels, ordered mesoporous carbons (OMCs), and high-performance carbons (HPCs) are investigated to enhance supercapacitor performance.

Hybrid electrode materials combining carbon with conducting polymers or metal oxides have been explored to take advantage of the strengths of each material. Novel material like metal chalcogenides, such as metal sulfides (e.g., MoS₂, WS₂) and metal oxides (e.g., RuO₂, MnO₂), have shown promising electrochemical properties for supercapacitor.

Metal ions coupled with organic ligands make up the family of porous materials known as MOFs. They have attracted attention as potential supercapacitor electrode materials owing to their large surface area, tunable pore size, and high porosity. 2D materials graphene, MXene and 3D materials with hierarchical structures, such as carbon nanotube (CNT) foams, graphene aerogels, and metal oxide nanowire arrays, have been explored as supercapacitor electrodes. It is worth noting that the supercapacitor performance depends on various factors, including electrode materials, electrolyte composition, and device architecture [Table 12.6]. Ongoing research aims to optimize these parameters and develop novel materials for even better supercapacitor performance.

Table 12.6: Electrode Material for Supercapacitor.

Material	Method	Sp. Cap. (F g ⁻¹)	Energy density (Wh kg ⁻¹)	Power Density (W kg ⁻¹)	Cyclic Stability (%)	Ref
Na-doped MoS ₂ @NiO/C	Hydrothermal	2540.63	36.93		97.6	[36]
Co ₃ O ₄	Wet chemical reduction	347.4	18.6	400	96	[37]
Gd ³⁺ doped V ₂ O ₅ /Ti ₃ C ₂ T _x MXene	wet chemical	585	-	-	96.12	[38]
ACC@MnO ₂ @PEDOT	Electrodeposition	1882.5 mF cm ⁻²	-	-	94.6	[39]
NiSe ₂ -CoSe	Wet chemical		54.9	8460	89.6	[40]
Ni-Co-Cu hydroxide based on Co-MOF	Synthetic route	1122.97	52.66	7500	92.69	[41]

12.3.3 Advances and Challenges of Green Materials:

There has been a recent shift towards harnessing renewable biomass as a feedstock for energy materials, driven by the need for sustainable and environmentally friendly solutions. Biomass with its diverse physicochemical properties is recognized as a sustainable and renewable resource for synthesizing high-performance materials. Biomass derived from various sources, including food waste, industrial residues, and natural materials, can be utilized through green processes to create energy materials with several advantages (Figure 12.1):

Green Materials Advances	Challenges
<p>Renewable and Sustainable: Biomass is derived from living or recently living organisms, such as plants, algae, or agricultural waste. Unlike fossil fuels, biomass is renewable as it can be regrown or replenished through natural processes. Its sustainable nature ensures a continuous supply of raw materials for synthesizing high-performance materials.</p> <p>Wide Range of Feedstocks: Biomass encompasses a wide range of feedstocks, including wood, agricultural residues, food waste, algae, and more. This diversity allows for the selection of feedstocks with specific properties, such as cellulose, lignin, or starch, which can be used to create materials with varied characteristics and applications.</p> <p>Tailorable Properties: Biomass-derived materials can be tailored to exhibit specific physicochemical properties by manipulating their composition, structure, and processing methods. Through various processing techniques, such as chemical modification, purification, or combination with other materials, the properties of biomass can be fine-tuned to meet the desired requirements of high-performance materials.</p> <p>Abundance and Availability: Biomass resources are abundant and widely available. The availability of biomass feedstocks offers opportunities for large-scale production of high-performance materials without depleting scarce resources. Furthermore, biomass can be sourced locally, reducing transportation costs and associated carbon emissions.</p> <p>Diverse Physicochemical Properties: Biomass exhibits a wide range of physicochemical properties due to its composition and structure. Different components of biomass, such as cellulose, hemicellulose, lignin, and extractives, possess distinct properties that can be leveraged to develop high-performance materials. For example, cellulose can provide strength and stiffness, while lignin can contribute to thermal stability and barrier properties.</p> <p>Biodegradability and Environmental Compatibility: Many biomass-derived materials are biodegradable and environmentally compatible, offering advantages in terms of waste management and end-of-life scenarios. These materials can degrade naturally without causing persistent pollution, reducing the environmental impact associated with traditional non-biodegradable materials.</p> <p>Circular Economy Potential: Biomass resources align with the principles of the circular economy by enabling the reuse, recycling, and upcycling of materials. Biomass waste and byproducts can be utilized to extract valuable components or converted into energy, contributing to a more sustainable and efficient resource utilization cycle.</p>	<p>Cost: The cost of using green materials for energy storage can be a significant challenge. Some green materials may be more expensive to produce or require complex manufacturing processes, which can impact the overall cost of energy storage systems.</p> <p>Performance and Efficiency: Achieving high energy density, fast charging/discharging rates, and long cycle life while using green materials can be challenging.</p> <p>Scalability: Scaling up production processes and ensuring a consistent supply of raw materials can be complex. Additionally, establishing large-scale recycling systems for green materials is crucial to minimize waste and environmental impact.</p> <p>Safety and Environmental Impact: While green materials aim to reduce the environmental impact of energy storage, it is essential to consider the safety and environmental implications of their production, use, and disposal. Proper handling, recycling, and disposal processes must be established to minimize any potential negative effects.</p> <p>Regulatory Frameworks: Regulations need to ensure the safety, performance, and environmental sustainability of energy storage systems while facilitating innovation and market growth. Harmonization of standards across different regions can promote the widespread adoption of green materials for energy storage.</p>

Figure 12.1: Advances and Challenges of Green Materials

12.4 Applications of Energy Storage:

12.4.1 Fuel Cells:

- **Transportation:** Electric vehicles (EVs) and hybrid cars are able to run on fuel cells as their power source. They offer longer driving ranges and shorter refueling times compared to traditional battery-powered EVs.
- **Portable Electronics:** Fuel cells can power portable devices such as laptops, smartphones, and tablets. Compared to batteries, they offer more energy for a longer period and can recharge fast.
- **Stationary Power Generation:** Electricity is usually produced using fuel cells for consumption in rural areas, industries, and households. They can provide clean and efficient power for off-grid applications and backup power during grid outages.

- **Military Applications:** Fuel cells are used in military applications such as portable power for soldiers, unmanned vehicles, and auxiliary power units for military aircraft and vehicles.

12.4.2 Batteries:

- **Electric Vehicles:** Electric cars frequently use batteries as their main power source. They hold the electrical energy needed to power the electric motor of the vehicle.
- **Renewable Energy Storage:** Extra energy produced by renewable energy sources like solar and wind is stored in batteries. When demand outpaces supply, this stored energy can be used.
- **Portable Electronics:** Numerous portable electronics, including smartphones, computers, cameras, and wearable technology, are powered by batteries.
- **Grid Energy Storage:** Large-scale batteries perhaps utilized for grid energy storage, helping to stabilize the electrical grid by storing excess energy during low-demand periods and releasing it during high-demand periods.
- **Medical Devices:** Batteries are used in various medical devices, including pacemakers, defibrillators, insulin pumps, and portable medical equipment.

12.4.3 Supercapacitors:

- **Energy Storage and Delivery:** Supercapacitors are capable of storing and delivering energy quickly. They are used when high-power bursts are required, such as in regenerative braking systems and the energy recovery systems of hybrid and electric vehicles.
- **Renewable Energy Integration:** Supercapacitors can be used in conjunction with batteries to enhance the performance of renewable energy systems. They can provide rapid energy delivery during peak demand periods, improving the overall efficiency of the system.
- **Power Quality and UPS Systems:** Supercapacitors are employed in uninterruptible power supply (UPS) systems to provide instant power backup during power outages.

They also help maintain stable power quality by compensating for voltage sags and surges.

- **Aerospace and Defense:** Supercapacitors are used in aerospace and defense applications for rapid energy storage and release, such as in aerospace systems, satellites, and military equipment.
- **Consumer Electronics:** Supercapacitors are utilized in consumer electronics for quick charging and energy storage in devices like cameras, wearable devices, and portable speakers.

12.4.4 Emerging Storage Technologies:

As potential electrodes for electrochemical energy conversion and storage, amorphous materials, 2D MXenes, bismuth-based materials, hydrogen storage materials, and Na-ion materials are developing.

These technologies are emerging and show promising potential, many more are still in the development and testing phases and may not be commercially available on a large scale yet.

Table 12.7: Applications of Energy Storage

Energy Storage	Type of fuel cell/Material	Application	Ref
Fuel Cell	Hydrogen fuel cell	Transportation	[42]
	Proton exchange membrane (PEM) fuel cell	Transportation	[43]
	Gadolinium (Gd/316L neutron shielding materials)	Nuclear Fuel transportation	[44]
	Direct methanol fuel cells	portable electronic devices	[45]
	Micro-Fuel Cell	portable electronic devices	[46]
	Thermal management of PEM fuel cell	portable electronic devices	[47]
	Flame-assisted Fuel Cells	Power generation	[48]
	Solid oxide fuel cell	Power generation	[49]
	Hydrogen fuel cell	Military vehicles	[50]
Batteries	phase change materials	Electric vehicles	[51]
	lithium-ion batteries	Electric vehicles	[52]
	sodium-ion batteries	Greed energy storage	[53]
	Nickel hydrogen gas batteries	Greed energy storage	[54]
	Thermally activated batteries	Greed energy storage	[55]
	Miniature pin-type lithium	Medical devices	[56]
	Hybrid cathode lithium batteries $\text{Ag}_2\text{V}_4\text{O}_{11}$ and CF_x	implantable medical applications	[57]
Supercapacitor	Solid state supercapacitor	Energy storage and delivery	[58]
	battery-type supercapacitor	Energy storage and delivery	[59]
	battery–supercapacitor	Renewable energy integration	[60]
	solid-state supercapacitors with wide working temperature range	Renewable energy	[61]
	battery–supercapacitor	power quality improvement	[62]
	hybrid power sources	UPS	[63]
	Nano supercapacitors	aerospace	[64]

Energy Storage	Type of fuel cell/Material	Application	Ref
	hybrid supercapacitor	wearable electronics	[65]
	flexible supercapacitors	wearable electronics	[66]
	New electrical model of supercapacitors	Hybrid electric vehicles	[67]
	battery–supercapacitor	Solar electric vehicles	[68]
	photo-supercapacitor	Electronic applications	[69]

12.5 Sustainable Developments: Constraints and Reality:

12.5.1 Materials Recycling:

Material recycling, including the recycling of carbon dioxide, is an important aspect of the circular economy. However, despite advancements in industrial processes, there are still challenges in achieving efficient material deconstruction. Additionally, knowledge management and the financial aspects play significant roles in promoting a circular economy. This includes considerations such as patents, royalties, and asset management. The life cycle of an industrial material typically involves several key steps (Figure 13.2) Knowledge management is crucial throughout the entire life cycle of a material. It involves capturing, organizing, and disseminating information and expertise related to the material and its production processes. Overall, effective knowledge management and financial considerations, including patents, royalties, and asset management, are essential components of promoting a circular economy and advancing material recycling practices.



Figure 12.2: Circular Economy for Material Recycling

12.5.2 Energy Management:

optimizing energy consumption in industries requires careful consideration of the entire process, including material selection, deconstruction, and environmental factors such as emissions and water usage. This holistic approach is necessary to address the complexities associated with energy management and strive for improved energy efficiency in industrial operations.

12.6 Challenges and Prospects:

While energy storage faces challenges related to cost, scalability, and environmental impact, it also holds great prospects for the future. Technological advancements, renewable energy integration, grid resilience, electrification, and decentralized solutions are expected to drive the growth and deployment of energy storage, enabling a more sustainable and reliable energy (Figure 13.3).



Figure 12.3: Challenges and Prospects of Energy Storages

12.7 Conclusion:

Advanced materials such as lithium-ion batteries, solid-state batteries, and supercapacitors have demonstrated improved energy density, longer lifespans, faster charging rates, and enhanced safety features compared to traditional energy storage technologies. They have opened the way for the widespread use of electric vehicles, grid-scale energy storage devices, and renewable energy sources. Progress in energy storage has also been aided by the production of nanomaterials like graphene and carbon nanotubes. These materials have a large surface area, great conductivity, and enhanced electrochemical characteristics, which increase battery and supercapacitor performance. Additionally, the investigation of novel possibilities has been sparked by the usage of sophisticated materials for energy storage. For instance, substances like perovskites and metal-organic frameworks (MOFs) appear to have promise in applications like fuel cells and solar cells, broadening the spectrum of energy storage technologies that are now accessible.

However, despite significant progress, challenges remain in the widespread commercialization and scalability of advanced energy storage materials. Issues such as cost, scalability, and environmental impact need to be addressed to ensure these technologies can be implemented on a larger scale. In summary, advanced materials have significantly transformed the field of energy storage, enabling more efficient, durable, and sustainable solutions. Continued research and development efforts, along with collaboration between academia, industry, and policymakers, will be crucial to further advance these materials and unlock their full potential for a clean and sustainable energy future.

12.8 References:

1. Kexin Yi, Wulin Yang, Bruce E. Logan, Defect free rolling phase inversion activated carbon air cathodes for scale-up electrochemical applications, *Chemical Engineering Journal*, 454 (2023) pp140411, <https://doi.org/10.1016/j.cej.2022.140411>
2. Ganesh Prasad Awasthi, Deval Prasad Bhattarai, Bikendra Maharjan, Kyung-Suk Kim
3. Chan Hee Park, Cheol Sang Kim, Synthesis and characterizations of activated carbon from *Wisteria sinensis* seeds biomass for energy storage applications, *Journal of Industrial and Engineering Chemistry*, 72 (2019) pp265-272, <https://doi.org/10.1016/j.jiec.2018.12.027>
4. Songtao Zhang, Mingbo Zheng, Zixia Lin, Nianwu Li, Yijie Liu, Bin Zhao, uan Pang, Jieming Cao, Ping He and Yi Shi, Activated carbon with ultrahigh specific surface area synthesized from natural plant material for lithium–sulfur batteries, *J. Mater. Chem. A*, 2 (2014) pp15889–15896; <https://doi.org/10.1039/C4TA03503H>
5. Jianfei Tu, Zhijun Qiao, Yuzuo Wang, Gaofeng Li, Xi Zhang, Guoping Li, Dianbo Ruan, American ginseng biowaste-derived activated carbon for high-performance supercapacitors, *International Journal of Electrochemical Science*, 18 (2023) pp16-24; <https://doi.org/10.1016/j.ijoes.2023.01.011>
6. Mohammad Bin Sabt, Mohamed Shaban and Ahmed Gamal, Nanocomposite Electrode of Titanium Dioxide Nanoribbons and Multiwalled Carbon Nanotubes for Energy Storage, *Materials* 16 (2023) pp595; <https://doi.org/10.3390/ma16020595>
7. Yujin Ren, Fanbo Meng, Siwen Zhang, Bu Ping, Hui Li, Bosi Yin Tianyi Ma, CNT@MnO₂ composite ink toward a flexible 3D printed micro-zinc-ion battery, *Carbon Energy*. 4 (2022) pp446–457, <https://doi.org/10.1002/cey2.177>
8. Vijay Kakani, Sivalingam Ramesh, H. M. Yadav, Chinna Bathula, Praveen Kumar Basivi, Ramasubba Reddy Palem, Heung Soo Kim, Visweswara Rao Pasupuletti, Handol Lee & Hakil Kim, Hydrothermal synthesis of CuO@MnO₂ on nitrogen-doped multiwalled carbon nanotube composite electrodes for supercapacitor applications, *Scientific Reports*, 12 (2022) pp12951; <https://doi.org/10.1038/s41598-022-16863-3>
9. Gu, E.J. Kim, S.K. Sharma, P.R. Sharma, S. Bliznakov, B.S. Hsiao, M.H. Rafailovich, Mesoporous carbon aerogel with tunable porosity as the catalyst support for enhanced proton-exchange membrane fuel cell performance, *Materials Today Energy*, Volume 19, March 2021, 100560; <https://doi.org/10.1016/j.mtener.2020.100560>
10. Hwei Zhao, Xiaolong Zeng, Tian Zheng, Shaojia Liu, Jie Yang, Rui Hao, Fengshi Li, Lin Guo, Three-dimensional porous aerogel assembly from ultrathin rGO@SnO₂ nanosheets for advanced lithium-ion batteries, *Composites Part B: Engineering*, Volume 231(2022) pp109591; <https://doi.org/10.1016/j.compositesb.2021.109591>

11. Zhou Liao, Jie Cheng b, Jian-Hua Yu c, Xiao-Long Tian c, Ming-Qiang Zhu, Graphene aerogel with excellent property prepared by doping activated carbon and CNF for free-binder supercapacitor, *Carbohydrate Polymers*, 286 (2022) pp119287; <https://doi.org/10.1016/j.carbpol.2022.119287>
12. Pitcheri Rosaiah, Theophile Niyitanga, Sangaraju Sambasivam c and Haekyoung Kim, Graphene based magnetite carbon nanofiber composites as anodes for high-performance Li-ion batteries, *New J. Chem.*, 47 (2023) pp482-490, DOI: 10.1039/D2NJ04821C
13. Juan Wang, Peimin Zhan, Dong Zhang, Luping Tang, Nickel cobalt sulfide composite nanosheet anchored on rGO as effective electrode for quasi-solid supercapacitor, *Journal of Energy Storage*, 70 (2023) pp107938; <https://doi.org/10.1016/j.est.2023.107938>
14. Zhi-Yong Li, Zhuo Li, Jia-Long Fu, Xin Guo, Sodium-ion conducting polymer electrolytes, *Rare Met.* (2023) 42:1–16; <https://doi.org/10.1007/s12598-022-02132-9>
15. Jongjun Lee, Seoungwoo Byun, Hyobin Lee, Youngjoon Roh, Dahee Jin, Jaejin Lim, Jihun Song, Cyril Bubu Dzakpasu, Joonam Park, Yong Min Lee, Digital-twin-driven structural and electrochemical analysis of Li⁺ single-ion conducting polymer electrolyte for all-solid-state batteries, 2 (2023) pp20220061, <https://doi.org/10.1002/bte2.20220061>
16. Shisong Nie, Zongyu Li, Zhen Su, Yingzhi Jin, Haijun Song, Haolan Zheng, Jiaying Song, Lin Hu, Xinxing Yin, Zhiguang Xu, Yuyuan Yao, Hao Wang, Zaifang, Highly Stable Supercapacitors Enabled by a New Conducting Polymer Complex PEDOT:CF₃SO₂(x)PSS(1-x), 16 (2023) ppe202202208, <https://doi.org/10.1002/cssc.202202208>
17. Madari Palliyalil Sidheekh, Aranhikundan Shabeeb, Lijin Rajan, Mohamed Shahin Thayyil and Yahya A. Ismail, Conducting Polymer/Hydrogel Hybrid Free-Standing Electrodes for Flexible Supercapacitors Capable of Self-Sensing Working Conditions: Large-Scale Fabrication Through Facile and Low Cost Route, *Eng. Sci.*, 23 (2023) pp890, 10.30919/es890
18. Xiaoteng Jia, Xuenan Ma, Li Zhao, Meiyong Xin, Yulei Hao, Peng Sun, Chenguang Wang, Danming Chao, Fangmeng Liu, Caiyun Wang, Geyu Lu and Gordon Wallace, A biocompatible and fully erodible conducting polymer enables implanted rechargeable Zn batteries, *Chem. Sci.*, (2023) pp2123-2130; DOI: 10.1039/D2SC06342E
19. Biao Zhang, Zikai Li, Huamei Xie, Yanling Dong, Pengfei Xu, Dan Wang, Anru Guo, Dong Liu, Cross-linking chemistry enables robust conductive polymeric network for high-performance silicon microparticle anodes in lithium-ion batteries, *Journal of Power Sources*, 556, (2023) 232495; <https://doi.org/10.1016/j.jpowsour.2022.232495>
20. Bo Wang, Simin Dai, Zehao Zhu, Lin Hu, Zhen Su, Yingzhi Jin, Liukang Xiong, Jiasong Gao, Jun Wan, Zaifang Li and Liang Huang, A two-dimensional conductive polymer/V₂O₅ composite with rapid zinc-ion storage kinetics for high-power aqueous zinc-ion batteries, *Nanoscale*, 14 (2022) pp12013-12021; <https://doi.org/10.1039/D2NR03147G>
21. Bhamini Bhujun, Michelle T.T. Tan, Anandan S. Shanmugam, Study of mixed ternary transition metal ferrites as potential electrodes for supercapacitor applications, *Results in Physics* 7 (2017) pp345–353, <http://creativecommons.org/licenses/by-nc-nd/4.0/>
22. Wen Qi, Xuan Li, Ying Wu, Hong Zeng, Chunjiang Kuang, Shaoxiong Zhou, Shengming Huang, Zhengchun Yang, Flexible electrodes of MnO₂/CNTs composite for

- enhanced performance on supercapacitors, *Surface & Coatings Technology* 320 (2017) pp624–629; <http://dx.doi.org/10.1016/j.surfcoat.2016.10.038>
23. Ramu Manikandan, C. Justin Raj, Goli Nagaraju, Rajavel Velayutham, Simon E. Moulton, J. Puigdollers, Byung Chul Kim, Selenium enriched hybrid metal chalcogenides with enhanced redox kinetics for high-energy density supercapacitors, *Materials Today Sustainability*, 19 (2022) pp100214; <https://doi.org/10.1016/j.cej.2021.128924>
 24. Jian Liang Cheong, Chen Hu, Wenwen Liu, Man-Fai Ng, Michael B. Sullivan, Jackie Y. Ying, 3D carbonaceous nanostructured transition metal nitride, carbonitride and carbide as polysulfide regulators for lithium-sulfur batteries, *Nano Energy*, 102 (2022) 107659; <https://doi.org/10.1016/j.nanoen.2022.107659>
 25. Qun Ma, Zhigui Zhang, Pengzu Kou, Dan Wang, Zhiyuan Wang, Hongyu Sun, Runguo Zheng, Yanguo Liu, In-situ synthesis of niobium-doped TiO₂ nanosheet arrays on double transition metal MXene (TiNbCTx) as stable anode material for lithium-ion batteries, *Journal of Colloid and Interface Science*, 617 (2022) pp147-155; <https://doi.org/10.1016/j.jcis.2022.03.007>
 26. Honglu Wu, Shuang Li, Yang Liu, Yixiang Shi, Self-assembled Zn-Co MOF nanospheres/rGO as cathode material for an asymmetric supercapacitor with high energy density, *Electrochimica Acta*, 462 (2023) pp142740; <https://doi.org/10.1016/j.electacta.2023.142740>
 27. J. Bonastre, J. Molina, F. Cases, Surface modification of jute fabrics by reduced graphene oxide-conducting polymer coatings for their application in low-cost and eco-friendly supercapacitors, *Journal of Energy Storage*, 69 (2023) pp107936; <https://doi.org/10.1016/j.est.2023.107936>
 28. Peng Tan, Bin Chen, Haoran Xu, Weizi Cai, Wei He, Houcheng Zhang, Meilin Liu, Zongping Shao, and Meng Ni, Integration of Zn–Ag and Zn–Air Batteries: A Hybrid Battery with the Advantages of Both, *ACS Appl. Mater. Interfaces* 10 (2018) pp36873–36881; <https://doi.org/10.1021/acsami.8b10778>
 29. Yingwen Cheng, Yuyan Shao, Ji-Guang Zhang, Vincent L. Sprenkle, Jun Liu and Guosheng Li, High Performance Batteries Based on Hybrid Magnesium and Lithium Chemistry, *Chem. Commun.*, 50 (2014) pp9644-9646; <https://doi.org/10.1039/C4CC03620D>
 30. S. Ramesh, Saurabh Khandelwal, Kyong Yop Rhee, David Hu, Synergistic effect of reduced graphene oxide, CNT and metal oxides on cellulose matrix for supercapacitor applications, *Composites Part B: Engineering*, 138 (2018) pp45-54; <https://doi.org/10.1016/j.compositesb.2017.11.024>
 31. Darina A. Lozhkina, Vladimir P. Ulin, Mikhail E. Kompan, Aleksander M. Rumyantsev, Irina S. Kondrashkova, Andrei A. Krasilin, Ekaterina V. Astrova, Influence of the Ni Catalyst on the Properties of the Si-C Composite Material for LIB Anodes, *Batteries* 8 (2022) pp102; <https://doi.org/10.3390/batteries8080102>
 32. Jaekwang Kim, Ilbok Lee, Young-Hoon Kim, Joong Ho Bae, Keebum Hwang, Hyunchul Kang, Jae-Hyun Shim, Ji-Soo Kim, Chul Wan Park, Young-Min Kim, Songhun Yoon, Ni-rich cathode material with isolated porous layer hindering crack propagation under 4.5 V high cut-off voltage cycling, *Chemical Engineering Journal*, 455 (2023) pp140578 <https://doi.org/10.1016/j.cej.2022.140578>
 33. Decheng Zhao, Zhen Zhang, Jinghui Ren, Yuanyuan Xu, Xiangyu Xu, Jian Zhou, Fei Gao, Hao Tang, Shupeii Liu, Zhoulu Wang, Di Wang, Yutong Wu, Xiang Liu, Yi Zhang, Fe₂VO₄ nanoparticles on rGO as anode material for high-rate and durable lithium and

- sodium ion batteries, *Chemical Engineering Journal*, 451 (2023) pp138882; <https://doi.org/10.1016/j.cej.2022.138882>
34. Junwu Sang, Xiangdan Zhang, Kangli Liu, Guoqin Cao, Ruxin Guo, Shijie Zhang, Zhiheng Wu, Yongshang Zhang, Ruohan Hou, Yonglong Shen, Guosheng Shao, Effective Coupling of Amorphous Selenium Phosphide with High-Conductivity Graphene as Resilient High-Capacity Anode for Sodium-Ion Batteries, *Advanced functional materials*, 33 (2023) pp2211640; <https://doi.org/10.1002/adfm.202211640>
 35. Qing-Chun Jiang, Jin Li, Yu-Jie Yang, Yu-Jie Ren, Lei Dai, Jia-Yi Gao, Ling Wang, Jia-Ye Ye, Zhang-Xing He, Ultrafine SnO₂ in situ modified graphite felt derived from metal–organic framework as a superior electrode for vanadium redox flow battery, *Rare Met.* 42 (2023) pp1214–1226, <https://doi.org/10.1007/s12598-022-02228-2>
 36. Monireh Faraji , Samira Yousefzadeh , Maadh Fawzi Nassar ^{c d}, Musaddak Maher Abdul Zahra, MnCo₂O₄/N-doped graphene quantum dot vigorously coupled to MXene nanosheet: A bifunctional Oxygen electrocatalyst outperforms Pt/IrO₂ benchmark electrocatalysts in metal-air batteries, *Journal of Alloys and Compounds*, 927 (2022) pp167115; <https://doi.org/10.1016/j.jallcom.2022.167115>
 37. Sheng Qiang Zheng, Siew Shee Lim, Chuan Yi Foo , Choon Yian Haw, Wee Siong Chiu, Chin Hua Chia, Poi Sim Khiew, Fabrication of sodium and MoS₂ incorporated NiO and carbon nanostructures for advanced supercapacitor application, *Journal of Energy Storage*, 63 (2023) 106980, <https://doi.org/10.1016/j.est.2023.106980>
 38. Qinghai Ma, Fang Cui, Jiajia Zhang, Xin Qi, Tiewu Cui, Surface engineering of Co₃O₄ nanoribbons forming abundant oxygen-vacancy for advanced supercapacitor, *Applied Surface Science*, 578 (2022) pp152001; <https://doi.org/10.1016/j.apsusc.2021.152001>
 39. Talya Tahir, Dalal Alhashmialameer, Sonia Zulfiqar, Amany M.E. Atia, Muhammad Farooq Warsi, Khadija Chaudhary, Heba M. El Refay, Wet chemical synthesis of Gd⁺³ doped vanadium Oxide/MXene based mesoporous hierarchical architectures as advanced supercapacitor material, *Ceramics International*, 48 (2022) pp24840-24849; <https://doi.org/10.1016/j.ceramint.2022.05.135>
 40. Abdul Rehman Akbar, Adil Saleem , Abdur Rauf , Rashid Iqbal, Muhammad Tahir, Gangqiang Peng , Abdul Sammed Khan, Arshad Hussain, Muhammad Ahmad, Mansoor Akhtar, Mumtaz Ali, Chuanxi Xiong, Quanling Yang, Ghaffar Ali, Fude Liu, Integrated MnO₂/PEDOT composite on carbon cloth for advanced electrochemical energy storage asymmetric supercapacitors, *Journal of Power Sources*, 579 (2023) pp233181; <https://doi.org/10.1016/j.jpowsour.2023.233181>
 41. Muhammad Sana Ullah Shah, Xiaoqing Zuo, A. Shah, Sameerah I. Al-Saeedi, Muhammad Zia Ullah Shah, Eman A. Alabbad , Hongying Hou, Syed Awais Ahmad, Muhammad Arif, Muhammad Sajjad, Tauseef Ul Haq, CoSe nanoparticles supported NiSe₂ nanoflowers cathode with improved energy storage performance for advanced hybrid supercapacitors, *Journal of Energy Storage*, 65 (2023) pp107267, <https://doi.org/10.1016/j.est.2023.107267>
 42. Lican Zhao , Fanbin Meng , Wei Zhang, Fabrication of 3D micro-flower structure of ternary Ni-Co-Cu hydroxide based on Co-MOF for advanced asymmetric supercapacitors, *Electrochimica Acta*, 461 (2023) pp142656 ; <https://doi.org/10.1016/j.electacta.2023.142656>
 43. Carlos Mendez , Marcello Contestabile , Yusuf Bicer, Hydrogen fuel cell vehicles as a sustainable transportation solution in Qatar and the Gulf cooperation council: a review, *International Journal of Hydrogen Energy*, 2023; <https://doi.org/10.1016/j.ijhydene.2023.04.194>
-

44. Steffen Dirkes, Julian Leidig, Philipp Fisch, Stefan Pischinger, Prescriptive Lifetime Management for PEM fuel cell systems in transportation applications, Part I: State of the art and conceptual design, *Energy Conversion and Management*, 277 (2023) pp116598; <https://doi.org/10.1016/j.enconman.2022.116598>
45. Zheng-Dong Qi , Zhong Yang , Xi-Gang Yang, Li-Ying Wang, Chang-Yuan Li, Ye Dai, Performance study and optimal design of Gd/316L neutron absorbing material for Spent Nuclear Fuel transportation and storage, *Materials Today Communications*, 34 (2023) pp105342; <https://doi.org/10.1016/j.mtcomm.2023.105342>
46. V. Raj, 16 - Direct methanol fuel cells in portable applications: materials, designs, operating parameters, and practical steps toward commercialization, *Direct Methanol Fuel Cell Technology*, (2020) Pages 495-525; <https://doi.org/10.1016/B978-0-12-819158-3.00016-1>
47. Robert Hockaday, Carlos Navas, Micro-Fuel Cells™ for portable electronics, *Fuel Cells Bulletin*, 2 (1999) pp 9-12, [https://doi.org/10.1016/S1464-2859\(99\)80068-6](https://doi.org/10.1016/S1464-2859(99)80068-6)
48. Yangyang Chen, Qifei Jian, Zhe Huang, Jing Zhao, Xingying Bai, Deqiang Li, Improvement of thermal management of proton exchange membrane fuel cell stack used for portable devices by integrating the ultrathin vapor chamber, *International Journal of Hydrogen Energy*, 46 (2021) pp36995-37006, <https://doi.org/10.1016/j.ijhydene.2021.08.185>
49. Xi Chen, Wenbo Li, Bhupendra Singh Chauhan, Saleh Mahmoud, Wael Al-Kouz, Abir Mouldi, Hassen Loukil, Yong Chen, Salema K. Hadrawi, Waste heat from a flame-assisted fuel cell for power generation using organic Rankine cycle: Thermoeconomic investigation with CO₂ emission considerations, *Process Safety and Environmental Protection*, 175 (2023) pp 585-598; <https://doi.org/10.1016/j.psep.2023.05.033>
50. Dibyendu Roy, Samiran Samanta, Sumit Roy, Andrew Smallbone, Anthony Paul Roskilly, Multi-objective optimisation of a power generation system integrating solid oxide fuel cell and recuperated supercritical carbon dioxide cycle, *Energy*, 281 (2023) pp128158; <https://doi.org/10.1016/j.energy.2023.128158>
51. Scott M. Katalenich, Mark Z. Jacobson, Toward battery electric and hydrogen fuel cell military vehicles for land, air, and sea, *Energy*, 254 (2022) pp124355; <https://doi.org/10.1016/j.energy.2022.124355>
52. Abdul Hai Alami , Hussein M. Maghrabie, Mohammad Ali Abdelkareem, Enas Taha Sayed, Zena Yasser, Tareq Salameh, S.M.A. Rahman, Hegazy Rezk, A.G. Olab, Potential applications of phase change materials for batteries' thermal management systems in electric vehicles, *Journal of Energy Storage*, 54 (2022) pp105204; <https://doi.org/10.1016/j.est.2022.105204>
53. Thi-Hai Anh Nguyen, Seok-Young Oh, Anode carbonaceous material recovered from spent lithium-ion batteries in electric vehicles for environmental application, *Waste Management*, 120, (2021) pp755-761; <https://doi.org/10.1016/j.wasman.2020.10.044>
54. Yunming Li, Yaxiang Lu, Chenglong Zhao, Yong-Sheng Hu, Maria-Magdalena Titirici b, Hong Li, Xuejie Huang, Liquan Chen, Recent advances of electrode materials for low-cost sodium-ion batteries towards practical application for grid energy storage, *Energy Storage Materials*, 7 (2017) pp130-151, <https://doi.org/10.1016/j.ensm.2017.01.002>
55. Taoli Jiang, Wei Chen, Nickel hydrogen gas batteries: From aerospace to grid-scale energy storage applications, *Current Opinion in Electrochemistry*, 30 (2021) pp100859, <https://doi.org/10.1016/j.coelec.2021.100859>

56. Minyuan M. Li^{1,2}, J. Mark Weller^{1,2}, David M. Reed¹, Vincent L. Sprenkle¹, Guosheng Li, Thermally activated batteries and their prospects for grid-scale energy storage, *Joule*, 7 (2023) pp619-623; <https://doi.org/10.1016/j.joule.2023.02.009>
57. Mikito Nagata, Ashok Saraswat, Hiroshi Nakahara, Hiroyuki Yumoto, David M. Skinlo, Kaname Takeya, Hisashi Tsukamoto, Miniature pin-type lithium batteries for medical applications, *Journal of Power Sources*, 146 (2005) pp762-765; <https://doi.org/10.1016/j.jpowsour.2005.03.156>
58. Kaimin Chen, Donald R. Merritt, William G. Howard, Craig L. Schmidt, Paul M. Skarstad, Hybrid cathode lithium batteries for implantable medical applications, *Journal of Power Sources*, 162 (2006) pp837-840; <https://doi.org/10.1016/j.jpowsour.2005.07.018>
59. Amr M. Obeidat, A.C. Rastogi, Co-electrodeposited poly (3, 4-ethylenedioxythiophene) (PEDOT)-multiwall carbon nanotubes (MWCNT) hybrid electrodes based solid-state supercapacitors using ionic liquid gel electrolyte for energy storage with pulsed power capabilities, *Journal of Energy Storage*, 67(2023) pp107563; <https://doi.org/10.1016/j.est.2023.107563>
60. Jiayi Xu, Hao Guo, Yuan Chen, Fan Yang, Yanrui Hao, Jiaying Tian, Yinsheng Liu, Zongyan Lu, Xiaoqin Wei, Wu Yang, In-situ construction of hierarchical NPO@CNTs derived from Ni-MOF as ultra-high energy storage electrode for battery-type supercapacitor, *Journal of Energy Storage*, 68 (2023) pp107819; <https://doi.org/10.1016/j.est.2023.107819>
61. Mahmoud F. Elmorshedy, M. R. Elkadeem, Kotb M. Kotb, Ibrahim B.M. Taha, Domenico Mazzeo, Optimal design and energy management of an isolated fully renewable energy system integrating batteries and supercapacitors, *Energy Conversion and Management*, 245 (2021) pp114584; <https://doi.org/10.1016/j.enconman.2021.114584>
62. <https://doi.org/10.1016/j.enconman.2021.114584>
63. Xiangya Wang, Qianqian Zhang, Lei Zhao, Mohammed Kamal Hadi, Sangaraju Sambasivam, Qi Zhou, Fen Ran, A renewable hydrogel electrolyte membrane prepared by carboxylated chitosan and polyacrylamide for solid-state supercapacitors with wide working temperature range, *Journal of Power Sources*, 560 (2023) pp232704; <https://doi.org/10.1016/j.jpowsour.2023.232704>
64. Nafih Muhammad Ismail, Mahesh Kumar Mishra, A multi-objective control scheme of a voltage source converter with battery–supercapacitor energy storage system used for power quality improvement, *International Journal of Electrical Power & Energy Systems*, 142 (2022) pp108253; <https://doi.org/10.1016/j.ijepes.2022.108253>
65. Yuedong Zhan, Youguang Guo, Jianguo Zhu, Li Li, Power and energy management of grid/PEMFC/battery/supercapacitor hybrid power sources for UPS applications, *International Journal of Electrical Power & Energy Systems*, 67 (2015) pp598-612; <https://doi.org/10.1016/j.ijepes.2014.12.044>
66. M.S.H. Al-Furjan, Z.H. Qi, L. Shan, A. Farrokhian, X. Shen, R. Kolahchi b, Nano supercapacitors with practical application in aerospace technology: Vibration and wave propagation analysis, *Aerospace Science and Technology*, 133 (2023) pp108082; <https://doi.org/10.1016/j.ast.2022.108082>
67. M.M. Harussani, S.M. Sapuan, Gohar Nadeem, Tahrir Rafin, W. Kirubaanand, Recent applications of carbon-based composites in defence industry: A review, *Defence Technology*, 18 (2022) pp1281-1300; <https://doi.org/10.1016/j.dt.2022.03.006>
68. Ruixue Li, Xiaoping Shen, Zhenyuan Ji, Yinxiu Xue, Peng Song, Hu Zhou, Lirong Kong, Shiping Zeng, Caixia Chen, Ultralight coaxial fiber-shaped zinc-ion hybrid

- supercapacitor with high specific capacitance and energy density for wearable electronics, *Chemical Engineering Journal*, 457 (2023) pp141266; <https://doi.org/10.1016/j.cej.2022.141266>
69. Zhuosheng Jiang, Shengli Zhai, Mingzhi Huang, Prayoon Songsirittigul, Su Htike Aung, Than Zaw Oo, Min Luo, Fuming Chen, 3D carbon nanocones/metallic MoS₂ nanosheet electrodes towards flexible supercapacitors for wearable electronics, *Energy*, 227 (2021) pp120419; <https://doi.org/10.1016/j.energy.2021.120419>
70. Punyavathi Ramineni , Alagappan Pandian, Malligunta Kiran Kumar, K. Mohana Sundaram, Improved operation of Li-ion battery with supercapacitor realized to solar-electric vehicle, *Energy Reports*, 8 (2022) pp256-264; <https://doi.org/10.1016/j.egy.2022.10.191>
71. Cigdem Tuc Altaf, Arpad Mihai Rostas, Maria Mihet, Mihaela Diana Lazar, Igor Iatsunskyi, Emerson Coy, Emre Erdem, Mehmet Sankir and Nurdan Demirci Sankir, Solar-assisted all-solid supercapacitors using composite nanostructures of ZnO nanowires with GO and rGO[†], *J. Mater. Chem. C*, 10 (2022) pp10748-10758; <https://doi.org/10.1039/D2TC02114E>

ABOUT THE EDITOR



Dr. V. D. Tripathi was born in Lucknow, Uttar Pradesh and completed his Graduation and Post-Graduation from University of Lucknow in 2003 and 2006 respectively. He qualified for CSIR NET-JRF and joined for research work at CSIR (Central Drug Research Institute) Lucknow. He was awarded Ph.D. degree by Jawaharlal Nehru University, New Delhi in 2012. He is professional medicinal chemist and has worked in different laboratories of esteemed organisations including Central Drug

Research Institute Lucknow, Jubilant Chemsys Noida, Zydus Cadila Healthcare Limited, LCC Toulouse France and University Paul Sabatier in field of Organic Synthesis and Medicinal Chemistry. He has the experience of working as one of the leading team members for the development of process for the first indigenous antidiabetic molecule Lipaglyn by Zydus Cadila Healthcare Limited. He was awarded prestigious CEFIPRA Indo French Research Fellowship in 2015 by DST, Government of India. He has a rich experience of research work in laboratory at CNRS-LCC Toulouse France in area of Dendrimer Synthesis. Presently he is working as Assistant Professor in the Department of Chemistry, C.M. Science College, Darbhanga. He has the experience of teaching Organic Chemistry to the students at undergraduate and Post Graduate level. He has over 35 research publications to his credit in reputed national and international journals. He has authored two books in Organic Chemistry. He has the experience as an Editor of book titled 'Future Science for Sustainable Development'. He has three Patents to his credit. He has delivered more than a dozen invited talks.



Kripa-Drishti Publications
A-503 Poorva Heights, Pashan-Sus Road, Near Sai Chowk,
Pune - 411021, Maharashtra, India.
Mob: +91 8007068686
Email: editor@kdpublications.in
Web: <https://www.kdpublications.in>

Price: ₹ 475

ISBN: 978-81-19149-17-9

